Visualizing Regular Tesselations:
Principal Congruence Links
and
Equivariant Morphisms from Surfaces to 3-Manifolds

by

Matthias Rolf Dietrich Goerner, Sr.

A dissertation submitted in partial satisfaction of the
requirements for the degree of
Doctor of Philosophy

in

Mathematics

in the

Graduate Division

of the

University of California, Berkeley

Committee in charge:

Professor Peter Teichner, Co-chair
Professor Ian Agol, Co-chair
Professor Carlo Sequin

Fall 2011

Abstract

Visualizing Regular Tesselations:
Principal Congruence Links
and
Equivariant Morphisms from Surfaces to 3-Manifolds

by

Matthias Rolf Dietrich Goerner, Sr.

Doctor of Philosophy in Mathematics

University of California, Berkeley

Professor Peter Teichner, Co-chair

Professor Ian Agol, Co-chair

We study embeddings of regular tessellations into S^3 such that some symmetries of the tessellation are directly visible in space. In the first chapter, we consider cusped hyperbolic 3-manifolds which arise from principal congruence subgroups and, therefore, are canonically tessellated by regular ideal hyperbolic tetrahedra. The codimension of an embedding of such a 3-manifold into S^3 is zero, and the embedding fills all of S^3 but a link, i.e., a disjoint union of knots. A new example constructed here is the 12-component link whose complement consists of 54 regular ideal hyperbolic tetrahedra. The link has 3-fold dihedral symmetry making some of the symmetries of its hyperbolic complement directly visible in the picture. In the second chapter, we embed surfaces F into 3-space. These surfaces are regular maps, i.e., regular tessellations by polygons.

The main result of the first chapter is the construction of two new principal congruence links. These links have hyperbolic complements arising from a natural number theoretic construction to obtain regular covers of Bianchi orbifolds. The datum for the construction of these arithmetic 3-manifolds is an ideal $\langle z \rangle$ in the ring of integers $\mathcal{O}_D$ in the imaginary quadratic number field $\mathbb{Q}(\sqrt{D})$ of discriminant $D < 0$. Results by Vogtman [Vog85], Lackenby [Lac00], and Agol [Ago00] imply that there are only finitely many principal congruence links. Here, we attempt to list all of the principal congruence links for the discriminant $D = -3$. Previously, only two such principal congruence links due to Dunfield and Thurston [DT03, Thu98] were known for the prime ideals generated by $z = 2$ and $z = 2 + \zeta$. We show that there are at most seven principal congruence links and explicitly construct two more for the non-prime ideals $z = 2 + 2\zeta$ and $z = 3$. For the construction, we use that the deck

transformation group of these Bianchi orbifold covers is a solvable extension to break down the construction into a sequence of branched cyclic covers starting from a known principal congruence orbifold diagram. Each cyclic cover can be obtained by either using Akbulut and Kirby's construction [AK80] or by unfolding the Euclidean (3,3,3)-triangle orbifold. The chapter finishes with a discussion of generic regular covers of the Bianchi orbifold for $\mathcal{O}_{-3}$ by explicitly constructing the category of all such covers with small fixed cusp modulus.

The second chapter gives an algorithm to determine how much symmetry of a surface F can be seen by mapping, immersing, or embedding F into Euclidean 3-space E^3. Here, F is a "regular map" as defined by, e.g., Coxeter [CM80] and is the generalization of the Platonic solids to higher genus surfaces, the genus 0 regular maps being exactly the surfaces of the Platonic solids. In this definition, the term "map" refers to a tessellation of a surface (as in countries of a geographic map) and a "regular map" is a tessellation by p-gons such that q of them meet at each vertex and fulfill an extra transitivity condition. Notice that any automorphism of the surface of a Platonic solid regarded as regular map is also realized by an isometry of the Platonic solid regarded as solid in E^3. However, embeddings of most higher-genus regular maps fail to make all symmetries directly visible in space. The Klein quartic is a regular map of genus 3 tessellated by heptagons and an embedding of it into E^3 is visualized by the sculpture "The Eightfold Way". We cannot rotate the sculpture so that one heptagon is rotated by a $\frac{1}{7}$th of a turn, even though this rotation is induced abstractly by an automorphism of the Klein quartic. However, the symmetries of the tetrahedron form a subgroup H of automorphisms that are visible in the sculpture. This gives rise to the question what the best sculpture for a given regular map F is in terms of symmetries directly made visible in space. We present algorithms to determine which subgroups H of the automorphism group of a given regular map F are realized by an *H-equivariant* morphism, immersion, or embedding into E^3. We show the results for the census of regular maps by Conder and Dobcsányi [CD01, Con09] up to genus 101.
To achieve this, we translate the question about the existence of an equivariant morphism into the existence of morphisms between the quotient spaces of F and E^3 by H with an extra condition on the holonomy. These quotient spaces are orbifolds and the orbifold fundamental group is a functor taking a morphism between orbifolds to a homomorphism between their orbifold fundamental groups. Here, we reverse the process: given a group homomorphism, is it coming from an orbifold morphism, immersion, or embedding from a 2-orbifold to a 3-orbifold? We develop algorithms to decide this using orbifold handle decompositions, extending normal surface theory, and applying the mapping class group.

Further connections intimately tie the two chapters together: For example, restricting the canonical triangulation of a principal congruence manifold to a cusp induces a regular map on the cusp torus, yielding an invariant we call cusp modulus. Furthermore, the 2-skeleton of the canonical triangulation of a principal congruence manifold is an immersed regular map, e.g., the Klein quartic in case of the complement of the Thurston congruence link [Ago].

To my parents.

Contents

Acknowledgments

I want to thank my two advisors, Peter Teichner and Ian Agol, very much. Peter helped me to get started in Berkeley and in topology and has taught me a very conceptual way to think about ideas. I really enjoyed his Algebraic Topology classes and the reading course on simplicial sets. He also provided generous funding and a nice network of advisees to help each other and bounce off ideas. Ian is an incredible expert on low-dimensional topology and I am very thankful for him sharing his insights, pointing out many helpful references to literature, making connections to experts in the field, and contributing several ideas to this thesis. He was very generous with his time and I was always welcomed to drop by his office and work out some ideas.

I also want to acknowledge Carlo Séquin. By introducing me to the Klein quartic and regular maps, he set off the first domino in a sequence of insights eventually resulting in the two chapters of my thesis. Carlo has a very concrete approach and loves visualizations, and my many visits to his office always have been fun and inspiring.

My thanks also go to Christian Zickert who has been a really solid math companion during half of my graduate school years. Christian's infectious enthusiasm spread beyond our collaboration of computing complex volumes of representations to the rest of my research. I wish him best of luck in Maryland.

Before graduate school, many people helped me on my path to math. In particular, I learned a lot of math and gained a lot of mathematical maturity from Dierk Schleicher who discovered my talent through "Jugend forscht" and from Desmond Sheiham who unfortunately cannot see the successful paths of his thankful students. I also want to acknowledge my high school teachers Bruno Hümmer who initiated the extracurricular math course and Rainer Göldel.

I also want to thank my many friends for their emotional support during many years, in particular, Tuğba Çolak, Rhea-Silvia Remus, and Felix Krahmer.

And Barb Waller, good spirit of the department and friend of all graduate students.

I want to acknowledge the Max-Planck Institute for Mathematics in Bonn for its funding.

Chapter 1

Congruence Links

1.1 Introduction

Let $\mathcal{O}_D$ be the ring of integers in the imaginary quadratic number field $\mathbb{Q}(\sqrt{D})$ of discriminant D with $D < 0$ and $D \equiv 0, 1\ (4)$. The group $\mathrm{PGL}(2, \mathcal{O}_D) \subset \mathrm{PGL}(2, \mathbb{C}) \cong \mathrm{PSL}(2, \mathbb{C})$ is a discrete subgroup of the orientation-preserving isometry group of hyperbolic 3-space $\mathbb{H}^3$ and contains the index 2 subgroup $\mathrm{PSL}(2, \mathcal{O}_D)$ which is called the *Bianchi group*. The quotient space

$$\mathrm{M}_1^D = \frac{\mathbb{H}^3}{\mathrm{PGL}(2, \mathcal{O}_D)} \quad \text{respectively} \quad \mathrm{N}_1^D = \frac{\mathbb{H}^3}{\mathrm{PSL}(2, \mathcal{O}_D)}$$

is a cusped hyperbolic 3-orbifold, called the *Bianchi orbifold*. Bianchi [Bia93, Bia92] (by hand and over a century ago) and Riley [Ril83] (by computer) have computed the Ford fundamental domains for the Bianchi orbifolds up to $D = -95$ and the orbifold diagrams can be found in [Hat83a].

The Bianchi orbifolds are prototypical in the sense that every arithmetic cusped hyperbolic 3-manifold is commensurable with a Bianchi orbifold M_1^D [MR03, Theorem 8.2.3]. For example, M_1^{-3} is covered by the Figure 8 knot complement and its sister. M_1^{-4} is covered by the complements of the Whitehead link and the Borromean rings.

The most straightforward way to construct arithmetic cusped hyperbolic 3-manifolds is by specifying an ideal $\langle z \rangle$ with $z \in \mathcal{O}_D$ and dividing $\mathbb{H}^3$ by the principal congruence subgroup to obtain a regular cover of the Bianchi orbifold for $\mathcal{O}_D$:

$$\mathrm{M}_z^D = \frac{\mathbb{H}^3}{\ker\left(\mathrm{PGL}\left(2, \mathcal{O}_D\right) \to \mathrm{PGL}\left(2, \frac{\mathcal{O}_D}{\langle z \rangle}\right)\right)}$$

respectively

$$\mathrm{N}_z^D = \frac{\mathbb{H}^3}{\ker\left(\mathrm{PSL}\left(2,\mathcal{O}_D\right) \to \mathrm{PSL}\left(2,\frac{\mathcal{O}_D}{\langle z\rangle}\right)\right)}.$$

These groups are called principal congruence subgroups of level $\langle z\rangle$ because they are formed by all matrices with coefficients in $\mathcal{O}_D$ that are invertible (M_z^D), respectively, have determinant one (N_z^D) and that are congruent to the identity modulo $\langle z\rangle$. We call the quotient spaces M_z^D and N_z^D *principal congruence manifold*. The orientation-preserving symmetry group is, up to a possible $\mathbb{Z}/2$ extension, $\mathrm{PSL}(2,\mathcal{O}_D/\langle z\rangle)$. Complex conjugation induces a reflection symmetry if $\langle z\rangle = \langle \bar{z}\rangle$.

Principal congruence subgroups have been studied extensively for $\mathbb{Z}$ and $\mathcal{O}_D$ yielding 2-, respectively, 3-orbifolds and manifolds such as the Klein quartic for $7 \in \mathbb{Z}$ (see Section 1.2.1) and have connections to many other areas of mathematics such as Group Theory, Algebraic Geometry, and Number Theory. Interesting examples included in this class are, e.g., the complement N_2^{-3} of the *minimally twisted 5-component chain link* yielding almost all census manifolds by Dehn fillings and the 4×5 chessboard complex $\mathrm{M}_{2+2\zeta}^{-3}$ studied in combinatorics (see Section 1.2.2). In fact, the family M_z^D even includes a manifold containing a geodesically immersed Klein quartic such that all symmetries of the Klein quartic are induced by symmetries of the 3-manifold ($\mathrm{M}_{2+\zeta}^{-3}$, see Section 1.2.1). Motivated by this relationship, Thurston managed to find a link with complement $\mathrm{M}_{2+\zeta}^{-3}$ [Thu98]. To the best of my knowledge, the *Thurston congruence link* for $\mathrm{M}_{2+\zeta}^{-3}$ and the *minimally twisted 5-component chain link* [DT03] for N_2^{-3} (see Section 1.13.1 for proof) are the only two examples of principal congruence links for $D=-3$ discovered so far (see Figure 1.4).

In more geometric terms, these two links are also examples of *Bianchi orbifold regular cover links* for $D=-3$, i.e., they have the following special property: the link complement posses a regular tessellation by regular ideal hyperbolic tetrahedra where regular means that the symmetry group of the link complement can take any tetrahedra to any other tetrahedra in all possible 12 rotations of the tetrahedron.

The two examples $\mathrm{M}_{2+\zeta}^{-3}$ and N_2^{-3} raise the question which of the manifolds M_z^D or N_z^D can be expressed as link complements and how much symmetry of the manifold is visible in the link. Cuspidal cohomology yields an obstruction to the Bianchi orbifold M_1^D being covered by a link complement. Using work of Grunewald, Mendoza, Rohlfs, Schwermer, and Zimmert [GS81, Men79, Roh85, Zim73], Vogtmann [Vog85] computes the rational cuspidal cohomology of the Bianchi groups implying:

Theorem 1.1.1. *If M_1^D can be covered by a link complement, then $D \in \mathcal{L}$ where*

$$\mathcal{L} = \{-3,-4,-7,-8,-11,-15,-19,-20,-23,-24,-31,-39,-47,-71\}.$$

In particular, a principal congruence manifold M_z^D can only be a link complement if $D \in \mathcal{L}$.

Hatcher [Hat83b] describes the structure of some of the Bianchi orbifolds in more detail and constructs link complements commensurable with them. Baker [Bak01] completes this work by constructing a link whose complement covers M_1^D for each $D \in \mathcal{L}$, thus turning Theorem 1.1.1 into "if and only if". However, Baker's links are not canonical and, in particular, the complement is not a principal congruence manifold or even a regular cover.

Whereas cuspidal cohomology restricts the possible values of D, Gromov and Thurston's 2π-Theorem [BH96] and later improvements by Agol [Ago00] and Lackenby [Lac00] restrict the possible values of z. Their theorems imply that for z large enough, any Dehn filling on M_z^D respectively N_z^D results in a hyperbolic manifold again. In particular, this implies that M_z^D and N_z^D cannot be link complements for all but finitely many values of z.

Together, these results imply that there are only finitely many principal congruence links, and, as shown in Section 1.7, at most seven potential principal congruence links for the case of discriminant $D = -3$. As mentioned earlier, two of those are known. The main part of this chapter is devoted to the construction of two more principal congruence links: $\mathrm{M}_3^{-3} \cong \mathrm{N}_3^{-3}$ in Section 1.12 and $\mathrm{M}_{2+2\zeta}^{-3} \cong \mathrm{N}_{2+2\zeta}^{-3}$ in Section 1.13.

The chapter is structured as follows:

Section 1.2 describes the connection of the principal congruence manifolds $\mathrm{M}_{2+\zeta}^{-3}$ and $\mathrm{M}_{2+2\zeta}^{-3}$ to the Klein Quartic and the 4×5 chessboard complex.

The next sections review prerequisites for the construction of the new principal congruence links: Section 1.3 proves some Lemmas about the groups PGL and PSL. It is fairly technical and can be skipped since references to the results are made explicitly when needed. Section 1.4 describes the Bianchi orbifold M_1^{-3}. Section 1.5 defines the cusp modulus as invariant of regular covers of Bianchi orbifolds. Section 1.7 lists all possible principal congruence links for $D = -3$ and Section 1.8 introduces congruence manifolds and the notation used later. Section 1.9 explains the orbifold diagram conventions and Section 1.10 details the construction of cyclic branched covers.

The principal congruence orbifolds $\mathrm{M}_{1+\zeta}^{-3}$ and M_2^{-3} discussed in Section 1.11 serve as starting point for the construction of the new principal congruence links.

The new principal congruence links are constructed in Section 1.12 and 1.13. Section 1.14 describes progress made on $\mathrm{N}_{3+\zeta}^{-3}$.

After the construction, a discussion of generic regular covers of M_1^{-3} follows in Section 1.15. To conclude, we discuss related and possible future work in Section 1.16

1.2 Relationship to Other Spaces

1.2.1 Relationship to the Klein Quartic

Similarly to M_z^D, the principal congruence subgroups of $\mathrm{PSL}(2,\mathbb{Z})$ yield Riemann surfaces as quotients of $\mathbb{H}^2$. An intuitive and geometric description of the action of these principal congruence subgroups on $\mathbb{H}^2$ is given in [Gra99]. Klein investigated these groups and, in particular, showed that for $z = 7$, the resulting quotient

$$\frac{\mathbb{H}^2}{\ker\left(\mathrm{PSL}\left(2,\mathbb{Z}\right) \to \mathrm{PSL}\left(2,\mathbb{Z}/7\right)\right)}$$

is the punctured version of the algebraic curve in $\mathbb{C}P^2$ that is given by the equation

$$xy^3 + yz^3 + zx^3 = 0$$

and that is now called the *Klein quartic* [Lev99]. The Klein quartic is also an example of a Hurwitz surface (see Section 2.2.2) and, hence, also a regular map (see Definition 2.2.1) of type $\{3,7\}$. The group of orientation-preserving symmetries is the unique simple group of order 168: $\mathrm{PSL}(2,\mathbb{Z}/7)$. The group $\mathrm{PGL}(2,\mathbb{Z}/7)$ of all symmetries of the Klein quartic is isomorphic to the symmetry group $\mathrm{PGL}(2,\mathbb{Z}[\zeta]/\langle 2+\zeta\rangle)$ of the chiral 3-manifold $\mathrm{M}_{2+\zeta}^{-3}$ where $\zeta = e^{\pi i/3} = \frac{1}{2} + \frac{\sqrt{3}}{2}i \in \mathbb{Z}[\zeta] = \mathcal{O}_{-3}$. The groups are isomorphic because $\mathbb{Z}[\zeta]/\langle 2+\zeta\rangle \cong \mathbb{Z}/7$ as the norm of $\langle 2+\zeta\rangle$ is $(2+\zeta)(2+\bar{\zeta}) = 7$. In fact, this group isomorphism is realized by a geodesic immersion of the punctured Klein quartic into $\mathrm{M}_{2+\zeta}^{-3}$, namely the Klein quartic is formed by the faces of the 28 regular ideal hyperbolic tetrahedra forming the Thurston congruence link complement [Ago].

1.2.2 Relationship to the 4×5 Chessboard Complex

The chessboard complex has been defined and investigated in [Gar79], [Zie94], and [BLVŽ94]. The $m \times n$ *chessboard complex* is a simplicial complex consisting of a k-simplex for every non-taking configuration of k rooks ("that is, no two rooks on the same row or column" [Zie94]) on the $m \times n$ chessboard. A face of a k-simplex is identified with the $k-1$-simplex corresponding to the respective subset of $k-1$ rooks.

The 2×3 chessboard complex is a 6-cycle. The 6-cycle is the link of a vertex in the 3×4 chessboard complex which is a torus with 24 triangles. This torus is the link of a vertex in the 4×5 chessboard which has 120 tetrahedra. Since 6 tetrahedra meet at an edge in a 6-cycle, the 4×5 chessboard complex can be given the structure of a cusped hyperbolic 3-manifold triangulated by regular ideal tetrahedra, as pointed out by David Eppstein [Epp].

The symmetry group of this manifold acts transitively on all flags of the triangulation. This means that the manifold is a regular cover of the Bianchi orbifold M_1^{-3}. The cusp modulus (as defined in Section 1.5) of the chessboard complex is the 3×4 chessboard complex. Up to multiplication by a unit, the only $z \in \mathbb{Z}[\zeta]$ with norm $\mathcal{N}(z) = \frac{24}{2}$ is $2 + 2\zeta$. Using the result on the category $\mathcal{C}_{2+2\zeta}$ of all Bianchi orbifold covers with this cusp modulus in Section 1.15.1, we have:

Theorem 1.2.1. *The 4×5 chessboard complex is isometric to the principal congruence manifold $\mathrm{M}_{2+2\zeta}^{-3}$.*

Section 1.13 constructs $\mathrm{M}_{2+2\zeta}^{-3}$ as link complement.

1.3 Properties of PGL and PSL

This section reviews and extends some well known properties of PGL and PSL and is rather technical. This section can be skipped. Later sections explicitly make references to results in this section when needed.

Section 1.3.1 discusses the structure of $\mathrm{PGL}(n, R/I)$ and $\mathrm{PSL}(n, R/I)$ for non-prime ideals I.
Lemma 1.3.11 and Example 1.3.12 in Section 1.3.2 state when N_z^{-3} is a double-cover of M_z^{-3}.
Lemma 1.3.15 and 1.3.18 in Section 1.3.3 give the symmetry groups of the principal congruence manifolds N_z^{-3} and M_z^{-3}.

1.3.1 PGL and PSL for Non-Prime Ideals

This section analyzes the structure of the groups $\mathrm{GL}, \mathrm{SL}, \mathrm{PGL}$, and PSL for a non-prime ideal I. Thus, this section can be used to compute the order of these groups by factoring an arbitrary ideal and using Remark 1.3.7 for the base case where I is prime.

Let R be a principal ideal domain. Recall the Chinese Remainder Theorem (see [Hun80, Chapter III, 2] or [Lan02, Chapter II, §2.]):

Theorem 1.3.1 (Chinese Remainder Theorem)**.** *Let I_j be pairwise coprime ideals in R. Then*

$$\frac{R}{\prod_{j=1}^{k} I_j} \cong \frac{R}{I_1} \times \cdots \times \frac{R}{I_k}$$

where the isomorphism is given by the projection onto each factor $R/\prod_{j=1}^{k} I_j \to R/I_j$.

Given a product of rings $A \times B$, the projections $A \times B \to A$ and $A \times B \to B$ induce maps between $M(n, \_)$ and yield an isomorphism $M(n, A \times B) \cong M(n, A) \times M(n, B)$. E.g., if A and B are quotients of a principal ideal domain, we can find a unique matrix on the left given two matrices on the right using the Chinese Remainder Theorem. In other words, $M(n, \_)$ is a product preserving functor.

Similarly, the units $(\_)^\times$ in the ring are given by

$$\left(\frac{R}{\prod_{j=1}^{k} I_j}\right)^\times \cong \left(\frac{R}{I_1}\right)^\times \times \cdots \times \left(\frac{R}{I_k}\right)^\times. \tag{1.1}$$

Lemma 1.3.2. *Let I_j be pairwise coprime ideals in R. Then*

$$\mathrm{GL}\left(n, \frac{R}{\prod_{j=1}^{k} I_j}\right) \cong \mathrm{GL}\left(n, \frac{R}{I_1}\right) \times \cdots \times \mathrm{GL}\left(n, \frac{R}{I_k}\right)$$

$$\mathrm{SL}\left(n, \frac{R}{\prod_{j=1}^{k} I_j}\right) \cong \mathrm{SL}\left(n, \frac{R}{I_1}\right) \times \cdots \times \mathrm{SL}\left(n, \frac{R}{I_k}\right).$$

Proof. Notice that the determinant commutes with the projections $M(n, A \times B) \to M(n, A)$, $M(n, A \times B) \to M(n, B)$. Hence, the above map between the GL is well-defined and an isomorphism because of Equation 1.1.
Similarly, 1 goes to 1 in each factor in Equation 1.1, hence the second isomorphism follows. □

For a unit r in a ring R, let $\sqrt[n]{r}_{R^\times}$ denote all units s such that $s^n = r$. Recall that $\mathrm{PGL}(n, R) \cong \mathrm{GL}(n, R)/R^\times$ and $\mathrm{PSL}(n, R) \cong \mathrm{SL}(n, R)/\sqrt[n]{1}_{R^\times}$. Equation 1.1 also holds for $\sqrt[n]{1}_{R^\times}$ implying:

Lemma 1.3.3. *Let I_j be pairwise coprime ideals in R. Then*

$$\mathrm{PGL}\left(n, \frac{R}{\prod_{j=1}^{k} I_j}\right) \cong \mathrm{PGL}\left(n, \frac{R}{I_1}\right) \times \cdots \times \mathrm{PGL}\left(n, \frac{R}{I_k}\right)$$

$$\mathrm{PSL}\left(n, \frac{R}{\prod_{j=1}^{k} I_j}\right) \cong \mathrm{PSL}\left(n, \frac{R}{I_1}\right) \times \cdots \times \mathrm{PSL}\left(n, \frac{R}{I_k}\right).$$

Lemma 1.3.4. *Let I be a prime ideal in R and $k \geq 2$. Then*

$$\ker\left(\mathrm{GL}\left(n, \frac{R}{I^{k+1}}\right) \to \mathrm{GL}\left(n, \frac{R}{I^k}\right)\right) \cong \quad M\left(n, \tfrac{R}{I}\right) \quad \cong \left(\frac{R}{I}\right)^{n^2}$$

$$\ker\left(\mathrm{SL}\left(n, \frac{R}{I^{k+1}}\right) \to \mathrm{SL}\left(n, \frac{R}{I^k}\right)\right) \cong \ker\left(\mathrm{tr} : M\left(n, \tfrac{R}{I}\right) \to \tfrac{R}{I}\right) \cong \left(\frac{R}{I}\right)^{n^2-1}$$

where we regard $M(n,R)$ and R/I as additive groups.

Proof. Let z be the generator of I. The matrices in the first kernel are exactly those of the form $\mathrm{Id}+z^kA$ where $A\in M(n,R/I)$. Two such matrices multiply as $(\mathrm{Id}+z^kA)(\mathrm{Id}+z^kB)=\mathrm{Id}+z^k(A+B)+z^{2k}AB\equiv\mathrm{Id}+z^k(A+B)\ (z^{k+1})$.
The matrices in the second kernel need to have $\mathrm{tr}(A)=0$. □

Remark 1.3.5. The matrices in the above kernel are the identity modulo I^k and can be regarded as the analogue of tangent vectors to the Lie group GL and SL at the identity in the I-adic expansion. Hence, the lemma is the analogue to computing the Lie algebra in the I-adic expansion.

Lemma 1.3.6. *Let I be a prime ideal in R.Then*

$$\ker\left(\mathrm{PGL}\left(n,\frac{R}{I^{k+1}}\right)\to\mathrm{PGL}\left(n,\frac{R}{I^k}\right)\right)\cong\left(\frac{R}{I}\right)^{n^2-1}.$$

Proof. Let z be the generator of the ideal I.

$$\begin{array}{ccc}\mathrm{GL}\left(n,\frac{R}{I^{k+1}}\right) & \twoheadrightarrow & \mathrm{PGL}\left(n,\frac{R}{I^{k+1}}\right)\\ \downarrow & & \downarrow\\ \mathrm{GL}\left(n,\frac{R}{I^k}\right) & \twoheadrightarrow & \mathrm{PGL}\left(n,\frac{R}{I^k}\right)\end{array}$$

The $\ker\left(\mathrm{GL}\left(n,\frac{R}{I^k}\right)\to\mathrm{PGL}\left(n,\frac{R}{I^k}\right)\right)$ is $\{r\mathrm{Id}\}$ with $r\in\left(\frac{R}{I^k}\right)^\times$. A preimage of such a matrix in $\mathrm{GL}\left(n,\frac{R}{I^{k+1}}\right)$ is of the form $r\mathrm{Id}+z^kA$ with $r\in\left(\frac{R}{I^{k+1}}\right)^\times$ and $A\in M(n,R/I)$. Notice that det is a unit again automatically, and so is $x=r+z^kA_{11}$. Hence, $x^{-1}(r\mathrm{Id}+z^kA)$ is the same in $\mathrm{PGL}\left(n,\frac{R}{I^{k+1}}\right)$ as $r\mathrm{Id}+z^kA$ and is of the form $\mathrm{Id}+z^kB$ with $B\in M(n,R/I)$ and $B_{11}=0$. These elements $\mathrm{Id}+z^kB$ form the kernel in the Lemma. □

Remark 1.3.7. For I a prime ideal in R, we have

$$\begin{aligned}\left|\mathrm{GL}\left(2,\frac{R}{I}\right)\right| &= (\mathcal{N}(I)^2-1)(\mathcal{N}(I)-1)\mathcal{N}(I)\\ \left|\mathrm{PGL}\left(2,\frac{R}{I}\right)\right|=\left|\mathrm{SL}\left(2,\frac{R}{I}\right)\right| &= (\mathcal{N}(I)^2-1)\mathcal{N}(I)\\ \left|\mathrm{PSL}\left(2,\frac{R}{I}\right)\right| &= \frac{1}{2}(\mathcal{N}(I)^2-1)\mathcal{N}(I)\quad\text{or}\quad(\mathcal{N}(I)^2-1)\mathcal{N}(I)\end{aligned}$$

where the factor $\frac{1}{2}$ has to be dropped for PSL if $2|\mathcal{N}(I)$.

1.3.2 Relationship between M_z^{-3} and N_z^{-3}

Let R be a principal ideal domain. Let $\mathcal{N}(I)$ denote the norm of the ideal I, i.e., the order of R/I.

Lemma 1.3.8. *Let I_j be distinct prime ideals, then -1 has a square root in $\frac{R}{\prod_{j=1}^{k} I_j^{m_j}}$ if and only if -1 has a square root in each factor $\frac{R}{I_j^{m_j}}$.*
Let I be a prime ideal with odd $\mathcal{N}(I)$, then -1 has a square root in $\frac{R}{I^m}$ if and only if $4|(\mathcal{N}(I)-1)$.

Proof. The first statement of the Lemma follows from -1 projecting to -1 in each factor under the isomorphism in the Chinese Remainder Theorem. We prove the other statement by induction on m:
For $m = 1$, $\frac{R}{I}$ is isomorphic to the field of order $\mathcal{N}(I)$. Under the group isomorphism $\left(\frac{R}{I}\right)^{\times} \cong \frac{\mathbb{Z}}{\mathcal{N}(I)-1}$, -1 corresponds to $\left[\frac{\mathcal{N}(I)-1}{2}\right]$, and, hence, -1 has a square root if and only if $4|(N(z)-1)$.
If R/I does not have a square root of -1, then neither does R/I^m because $R/I^m \twoheadrightarrow R/I$. For the induction step, pick $r \in R$ such that $r^2 \equiv -1\ (I^m)$. There exists $\bar{r} \in I^m$ such that $(r+\bar{r})^2 \equiv r^2 + 2r\bar{r} \equiv -1\ (I^{m+1})$ because $\frac{I^m}{I^{m+1}}$ is a field. Hence, $r+\bar{r}$ is a square root of -1 in $\frac{R}{I^{m+1}}$. □

Example 1.3.9. Let $R = \mathbb{Z}[\zeta]$ with $\zeta = e^{\pi i/3}$ be the Eisenstein integers. Consider the rings $\frac{R}{\langle z\rangle}$. For $z = 2$, we obtain the finite field of order 4, so -1=1 has a square root. For $z = 4$, and hence for $z = 2^k$ with $k \geq 2$, one can check that -1 does not have a square root. Recall that $\mathcal{N}(a+b\zeta) = a^2 + ab + b^2$. Using the Lemma, we obtain Table 1.1.

Let S be a ring, typically, $\frac{\mathbb{Z}[\zeta]}{\langle z\rangle}$. The determinant map $\det : \mathrm{GL}(n,S) \to S^{\times}$ descends to

$$\det : \mathrm{PGL}(n,S) \cong \frac{\mathrm{GL}(n,S)}{S^{\times}} \to \frac{S^{\times}}{(S^{\times})^n}. \tag{1.2}$$

Lemma 1.3.10. *The bottom row of the following diagram is exact:*

$$\begin{array}{ccccc}
\frac{\mathrm{SL}(2,S)}{\sqrt{1}_{S^{\times}}} & \hookrightarrow & \frac{\mathrm{GL}(2,S)}{\sqrt{1}_{S^{\times}}} & \twoheadrightarrow & \frac{\mathrm{GL}(2,S)}{S^{\times}} \\
\downarrow \cong & & & & \downarrow \cong \\
\mathrm{PSL}(2,S) & \xhookrightarrow{k} & \mathrm{PGL}(2,S) & \xrightarrow{\det} & \frac{S^{\times}}{(S^{\times})^2}
\end{array}$$

Table 1.1: Existence of $\sqrt{-1}$ in $\frac{\mathbb{Z}[\zeta]}{\langle z \rangle}$.

z	prime factors	$\sqrt{-1}$ exists
$1+\zeta$	-	No
2	-	Yes
$2+\zeta$	-	No
$2+2\zeta$	$2(1+\zeta)$	No
3	$\langle 1+\zeta \rangle^2$	No
$3+\zeta$	-	Yes
$3+2\zeta$	-	No
$3+3\zeta$	$\langle 1+\zeta \rangle^3$	No
4	2^2	No
$4+\zeta$	$\langle 1+\zeta \rangle \ \langle 2+\zeta \rangle$	No
$4+2\zeta$	$2(2+\zeta)$	No
$4+3\zeta$	-	Yes
$4+4\zeta$	$2^2(1+\zeta)$	No
5	-	Yes
$5+\zeta$	-	No
$5+2\zeta$	$(1+\zeta)(3+\bar{\zeta})$	No
$5+3\zeta$	$\langle 2+\zeta \rangle^2$	No
$5+4\zeta$	-	Yes
$5+5\zeta$	$5(1+\zeta)$	No
6	$\langle 2 \rangle \ \langle 1+\zeta \rangle^2$	No
$6+\zeta$	-	No
$6+2\zeta$	$2(3+\zeta)$	Yes

Proof. The neutral element in $\mathrm{GL}(2,S)/S^\times$ has representatives $\begin{pmatrix} s & 0 \\ 0 & s \end{pmatrix} \in \mathrm{GL}(2,S)$ with $s \in S$. Such a representative lifts to $\mathrm{SL}(2,S)$ only if $s \in \sqrt{1}_{S^\times}$, hence is zero in $\mathrm{SL}(2,S)/\sqrt{1}_{S^\times}$. Hence, k is injective.
An element $[M] \in \mathrm{PGL}(2,S)$ lifts to $\mathrm{PSL}(2,S)$ if and only if there is a representative $M \in \mathrm{GL}(2,S)$ with $\det M = 1 \in S$, i.e., $[M] \in \ker(\det)$. □

Consider the principal congruence subgroups $\ker(p_{\mathrm{PGL}})$ and $\ker(p_{\mathrm{PSL}})$ yielding M_z^{-3} and N_z^{-3}:

$$\begin{array}{ccccc} \ker(p_{\mathrm{PSL}}) & \hookrightarrow & \mathrm{PSL}(2,\mathbb{Z}[\zeta]) & \xrightarrow{p_{\mathrm{PSL}}} & \mathrm{PSL}\left(2,\frac{\mathbb{Z}[\zeta]}{\langle z\rangle}\right) \\ \downarrow i & & \downarrow j & & \downarrow k \\ \ker(p_{\mathrm{PGL}}) & \hookrightarrow & \mathrm{PGL}(2,\mathbb{Z}[\zeta]) & \xrightarrow{p_{\mathrm{PGL}}} & \mathrm{PGL}\left(2,\frac{\mathbb{Z}[\zeta]}{\langle z\rangle}\right) \end{array} \tag{1.3}$$

We have $\ker(p_{\mathrm{PSL}}) = j^{-1}(\ker(p_{\mathrm{PGL}}))$ or, as subgroup of $\mathrm{PSL}(2,\mathbb{C}) \cong \mathrm{PGL}(2,\mathbb{C})$,

$$\ker(p_{\mathrm{PSL}}) = \mathrm{PSL}(2,\mathbb{Z}[\zeta]) \cap \ker(p_{\mathrm{PGL}}).$$

Lemma 1.3.11. *The index of the map i is at most two, i.e., N_z^{-3} is isometric to M_z^{-3} or a double cover of M_z^{-3}. The index is two if and only if -1 has a square root in $S = \frac{\mathbb{Z}[\zeta]}{\langle z\rangle}$.*

Proof. The index of the inclusion j is two, therefore, the index of i is at most two.
The index of the map i is one if and only if

$$\ker(p_{\mathrm{PGL}}) \subset \mathrm{Im}(j) \cong \mathrm{PSL}(2,\mathbb{Z}[\zeta]).$$

Hence, the index is two if and only if there is a matrix $M \in \mathrm{GL}(2,\mathbb{Z}[\zeta])$ with $\det(M) = -1$ such that M is 1 in $\mathrm{PGL}(2,S)$. Such a matrix has $\det(p_{\mathrm{PGL}}(M)) = 1 \in \frac{S^\times}{(S^\times)^2}$, so it is a necessary condition that -1 is send to 1 in $\frac{S^\times}{(S^\times)^2}$.
This condition is sufficient: Assume there is $s \in S$ with $s^2 = -1$. Pick a representative $s' \in \mathbb{Z}[\zeta]$ of s. We need to prove that there is a matrix $M \in \mathrm{GL}(2,\mathbb{Z}[\zeta])$ that is $\begin{pmatrix} s & 0 \\ 0 & s \end{pmatrix}$ in $\mathrm{GL}(2,S)$. Consider $M = \begin{pmatrix} s'+za' & zb' \\ z & s' \end{pmatrix}$. We need to find $a', b' \in \mathbb{Z}[\zeta]$ such that

$$\det(M) = (s')^2 + s'za' + z^2b' = -1. \tag{1.4}$$

Because $s^2 = -1 \in S$, Equation 1.4 is true modulo z. Since s' has an inverse modulo z, we can pick a' such that the equation is fulfilled modulo z^2. Hence, we can pick b' such that the equation is exact. □

Example 1.3.12. "Yes" entries in Example 1.3.9 are cases where N_z^{-3} is a double cover of M_z^{-3}. The matrix $M = \begin{pmatrix} 12 & 5 \\ 5 & 2 \end{pmatrix}$ serves as an example of the proof for $z = 5$.

1.3.3 The Symmetry Group of M_z^{-3} and N_z^{-3}

Lemma 1.3.13. *The map p_{PSL} in the Commutative Diagram 1.3 is surjective. The map p_{PGL} has image $\det^{-1}(\{\pm 1\})$ with $\det$ as defined by Equation 1.2.*

Proof. We can pick a representative $M \in \mathrm{GL}(2, \mathbb{Z}[\zeta])$ with $\det M = \pm 1$ for every element in $\mathrm{PGL}(2, \mathbb{Z}[\zeta])$, hence $\mathrm{Im}(p_{\mathrm{PGL}}) \subset \det^{-1}(\{\pm 1\})$.
It is left to show that an element in $\mathrm{PSL}(2, S)$ respectively $\det^{-1}(\{\pm 1\})$ is in the image of p_{PSL} respectively p_{PGL}. Pick a matrix $M = \begin{pmatrix} a & b \\ c & d \end{pmatrix} \in \mathrm{GL}(2, S)$ to represent such an element. In case of PSL, we have $\det M = 1$. In case of PGL, we can assume that $\det M = \pm 1$, because $\det M \mapsto \pm 1 \in \frac{S^\times}{(S^\times)^2}$ and we can multiply M by a unit in $S^\times$ without changing the element in $\mathrm{PGL}(2, S)$ that M represents.
Recall that $\mathbb{Z}[\zeta]$ is a Euclidean domain (see, e.g., [Hun80, Chapter III, Definition 3.8]) with norm $\rho(a + b\zeta) = a^2 + ab + b^2$. This induces a function $\rho : S = \frac{\mathbb{Z}[\zeta]}{\langle z \rangle} \to \mathbb{N}_0$ defined by $\rho(s)$ being the minimal $\rho(s')$ among all representatives $s' \in \mathbb{Z}[\zeta]$ of $s \in S$. The function ρ does not turn S into a Euclidean domain, but still fulfills that, for $a, b \in S \setminus 0$ with $\rho(b) \leq \rho(a)$, there exists $k \in \mathbb{Z}$ such that $\rho(a - \zeta^k b) < \rho(a)$. Hence, we can still perform the Euclidean algorithm on S.
Perform the Euclidean algorithm on the pair (a, b). Apply the same steps to (c, d). This means that we can think of the Euclidean algorithm as performing column operations on M, i.e., multiplying M by elementary matrices $\begin{pmatrix} 1 & \zeta^k \\ 0 & 1 \end{pmatrix}$ and $\begin{pmatrix} 1 & 0 \\ \zeta^k & 1 \end{pmatrix}$. At the end of the Euclidean algorithm, M is of the form $\begin{pmatrix} 0 & b \\ c & d \end{pmatrix}$ or $\begin{pmatrix} a & 0 \\ c & d \end{pmatrix}$. By multiplication with the counter-diagonal matrix $\begin{pmatrix} 0 & 1 \\ -1 & 0 \end{pmatrix}$, we can exclude the first form. By multiplication with the elementary matrix $\begin{pmatrix} 1 & 0 \\ -a^{-1}c & 1 \end{pmatrix}$, we can bring the matrix into the form $M_0 = \begin{pmatrix} a & 0 \\ 0 & d \end{pmatrix} \in \mathrm{GL}(2, S)$ with $ad = 1$ respectively $ad = \pm 1$.
Pick $s', t' \in \mathbb{Z}[\zeta]$ such that they map to $a, d \in S$. Similarly to the proof of Lemma 1.3.11, we can find $a', b' \in \mathbb{Z}[\zeta]$ such that $\begin{pmatrix} s' + za' & zb' \\ z & t' \end{pmatrix} \in \mathrm{GL}(2, \mathbb{Z}[\zeta])$ goes to M_0.
Notice that the elementary matrices and the counter-diagonal matrix lift to $\mathrm{SL}(2, \mathbb{Z}[\zeta])$ as

well. Hence, M has a preimage under p_{PGL} respectively p_{PSL}. □

Remark 1.3.14. The surjectivity of p_{PSL} for prime ideals is also shown in [MR03, Lemma 6.5.6] using Hensel's Lemma (see, e.g., [Eis95, Theorem 7.18]).

Lemma 1.3.15. *Let M be a regular manifold cover of M_1^{-3}. Then $\mathrm{Isom}^+(M)$ is isomorphic to the group of deck transformations of $M \to \mathrm{M}_1^{-3}$. Hence, $\mathrm{Isom}^+(\mathrm{M}_z^{-3}) \cong \det^{-1}(\{\pm 1\}) \subset \mathrm{PGL}\left(2, \frac{\mathbb{Z}[\zeta]}{\langle z \rangle}\right)$ where $\det$ as defined by Equation 1.2.*

Proof. Every deck transformation of $M \to \mathrm{M}_1^{-3}$ induces an orientation-preserving symmetry. If $M = \mathrm{M}_z^{-3}$, the holonomy of this covering space is given by $\pi_1^{orb}(\mathrm{M}_1^{-3}) \cong \mathrm{PGL}(2, \mathbb{Z}[\zeta]) \twoheadrightarrow \mathrm{Im}\,(p_{\mathrm{PGL}}) = \det^{-1}(\{\pm 1\})$ using Lemma 1.3.13.
We need to exclude that there are "hidden symmetries", i.e., orientation-preserving symmetries of M not induced by a deck transformation. Notice that the canonical cell decomposition of M (see, e.g., [EP88]) is the triangulation by regular ideal hyperbolic tetrahedra induced from M_1^{-3}. Hence, every orientation-preserving isometry of M comes from mapping some tetrahedra to some other tetrahedra with a choice of 12 possible orientations, i.e., from a deck transformation of $M \to \mathrm{M}_1^{-3}$.

The orbifold diagrams for the orbifold cases M_1^{-3}, $\mathrm{M}_{1+\zeta}^{-3}$ and M_2^{-3} are shown in Section 1.11 and reveal that there are no hidden symmetries. □

Remark 1.3.16. This also follows from the theorem in [Mey86] which states that M_1^{-3} is the minimal volume cusped orientable hyperbolic 3-orbifold.

Remark 1.3.17. If M is a generic cover of M_1^{-3}, the argument fails. For example, $M = \mathrm{M}_{3+\zeta}^{-3}(P)$ (also discussed in Section 1.14; see Section 1.8 for notation) with $P = \left\{ \begin{pmatrix} 1 & x \\ 0 & 1 \end{pmatrix} \right\}$ has an orientation-preserving symmetry that exchanges the two cusps and, hence, is not a deck transformation of $M \to \mathrm{M}_1^{-3}$. This symmetry will take one triangulation by regular ideal tetrahedra to a distinct triangulation by regular ideal tetrahedra.

Lemma 1.3.18. *If $\mathrm{N}_z^{-3} \ncong \mathrm{M}_z^{-3}$ (i.e., if -1 has no square root in $S = \mathbb{Z}[\zeta]/\langle z \rangle$), then*

$$\mathrm{Isom}^+(\mathrm{N}_z^{-3}) \cong \frac{\mathbb{Z}}{2} \times \mathrm{Isom}^+(\mathrm{M}_z^{-3}) \cong \frac{\mathbb{Z}}{2} \times \mathrm{PSL}\left(2, \frac{\mathbb{Z}[\zeta]}{\langle z \rangle}\right).$$

Proof. Recall that N_z^{-3} is a regular cover of both M_1^{-3} and its double-cover N_1^{-3}.
Therefore, the symmetries of N_z^{-3} are induced from the action of $\mathrm{PGL}(2, \mathbb{Z}[\zeta])$ on $\mathbb{H}^3$ by Lemma 1.3.15, let m be the map $\mathrm{PGL}(2, \mathbb{Z}[\zeta]) \to \mathrm{Isom}^+(\mathrm{N}_z^{-3})$.
The deck transformations of $\mathrm{N}_z^{-3} \to \mathrm{N}_1^{-3}$ are $\mathrm{PSL}\left(2, \frac{\mathbb{Z}[\zeta]}{\langle z \rangle}\right)$ by Lemma 1.3.13 and form a subgroup of $\mathrm{Isom}^+(\mathrm{N}_z^{-3})$, call the inclusion l. The index of $\mathrm{Im}(l)$ in $\mathrm{Isom}^+(\mathrm{N}_z^{-3})$ is two

because N_z^{-3} is a double-cover of M_z^{-3} by Lemma 1.3.11. Hence we obtain the following commutative diagram:

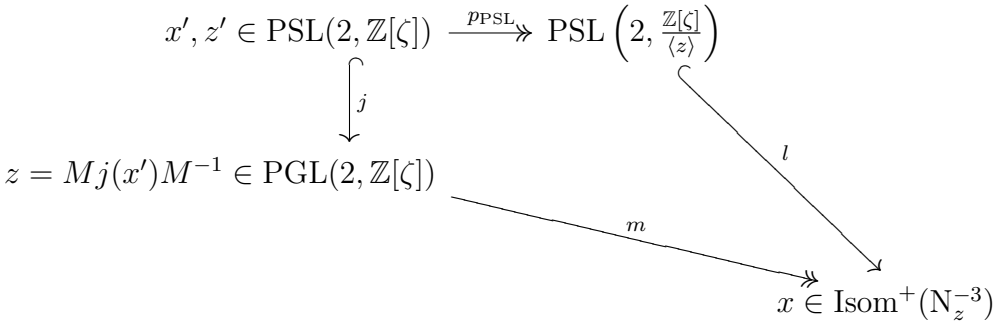

(1.5)

Because $\frac{\mathbb{Z}[\zeta]}{\langle z \rangle}$ has a square root of -1 by Lemma 1.3.11, the map k from Lemma 1.3.10 gives an isomorphism onto the image of p_{PGL}. Hence Commutative Diagram 1.3 becomes:

$$\begin{array}{ccc} \mathrm{PSL}(2, \mathbb{Z}[\zeta]) & \xrightarrow{p_{\mathrm{PSL}}} & \mathrm{PSL}\left(2, \frac{\mathbb{Z}[\zeta]}{\langle z \rangle}\right) \\ \downarrow j & & \downarrow k \cong \\ \mathrm{PGL}(2, \mathbb{Z}[\zeta]) & \xrightarrow{p_{\mathrm{PGL}}} & \det^{-1}(\{\pm 1\}) \end{array} \tag{1.6}$$

A matrix $y \in \mathrm{PGL}(2, \mathbb{Z}[\zeta])$ has $\det y \in \frac{\mathbb{Z}[\zeta]^\times}{(\mathbb{Z}[\zeta]^\times)^2}$. If $\det y = +1$, then it lifts to $\mathrm{PSL}(2, \mathbb{Z}[\zeta])$ and induces a deck transformation of $\mathrm{N}_z^{-3} \to \mathrm{N}_1^{-3}$. If $\det y = -1$, y induces the non-trivial symmetry of N_1^{-3} and $m(y) \notin \mathrm{Im}(l)$.
The matrix $M \in \mathrm{PGL}(2, \mathbb{Z}[\zeta])$ in the proof Lemma 1.3.11 is an example of the case $\det M = -1$ such that $p_{\mathrm{PGL}}(M) = 1$. Let $i : \mathbb{Z}/2 \hookrightarrow \mathrm{Isom}^+(\mathrm{N}_z^{-3})$ map 1 to $m(M)$. Then l is a splitting of the following central extension:

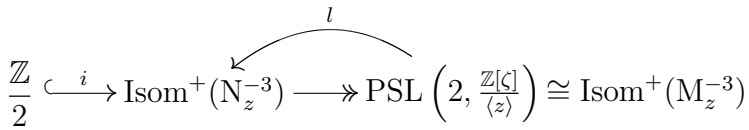

It is left to show that N_z^{-3} is a central extension, i.e., that $m(M)$ commutes with an element $x \in \mathrm{Im}(l)$.
Lift x to $x' \in \mathrm{PSL}(2, \mathbb{Z}[\zeta])$. Let $z = Mj(x')M^{-1}$. Pick the unique $z' \in \mathrm{PSL}(2, \mathbb{Z}[\zeta])$ with $j(z') = z$. Commutative Diagram 1.6 implies

$$\begin{aligned} p_{\mathrm{PSL}}(z') &= k^{-1}(p_{\mathrm{PGL}}(j(z'))) = k^{-1}(p_{\mathrm{PGL}}(z)) = k^{-1}(p_{\mathrm{PGL}}(Mj(x')M^{-1})) \\ &= k^{-1}(p_{\mathrm{PGL}}(M)p_{\mathrm{PGL}}(j(x'))p_{\mathrm{PGL}}(M)^{-1}) = k^{-1}(p_{\mathrm{PGL}}(j(x'))) \\ &= p_{\mathrm{PSL}}(x') \\ l(p_{\mathrm{PSL}}(z')) &= l(p_{\mathrm{PSL}}(x')) = x. \end{aligned}$$

Since Diagram 1.5 commutes, we have

$$\begin{aligned} l(p_{\mathrm{PSL}}(z')) &= m(j(z')) \\ &= m(z) = m(Mj(x')M^{-1}) = m(M)m(j(x'))m(M)^{-1} \\ &= m(M)xm(M)^{-1}. \end{aligned}$$

Therefore $x = m(M)xm(M)^{-1}$. □

Remark 1.3.19. This proof is rather subtle. The two Commutative Diagrams 1.5 and 1.6 do not commute together. For example, take an element $M \in \mathrm{PGL}(2, \mathbb{Z}[\zeta])$ with $\det M = -1$. Then $m(M) \neq l(k^{-1}(p_{\mathrm{PGL}}(M)))$.

1.4 The Bianchi Orbifold for $D = -3$

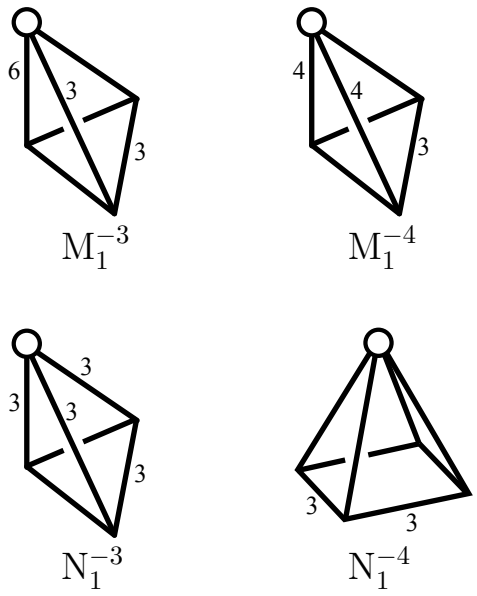

Figure 1.1: Bianchi orbifolds for $D = -3$ and -4.

Let $\zeta = e^{\pi i/3} = \frac{1}{2} + \frac{\sqrt{3}}{2}i$ such that $\mathcal{O}_{-3} = \mathbb{Z}[\zeta]$ are the Eisenstein integers. The group $\mathrm{PGL}(2, \mathcal{O}_{-3})$ is the orientation-preserving subgroup of a Coxeter reflection group [MR03, Section 9.1] (as is $\mathrm{PGL}(2, \mathcal{O}_{-4})$, see Figure 1.1). In other words, M_1^{-3} is obtained by dividing $\mathbb{H}^3$ by the orientation-preserving symmetries of the tessellation $\mathbb{H}^3$ by regular ideal tetrahedra. 12 copies of a fundamental domain of M_1^{-3} form one such regular ideal tetrahedron. The cusp respectively vertices of the singular locus correspond to the ideal vertex respectively the edge-center, face-center, and center of the regular ideal tetrahedron.

1.5 Cusp Modulus

Let $M \cong \frac{\mathbb{H}^3}{\Gamma}$ be a regular cover of M_1^{-3}. If M is a manifold, it inherits a triangulation by regular ideal hyperbolic tetrahedra. Intersecting this triangulation with a horosphere about an ideal vertex of a tetrahedron induces a triangulation of the cusp torus by equilateral Euclidean triangles that is regular.

This triangulation lifts to a triangulation of the universal cover of the torus (compare to classification of genus 1 regular maps in Section 2.2.2). The vertices of this triangulation can be associated with the lattice $\mathbb{Z}[\zeta] \subset \mathbb{C}$, and the torus can be obtained by dividing $\mathbb{Z}[\zeta] \subset \mathbb{C}$ by an ideal $\langle z \rangle$ in $\mathbb{Z}[\zeta]$. We refer to the triangulation of the torus respectively the generator $z \in \mathbb{Z}[\zeta]$ as *cusp modulus* of M. Because M is a regular cover, the cusp modulus is the same for every cusp, hence an invariant of M.

The number of vertices, edges, and triangles in the triangulation of a cusp with cusp modulus z is given by

$$v = \mathcal{N}(z), \qquad e = 3\mathcal{N}(z), \qquad f = 2\mathcal{N}(z)$$

where $\mathcal{N}(z)$ is the norm of the ideal $\langle z \rangle$ given by

$$\mathcal{N}(z) = \left| \frac{\mathbb{Z}[\zeta]}{\langle z \rangle} \right| = a^2 + ab + b^2 \qquad \text{with } z = a + bi.$$

In other words, look at the elements $\left[\begin{pmatrix} 1 & x \\ 0 & 1 \end{pmatrix} \right] \in \Gamma \subset \mathrm{PGL}(2, \mathbb{C})$ fixing ∞. These correspond to the translations of the above lattice $\mathbb{Z}[\zeta]$ that give the torus as quotient. The group of all $x \in \mathbb{Z}[\zeta]$ occurring this way is an ideal $\langle z \rangle$ in $\mathbb{Z}[\zeta]$ because Γ is invariant under conjugation by $\begin{pmatrix} \zeta & 0 \\ 0 & 1 \end{pmatrix}$. The generator $z \in \mathbb{Z}[\zeta]$ is again the cusp modulus.

Figure 1.2 shows a fundamental domain of a triangulation of a torus forming the link of an ideal vertex for the cusp modulus $z = 2 + \zeta$.

If M is an orbifold, the regular cover structure makes the cusp an interval $\times$ a regular cover of the Euclidean (2,3,6)-triangle orbifold. This regular cover of the (2,3,6)-triangle orbifold is again encoding the "cusp modulus" (this time z and some rotations of $\mathbb{C}$ such that the quotient is an orbifold) and can be recovered by looking at the elements $\left[\begin{pmatrix} \zeta^k & x \\ 0 & 1 \end{pmatrix} \right] \in \Gamma \subset \mathrm{PGL}(2, \mathbb{C})$ which act as $z \mapsto \zeta^k z + x$ on $\mathbb{C}$. Notice that these torsion elements with $k \not\equiv 0(6)$ make the topology of a cusp an interval $\times$ a sphere.

The maximally embedded horocusp neighborhood of M_1^{-3} corresponds to a horoball above the horosphere with height 1 in the upper half plane model. This induces an embedded

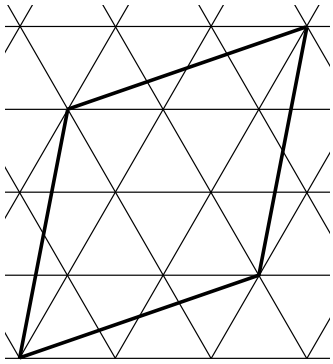

Figure 1.2: Cusp modulus $z = 2 + \zeta$.

horocusp neighborhood C on a regular cover M. Hence, the length of a geodesic peripheral curve in ∂C is the same as the one obtained from the natural Euclidean metric on the torus $\mathbb{C}/\langle z \rangle$.

In Section 1.15.1, we discuss universal Bianchi orbifold covers defined by cusp modulus being the only relation.

1.6 Bound on the Cusp Modulus for a Link Complement

The goal of this section is to prove Corollary 1.6.2 stating that a principal congruence link for discriminant $D = -3$ has cusp modulus $|z| < 6$.

Let M be a cusped orientable hyperbolic 3-manifold with an embedded horocusp neighborhood C. Pick a closed curve γ_i in each connected component of ∂C such that γ_i is geodesic with respect to the Euclidean metric on ∂C. Gromov and Thurston's 2π-Theorem (see [BH96] for proof) says that the manifold $M(\gamma_1, \ldots, \gamma_n)$ obtained by Dehn filling M along the γ_i again admits a hyperbolic metric if the length of each γ_i is $> 2\pi$. Agol [Ago00, Theorem 6.2] and Lackenby [Lac00, Theorem 3.1] improve this bound to > 6 (using the Geometrization Theorem).

Lemma 1.6.1. *If the length of each γ_i is ≥ 6, the cores of the Dehn fillings have infinite order in $\pi_1(M(\gamma_1, \ldots, \gamma_n))$.*

Proof. This lemma is the first step in the proofs of [Ago00, Theorem 6.2] and [Lac00, Theorem 3.1] and both proofs still hold when replacing > 6 by ≥ 6:

Both proofs start assuming there exists a map of a disk into $M(\gamma_1, \ldots, \gamma_n)$ such that the boundary becomes a multiple of a core. Both papers show that such a disk can be turned into a pleated surface S (in [Ago00]) respectively F (in [Lac00]) in $M \setminus C$ with boundary being a collection of γ_i. We might need to replace C with a slightly smaller horocusp, retaining the property that the length of γ_i is $> 6 - \epsilon$ where we can pick any $\epsilon > 0$. The proofs then continue to derive an inequality for the area of the surface that results in a contradiction. To make this part of the proofs work, we have to modify the inequalities as follows. For the proof of Theorem 3.1 in [Lac00]:

$$2\pi(|F \cap \partial M| - 2) = \text{Area}(F - \partial F) \geq |F \cap \partial M|(\pi/3) \min \text{Length}(s_i) > (2\pi - \epsilon\pi/3)|F \cap \partial M|.$$

For the proof of Theorem 6.2 in [Ago00]:

$$6(n-2) = 6|\chi(S)| \geq (n-1) \cdot l_C(\alpha) > (6 - \epsilon)(n-1).$$

□

Corollary 1.6.2. *If the manifold M is a regular cover of the Bianchi orbifold M_1^{-3} with cusp modulus $|z| >= 6$, e.g., M_z^{-3} or N_z^{-3}, then M cannot be a link complement.*

Proof. Pick embedded horocusp neighborhood in M as described in 1.5. Assume M is a link complement. Let γ_i be the meridians of $M \subset S^3$. Then Dehn filling along them yields $M(\gamma_1, \ldots, \gamma_n) \cong S^3$. Pick geodesics in ∂C homotopic to γ_i. By the remark in Section 1.5, the length of these geodesics is at least $|z|$. By Gromov, Thurston, Agol, and Lackenby's results, $M(\gamma_1, \ldots, \gamma_n)$ is hyperbolic or has at least infinite fundamental group. A contradiction. □

1.7 Principal Congruence Links

Multiplying z with ζ^k does not change the ideal $\langle z \rangle$. Complex conjugation only changes the orientation of M_z^{-3} respectively N_z^{-3}. Hence, from now on we assume that z is of the form $z = a + b\zeta$ with $a \geq b \geq 0$. The space M_z^{-3} is amphicheiral if and only if $z \in \{1, 1 + \zeta\} \cdot \mathbb{N}$.

Recall that $[M] \in \mathrm{PGL}(2, \mathbb{C})$ is parabolic if and only if $\frac{\text{tr } M}{\pm\sqrt{\det M}} \in (-2, 2)$. Hence the principal congruence subgroup is torsion-free and the quotient M_z^{-3} a manifold except for $|z| \leq 2$. The orbifold cases are covered in Section 1.11.

A computer program generated the triangulations for the manifold cases with $|z| < 6$ as input for SnapPy [CDW]. Table 1.2 shows the homologies of these manifolds. If H_1 has torsion or Betti number larger than the number of cusps, the manifold cannot be a link complement. Together with Corollary 1.6.2, this yields:

Theorem 1.7.1. *If* N_z^{-3} *is a link complement, then*

$$z \in \{2, 2+\zeta, 2+2\zeta, 3, 3+\zeta, 3+2\zeta, 5+\zeta\}.$$

If M_z^{-3} *is a link complement, then* $\mathrm{M}_z^{-3} \cong \mathrm{N}_z^{-3}$.

Figure 1.3 gives an overview of the z for which we know whether N_z^{-3} is a link complement or not. The corresponding links or orbifold diagrams are shown in Figure 1.4. The link for N_3^{-3} is constructed in Section 1.12 and for $\mathrm{N}_{2+2\zeta}^{-3}$ in Section 1.13. Section 1.13.1 also contains a proof that the complement of the minimally twisted 5-component chain link is N_2^{-3}.

Remark 1.7.2. The table in Example 1.3.9 lists when $\mathrm{N}_z^{-3} \ncong \mathrm{M}_z^{-3}$.

Remark 1.7.3. The difference between 2π and 6 rules out the cases $z = 4{+}3\zeta$ and $z = 5{+}2\zeta$.

Table 1.2: Homologies of principal congruence manifolds M_z^{-3} and N_z^{-3} (when $\mathrm{M}_z^{-3} \ncong \mathrm{N}_z^{-3}$). SnapPy [CDW] crashes for larger z.

	M_z^{-3}			N_z^{-3}
z	Tetrahedra	cusps	$H_1(\mathrm{M}_z^{-3})$	$H_1(\mathrm{N}_z^{-3})$
$2+\zeta$	28	8	$\mathbb{Z}^8$	
$2+2\zeta$	120	20	$\mathbb{Z}^{20}$	
3	54	12	$\mathbb{Z}^{12}$	
$3+\zeta$	91	14	$\mathbb{Z}^{14} \oplus \mathbb{Z}/2$	$\mathbb{Z}^{28}$
$3+2\zeta$	570	60	$\mathbb{Z}^{60}$	
$3+3\zeta$	1458	108	$\mathbb{Z}^{126}$	
4	160	20	$\mathbb{Z}^{20} \oplus \mathbb{Z}/4$	
$4+\zeta$	336	32	$\mathbb{Z}^{32} \oplus \mathbb{Z}/2$	
$4+2\zeta$	1680	120	$\mathbb{Z}^{120} \oplus (\mathbb{Z}/2)^8$	
$4+3\zeta$	2109	114	$\mathbb{Z}^{114} \oplus \mathbb{Z}/2$	?
$4+4\zeta$	1920	80	$\mathbb{Z}^{125} \oplus (\mathbb{Z}/2)^3$	
5	650	52	$\mathbb{Z}^{52} \oplus (\mathbb{Z}/2)^{14}$	$\mathbb{Z}^{117}$
$5+\zeta$	2480	160	$\mathbb{Z}^{160}$	
6	3240	180	?	

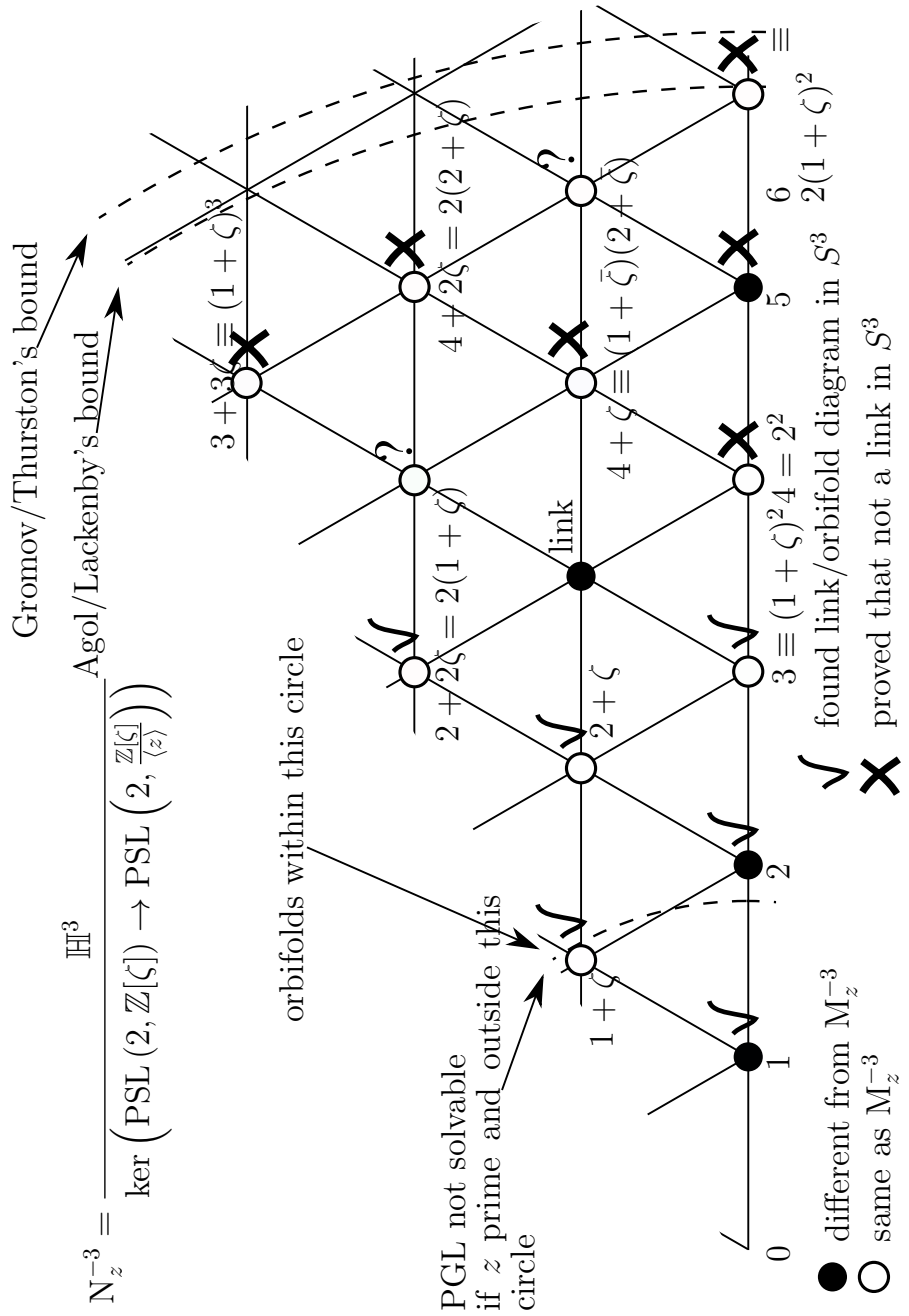

Figure 1.3: Principal congruence manifolds N_z^{-3} for $D = -3$.

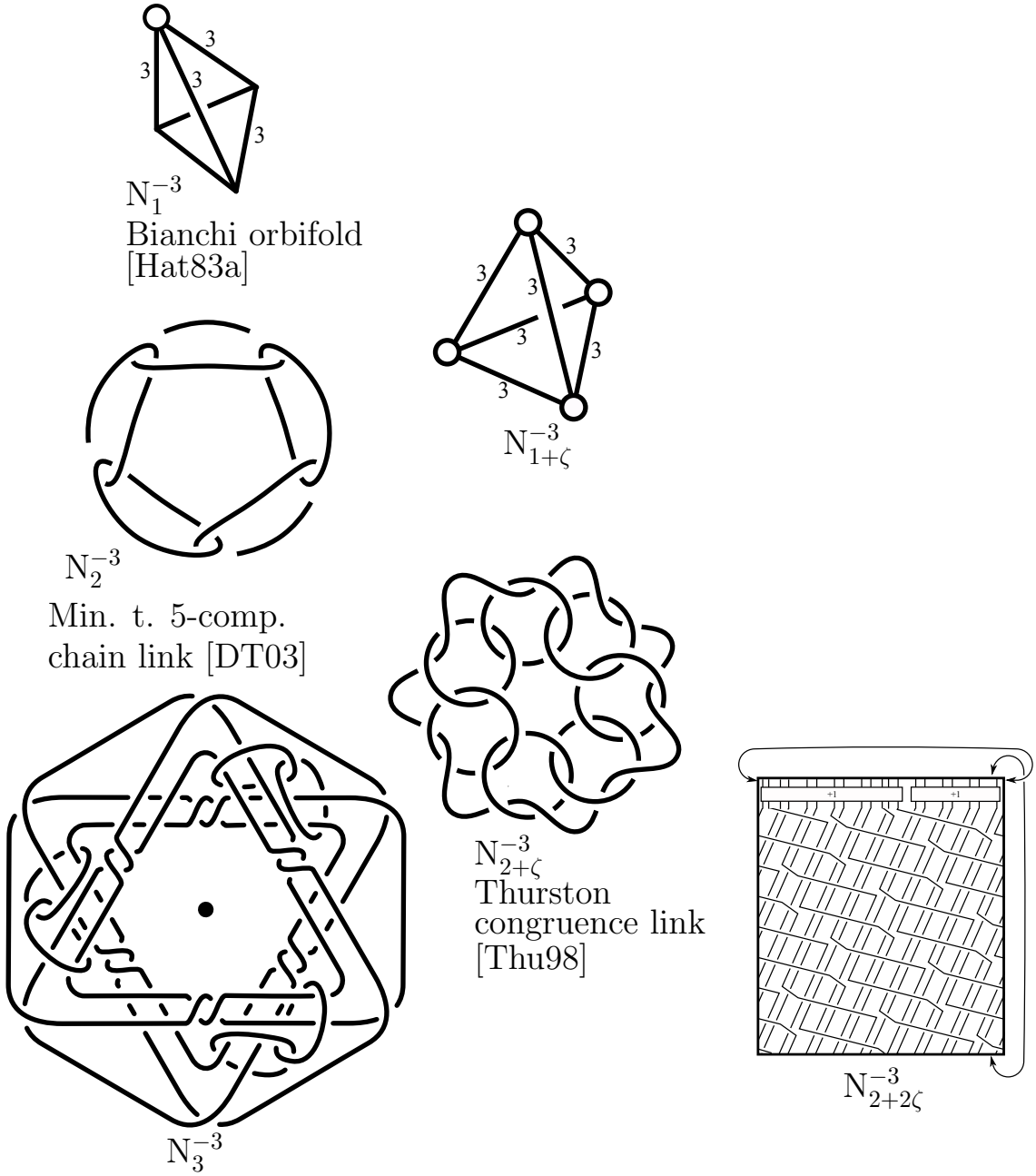

Figure 1.4: Known principal congruence orbifold diagrams and links for $D = -3$.

1.8 Congruence Orbifolds and Manifolds

We will construct congruence links through a sequence of covering spaces. We describe the intermediate covering spaces by subgroups G of $\mathrm{PGL}\left(2, \frac{\mathbb{Z}[\zeta]}{\langle z \rangle}\right)$ as follows: Let p denote the natural map $\mathrm{PGL}(2, \mathbb{Z}[\zeta]) \to \mathrm{PGL}\left(2, \frac{\mathbb{Z}[\zeta]}{\langle z \rangle}\right)$. Let $\Delta(z) = \ker(p)$. Now associate to G the orbifold $\mathrm{M}_z^{-3}(G)$ defined by

$$\begin{array}{ccc} \frac{\mathbb{H}^3}{p^{-1}(G)} & \xleftarrow[\mathrm{M}_z^{-3}(\_)]{} & G \end{array}$$

$$\begin{array}{ccc} p^{-1}(G) & \longrightarrow & G \\ \downarrow & & \downarrow \\ \mathrm{PGL}(2, \mathbb{Z}[\zeta]) & \xrightarrow[p]{} & \mathrm{PGL}\left(2, \frac{\mathbb{Z}[\zeta]}{\langle z \rangle}\right) \end{array}$$

Notice that $G \subset \mathrm{PGL}(2, \mathbb{Z}[\zeta]/\langle z \rangle)$ can be identified with a subgroup of deck transformations of M_z^{-3}. We have $\mathrm{M}_z^{-3}(G) \cong \frac{\mathrm{M}_z^{-3}}{G}$. The space $\mathrm{M}_z^{-3}(G)$ is called *congruence orbifold* respectively *congruence manifold*. If the discriminant D and the ideal $\langle z \rangle$ are clear from context, we abbreviate it by $[G]$.

The functor $[\_]$ is a category equivalence between subgroups of $\mathrm{Im}(p)$ and intermediate covering spaces between M_z^{-3} and the Bianchi orbifold M_1^{-3}. The functor maps an inclusion $G \subset H$ to a cover $[G] \to [H]$ whose holonomy $\pi_1^{orb}([H]) \cong p^{-1}(H) \to S_{H/G}$ is given by the action on the cosets H/G. In particular, it maps

- a normal subgroup $G \subset H$ to a regular cover $[G] \to [H]$ whose holonomy $\pi_1^{orb}([H]) \to p^{-1}(H) \to H/G$ is given by the action on the quotient group H/G.
- a p-cyclic extension $G \hookrightarrow H \to \mathbb{Z}/p$ to a p-cyclic cover.

Analogous constructions can be done for PSL.

Remark 1.8.1. It is still an open question whether there are infinitely many congruence links. Let

$$P = \left\{ P_x = \pm \begin{pmatrix} 1 & x \\ 0 & 1 \end{pmatrix} \right\}.$$

Consider the congruence orbifolds respectively manifolds $[P]$ and $\mathrm{N}_z^{-3}(P)$. When the horocusp from M_1^{-3} is lifted to these covering spaces, there is one cusp with cusp modulus 1,

Table 1.3: Homologies of the congruence manifolds $\mathrm{M}_z^{-3}(P)$.

z	Tetrahedra	cusps	H_1	Complement of Link
$3+\zeta$	7	2	$\mathbb{Z}/2 \oplus \mathbb{Z}^2$	No (but in $\mathbb{R}P^3$)
$3+2\zeta$	30	6	$\mathbb{Z}^6$	Yes
$3+3\zeta$	54	10	$\mathbb{Z}^{10}$	Yes
4	10	5	$\mathbb{Z}^5$	Yes
$4+\zeta$	16	4	$\mathbb{Z}/2 \oplus \mathbb{Z}^4$	No (but in $\mathbb{R}P^3$)
$4+2\zeta$	60	12	$\mathbb{Z}^{12}$	Yes
$4+3\zeta$	57	6	$\mathbb{Z}/2 \oplus \mathbb{Z}^6$	No
$4+4\zeta$	40	10	$\mathbb{Z}^{10}$	Yes
5	26	4	$(\mathbb{Z}/2)^2 \oplus \mathbb{Z}^4$	No
$5+\zeta$	80	10	$\mathbb{Z}^{10}$	Yes
$5+2\zeta$	56	8	$\mathbb{Z}/2 \oplus \mathbb{Z}^8$	No
6	90	16	$\mathbb{Z}^{16}$	Yes

hence the argument in Corollary 1.6.2 does not work, even if $|z| > 6$.
Table 1.3 lists the homologies for these spaces for small z and whether we could find Dehn fillings trivializing π_1 in SnapPy [CDW].

1.9 Orbifold Diagram Conventions

Dunbar [Dun88, Introduction] and Ratcliffe [Rat94, Chapter 13] summarize the definitions of orbifolds, respectively, the fundamental group of an orbifold, here denoted by $\pi_1^{orb}(M)$. For a hyperbolic 3-manifold $M \cong \frac{\mathbb{H}^3}{\Gamma}$, the orbifold fundamental group π_1^{orb} is isomorphic to Γ. A definition is also given in Section 2.3.3. We write $X(M)$ for the underlying topological space and $\Sigma(M)$ for the singular locus of an orbifold M. Here, we regard only oriented 3-orbifolds, hence $X(M)$ is an oriented 3-manifold and $\Sigma(M)$ a trivalent graph embedded in $X(M)$. Near $\Sigma(M)$, the orbifold is modeled on a quotient of $\mathbb{R}^3$ by a finite subgroup Γ of $\mathrm{SO}(3,\mathbb{R})$. The edges of the graph carry labels n indicating that Γ is a cyclic group C_n and the orbifold chart near that edge is an n-cyclic branched cover of $\mathbb{R}^3$. Near a vertex of $\Sigma(M)$, the group Γ is the orientation-preserving subgroup of a spherical triangle group (that is a Coxeter group with three generators), i.e., either a dihedral group D_n or the orientation-preserving symmetry group of a Platonic solid.
An orbifold can have cusps that are ends modeled on either $T^2 \times (0,1)$ or $S^2 \times (0,1)$ containing some edges of Σ_M modeled on lines $p \times (0,1)$.

Figure 1.5 shows the conventions used here for orbifold diagrams that are projections of $S^3 = \mathbb{R}^3 \cup \{\infty\}$ and that can contain cusps, singular locus, and Dehn surgeries. Notice that surgery coefficients always carry a sign to distinguish them from labels of edges of the singular locus. If a line segment of a diagram can only be part of the singular locus and does not carry a label, the order is implied to be 2. A knot carrying no label is denoting a cusp.

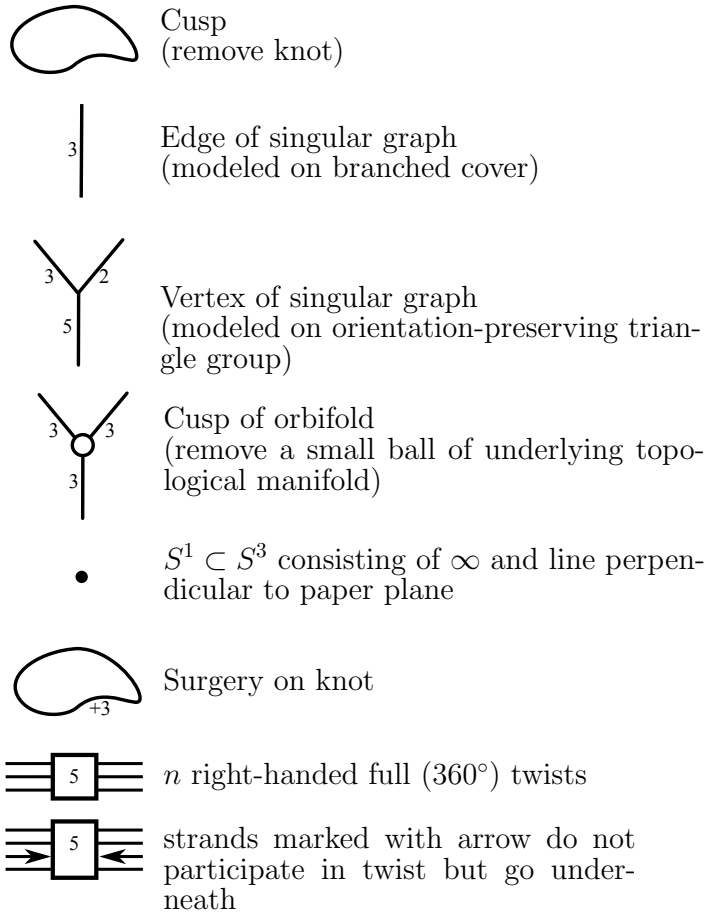

Figure 1.5: Conventions for orbifold diagrams.

1.10 Construction of Cyclic Branched Covers

We follow the construction of p-cyclic branched covers by Akbulut and Kirby [AK80]. Whereas [AK80] constructs covers of B^4 branched over a Seifert surface, we are only interested here in what happens on the 3-manifold boundary.

Since we need to lift the embedded singular graph, surgeries, and cusps of the orbifold diagram to the branched cover, we review the construction in [AK80] to give an explicit description of the diagram for the branched cover together with fundamental domains.

We start with an orbifold diagram $\mathcal{O}$ in S^3 and an oriented Seifert surface $F \subset S^3$ that is bounded by a link serving as branching locus for the p-fold branched cover $\widetilde{\mathcal{O}} \to \mathcal{O}$.

We take a handle decomposition of the Seifert surface F having only one 0-handle D. The 0-handle is drawn as half-disk with the 1-handles being drawn above D and attached to the straight top edge of D. See Figure 1.6.

First, thicken the Seifert surface F in S^3. Split the thickened Seifert surface $F \times I \subset S^3$ into $p-1$ layers $F \times I_1, \ldots, F \times I_{p-1}$ where I_j are subintervals forming the interval I. Each of these layers $F \times I_j$ together with the complement $S^3 \setminus (F \times I)$ will form one fundamental domain of the branched cover. The boundaries of these fundamental domains will be the preimages of F. To match the topology of the layers $F \times I_j$ with the complement $S^3 \setminus (F \times I)$, surgeries on each $F \times I_j$ are necessary. To finish the process, divide out the fibers of $\partial F \times I$. They will collapse to the branching locus.

For each layer $F \times I_j$, we now construct the surgeries: Move the cores of the 1-handles of F into the center $F \times p$ of the layer ($p \in I_j$). Take a copy of these cores and flip them along the top edge of $D \times p$ into $D \times I_j$. Connect the cores and their flipped copies to obtain a link in $F \times I_j$. The surgery coefficient for each component γ of the link is twice the number of twists of the corresponding 1-handle. Here, the 1-handle is said to have 0 twists if it lies in a Seifert surface for γ. "Thus the left handed trefoil knot in Figure 1.6 gives -3 full twists to that 1-handle; hence the -6 framing in the [...] cover" [AK80].

Remark: If the Seifert surface is bounded by a a/b surgery component of the link, then p has to divide a and the surgery becomes $a/(bp)$.

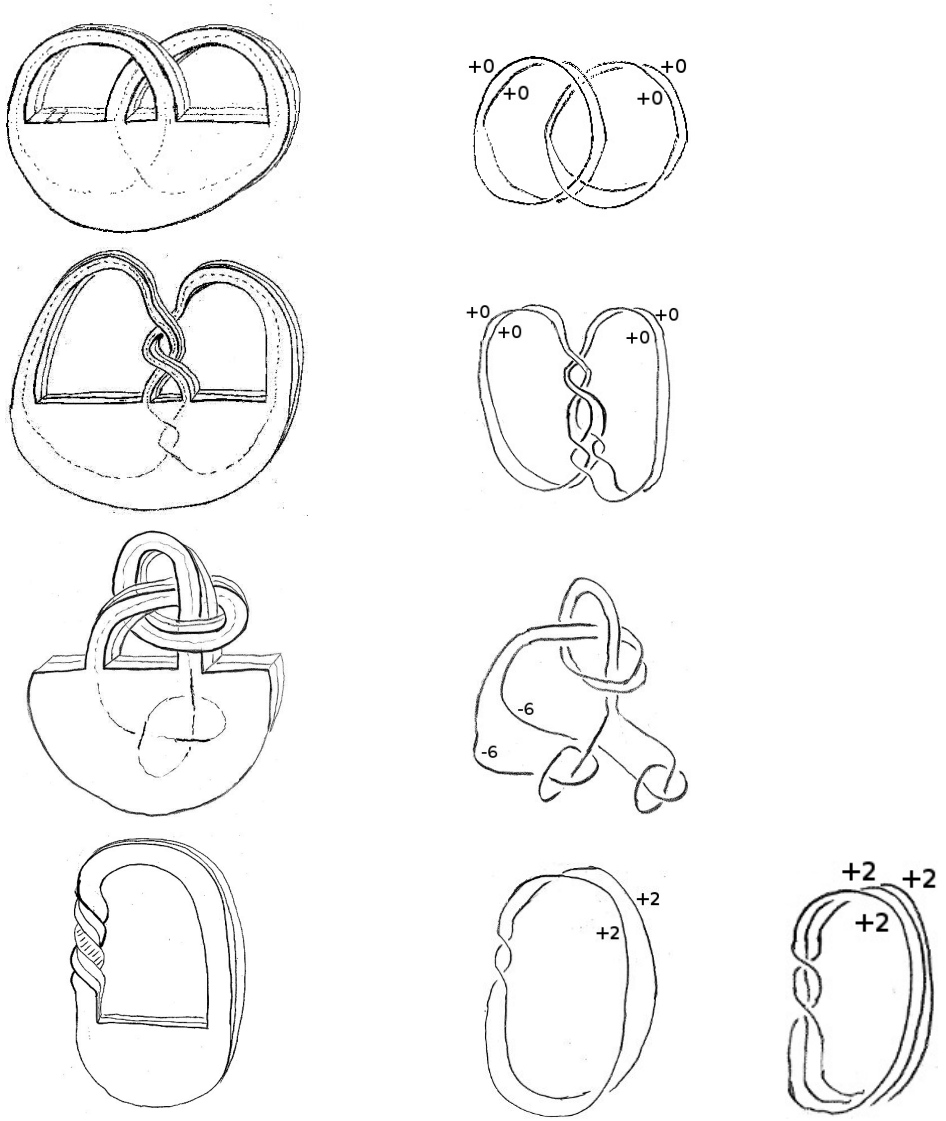

Thickened Seifert surface 3-cyclic 4-cyclic

Figure 1.6: Examples of constructing cyclic branched covers according to Akbulut and Kirby [AK80].

1.11 The Orbifold Cases for $D = -3$

Here, we describe the orbifolds $\mathrm{M}^{-3}_{1+\zeta}$ and M^{-3}_{2}. The Bianchi orbifold M^{-3}_{1} was already discussed in Section 1.4 with Figure 1.1 showing the orbifold diagram.

The subgroup of elements

$$\left[\begin{pmatrix} \zeta^k & x \\ 0 & 1 \end{pmatrix}\right] \in \ker(p)$$

fixing ∞ is generated by translations and the torsion elements

$$\begin{pmatrix} \zeta^2 & 0 \\ 0 & 1 \end{pmatrix} \quad \text{for} \quad z = 1+\zeta \quad \text{and} \quad \begin{pmatrix} -1 & 0 \\ 0 & 1 \end{pmatrix} \quad \text{for} \quad z = 2.$$

As described in Section 1.5, the topology of the cusps of $\mathrm{M}^{-3}_{1+\zeta} \cong \mathrm{N}^{-3}_{1+\zeta}$ and M^{-3}_{2} is an interval $\times$ sphere. As an orbifold, such a cusp is an interval $\times$ an orbifold $\mathcal{O}$ covering the $(2,3,6)$-triangle group. In the two cases $z = 1+\zeta$ and $z = 2$, the orbifold $\mathcal{O}$ can be triangulated by equilateral Euclidean triangles such that singular points are the vertices. Hence, the orbifolds $\mathrm{M}^{-3}_{1+\zeta}$ and M^{-3}_{2} are triangulated by regular ideal hyperbolic tetrahedra with the singular locus formed by the edges.

For $\mathrm{M}^{-3}_{1+\zeta}$, the cusp structure $\mathcal{O}$ is the (3,3,3)-triangle orbifold divided into two Euclidean equilateral triangles belonging to the two tetrahedra meeting at a cusp. For M^{-3}_{2}, the triangulation of the $\mathcal{O}$ is the boundary of a tetrahedron with each vertex being an order two cone point. We can construct triangulations by gluing tetrahedra such as to enforce these cusp structures and obtain the universal regular cover with fixed cusp structure (see Section 1.15.1 with the torsion elements as additional generators). These triangulations have two, respectively, five regular ideal tetrahedra and topologically form punctured S^3. The latter triangulation is also the boundary of a 4-simplex. The orbifold diagrams for $\mathrm{M}^{-3}_{1+\zeta}$ and M^{-3}_{2} are shown in Figure 1.4. The latter diagram is called the Pentacle and is taken from [DT03].

To check that the orbifolds we constructed are indeed $\mathrm{M}^{-3}_{1+\zeta}$ and M^{-3}_{2}, we can compute their degrees as orbifold covers of M^{-3}_{1}: the group of the deck transformations of $\mathrm{M}^{-3}_{1+\zeta}$ is $\mathrm{PGL}(2, \mathbb{Z}[\zeta]/\langle 1+\zeta \rangle)$ and its order is $24 = 2 \cdot 12$. Similarly $\mathrm{PGL}(2, \mathbb{Z}[\zeta]/\langle 2 \rangle)$ has order $60 = 5 \cdot 12$.

1.12 Construction of M_3^{-3}

The manifold M_3^{-3} has a triangulation consisting of 54 regular ideal hyperbolic tetrahedra such that 18 form one of 12 cusps of the manifold.

Theorem 1.12.1. *The complement of the top link in Figure 1.7 is* M_3^{-3}.

Proof. We will construct the link in five steps through the covering spaces $\widetilde{\mathrm{M}}^{\mathrm{I}}_{1+\zeta}$, $\widetilde{\mathrm{M}}^{\mathrm{II}}_{1+\zeta}$, $\widetilde{\mathrm{M}}^{\mathrm{III}}_{1+\zeta}$, and $\widetilde{\mathrm{M}}^{\mathrm{IV}}_{1+\zeta}$ of the orbifold $\mathrm{M}^{-3}_{1+\zeta}$ as shown in Figure 1.7. At each step, we will show that the covering space is an Abelian cover of $\mathrm{M}^{-3}_{1+\zeta}$. By lemma 1.12.2, the manifold M_3^{-3} must be a 3-cyclic cover of $\widetilde{\mathrm{M}}^{\mathrm{IV}}_{1+\zeta}$. There is a unique 3-cyclic cover of $\widetilde{\mathrm{M}}^{\mathrm{IV}}_{1+\zeta}$ such that the sizes of the cusp matches with those of M_3^{-3}. Hence this unique 3-cyclic cover has to be M_3^{-3}. □

Notice that $\Delta(3)$ (see Section 1.8) is a normal subgroup of $\Delta(1+\zeta)$, hence the manifold M_3^{-3} is a regular cover of $\mathrm{M}^{-3}_{1+\zeta}$ with holonomy given by

$$\pi_1^{orb}\left(\mathrm{M}^{-3}_{1+\zeta}\right) \twoheadrightarrow G := \frac{\Delta(1+\zeta)}{\Delta(3)} \cong \ker\left(\mathrm{PGL}\left(2, \frac{\mathbb{Z}[\zeta]}{\langle 3\rangle}\right) \to \mathrm{PGL}\left(2, \frac{\mathbb{Z}[\zeta]}{\langle 1+\zeta\rangle}\right)\right).$$

The orbifold diagram for $\mathrm{M}^{-3}_{1+\zeta}$ is shown in Figure 1.7 and serves as starting point for the construction of a link for M_3^{-3}. The group G is $(\mathbb{Z}/3)^3$ by Lemma 1.3.6.

Lemma 1.12.2. *The manifold* M_3^{-3} *is the universal Abelian cover of* $\mathrm{M}^{-3}_{1+\zeta}$.

Proof. The complement of the singular locus $X(\mathrm{M}^{-3}_{1+\zeta})\backslash\Sigma(\mathrm{M}^{-3}_{1+\zeta})$ is a genus 3 handlebody. We can pick three loops around $\Sigma(\mathrm{M}^{-3}_{1+\zeta})$ generating its fundamental group and becoming order 3 elements under the map $\pi_1(X(\mathrm{M}^{-3}_{1+\zeta}) \setminus \Sigma(\mathrm{M}^{-3}_{1+\zeta})) \to \pi_1^{orb}(\mathrm{M}^{-3}_{1+\zeta})$. Hence, the Abelianization $\pi_1^{orb}(\mathrm{M}^{-3}_{1+\zeta})^{ab}$ is a quotient of $\left(\frac{\mathbb{Z}}{3}\right)^3$ and G being Abelian is a quotient of $\pi_1^{orb}(\mathrm{M}^{-3}_{1+\zeta})^{ab}$. So $\pi_1^{orb}\left(\mathrm{M}^{-3}_{1+\zeta}\right) \cong G$. □

This suggests that M_3^{-3} can be obtained by consecutively constructing three cyclic branched covers. However, after two such steps motivated by the elimination of singular locus, the remaining singular locus in $\widetilde{\mathrm{M}}^{\mathrm{II}}_{1+\zeta}$ is too complicated to proceed directly. If we divide the diagram by the C_3 symmetry, we can use previous techniques again and undo the division by constructing an appropriate cover in the last step.

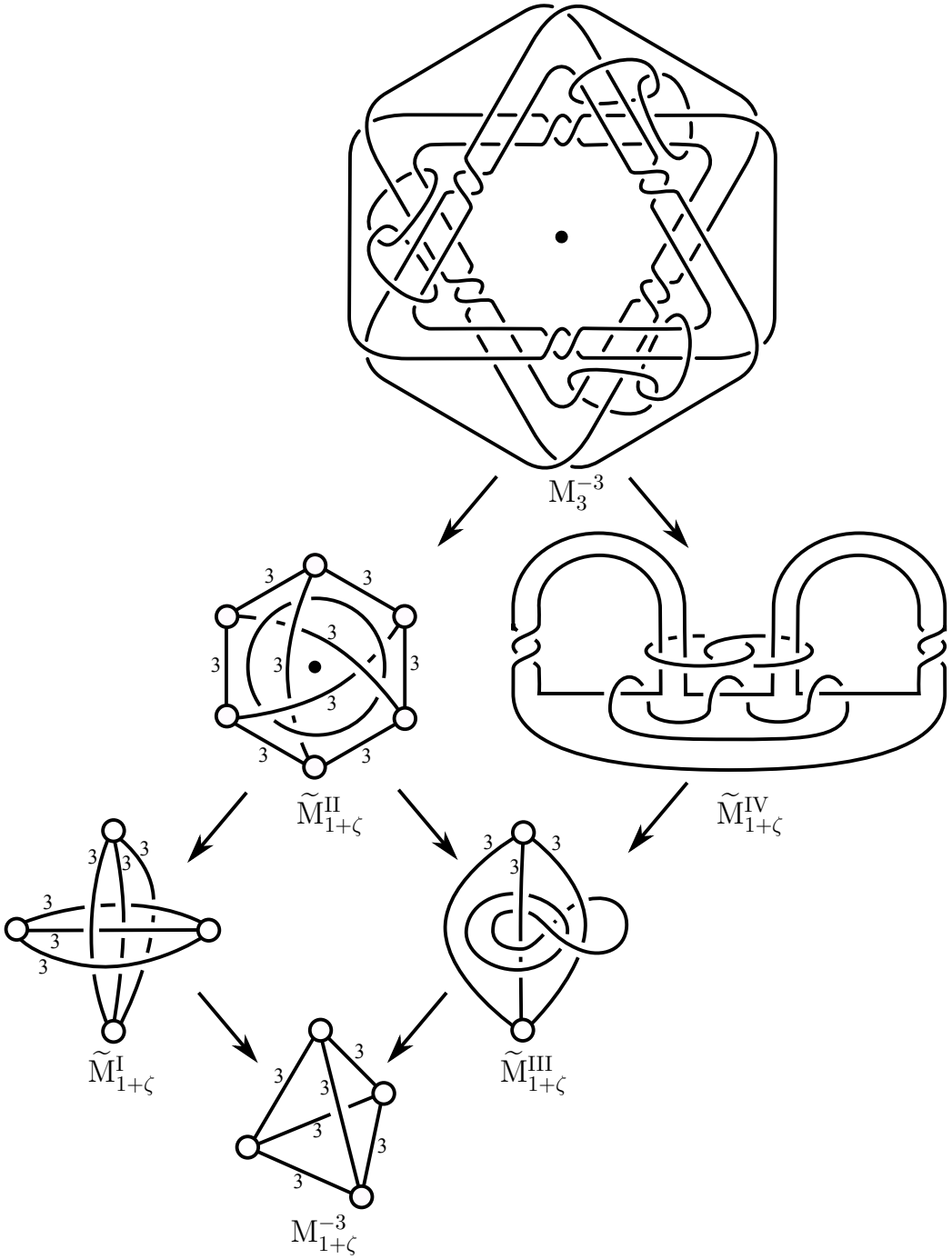

Figure 1.7: Abelian covers of the Bianchi orbifold for $\mathcal{O}_{-3}$ involved in the construction of M_3^{-3}. Each arrow is a 3-cyclic cover.

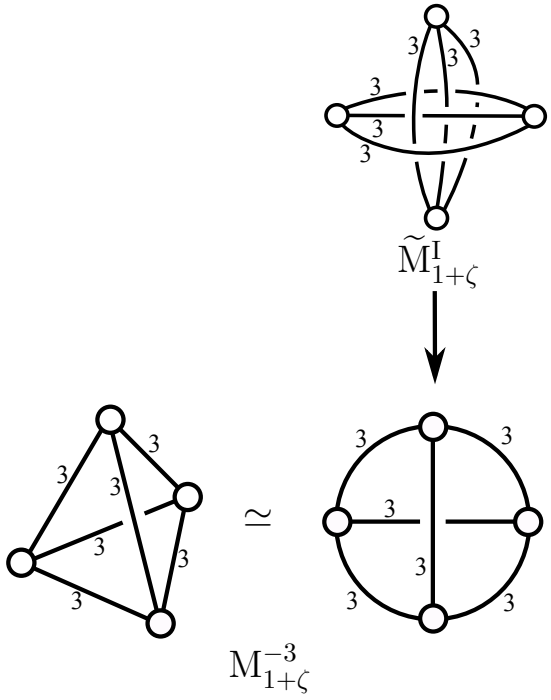

Figure 1.8: Construction of $\widetilde{\mathrm{M}}^{\mathrm{I}}_{1+\zeta}$.

1.12.1 Construction of $\widetilde{\mathrm{M}}^{\mathrm{I}}_{1+\zeta}$

The construction of the 3-cyclic cover $\widetilde{\mathrm{M}}^{\mathrm{I}}_{1+\zeta} \to \mathrm{M}^{-3}_{1+\zeta}$ is shown in Figure 1.8. Pick four edges of the singular locus of $\mathrm{M}^{-3}_{1+\zeta}$ that form an unknot spanning a disk. For the projection of $\mathrm{M}^{-3}_{1+\zeta}$ shown on the left in Figure 1.8, this disk is shown in [Thu86, Figure 3.3]. Here, we use the projection shown on the right in Figure 1.8 and pick the four outer edges.
This disk serves as a Seifert surface for constructing the 3-cyclic cover according to Akbulut and Kirby [AK80]. In other words, cut S^3 along this disk to obtain a ball B^3 and glue three copies of B^3 together. The four edges of the singular locus become regular and disappear in the branched cover.

Notice that the deck transformations of $\widetilde{\mathrm{M}}^{\mathrm{I}}_{1+\zeta}$ act by cyclic permutations of the edges of each connected components of the singular locus.

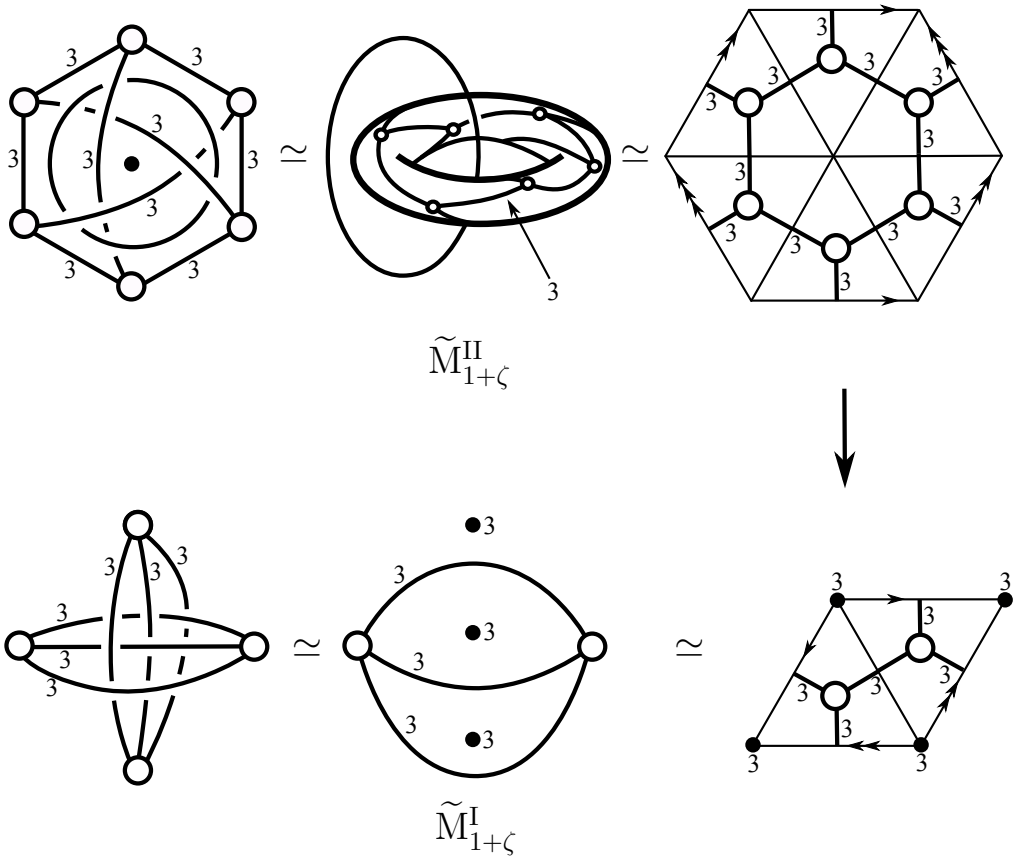

Figure 1.9: Construction of $\widetilde{\mathrm{M}}^{\mathrm{II}}_{1+\zeta}$.

1.12.2 Construction of $\widetilde{\mathrm{M}}^{\mathrm{II}}_{1+\zeta}$

The construction of the 3-cyclic cover $\widetilde{\mathrm{M}}^{\mathrm{II}}_{1+\zeta} \to \widetilde{\mathrm{M}}^{\mathrm{I}}_{1+\zeta}$ is shown in Figure 1.9. Ignoring one of the connected components of the singular locus, the orbifold $\widetilde{\mathrm{M}}^{\mathrm{I}}_{1+\zeta}$ is the product $\mathcal{O} \times (0,1)$ where $\mathcal{O}$ is the Euclidean 2-orbifold $(3,3,3)$ with underlying topological space $X(\mathcal{O}) = S^2$. The middle picture in Figure 1.9 shows a projection of $\widetilde{\mathrm{M}}^{\mathrm{I}}_{1+\zeta}$ with two cusps being at infinity, thus revealing the structure of $\mathcal{O}$ and showing how the other connected component of the singular locus embeds. The right picture displays a fundamental domain of $\mathcal{O}$. The 3-cyclic cover of $\mathcal{O}$ is a torus T^2 and its fundamental domain appears in the picture above. We project the fundamental domain onto the torus T^2 in the Hopf link complement $T^2 \times (0,1)$. The left picture shows a different projection of $\widetilde{\mathrm{M}}^{\mathrm{II}}_{1+\zeta}$.

Lemma 1.12.3. *The covering space* $\widetilde{\mathrm{M}}^{\mathrm{II}}_{1+\zeta} \to \mathrm{M}^{-3}_{1+\zeta}$ *is Abelian.*

Proof. More generally, let $A \to B \to C$ be a sequence of consecutive Abelian covering spaces. The orbifold fundamental group $\pi_1^{orb}(C)$ acts on B by deck transformations, hence it acts on the Abelianization of the orbifold fundamental group $\pi_1^{orb}(B)^{ab}$. The cover $A \to C$ is Abelian if and only if the holonomy $\pi_1^{orb}(B) \to H$ corresponding to the cover $A \to B$ stays invariant under this action.

For $\widetilde{\mathrm{M}}^{\mathrm{I}}_{1+\zeta}$, look at the small loops winding once around an edge of a fixed component of the singular locus in the same orientation. The holonomy of $\widetilde{\mathrm{M}}^{\mathrm{II}}_{1+\zeta} \to \widetilde{\mathrm{M}}^{\mathrm{I}}_{1+\zeta}$ is uniquely determined by sending each such loop to $1 \in \mathbb{Z}/3$ and other generators to zero. The deck transformations of $\widetilde{\mathrm{M}}^{\mathrm{I}}_{1+\zeta} \to \mathrm{M}^{-3}_{1+\zeta}$ leave this holonomy invariant. □

Look at the top right hexagon in Figure 1.9 which becomes the torus T^2. The deck transformation group of $\widetilde{\mathrm{M}}^{\mathrm{II}}_{1+\zeta} \to \mathrm{M}^{-3}_{1+\zeta}$ is the direct sum of deck transformations of $\widetilde{\mathrm{M}}^{\mathrm{I}}_{1+\zeta} \to \mathrm{M}^{-3}_{1+\zeta}$ and deck transformations of $\widetilde{\mathrm{M}}^{\mathrm{II}}_{1+\zeta} \to \widetilde{\mathrm{M}}^{\mathrm{I}}_{1+\zeta}$. The first acts by rotating T^2 by $2/3\pi$ about a vertex of the singular locus. The second acts by rotating T^2 by $2/3\pi$ about the center of the hexagon. Together, they form a translation of T^2 as deck transformation.

The deck transformation group is $\left(\frac{\mathbb{Z}}{3}\right)^2$.

1.12.3 Construction of $\widetilde{\mathrm{M}}^{\mathrm{III}}_{1+\zeta}$

Dividing $\widetilde{\mathrm{M}}^{\mathrm{II}}_{1+\zeta}$ by the C_3 symmetry displayed in Figure 1.7 yields the orbifold $\widetilde{\mathrm{M}}^{\mathrm{III}}_{1+\zeta}$. This C_3 symmetry corresponds to deck transformations by translations of T^2 as described in the previous Section. These deck transformations have to form a normal subgroup since $\widetilde{\mathrm{M}}^{\mathrm{II}}_{1+\zeta} \to \mathrm{M}^{-3}_{1+\zeta}$ is Abelian. Hence, the cover $\widetilde{\mathrm{M}}^{\mathrm{III}}_{1+\zeta} \to \mathrm{M}^{-3}_{1+\zeta}$ is 3-cyclic.

Recall that there is another subgroup of deck transformations of $\widetilde{\mathrm{M}}^{\mathrm{II}}_{1+\zeta} \to \mathrm{M}^{-3}_{1+\zeta}$ generated by a rotation of T^2 by $2/3\pi$ about a vertex of the singular locus. This subgroup commutes with C_3 and descends to the deck transformations of $\widetilde{\mathrm{M}}^{\mathrm{III}}_{1+\zeta} \to \mathrm{M}^{-3}_{1+\zeta}$. On $\widetilde{\mathrm{M}}^{\mathrm{III}}_{1+\zeta}$, these deck transformations act by 3-cyclically permuting the edges of the singular graph.

1.12.4 Construction of $\widetilde{\mathrm{M}}^{\mathrm{IV}}_{1+\zeta}$

The construction of the 3-cyclic cover $\widetilde{\mathrm{M}}^{\mathrm{IV}}_{1+\zeta} \to \widetilde{\mathrm{M}}^{\mathrm{III}}_{1+\zeta}$ is shown in Figure 1.10 and follows the same idea of unfolding the Euclidean orbifold $\mathcal{O}$ in Section 1.12.2 for the 3-cyclic cover $\widetilde{\mathrm{M}}^{\mathrm{II}}_{1+\zeta} \to \widetilde{\mathrm{M}}^{\mathrm{I}}_{1+\zeta}$. The top right picture in Figure 1.10 shows a projection of $\widetilde{\mathrm{M}}^{\mathrm{IV}}_{1+\zeta}$ revealing the torus T^2 inside the Hopf link complement that is formed by the components bl and br. The top left picture in Figure 1.10 shows a projection of the same link revealing the Seifert

surface that is bounded by the components al, ac, and ar and that is needed in the next step of the construction. Figure 1.11 illustrates the isotopy between the two projections of $\widetilde{\mathrm{M}}^{\mathrm{IV}}_{1+\zeta}$.

By the same argument as used in Lemma 1.12.3, the cover $\widetilde{\mathrm{M}}^{\mathrm{IV}}_{1+\zeta} \to \mathrm{M}^{-3}_{1+\zeta}$ is Abelian.

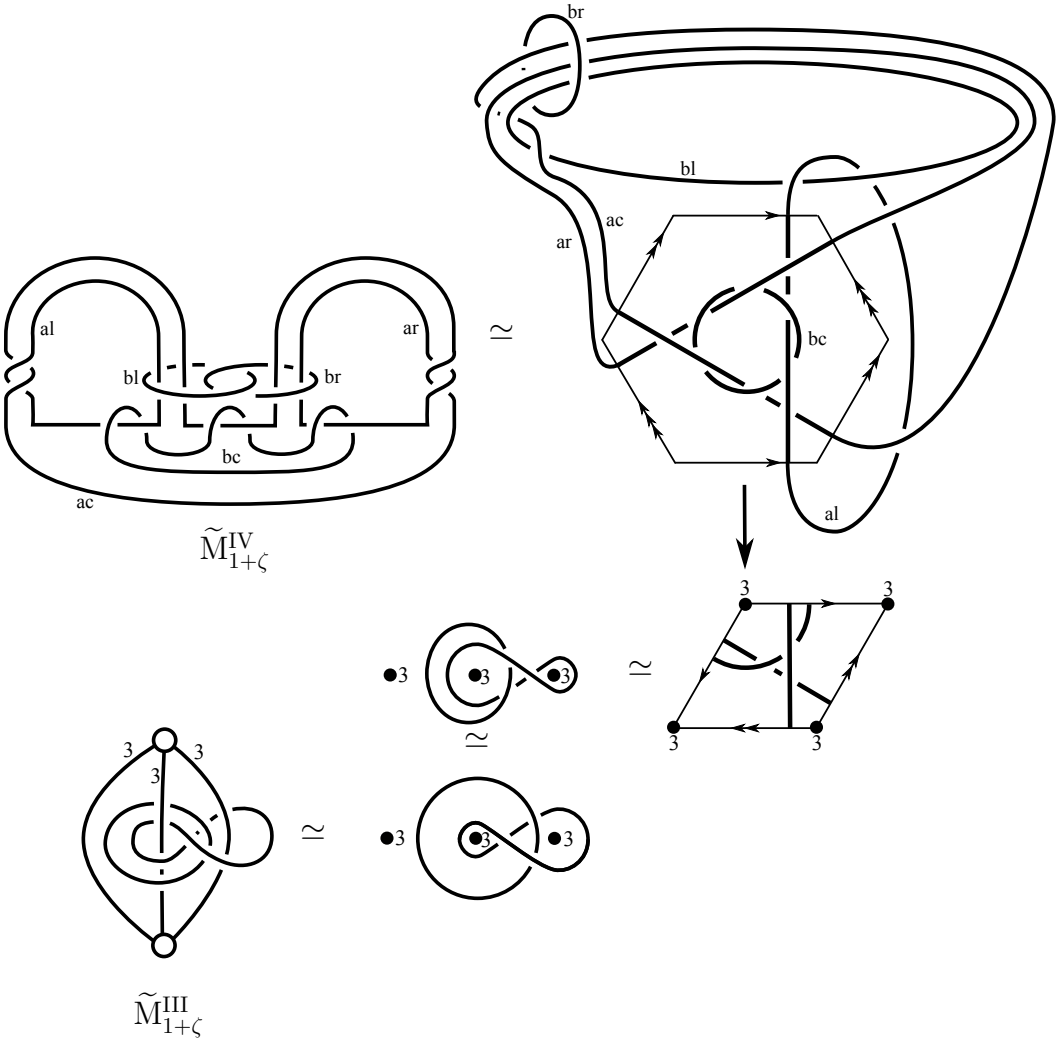

Figure 1.10: Construction of $\widetilde{\mathrm{M}}^{\mathrm{IV}}_{1+\zeta}$.

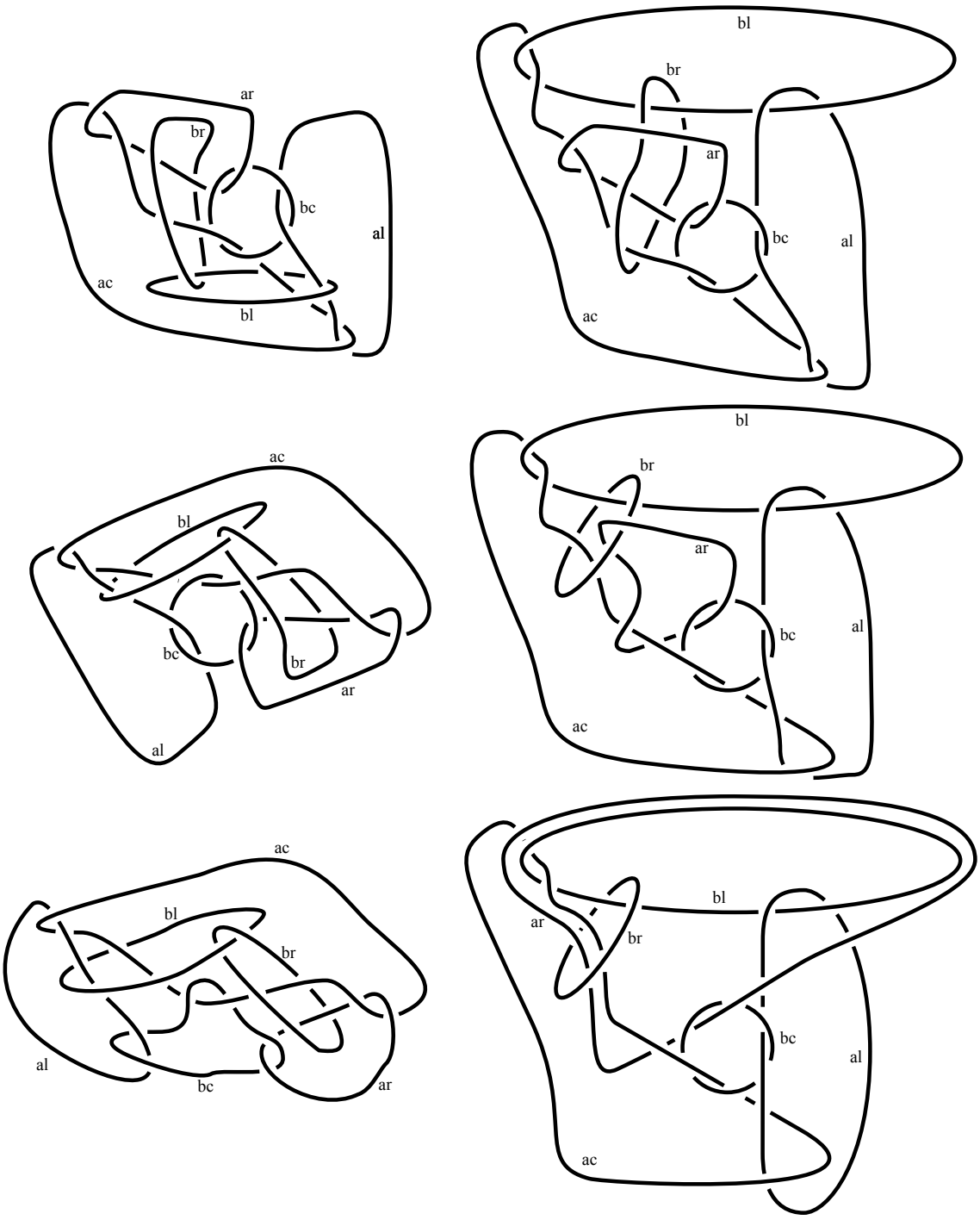

Figure 1.11: Different projections of $\widetilde{\mathrm{M}}^{\mathrm{IV}}_{1+\zeta}$ arranged counter-clockwise starting from bottom right. The last two projections are homeomorphic to the one revealing the Seifert surface.

1.12.5 Construction of M_3^{-3}

Determination of the Seifert surface

To construct the last 3-cyclic branched cover $\mathrm{M}_3^{-3} \to \widetilde{\mathrm{M}}^{\mathrm{IV}}_{1+\zeta}$, we need to determine the right holonomy $\pi_1\left(\widetilde{\mathrm{M}}^{\mathrm{IV}}_{1+\zeta}\right) \to \mathbb{Z}/3$ and then find a suitable Seifert surface in $\widetilde{\mathrm{M}}^{\mathrm{IV}}_{1+\zeta}$ for the construction of the cyclic cover according to Akbulut and Kirby [AK80]. Notice that the holonomy factors through $H_1\left(\widetilde{\mathrm{M}}^{\mathrm{IV}}_{1+\zeta}\right)$ which is generated by meridians.

We trace the number of tetrahedra that meet at each cusp when triangulating the orbifolds by regular ideal tetrahedra. For example, this number is 2 for the cusps in $\mathrm{M}^{-3}_{1+\zeta}$ and 6 for $\widetilde{\mathrm{M}}^{\mathrm{I}}_{1+\zeta}$. For $\widetilde{\mathrm{M}}^{\mathrm{IV}}_{1+\zeta}$, this number is 6 for the cusps al, ac, and ar, and 18 for the cusps bl, bc, and br (see Figure 1.10). Hence the link components al, ac, and ar have to serve as branching locus for the cyclic cover. Each of the other cusps bl, bc, and br has to lift to three copies in the covering space, hence their meridians and longitudes are zero under the holonomy $H_1\left(\widetilde{\mathrm{M}}^{\mathrm{IV}}_{1+\zeta}\right) \to \mathbb{Z}/3$. This determines the holonomy uniquely. A Seifert surface realizing that holonomy is shown in Figure 1.10, as can be easily checked by noticing that each bl, bc, and br intersects the surface a multiple of 3 times.

Construction of the Cyclic Cover

Figure 1.12 shows the construction of the 3-cyclic cover according to Akbulut and Kirby [AK80] and as described in Section 1.10. The components bl, bc, and br are drawn to lie just in front of the Seifert surface with small circles around the branched locus such that their lifts to the branched cover are easier to visualize.

We perform Rolfsen twists (see [Rol90, Chapter 9.H] or [GS99, Chapter 5.3]) and blow-downs (see [GS99, Chapter 5.1]) to eliminate the surgeries. Figure 1.13 shows the results of the first Rolfsen twists about al respectively ar. Figure 1.14 shows the result of the blow-downs about each of the unknots with +1 surgery coefficient. The resulting link is shown in its entirety in Figure 1.15. A projection revealing the D_6 symmetry of the link is shown in Figure 1.7.

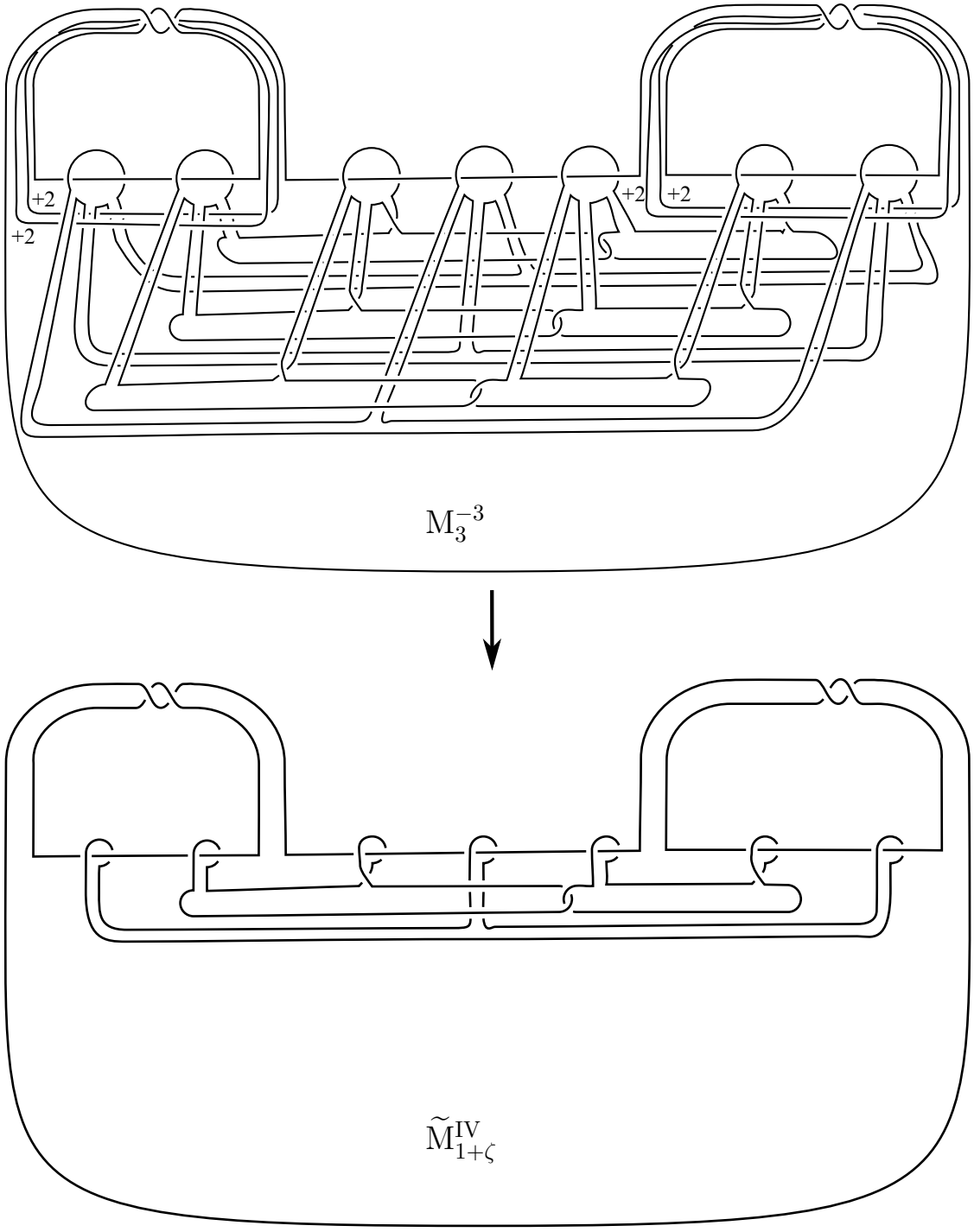

Figure 1.12: Construction of 3-cyclic branched cover $M_3^{-3} \to \widetilde{M}^{IV}_{1+\zeta}$. The resulting link diagram of M_3^{-3} has four $+2$ surgeries.

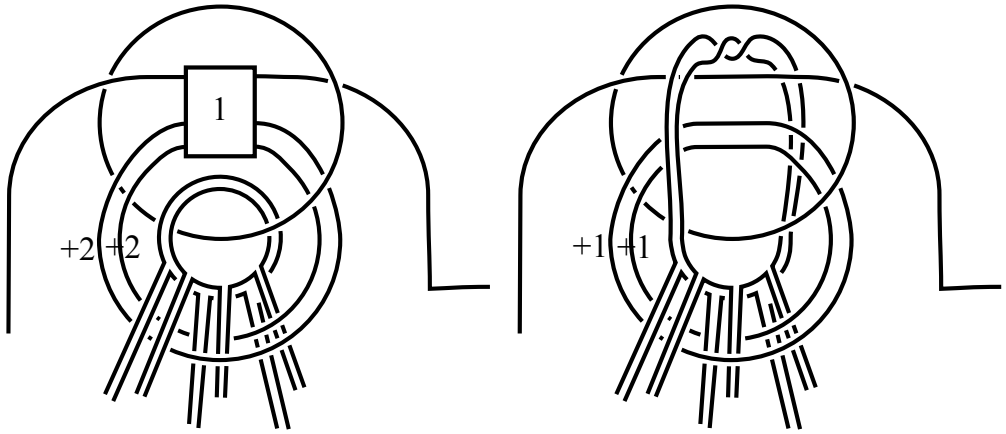

Figure 1.13: Rolfsen twist on the link for M_3^{-3} about al respectively ar resulting in +1 surgeries.

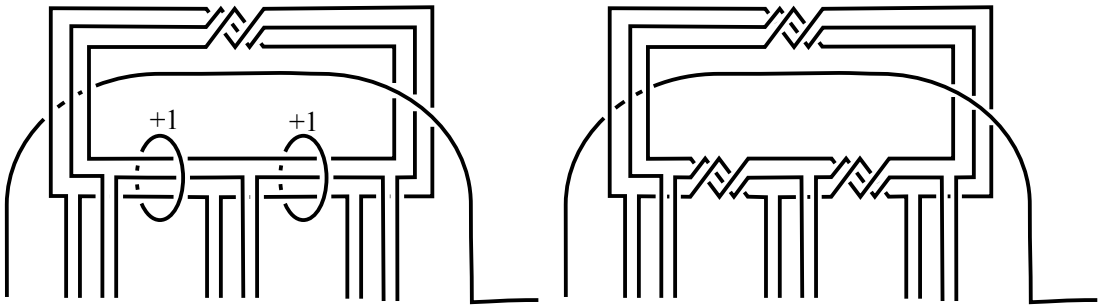

Figure 1.14: Blow-downs on the link for M_3^{-3} about the +1 surgery unknots eliminating the surgeries.

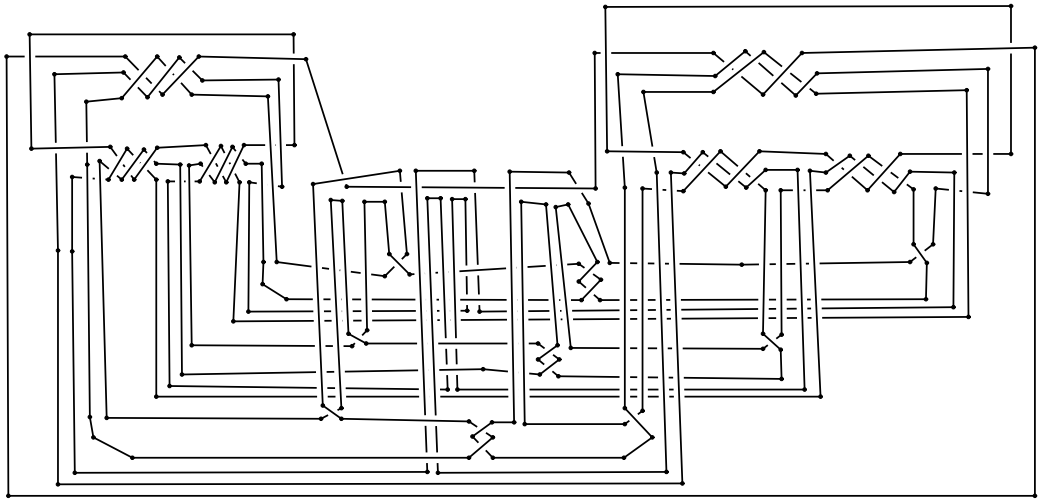

Figure 1.15: The link for M_3^{-3}.

1.13 Construction of $\mathrm{M}^{-3}_{2+2\zeta}$

The manifold $\mathrm{M}^{-3}_{2+2\zeta}$ has a triangulation consisting of 120 regular ideal hyperbolic tetrahedra such that 24 form one of 20 cusps of the manifold.

Theorem 1.13.1. *The complements of the link in $\mathbb{R}P^3$ in Figure 1.26 respectively in S^3 in Figure 1.27 are $\mathrm{M}^{-3}_{2+2\zeta}$.*

Proof. Following the notation in Section 1.8, we will construct the links through a sequence of cyclic covers starting with $[A_4 \times 1]$ as shown in Figure 1.16. We will prove the correctness of each step in a way that can be checked by hand. □

Recall the following identities [CM80]:

- $A_4 \cong \mathrm{PSL}(2,3) \cong \mathrm{PSL}(2, \mathbb{Z}[\zeta]/\langle 1+\zeta \rangle)$
- $S_4 \cong \mathrm{PGL}(2,3) \cong \mathrm{PGL}(2, \mathbb{Z}[\zeta]/\langle 1+\zeta \rangle)$
- $A_5 \cong \mathrm{PSL}(2,4) \cong \mathrm{SL}(2,4) \cong \mathrm{PGL}(2,4) \cong \mathrm{PGL}(2, \mathbb{Z}[\zeta]/\langle 2 \rangle)$
- $S_5 \cong \mathrm{PGL}(2,5)$

Using Lemma 1.3.3 and 1.3.15, notice that the symmetry group of $\mathrm{M}^{-3}_{2+2\zeta}$ factors as

$$\mathrm{PGL}\left(2, \frac{\mathbb{Z}[\zeta]}{\langle 2+2\zeta \rangle}\right) \cong \mathrm{PGL}\left(2, \frac{\mathbb{Z}[\zeta]}{\langle 1+\zeta \rangle}\right) \times \mathrm{PGL}\left(2, \frac{\mathbb{Z}[\zeta]}{\langle 2 \rangle}\right) \cong S_4 \times A_5.$$

We already have orbifold diagrams for (notation $[G]$ as defined in Section 1.8)

$$\mathrm{M}^{-3}_2 \cong [S_4 \times 1] \quad \text{and} \quad \mathrm{M}^{-3}_{1+\zeta} \cong [1 \times A_5]\,.$$

Since A_5 is not solvable, $\mathrm{M}^{-3}_{2+2\zeta}$ cannot be constructed as series of cyclic covers of $\mathrm{M}^{-3}_{1+\zeta}$. However, the group S_4 is solvable, hence we start our construction of a link for $\mathrm{M}^{-3}_{2+2\zeta}$ with M^{-3}_2. Recall that a solution of S_4 is given by $[S_4, S_4] = A_4$ and $[A_4, A_4] = \langle (12)(34), (13)(24) \rangle \cong (\mathbb{Z}/2)^2$ which is Abelian, namely the Klein four group.

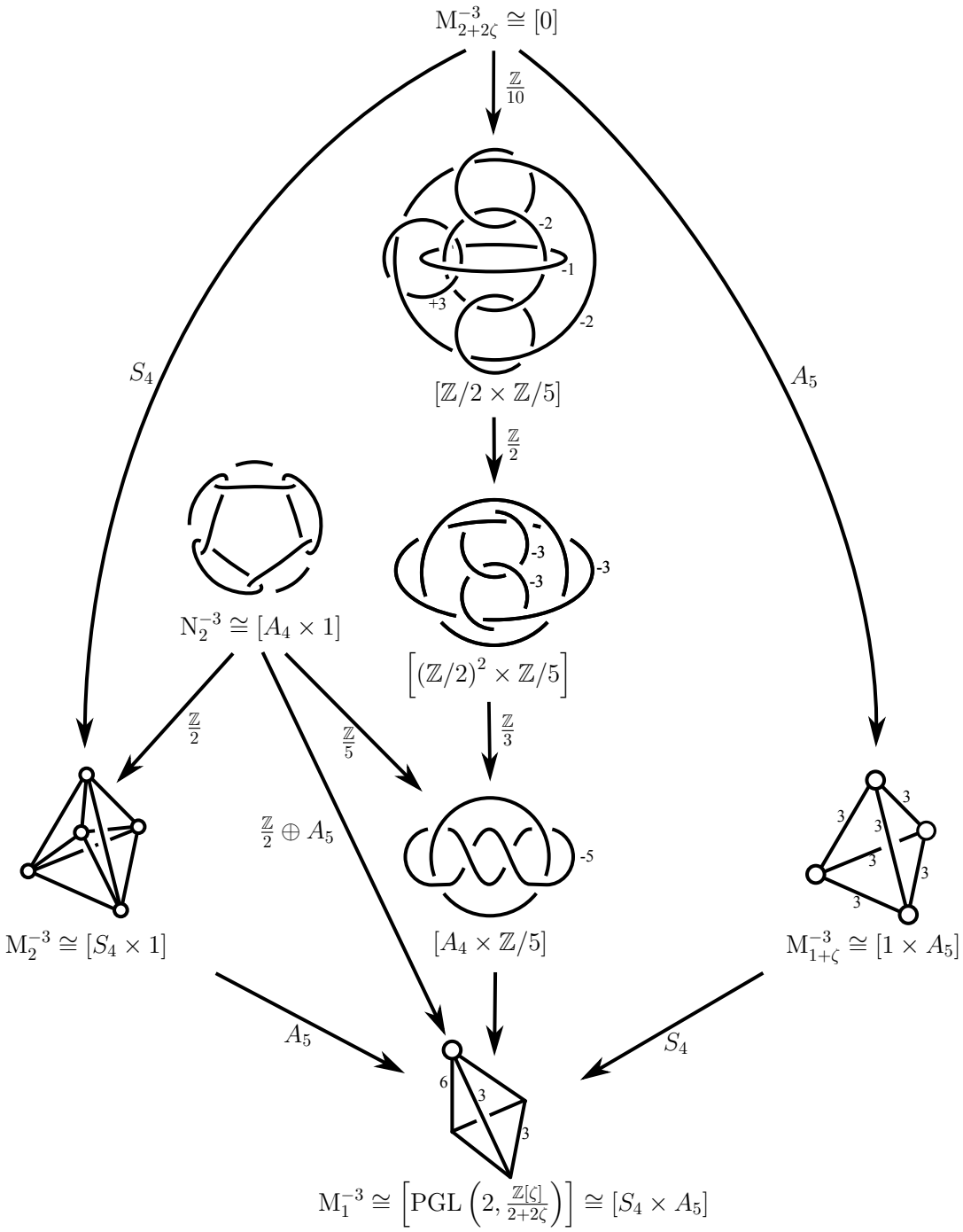

Figure 1.16: Covers of the Bianchi orbifold for $\mathcal{O}_{-3}$ involved in the construction of $\mathrm{M}^{-3}_{2+2\zeta}$. An arrow indicates a regular cover if and only if it is labeled by the group of deck transformations.

Lemma 1.13.2. *Let M be a 3-manifold with r cusps such that the free part of*

$$H_1(M) \cong \mathbb{Z}^r \times \left(\frac{\mathbb{Z}}{p}\right)^k \times \textit{non-}p\textit{ torsion}$$

is generated by peripheral curves of the cusps. Then connected p-cyclic covering spaces with rp cusps are in 1-1 correspondence to maps $\left(\frac{\mathbb{Z}}{p}\right)^k \to \frac{\mathbb{Z}}{p}$ up to isomorphisms of $\frac{\mathbb{Z}}{p}$. In particular, such a covering space is unique if $k = 1$. If p is prime, there are $\frac{p^k-1}{p-1}$ such covering spaces.

Proof. The holonomy $\pi_1(M) \to \frac{\mathbb{Z}}{p}$ factors through $H_1(M)$. Since each cusp has to lift to p copies, the free part is sent to zero. □

1.13.1 Construction of $[A_4 \times 1] \cong \mathrm{N}_2^{-3}$

The orbifold M_2^{-3} is the pentacle as described in [DT03] and shown in Figure 1.16. A triangulation of M_2^{-3} by regular ideal tetrahedra is given by the boundary of a 4-simplex. Each edge is singular locus of order 2.

Lemma 1.13.3. *The quotient $[A_4 \times 1]$ is a manifold.*

Proof. By definition

$$[A_4 \times 1] \cong [[S_4; S_4] \times 1] \cong \frac{\mathbb{H}^3}{\Gamma}$$

where

$$\Gamma = \left[p^{-1}\left(S_4 \times 1\right), p^{-1}\left(S_4 \times 1\right)\right] = [\Delta(2), \Delta(2)] = \ker\left(\mathrm{PSL}\left(2, \mathbb{Z}[\zeta]\right) \to \mathrm{PSL}\left(2, \frac{\mathbb{Z}[\zeta]}{\langle 2\rangle}\right)\right).$$

The group Γ misses the involution $\begin{pmatrix} 1 & 0 \\ 0 & -1 \end{pmatrix}$ that caused the singular locus of the pentacle $[S_4 \times 1] \cong \mathrm{M}_2^{-3}$. Furthermore Γ is normal in $\mathrm{PGL}(2, \mathbb{Z}[\zeta])$, hence all singular locus of the pentacle will disappear and $[A_4 \times 1]$ is a manifold. □

Lemma 1.13.4. M_2^{-3} *has a unique manifold double cover.*

Proof. Small loops γ winding once around an edge of the singular locus of M_2^{-3} generate $\pi_1^{orb}\left(\mathrm{M}_2^{-3}\right)$. Each γ has to go to 1 under the holonomy $\pi_1^{orb}\left(\mathrm{M}_2^{-3}\right) \to \mathbb{Z}/2$ to obtain a manifold, determining the holonomy completely. □

The unique manifold double cover of $\mathrm{M}_2^{-3} \cong [S_4 \times 1]$ is N_2^{-3} and the complement of the minimally twisted 5-component chain link as described in [DT03]. The involution of the link acts by a rotation around the dashed circle in Figure 1.17. A fundamental domain for the quotient of the link complement under the involution is the ball whose equator is the dashed circle. Cut away the outside of the ball and blow it up to get S^3 identifying the top and bottom of the ball. The tori of the 5-component chain link become elongated balls. When removing them, the circle splits into 10 line segments. When shrinking the balls so that they become the cusps of the pentacle $[S_4 \times 1]$, these line segments become the order 2 singular locus.

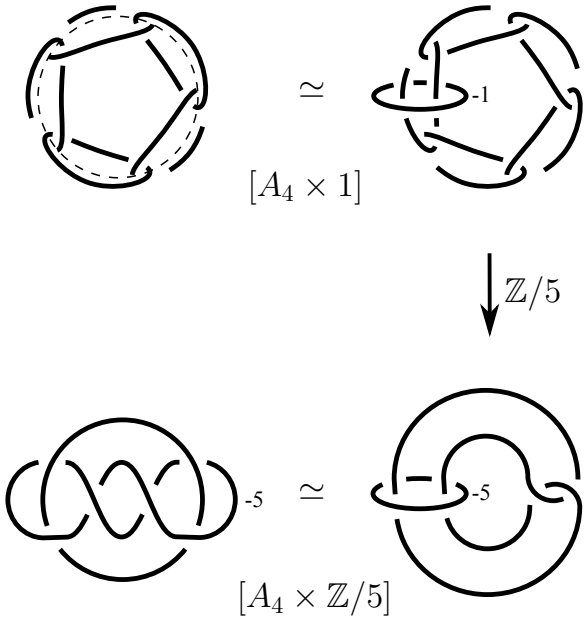

Figure 1.17: Construction of $\left[A_4 \times \frac{\mathbb{Z}}{5}\right]$.

1.13.2 Construction of $[A_4 \times \mathbb{Z}/5]$

A blow-up [GS99, Chapter 5.1] of the diagram for the minimally-twisted 5-component chain link makes the C_5 symmetry visible, see top of Figure 1.17. We divide by this C_5 symmetry which is turning the -1-surgery into a -5-surgery, see Figure 1.17.

The resulting manifold has to be $[A_4 \times \mathbb{Z}/5]$ because the action of C_5 on the manifold $[A_4 \times 1]$ is unique up to conjugation. In other words, the orientation-preserving symmetry group of $[A_4 \times 1]$ is $\mathbb{Z}/2 \times A_5$ and has only one conjugacy class of order 5.

The manifold $[A_4 \times \mathbb{Z}/5]$ is isometric to m003, the sister of the Figure 8 knot complement.

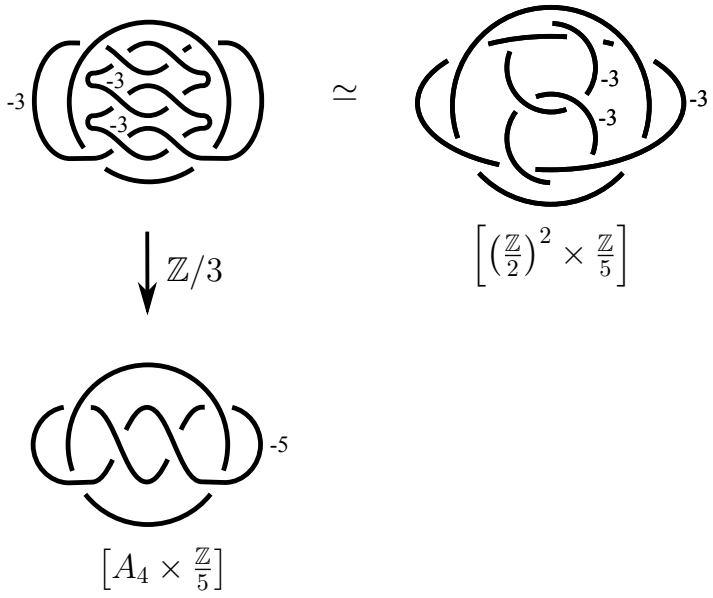

Figure 1.18: Construction of $\left[\left(\frac{\mathbb{Z}}{2}\right)^2 \times \frac{\mathbb{Z}}{5}\right]$.

1.13.3 Construction of $\left[(\mathbb{Z}/2)^2 \times \mathbb{Z}/5\right]$

The manifold $\mathrm{M}^{-3}_{2+2\zeta}$ is a 60-fold cover of $[A_4 \times \mathbb{Z}/5]$. The manifold $\mathrm{M}^{-3}_{2+2\zeta}$ has 20 cusps, whereas $[A_4 \times \mathbb{Z}/5]$ has only one. The manifold $[A_4 \times \mathbb{Z}/5]$ has eight tetrahedra meeting at a cusp ($[A_4 \times 1]$ being the double cover of M^{-3}_2). The manifold $\mathrm{M}^{-3}_{2+2\zeta}$ has 24 tetrahedra meeting at a cusp. This means that the 3-cyclic cover $\left[(\mathbb{Z}/2)^2 \times \mathbb{Z}/5\right] \to [A_4 \times \mathbb{Z}/5]$ has to triple the size of the cusp, hence the corresponding component of the link has to serve as branching locus. Each of the following p-cyclic covers in the construction has to lift the cusps to p copies.

Notice that $H_1\left([A_4 \times \mathbb{Z}/5]\right) \cong \mathbb{Z} \oplus \mathbb{Z}/5$ (the two components of the link have linking number zero). Hence, the 3-cyclic cover is unique.

Figure 1.18 illustrates the construction of the 3-cyclic cover as described in Section 1.10. Notice that each of -5 surgeries becomes a -3 surgery. To see this, blow-up about the clasp of the -5 surgery component in the diagram for $[A_4 \times \mathbb{Z}/5]$ to unlink the components, undo the blow-ups by three blow-downs in the 3-cyclic cover.

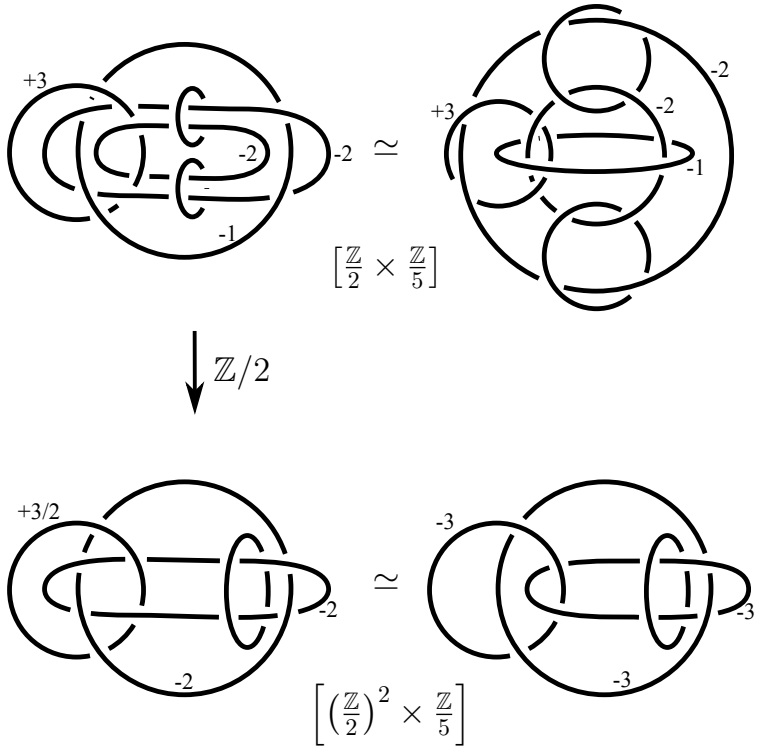

Figure 1.19: Construction of $\left[\frac{\mathbb{Z}}{2} \times \frac{\mathbb{Z}}{5}\right]$.

1.13.4 Construction of $[\mathbb{Z}/2 \times \mathbb{Z}/5]$

Pick one surgery component of the link for $\left[(\mathbb{Z}/2)^2 \times \mathbb{Z}/5\right]$ to perform a Rolfsen twist with $n = 1$ about (see bottom of Figure 1.19), then construct the 2-cyclic cover with one of the -2-surgery components as branching locus (see top of Figure 1.19). Different choices result in three covers that are different as covering spaces but not as manifolds. Since $H_1\left([(\mathbb{Z}/2)^2 \times \mathbb{Z}/5]\right) \cong \mathbb{Z} \oplus (\mathbb{Z}/2)^2 \oplus \mathbb{Z}/5$, these are all possible 2-cyclic covers by Lemma 1.13.2.

1.13.5 Construction of $\mathrm{M}^{-3}_{2+2\zeta}$

Representing $[\mathbb{Z}/2 \times \mathbb{Z}/5]$ as Link Complement in the Lens Space $L(20, 11)$

Without the cusps, the diagram for $[\mathbb{Z}/2 \times \mathbb{Z}/5]$ in Figure 1.19 is a plumbing diagram. After a blow-down about the -1 surgery, it is a linear plumbing diagram with coefficients -2, +4, -2. Following [Rol90, Section 9.H] or [GS99, Section 5.3], the resulting space is a lens space $L(20, 11) \cong L(20, -9)$ whose type is determined by the continued fraction

$$-\frac{20}{9} = -2 - \frac{1}{+4 - \frac{1}{-2}}.$$

The moves on the plumbing diagram revealing the lens space structure are shown in Figure 1.20. Figure 1.21, 1.22, 1.23, 1.24, and 1.25 trace the other components of the link diagram for $[\mathbb{Z}/2 \times \mathbb{Z}/5]$ through the moves on the plumbing diagram.

Construction of the 10-Cyclic Cover in $\mathbb{R}P^3$

The components of the link in Figure 1.25 corresponding to cusps wind 10 times around the $+20/11$-surgery unknot. Hence, $H_1([\mathbb{Z}/2 \times \mathbb{Z}/5]) \cong \mathbb{Z} \oplus \mathbb{Z} \oplus \mathbb{Z}/10$ and the 10-cyclic cover is uniquely determined by Lemma 1.13.2. During the construction of the 10-cyclic cover, the $+20/11$-surgery unknot serves as branching locus and turns into $+2/11$ surgery, hence we obtain a link for $\mathrm{M}^{-3}_{2+2\zeta}$ in $L(2, 11) \cong L(2, -1) \cong \mathbb{R}P^3$. Figure 1.26 shows this link after simplification by a Rolfsen twist with $n = -6$ about the $+2/11$ surgery unknot. Each of the 20 components is an unknot parallel to a meridian around the surgery unknot. The link has at least D_{20}-symmetry.

When drawing Figure 1.26, it is helpful to compute the slopes (number of meridians divided by number of longitudes around the surgery unknot) of the resulting curves after the construction of the cyclic cover and the Rolfsen twists. The surgery slope is $+20/11$, the slopes of the straight lines in Figure 1.25 are $+1/1$ and $+9/5$. The 10-cyclic cover will turn those into $+2/11$, $+1/10$, and $+9/50$. The $n = -6$ Rolfsen twists will result in -2/1, $+1/4$, and -9/4.

Link Diagram in S^3

Pick one of the link components, say γ, in the link diagram from Figure 1.26. Perform a Rolfsen twist about γ. The seven components that are linked to γ get twisted and unlinked from the surgery unknot. The surgery unknot turns to -1. Hence, a blow-down about this

surgery unknot results in a link diagram for $M^{-3}_{2+2\zeta}$ in S^3 shown in Figure 1.27, unfortunately breaking the D_{20} symmetry.

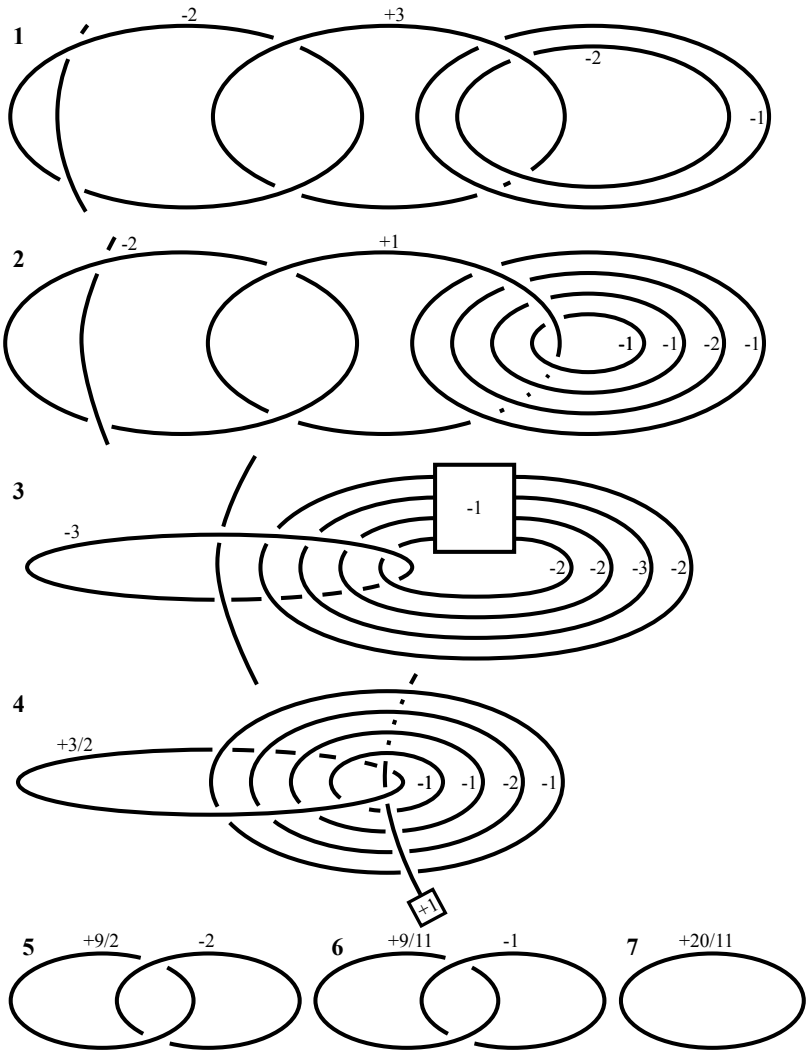

Figure 1.20: Moves on the Plumbing Diagram for $\left[\frac{\mathbb{Z}}{2} \times \frac{\mathbb{Z}}{5}\right]$. In this Figure, we ignore the other link components. However, we trace a small line segment for some of the moves to guide the construction of Figure 1.22.

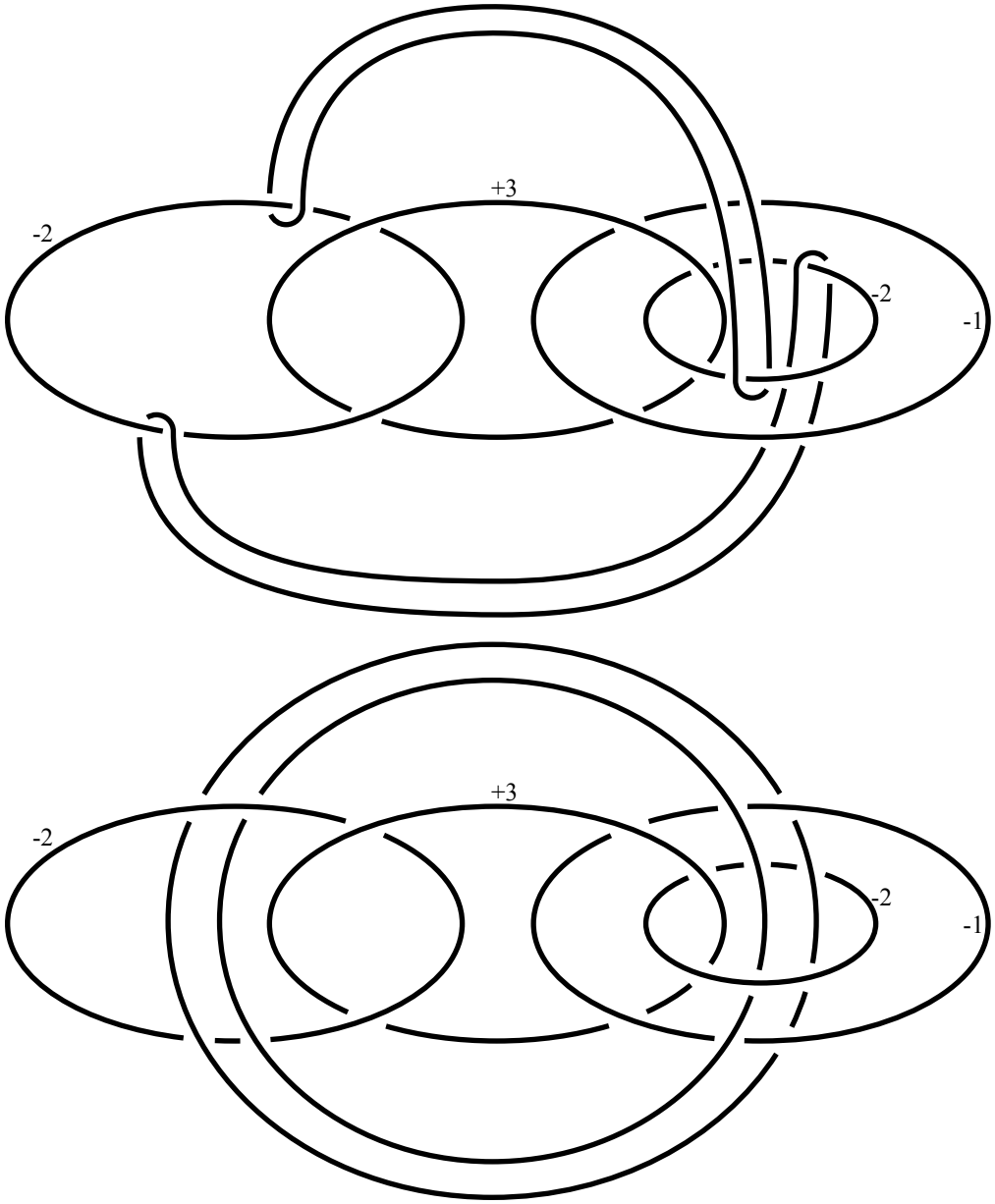

Figure 1.21: Two different projections of Plumbing Diagram 1 from Figure 1.20 with cusps for $\left[\frac{\mathbb{Z}}{2} \times \frac{\mathbb{Z}}{5}\right]$.

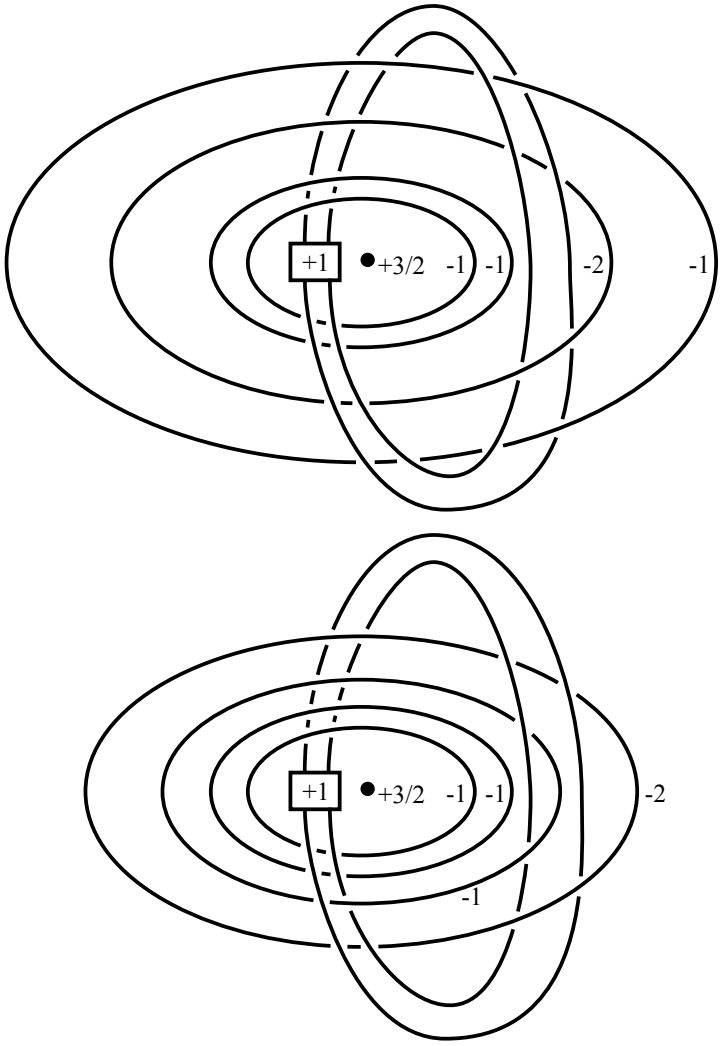

Figure 1.22: Two different projections of Plumbing Diagram 4 from Figure 1.20 with cusps for $\left[\frac{\mathbb{Z}}{2} \times \frac{\mathbb{Z}}{5}\right]$.

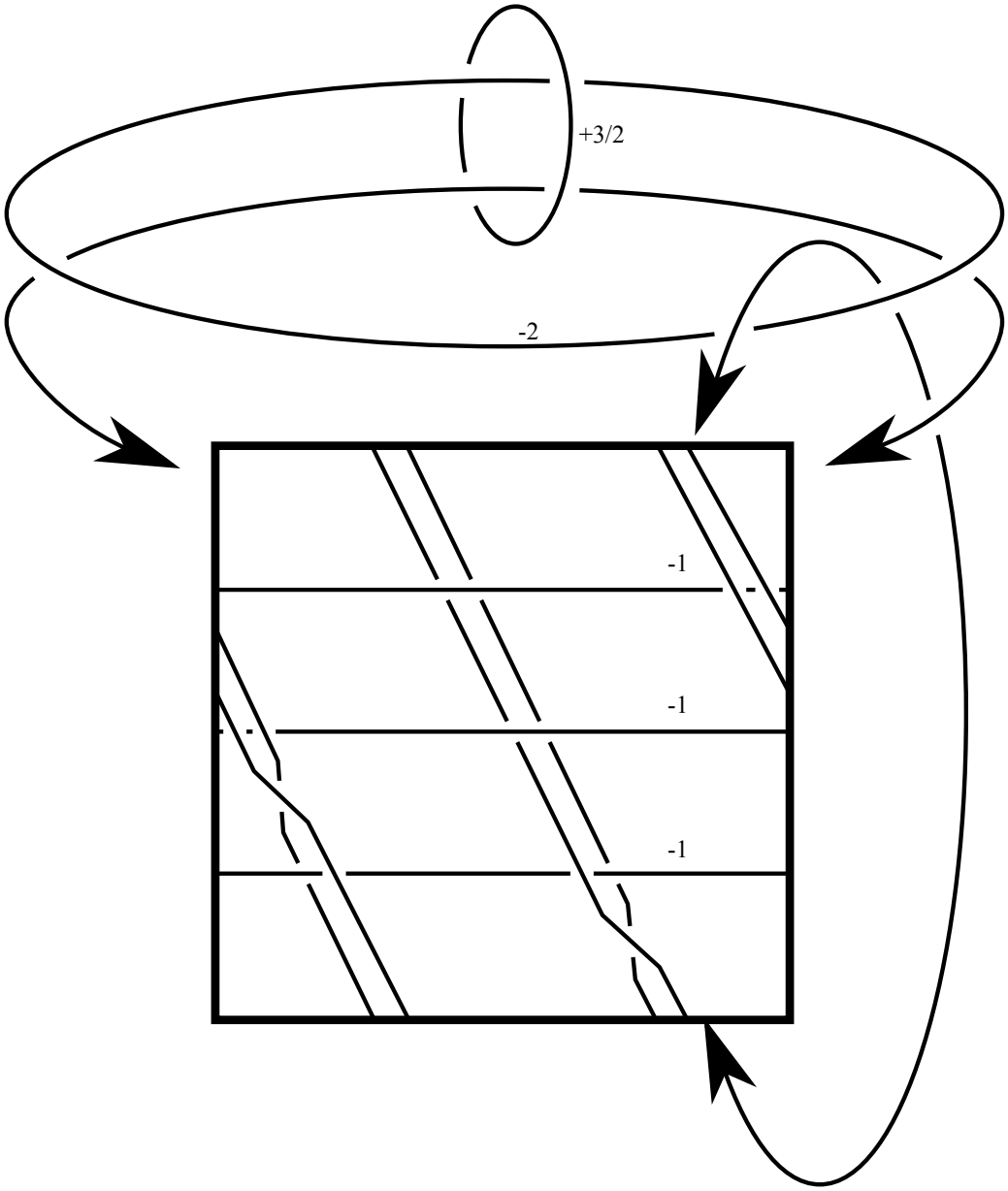

Figure 1.23: Plumbing Diagram 4 from Figure 1.20 with cusps for $\left[\frac{\mathbb{Z}}{2} \times \frac{\mathbb{Z}}{5}\right]$ projected onto torus sitting in the Hopf link formed by the -2 and $+3/2$ surgery unknots.

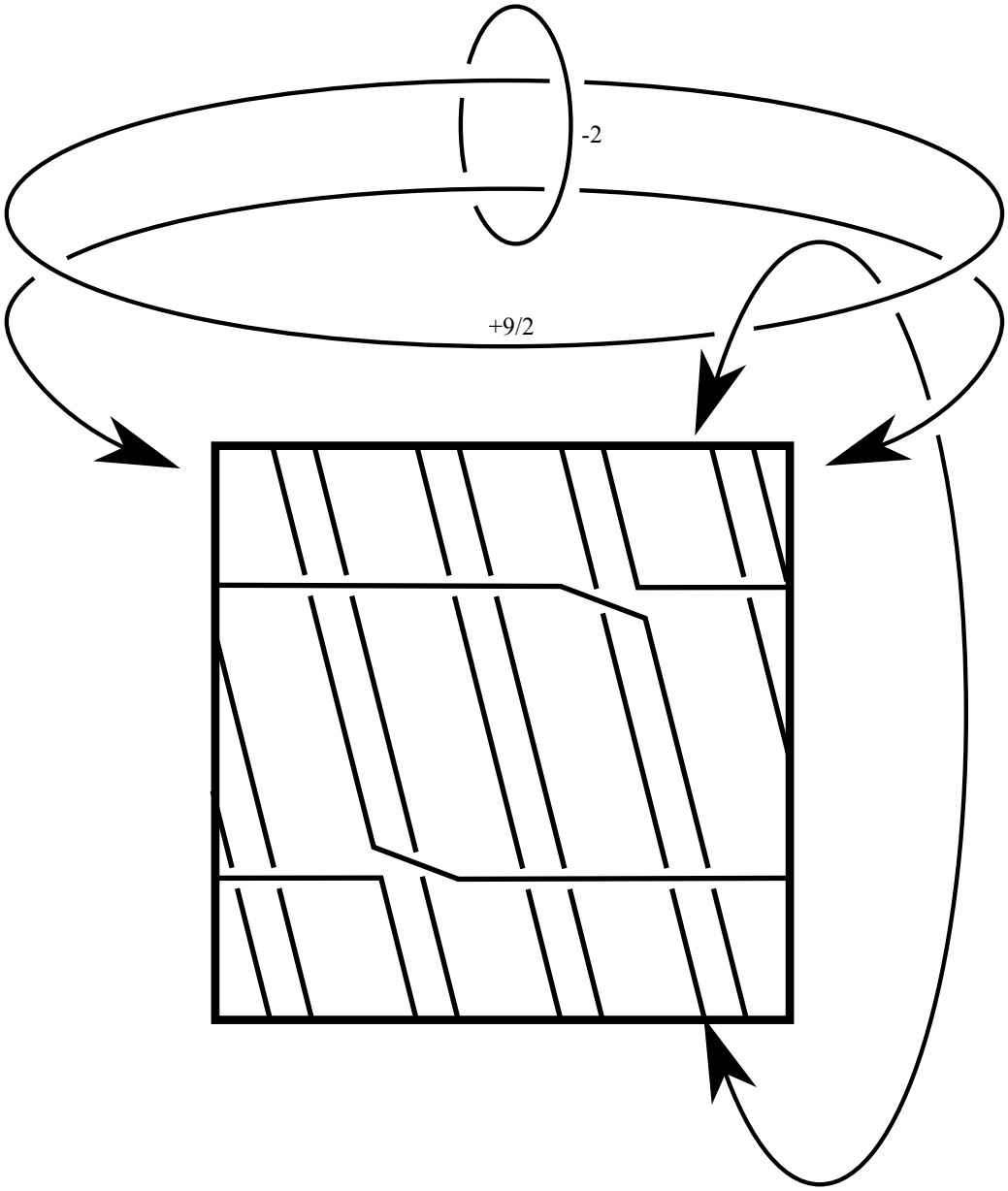

Figure 1.24: Plumbing Diagram 5 from Figure 1.20 with cusps for $\left[\frac{\mathbb{Z}}{2} \times \frac{\mathbb{Z}}{5}\right]$ projected onto torus sitting in the Hopf link formed by the -2 and $+9/2$ surgery unknots.

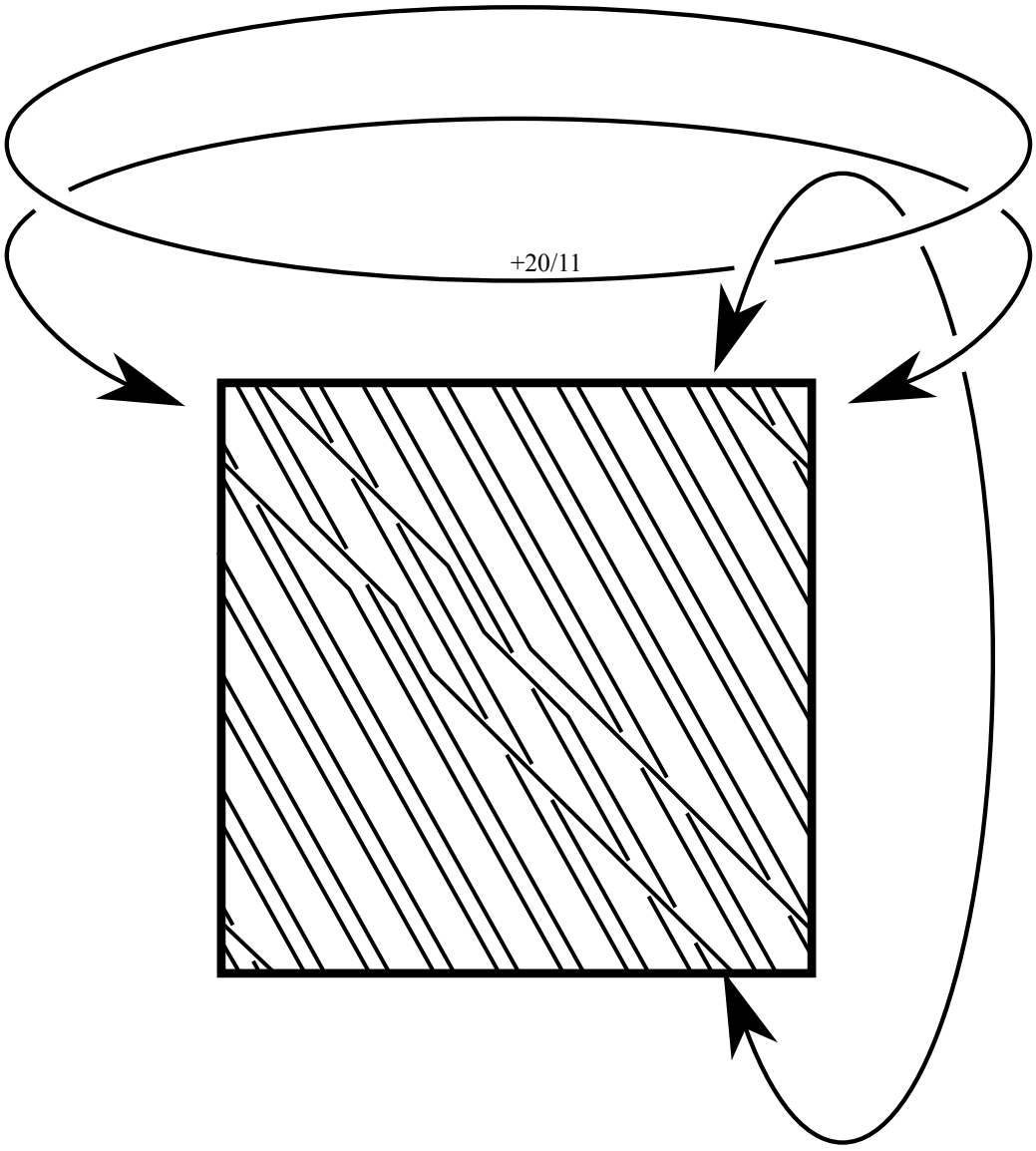

Figure 1.25: Plumbing Diagram 7 from Figure 1.20 with cusps for $\left[\frac{\mathbb{Z}}{2} \times \frac{\mathbb{Z}}{5}\right]$.

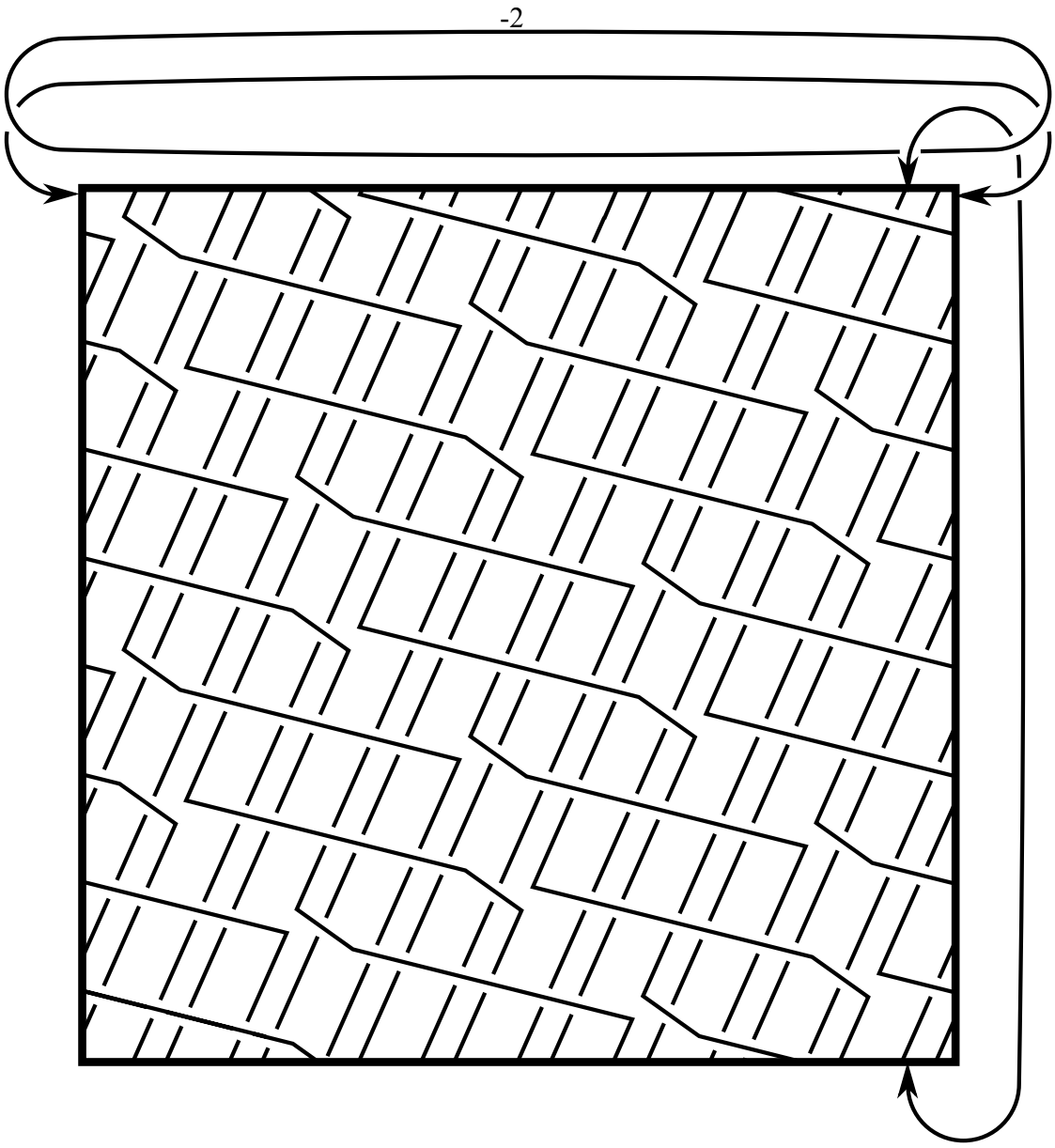

Figure 1.26: Link for $\mathrm{M}^{-3}_{2+2\zeta}$ in $\mathbb{R}P^3$.

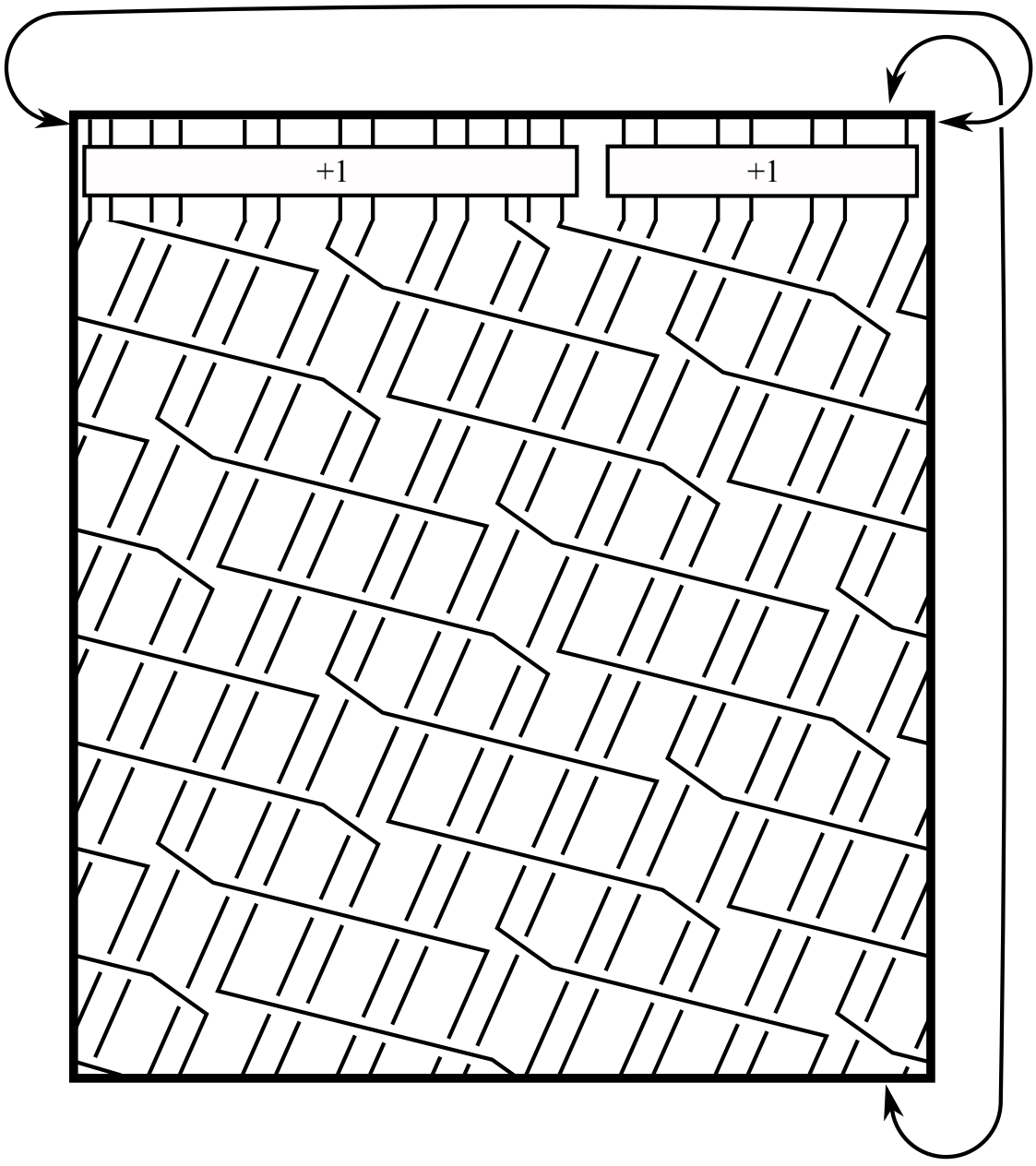

Figure 1.27: Link for $\mathrm{M}^{-3}_{2+2\zeta}$ in S^3.

1.14 Attempt to Construct $\mathrm{N}^{-3}_{3+\zeta}$

For $3+\zeta$, a SnapPy [CDW] computation shows that a suitable Dehn filling of $\mathrm{N}^{-3}_{3+\zeta}$ trivializes the fundamental group. Hence, by Perelman's Theorem, $\mathrm{N}^{-3}_{3+\zeta}$ is a link complement. The manifold $\mathrm{M}^{-3}_{3+\zeta}(P)$ (notation defined in 1.8) with

$$P = \left\{ \begin{pmatrix} 1 & x \\ 0 & 1 \end{pmatrix} \right\}$$

is shown in Figure 1.28. The manifold $\mathrm{M}^{-3}_{3+\zeta}(P)$ has 14 13-cyclic covers, but only two of those have 14 cusps, each of the two is isometric to $\mathrm{M}^{-3}_{3+\zeta}$ which is the complement of a 14-component link in $\mathbb{R}P^3$. The double-cover of $\mathbb{R}P^3$ yields a 28-component link in S^3 whose complement is $\mathrm{N}^{-3}_{3+\zeta}$.

The manifold $\mathrm{N}^{-3}_{3+\zeta}(P)$ is the complement of a 4-component link in S^3. Analogously, the two of those 13-cyclic covers with 28 cusps are isometric to $\mathrm{N}^{-3}_{3+\zeta}$.

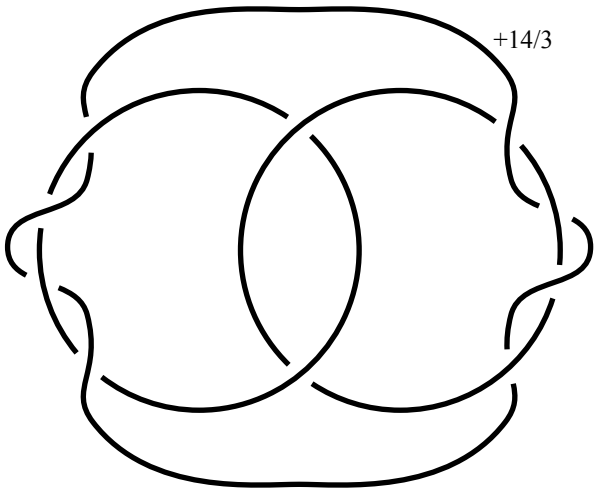

Figure 1.28: Surgery diagram for $\mathrm{M}^{-3}_{3+\zeta}(P)$.

1.15 Generic Regular Covers of Bianchi Orbifolds

1.15.1 Category of Regular Covers of the Bianchi Orbifold with Fixed Cusp Modulus

Let $\mathcal{C}_z$ be the category with objects being pointed, connected regular covering spaces of the Bianchi orbifold M_1^{-3} with toroidal cusp modulus z (see Section 1.5). Morphisms are topological morphisms commuting with the projections onto M_1^{-3}. Note that we obtain the same category if we drop the condition on a topological morphism to commute and let morphisms instead be covering maps, regular covering maps, or hyperbolic morphisms by Lemma 1.3.15. Clearly, M_z^{-3} and N_z^{-3} are objects in this category. Let

$$\widehat{\Delta}(z) = \text{normal subgroup of } \mathrm{PGL}(2,\mathbb{Z}[\zeta]) \text{ generated by } P_z = \pm \begin{pmatrix} 1 & z \\ 0 & 1 \end{pmatrix}.$$

The quotient $\widehat{\mathrm{N}}_z^{-3} = \frac{\mathbb{H}^3}{\widehat{\Delta}(z)}$ is the initial object in $\mathcal{C}_z$ because, if $\frac{\mathbb{H}^3}{\Gamma}$ is an object in $\mathcal{C}_z$, the group Γ is normal in $\mathrm{PGL}(2,\mathbb{Z}[\zeta])$ by definition and the cusp modulus implies that $P_z \in \Gamma$.

An algorithmic attempt to construct a triangulation of $\widehat{\mathrm{N}}_z^{-3}$ is given in Table 1.4. This algorithm terminates within reasonable time in the cases indicated in Table 1.5.

Given $\widehat{\mathrm{N}}_z^{-3}$, we can find all objects in $\mathcal{C}_z$ by looking for normal subgroups of $\mathrm{Isom}^+(\widehat{\mathrm{N}}_z^{-3})$ containing no non-trivial element fixing a cusp. SnapPy [CDW] can represent the symmetry group by its action on the cusps. If this action is faithful (e.g., the involution of the minimally twisted 5-component chain link does *not* permute the cusps, see Section 1.13.1), this gives a permutation representation which can be used in gap [GAP08].

This allows us to compute $\mathcal{C}_z$ (up to category equivalence) for small z (degree of covering map is 2 unless indicated otherwise):

$$\begin{aligned}
\mathcal{C}_z &= \left\{\mathrm{N}_z^{-3}\right\} \quad \text{for} \quad z \in \{2, 2+\zeta, 2+2\zeta, 3, 3+2\zeta\} \\
\mathcal{C}_{3+\zeta} &= \left\{\mathrm{M}_{3+\zeta}^{-3} \leftarrow \mathrm{N}_{3+\zeta}^{-3}\right\} \\
\mathcal{C}_4 &= \left\{\mathrm{N}_4^{-3} \leftarrow \widetilde{\mathrm{N}}_4^{-3} \leftarrow \widehat{\mathrm{N}}_4^{-3}\right\} \\
\mathcal{C}_{4+\zeta} &= \left\{\mathrm{M}_{4+\zeta}^{-3}\left((\mathbb{Z}/2)^2\right) \overset{4}{\leftarrow} \mathrm{N}_{4+\zeta}^{-3} \leftarrow \widetilde{\mathrm{N}}_{4+\zeta}^{-3}\right\}
\end{aligned}$$

where $\widetilde{\mathrm{N}}_z^{-3}$ is defined as

$$\widetilde{\mathrm{N}}_z^{-3} = \frac{\mathbb{H}^3}{\ker\left(\mathrm{PSL}(2,\mathbb{Z}[\zeta]) \to \frac{\mathrm{SL}(2,\mathbb{Z}[\zeta]/\langle z\rangle)}{\pm\mathrm{Id}}\right)}.$$

Table 1.4: An algorithm attempting to construct the universal triangulation with fixed cusped modulus.

1. Start with a single regular ideal hyperbolic tetrahedron.
2. While there are tetrahedra with open faces:
   (a) Add a regular ideal tetrahedron and glue it to an open face. The open face is chosen to be a face participating in a cusp that already has a lot of tetrahedra, i.e., finishing one cusp first is preferred over moving on to the next.
   (b) For each cusp, enforce the right cusp modulus by identifying appropriate tetrahedra.

By working with right-handed flags instead of tetrahedra to encode a triangulation, this algorithm also works if $\widehat{\mathrm{N}}_z^{-3}$ is an orbifold.

Table 1.5: Homologies of universal Binachi orbifold covers $\widehat{\mathrm{N}}_z^{-3}$.

z	Tetrahedra	cusps	H_1
2 $2+\zeta$ $2+2\zeta$ 3 $3+\zeta$ $3+2\zeta$	isometric to N_z^{-3}		
4	640	80	$\mathbb{Z}^{80}$
$4+\zeta$	672	64	$\mathbb{Z}^{64}$

Notice that $\mathrm{M}_z^{-3} \leftarrow \mathrm{N}_z^{-3} \leftarrow \widetilde{\mathrm{N}}_z^{-3} \leftarrow \widehat{\mathrm{N}}_z^{-3}$ where maps are covering maps or isomorphisms and $\widehat{\mathrm{N}}_z^{-3}$ might not be finite volume. Lemma 1.3.11 gives a complete answer to when the first map is a double cover, also see Example 1.3.12.

The initial objects in $\mathcal{C}_4$ and $\mathcal{C}_{4+\zeta}$ are homology link complements, even though the other objects in those categories are not, e.g., $H_1(\widetilde{\mathrm{N}}_4^{-3}) = \mathbb{Z}^{40} \oplus \mathbb{Z}/2$.

1.15.2 Another Universal Property

Theorem 1.15.1. *For any finite volume (not necessarily regular) cover N of the Bianchi orbifold M_1^{-3}, there exists z such that $\widehat{\mathrm{N}}_z^{-3}$ covers N.*

Proof. Even though N is not a regular cover, there are still natural coordinates on the cusps as discussed in Section 1.5. The natural coordinates are defined up to ζ^k. N posses a triangulation (not necessarily the canonical triangulation) by regular ideal tetrahedra coming from the covering map $N \to \mathrm{M}_1^{-3}$. In the natural coordinates, the edges of this triangulation intersect a cusp torus in the lattice $\mathbb{Z}[\zeta]$. Let μ_i and λ_i be the translations induced by two peripheral curves generating the homology of the i-th cusp.

Notice μ_i and λ_i span $\mathbb{Q}[\zeta]$ as a $\mathbb{Q}$-vector space. Hence, there are $a_i, b_i, c_i \in \mathbb{Z}$ such that $a_i\mu_i + b_i\lambda_i = c_i\zeta\mu_i \neq 0$. Notice that, for each k, $a_ic_i\zeta^k\mu_i$ is a $\mathbb{Z}$-linear combination of μ_i and λ_i. Let $z = \prod a_ic_i\mu_i$, then $\langle z \rangle \subset \mathbb{Z}\mu_i + \mathbb{Z}\lambda_i$ for every i.

Let $\Gamma \subset \mathrm{PGL}(2, \mathbb{Z}[\zeta])$ such that $N = \frac{\mathbb{H}^3}{\Gamma}$. We need to show that $\Gamma \supset \widehat{\Delta}_z$. As a group, $\widehat{\Delta}_z$ is generated by matrices MP_zM^{-1} with $M \in \mathrm{PGL}(2, \mathbb{Z}[\zeta])$. Hence, it suffices to prove that every MP_zM^{-1} is in Γ. By conjugation of Γ with M, we can reduce to the case P_z which fixes $\infty \in \partial\mathbb{H}^3$.

By choice of z, it is a linear combination of μ_i and λ_i for the cusp at ∞. The corresponding translation is an element of Γ, thus $P_z \in \Gamma$. □

Remark 1.15.2. Using [MR03, Theorem 8.2.3], this theorem implies that every arithmetic cusped hyperbolic 3-manifold is covered by some, not necessarily finite volume, $\widehat{\mathrm{N}}_z^{-3}$.

1.16 Discussion and Future Work

We have made substantial progress in classifying all principal congruence links of discriminant $D = -3$. We have shown that there are at most seven principal congruence links where we regard two links as equivalent if they have the same link complement.[1] We have found two of these principal congruence links explicitly. Together with the two examples due to Dunfield and Thurston [DT03, Thu98], there are three cases left of potential prinicipal congruence links that need to be found. For one case, we have shown that the prinicipal congruence link exists.

There are several ways of extending this work:

- **Bianchi orbifold regular cover links.** Classify generic regular covers of a Bianchi orbifold with a given cusp modulus as defined in Section 1.5 and determine which ones are link complements. The universal regular Bianchi orbifold cover with a given cusp modulus (as defined in Section 1.15.1) appears to be infinite for large enough cusp modulus. Hence, there might be infinitely many regular covers with given cusp modulus z. If this happens for a cusp modulus $|z| < 6$, there might even be an infinite class of Bianchi orbifold regular cover links. The exact bound when the universal regular Bianchi orbifold cover becomes infinite and the existence of an infinite family of Bianchi orbifold regular cover links are interesting open questions.

- **Other discriminants.** Classify the finitely many principal congruence links for discriminants $D \neq -3$ (see introduction in Section 1.1). Similarly to $D = -3$, the group $\mathrm{PGL}(2, \mathcal{O}_{-4})$ is again a Coxeter group, this time related to the octahedron (also, see next paragraph).

- **Other regular ideal polyhedra.** We can look at regular tessellations of cusped manifolds by other regular ideal polytopes, i.e., quotients by finite index normal subgroups of Coxeter groups. Aitchison and Rubinstein [AR92] list all possible polytopes, respectively, Coxeter groups and construct a link for each case such that the link complement is tessellated by these polytopes. However, their tessellations are not regular.

Polytope	Coxeter group
Tetrahedron	$\{3, 3, 6\}$
Octahedron	$\{3, 4, 4\}$
Cube	$\{4, 3, 6\}$
Dodecahedron	$\{5, 3, 6\}$

[1] Unlike knots, links are not determined by their complement and all links representing the same manifold can be obtained through Kirby calculus

We modified the algorithm in Table 1.4 to use these polytopes. For, e.g., the octahedron, the algorithm terminates for $z \in \{1, 1+i, 2, 2+i, 2+2i, 3, 3+i, 3+2i\}$.

The following questions are related to this work and possible future work:

- **Is a given hyperbolic manifold M a link complement?** M is a link complement if and only if there are Dehn fillings resulting in S^3. In theory, the 3-sphere recognition is algorithmic [Mat07]. Even though there might be infinitely many Dehn fillings resulting in S^3, Gordon [Gor02] lists a finite (though intractable) set of slopes sufficient for recognizing link complements of a certain class.

- **What is the maximal symmetry of a link with complement being a given hyperbolic manifold M?** The symmetry group $\mathrm{Sym}(M)$ can be computed effectively through the canonical triangulation in SnapPy [CDW]. $\mathrm{Sym}(M)$ acts on the cusps and their peripheral curves. A subgroup $H \subset \mathrm{Sym}(M)$ can be seen in the link if the Dehn fillings resulting in S^3 are invariant under H. If an element $h \in H$ fixes a cusp, then h cannot change the peripheral curves on the cusp other than by flipping their orientations. To determine all possible H, we can find all H (up to conjugation in $\mathrm{Sym}(M)$) fulfilling this condition and search for H-invariant Dehn fillings resulting in S^3.

- **Is M a congruence manifold?** Given a hyperbolic manifold M, can we effectively detect whether there is a $z \in \mathcal{O}_D$ and a subgroup $G \subset \mathrm{PGL}(2, \mathcal{O}_D/\langle z \rangle)$ such that M is isometric to the congruence manifold $\mathrm{M}_z^D(G) = \mathbb{H}^3/p^{-1}(G)$ as defined in Section 1.8?

- **What chain links are arithmetic?** Neumann and Reid completely classify all arithmetic chain links [NR92, Theorem 5.1]. All arithmetic chain links with discriminant $D = -3$ are $C(1,-3), C(1,2), C(4,-4), C(4,0)$, and $C(5,-2)$. Among those, only the minimally twisted 5-component chain link $C(5,-2)$ is a principal congruence link.

Chapter 2

Equivariant Morphisms from Regular Maps to S^3

2.1 Introduction

This chapter generalizes the idea behind the sculpture of the Klein quartic by Helaman Ferguson at the Mathematical Science Research Institute in Berkeley, see Figure 2.1. The center piece of the sculpture is a genus 3 handlebody obtained by taking the edges of a tetrahedron and thickening them. There is a pattern of edges and vertices on the surface of the sculpture dividing the surface into 24 heptagons. Each of the 56 vertices is surrounded by three heptagons. Any rotational symmetry of the tetrahedron can be applied to the sculpture and leaves the pattern invariant meaning that the image of a vertex or edge under this symmetry is again a vertex or edge of the pattern.

This pattern is an example of a *regular map*. Here, "map" refers to a tessellation of a surface, similar to a geographic map with countries. In fact, several regular maps have been found while studying the four-color problem [CM80]. A regular map is a tessellation of a surface by p-gons such that q of them meet at each vertex and such that an extra transitivity condition holds: any p-gon can be taken to any other p-gon in all possible p rotations by an automorphism of the tessellation. We say that such a regular map is of type $\{p, q\}$. Here, an automorphism of the tessellation is a surface homeomorphism taking the tessellation to itself, i.e., a bicontinuous 1-1 function from the surface to itself that takes vertices to vertices, edges to edges, p-gons to p-gons. As such, regular maps are the generalization of the Platonic solids to higher genus surfaces, the genus 0 regular maps being exactly the surfaces of the five Platonic solids. The transitivity condition simply says that a person living in the surface cannot tell through intrinsic measurements what p-gon he or she is in and at what edge of

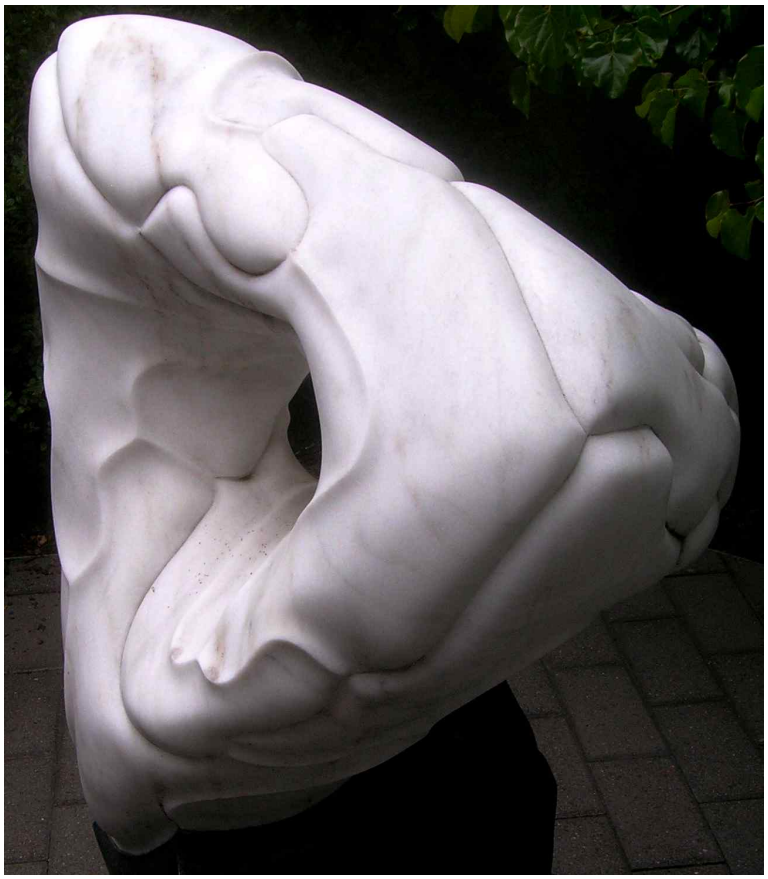

Figure 2.1: Sculpture "The Eightfold Way" by Helaman Ferguson.

the p-gon he or she is looking at. The Klein quartic is a regular map of type $\{7, 3\}$ (or $\{3, 7\}$ depending on convention) and genus 3 which has many connections to other areas of math and which reoccurs in this thesis in Section 1.2.1 and 2.2.2.

As explained earlier, every rotational symmetry of Ferguson's sculpture induces an automorphism of the Klein quartic. In other words, some symmetries of the Klein quartic are "directly visible as symmetries of space" (William Thurston [Lev99]). However, there are symmetries of the Klein quartic that do not extend to a symmetry of the tetrahedral sculpture. For example, we fail to find a symmetry of the sculpture that rotates one heptagon by a $\frac{1}{7}$th of a turn. The failure to capture this seven fold symmetry of the Klein quartic is not particular to this sculpture, but intrinsic to any embedding of the Klein quartic. As shown in Section 2.13, no embedding of the Klein quartic into Euclidean 3-space makes this order seven symmetry visible. Even though the sculpture is not a perfect representation of the Klein quartic, it is still the best possible in the sense that no other sculpture could make a

larger subgroup of the symmetries of the Klein quartic visible.

The goal of this chapter is to look for the "best sculpture" of a given regular map F.

More precisely, we develop a theory to find all subgroups H of the automorphism group of a regular map F that can be realized by isometries of Euclidean 3-space E^3 when mapping, immersing, or embedding F into E^3. This idea is captured by the notion of *equivariant morphisms*. We give a complete theoretic solution to this problem resulting in algorithms. We have implemented some of the algorithms showing that they are feasible on current hardware.

This chapter is structured as follows:

An equivariant morphism $F \to M$ carries as extra datum an (H, B, η)-triple where H is a subgroup of automorphisms of F, B a subgroup of isometries of M, and $\eta : H \cong B$ an isomorphism relating an automorphism of F to an isometry of M. First, given a regular map F, we find all (H, B, η)-triples up to the equivalence defined in Section 2.5. Then, we determine for a triple whether there exists an (H, B, η)-equivariant morphism, immersion, or embedding. For this, Section 2.6 translates the question to the quotient spaces $F/H \to M/B$ which, in general, are orbifolds reviewed in Section 2.3. If $M = S^3$, we obtain a map

$$\tau : \pi_1^{orb}(F/H, p) \xrightarrow{h} H \cong B \cong \pi_1^{orb}(S^3/B, p)$$

and develop a theory in Section 2.7 and 2.8 to decide whether τ is induced by a morphism, immersion, or embedding.

Section 2.10 and 2.11 describe the resulting algorithms to find all (H, B, η)-triples, respectively, determine whether a (H, B, η)-equivariant morphism, immersion, or embedding exists.

Interesting examples of mappings, immersions, and embeddings of regular maps appear in Section 2.12 as application of the theory and the algorithms.

To conclude this chapter, we implement some of the algorithms in gap [GAP08] and apply them in Section 2.13 to the orientable regular maps up to genus 101 in Conder's census [CD01, Con09]. For each of those regular maps, we list the subgroups H which fulfill the necessary or sufficient conditions for an equivariant morphism, immersion, or embedding.

Several theoretical obstacles had to be overcome for these results. An example of an algebraic subtlety is the right notion of equivalence of two equivariant morphism. The Klein quartic, for example, has a C_7 symmetry given by a rotation about one heptagon, and another such symmetry group when taking rotations about another heptagon. These symmetries are showing the same phenomenon but are technically speaking different subgroups. We choose the definition of equivalence of equivariant morphisms to account for this.

Given that a subgroup of the automorphisms of a regular map and a finite group of isometries

of Euclidean 3-space are the same algebraically, there is the topological question whether the (algebraic) group isomorphism is realized by a topological morphism. To address this problem, we apply orbifold theory, normal surface theory, and the mapping class group.

While developing this theory in Section 2.7.7, we encounter a cohomology obstruction $[c(\tau)] \in H^2(X(F); \mathbb{Z}/2)$ that is an equivariant analog to the Stiefel-Whitney class serving as obstruction for an immersion (see, e.g., [MS74, §4., Immersions]). We give an example of how to compute it effectively in Section 2.11.5 and 2.12.1.

The algorithm for deciding the existence of equivariant immersions described here allows a feasible implementation and would find all subgroups that allow equivariant immersions in reasonable time on current hardware (days) for all regular map in Conder's census.

This work is related to a SIGGRAPH paper by Jack van Wijk [vW09] on visualizing regular maps. Professor Carlo Séquin who got me interested in this topic is also working on producing visualizations of regular maps. The "Regular Map Database" [Wed] also contains pictures of various models of regular maps.

2.1.1 Conventions

We use the term "regular map" from graph theory as it has been defined and used by, e.g., Coxeter and Moser [CM80, Cox69], Conder and Marsden [CD01, Con09], and Jack van Wijk [vW09].

Unfortunately, there is potential for confusion because the term "map" in topology can also refer to a continuous or smooth function between spaces, i.e., a morphism in the category of topological spaces or smooth manifolds. Here, the term "regular map" always refers to a tessellation of a surface as defined in Section 2.2.1. When talking about a topological morphism, we always say "mapping", "morphism", or "smooth function". Unless otherwise indicated, all manifolds, orbifolds, and morphisms are supposed to be smooth or piecewise-linear, thus ruling out pathological cases such as the Alexander horned sphere.

Throughout this chapter, we assume that every orbifold M is good, closed, orientable, and connected and has a base point p not in the singular locus $\Sigma(M)$ of M. We usually denote a 2-orbifold by F and a 3-orbifold by M.

2.2 Regular Maps

2.2.1 Definition

Coxeter and Moser [Cox69, CM80] give an introduction to regular maps. We summarize the definition of regular map here and fix the notation used in later sections.

Definition 2.2.1. *A regular map of type $\{p, q\}$ is a surface with a CW-structure dividing the surface into p-gons such that q of the polygons meet at each vertex and such that each p-gon can be taken to any other p-gon in all possible p choices of rotation by some cellular automorphism.*

A regular map is called orientable or non-orientable if the underlying topological space is orientable or non-orientable.

We can give each p-gon a constant-curvature geometry such that the p-gon is regular, the edges are geodesics, and the angle at a vertex is $2\pi/q$. This geometrizes a regular map. The triangle orbifold $(2, p, q)$ is a 2-orbifold (see Section 2.3.4) that is topologically S^2 and that has three singular points of order 2, p, and q. A triangle orbifold has a unique geometric structure. Hence, the following definition of a regular map is equivalent if we consider only orientable regular maps and do not distinguish between a regular map of type $\{p, q\}$ and its dual of type $\{q, p\}$:

Definition 2.2.2. *An orientable regular map F of type $\{p, q\}$ respectively $\{q, p\}$ is a Riemannian manifold that is a regular branched cover of the triangle orbifold $(2, p, q)$. The automorphisms respectively orientation-preserving automorphisms of F are $\mathrm{Aut}_{reg}(F) = \mathrm{Isom}(F)$, $\mathrm{Aut}^+_{reg}(F) = \mathrm{Isom}^+(F)$.*

Notice that $\mathrm{Aut}_{reg}(F)$ is a finite group and $\mathrm{Aut}^+_{reg}(F)$ is isomorphic to the deck transformations of F as a covering space over the triangle orbifold.

The orientation-preserving automorphisms $\mathrm{Aut}^+_{reg}(F)$ of an orientable regular map are generated by R which rotates a polygon by one notch and S which rotates F about one vertex by one notch. Furthermore R and S can be chosen such that $T = RS$ reverses an edge, see Figure 2.2. Hence, $\mathrm{Aut}^+_{reg}(F)$ is a quotient of the orientation-preserving triangle group

$$[p, q]^+ \cong \langle R, S | R^p = S^q = (RS)^2 = 1 \rangle. \tag{2.1}$$

We usually only consider orientable regular maps F here. If F is orientable, it is called *reflexible* if there is an orientation-reversing automorphism, otherwise it is called *chiral*.

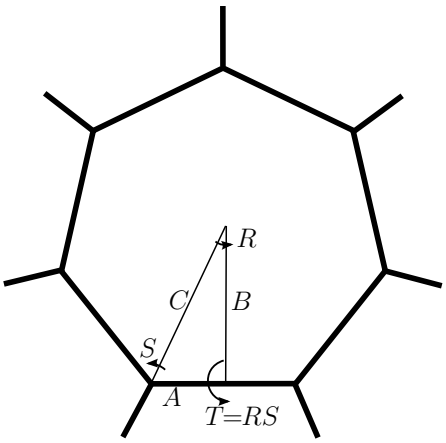

Figure 2.2: Generators of the triangle group or automorphisms of a regular map (here of type $\{7, 3\}$).

If F is reflexible or non-orientable, then all automorphisms $\mathrm{Aut}(F)$ are generated by R, S, and a reflection C. Hence, $\mathrm{Aut}(F)$ is a quotient of the triangle group $[p, q]$ (notation from [CM80]) given by

$$[p, q] \cong \langle R, S, C | R^p = S^q = (RS)^2 = C^2 = (CR^{-1})^2 = (CS)^2 = 1 \rangle \tag{2.2}$$

which is isomorphic to

$$[p, q] \cong \langle A, B, C | A^2 = B^2 = C^2 = (BC)^p = (CA)^q = (AB)^2 = 1 \rangle$$

where A, B, C are reflections about the sides of the orbifold triangle and the isomorphism is given by $R = BC, S = CA$. Notice that $[p, q]^+$ is the index 2 subgroup of $[p, q]$ generated by R and S.

In other words, the universal cover of a regular map is a regular tessellation of spherical, Euclidean, or hyperbolic 2-space. The corresponding triangle group is acting on this regular tessellation. The regular map is obtained as quotient of the space by a normal subgroup of the triangle group. Conder presents a regular map by giving the generators of this normal subgroup in [CD01]. Notice, however, that he denotes the reflection C by T.

2.2.2 Classification Results

This section reviews known classification results about regular maps. Coxeter and Moser [Cox69] and [CM80] review early classification results on regular maps. Conder and Marsden

have classified all regular maps up to genus $g = 101$ in 2006 [CD01, Con09]. We use their notation for regular maps.

For genus $g = 0$, orientable regular maps are just the Platonic solids.

For $g = 1$, there are only two possible types of regular maps up to duality: $\{3, 6\}$ and $\{4, 4\}$. The universal covering space of such a map has vertices which can be identified with the lattice $\mathbb{Z}[\zeta] \subset \mathbb{C}$ with $\zeta = e^{2\pi i/3}$ respectively $\mathbb{Z}[i] \subset \mathbb{C}$. Each regular map can be obtained by dividing $\mathbb{Z}[\zeta] \subset \mathbb{C}$ by an ideal $\langle z \rangle$ in the Eisenstein integers $\mathbb{Z}[\zeta]$ respectively Gaussian integers $\mathbb{Z}[i]$ to obtain a torus. This completely classifies orientable regular maps of genus 1.

A particular interesting regular map is the *Klein quartic* (R3.1 in [Con09]). This regular map of genus $g = 3$ and type $\{3, 7\}$ can also be described as algebraic curve [Kle78, Kle99], see Section 1.2.1. Hurwitz showed that $\left|\mathrm{Aut}^+_{reg}(F)\right| \leq 84(g-1)$ for any Riemann surface with $g \geq 2$ and, in particular, any orientable regular map F [Hur92]. A regular map that achieves this upper bound is called a *Hurwitz surface*. Equivalently, a Hurwitz surface is a regular cover of the minimal volume hyperbolic orbifold of type $(2, 3, 7)$, hence, it is a regular map of type $\{3, 7\}$ or $\{7, 3\}$. The Klein quartic is the minimal volume Hurwitz surface. The next Hurwitz surface is the *Macbeath surface* (R7.1 in [Con09]) of genus $g = 7$ which has orientation-preserving symmetry group $\mathrm{PSL}(2, 8)$. For genus $g = 14$, there are three different Hurwitz surfaces up to duality [Con09], two of them have the same symmetry group $\mathrm{PSL}(2, 13)$ but come from different representations of $\mathrm{PSL}(2, 13)$ as quotients of the $[3, 7]^+$ triangle group (see [Mac99] or [CM80, Chapter 7.5]). Macbeath constructs an infinite family of Hurwitz surfaces [Mac61]. Starting with a Hurwitz surface F of genus g, Macbeath uses the holonomy $\pi_1(F) \twoheadrightarrow H_1(F; \mathbb{Z}/m)$ to construct a covering space that is a new Hurwitz surface of genus $(g-1)m^{2g}$. Larsen shows that the genuses g of Hurwitz surfaces are distributed like perfect cubes [Lar01]. The connections of the Klein quartic to other areas of mathematics such as Number Theory and Algebraic Geometry are covered in [Lev99].

2.3 Review of Orbifold Theory

This section is reviewing orbifolds, the orbifold fundamental group, and covering space theory for orbifolds. It can be skipped by readers familiar with orbifolds. It is assumed that the reader is familiar with covering space theory for topological spaces as it is treated in, e.g., [Hat02, Chapter 1].

Orbifolds and the orbifold fundamental group are also treated in [Rat94] and [Sco83]. A visual explanation of 2-orbifolds can be found in [CDGT91].

2.3.1 Orbifolds

We consider only 2- and 3-dimensional orientable orbifolds M. Recall that an orbifold is locally modeled on the quotient of a subset V_i of Euclidean n-space E^n by a discrete subgroup Γ_i of $\mathrm{SO}(n)$. Or more formally, M is a topological manifold $X(M)$ together with compatible orbifold charts $\{\phi_i : V_i \twoheadrightarrow V_i/\Gamma_i \cong U_i\}$ where $V_i \subset E^n$ and $U_i \subset X(M)$ are open subsets and the U_i cover $X(M)$. Given a connected $U \subset U_i$, the preimage $\phi_i^{-1}(U)$ splits into several connected components, pick one, say V. Let Γ be the subgroup of Γ_i fixing V. The restriction of the orbifold chart ϕ_i yields a new orbifold chart $\phi : V \twoheadrightarrow V/\Gamma \cong U$. For example, when restricting a 3-orbifold near a trivalent vertex to a small neighborhood intersecting an edge, Γ becomes a cyclic group. Two orbifold charts on V_i and V_j are compatible if their restrictions to $V_i \cap V_j$ yield isomorphic Γ and the two restrictions are related through a Γ-equivariant isomorphism.

We use the notation $X(M)$ for the topological space underlying an orbifold M and $\Sigma(M)$ for the singular locus, i.e., the set of the points where there is no orbifold chart with trivial Γ_i.

A 2-orbifold has as underlying topological space $X(M)$ a genus g surface. The singular locus $\Sigma(M) \subset X(M)$ is a discrete set of points labeled by natural numbers. Near a singular point s of order k, the orbifold is modeled on a k-cyclic cover $V_i \to U_i$ branched over s.

Section 1.9 describes the structure of 3-orbifolds and their singular locus $\Sigma(M)$.

A manifold can be regarded as an orbifold with empty singular locus.

2.3.2 Orbifold Morphisms

General Orbifold Morphism

An orbifold morphism $t : F \to M$ is a mapping $X(F) \to X(M)$ of the underlying topological spaces that locally lifts to the orbifold charts. This means that every point $p \in X(F)$ has a neighborhood $U \ni p$ in $X(F)$ and a Γ-equivariant mapping $\tilde{t} : V \to V'$ making the following diagram commute:

$$\begin{array}{ccc} V & \xrightarrow{\tilde{t}} & V' \\ \downarrow{\scriptstyle \phi} & & \downarrow{\scriptstyle \phi'} \\ X(F) \supset U & \xrightarrow{t} & U' \subset X(M) \end{array}$$

where ϕ and ϕ' are (restrictions of) the orbifold charts on F and M and Γ is the group associated to the orbifold chart ϕ.

From 2-Orbifold to 3-Orbifold

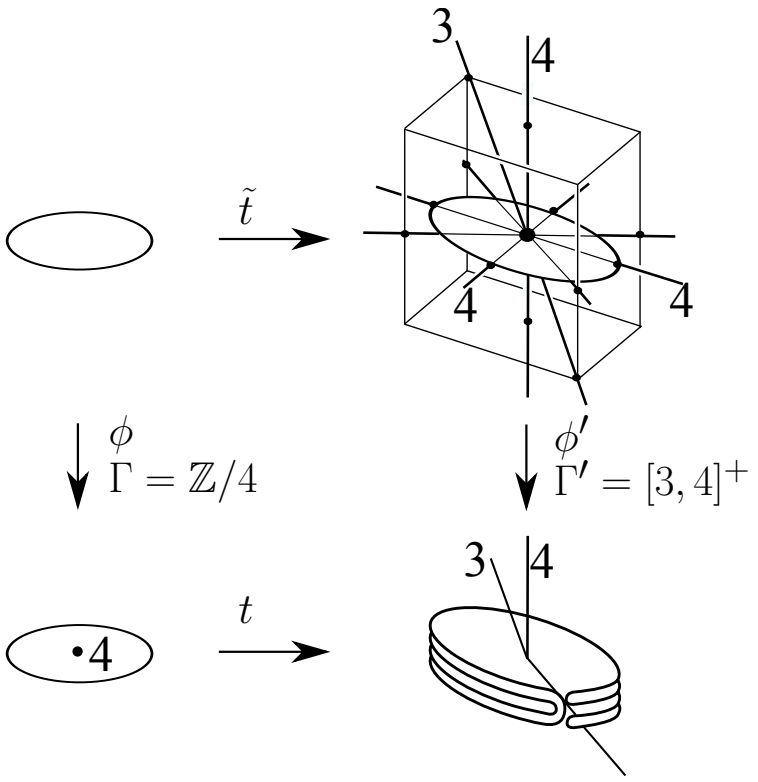

Figure 2.3: 2-orbfiold F intersecting vertex of $\Sigma(M)$.

An orbifold morphism $t : F \to M$ from a 2-orbifold to a 3-orbifold can potentially intersect $\Sigma(M)$ in a vertex of the trivalent graph. Figure 2.3 shows this in the case where F is locally modeled on a 4-cyclic branched cover and M is locally modeled on the quotient by $\Gamma' = [3, 4]^+$, the rotations of a cube. The figure shows the orbifold morphism $t : F \to M$ and its lift to the orbifold charts. On the orbifold charts, we have a $\mathbb{Z}/4$-equivariant embedding of the disk into a cube. We can perturb the embedding to avoid the center of the cube. Notice that on the orbifold charts, the perturbed disk intersects an order 3 axis, hence, a non-singular n point of F is sent to M. Sending a non-singular point n to a singular point possible because the perturbed $X(F) \to X(M)$ is a 3-cyclic cover branched at n.

Similarly, $X(F)$ might intersect $\Sigma(M)$ non-transversely. We again perturb the morphism a bit. From now on, we assume that $X(F)$ intersects $\Sigma(M)$ transverse, and if dim $F = 2$ and dim $M = 3$, $X(F)$ does not intersect the vertices of the trivalent graph $\Sigma(M)$.

2.3.3 Orbifold Fundamental Group

Definition 2.3.1. *The orbifold fundamental group of an orientable orbifold (M, p) has as elements the equivalence classes of loops in $X(M) \setminus \Sigma(M)$ and the usual addition:*

$$\pi_1^{orb}(M,p) = \frac{\{\gamma : (S^1, p) \to (X(M) \setminus \Sigma(M), p)\}}{\sim}.$$

Here, we consider two loops γ and γ' equivalent if they span a cylinder in M, i.e., if there is an orbifold morphism $h : (S^1 \times I, p \times I) \to (M, p)$ such that $h_{|0} = \gamma, h_{|1} = \gamma'$. In particular, a loop is zero, if it spans a disk $D \to M$.

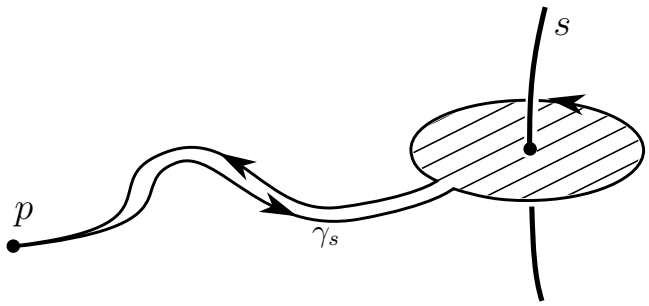

Figure 2.4: Simple singular loop.

Definition 2.3.2 (Simple singular loop)**.** *Let (M, p) be an orientable 2- or 3-orbifold. Take a loop bounding a small embedded disk in $X(M)$ that intersects $\Sigma(M)$ in one point s (not being a vertex of the trivalent singular graph if $\dim M = 3$). Connecting this loop through a path to p gives an element $\gamma_s \in \pi_1(X(M) \setminus \Sigma(M), p)$, see Figure 2.4. We call γ_s a* **simple singular loop (ssl)**. *The order $\operatorname{ord}(\gamma_s)$ of γ_s is the order of s as singular point.*

Remark 2.3.3. Given s, the loop $\gamma_s^{\pm 1}$ is defined only up to conjugacy, but this choice does not matter in theorems involving, e.g., the order of γ_s.

By Lemma 2.3.5 proven later, the following definition is equivalent to Definition 2.3.1:

Definition 2.3.4. *Let (M, P) be an orientable 2- or 3-orbifold. The orbifold fundamental group $\pi_1^{orb}(M, p)$ is*

$$\pi_1^{orb}(M,p) = \frac{\pi_1\left(X(M) \setminus \Sigma(M), p\right)}{\langle \gamma_s^{\operatorname{ord}(\gamma_s)} : \gamma_s \text{ is ssl} \rangle}.$$

Simple Singular Loops

Consider a disk D without singular points and embed it topologically into $X(M)$ such that it intersects the singular locus of $X(M)$ in a single point s of order k. The embedding of the topological spaces is not an orbifold morphism because there is no choice for the top horizontal arrow making the following diagram commute:

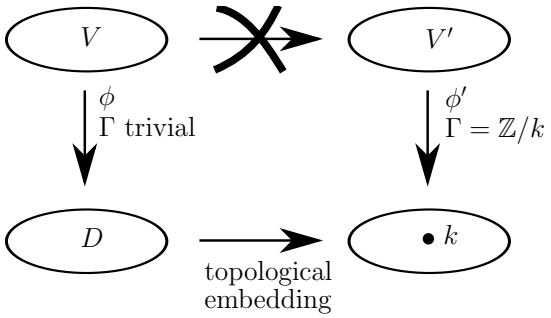

Connecting this disk by a little strip to the base point p gives again a disk whose boundary is a ssl γ_s. Because the embedding of D into the topological space $X(M)$ is not an orbifold morphism, this disk does not trivialize γ_s in $\pi_1^{orb}(M,p)$. In fact, γ_s is non-trivial in $\pi_1^{orb}(M,p)$ if M is a good orbifold.

However, the loop γ_s^k bounds a disk $D \to X(M)$ mapped through a branched k-cyclic cover. This mapped disk lifts to an embedding on the orbifold charts. Hence, $D \to M$ is an orbifold morphism making γ_s^k zero in $\pi_1^{orb}(M,p)$:

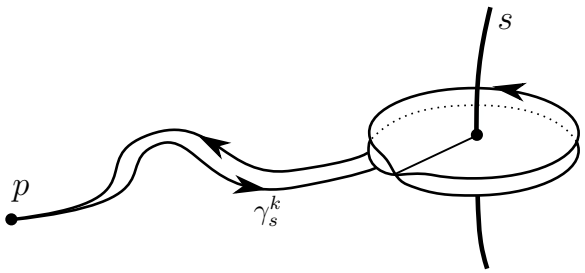

Orbifold Morphisms and Immersions in Dimension 2 and 3

In general, if a topological morphism $t : X(F) \to X(M)$ sends an order m singular point s in F to an order k singular point in M and t is a n-cyclic cover branched over the singular point near that point, then it is an orbifold morphism near this point if and only if $k|mn$. In this case, an l-cyclic cover with $l = mn/k$ makes the following diagram commute (where

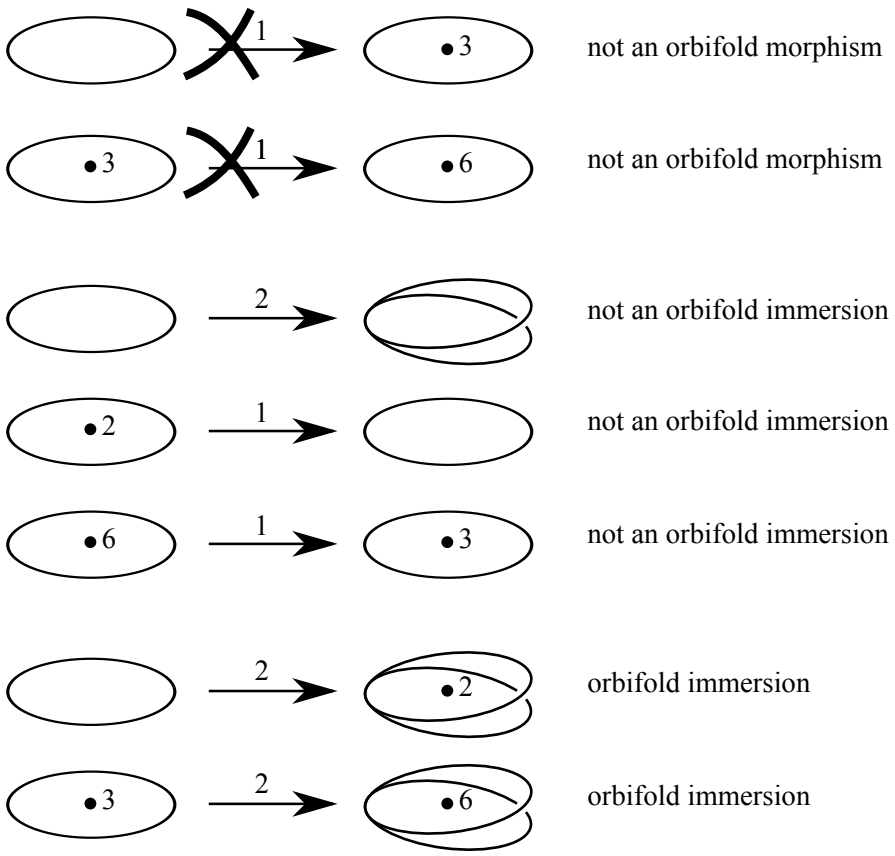

Figure 2.5: Examples of orbifold morphisms and immersions and non-morphisms.

labels on arrows denote the degree of the cyclic branched cover):

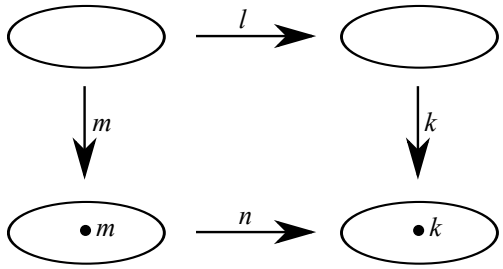

(2.3)

If $l = \pm 1$, the orbifold morphism is an orbifold immersion because it is an immersion when lifted to the orbifold charts.

Figure 2.5 shows examples of topological mappings $X(F) \to X(M)$ that are or are not orbifold morphisms or immersions.

Orbifold Fundamental Group Revisited

The group homomorphism

$$j : \pi_1(X(M) \setminus \Sigma(M), p) \to \pi_1^{orb}(M, p) \tag{2.4}$$

is well defined: two loops equivalent in $\pi_1(X(M) \setminus \Sigma(M), p)$ are equivalent in $\pi_1^{orb}(M, p)$ because a cylinder $(S^1 \times I, p \times I) \to (X(M) \setminus \Sigma(M), p)$ between them is a valid orbifold morphism into M.

Lemma 2.3.5. *Definition 2.3.1 and 2.3.4 of the orbifold fundamental group $\pi_1^{orb}(M, p)$ are equivalent.*

Proof. We already have seen that $\gamma_s^{\mathrm{ord}(s)}$ is in $\ker(j)$. It is left to show that a loop trivial in $\pi_1^{orb}(M, p)$ is in $\left\langle \gamma_s^{\mathrm{ord}(\gamma_s)} \right\rangle$, i.e., if a loop γ bounds a disk $i : D \to M$ in M, then γ is homotopic to a product of ssl's. Assume that $i^{-1}(\Sigma(M))$ consists of only one point $s \in D$ mapped to an order k singular point in M. We can pick a small disk-like neighborhood U of s such that $i_{|U}$ is topologically a mk-cyclic cover branched over s. Connect U to the base-point p by a path in D. The boundary of U together with the path is $\gamma_{i(s)}^{mk}$ with $\gamma_{i(s)}$ being a ssl. The rest of the disk serves as homotopy between $\gamma_{i(s)}$ and $\gamma = \partial D$ in $(X(M) \setminus \Sigma(M), p)$. If several points $s_i \in D$ are sent to $\Sigma(M)$, pick disjoint neighborhoods U_i and disjoint paths to p. Now γ is homotopic to a product of powers of ssl's, see Figure 2.6. □

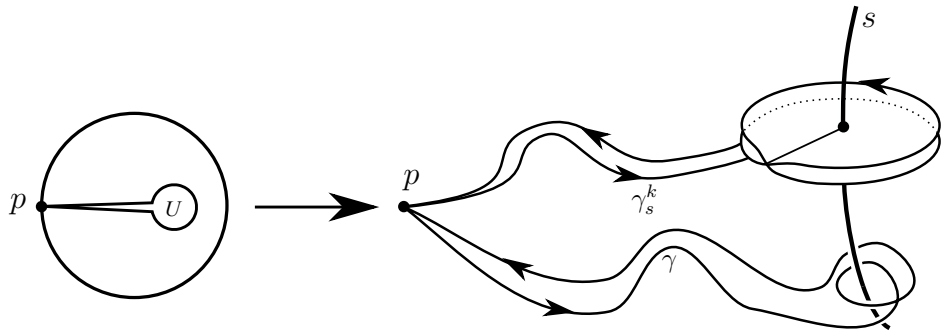

Figure 2.6: A disk intersecting the singular locus once is a power of a ssl.

2.3.4 Orbifold Covering Space Theory

Orbifold Covering Spaces

An orbifold morphism $p : \tilde{M} \to M$ is an orbifold covering space if every point $\alpha \in M$ has a neighborhood U_α such that p restricted to U_α and lifted to the orbifold charts is a topological covering space. In other words, $p^{-1}(U_\alpha) = \cup_i V_{i,\alpha}$ is a union of disjoint open sets $V_{i,\alpha}$ such that $p_{|V_{i,\alpha}}$ is an orbifold immersion onto U_α.

Notice that an orbifold covering space $p : \tilde{M} \to M$ can be a branched cover on the underlying topological spaces, but when lifted to the orbifold charts, the branch points of p have to disappear.

Example 2.3.6. Every orbifold immersion in Figure 2.5 is a covering space.

Example 2.3.7. Given a smooth, orientable manifold M and a properly discontinuous, orientation-preserving group action G, the quotient space M/G is an orbifold, the singular points coming from fixed points of M under an element $g \in G$. The morphism $M \to M/G$ is a covering space in the orbifold category.

Example 2.3.8. The triangle group $[p, q]^+$ is acting on S^2, E^2, respectively, $\mathbb{H}^2$. The quotient space is topologically S^2 with three singular points of order two, p, and q. We call this orbifold the triangle orbifold. Regular maps are exactly the regular covering spaces of a triangle orbifold that are compact and manifolds.

Universal Covering Space

Definition 2.3.9. *Let (M, p) be a connected, orientable orbifold. The universal orbifold covering space $(\tilde{M}, p)$ is the unique orbifold covering space with $\pi_1^{orb}(\tilde{M}, p) = 0$.*

The universal orbifold covering space always exists. To see this, drill out the singular locus: $X(M) \setminus \Sigma(M)$. Take the normal subgroup G of $\pi_1(X(M) \setminus \Sigma(M), p)$ generated by all $\gamma_s^{\mathrm{ord}(s)}$ where γ_s is a ssl around the singular point s of order $\mathrm{ord}(s)$. By [Hat02, Theorem 1.38], G determines a (topological) covering space of $X(M) \setminus \Sigma(M)$. Fill back the singular locus into this covering space to obtain $\tilde{M}$.

Definition 2.3.10. *Let (M, p) be a connected, orientable orbifold. We say (M, p) is good if the universal orbifold covering space is a manifold.*

Remark 2.3.11. It is already sufficient (and necessary) that (M, p) has any covering space that is a manifold (i.e., any covering space branched over the singular locus such that the singular locus disappears). This is equivalent to saying that the order of a ssl γ_s as group element in $\pi_1^{orb}(M, p)$ is the order of the singular point s.

Example 2.3.12. Take S^2 and add a single singular point s. This is a bad orbifold because a ssl γ_s is zero in $\pi_1^{orb}(M, p)$.

Classification of Orbifold Covering Spaces in Category Theory Language

Classical results about topological covering spaces (see [Hat02, Chapter 1]) carry over to orbifold covering spaces when replacing the fundamental group by the orbifold fundamental group.

The following theorem summarizes these results in the language of categories:

Theorem 2.3.13. *Let (M, p) be an orientable, connected orbifold. The category of orbifold covering spaces $(\bar{M}, p) \to (M, p)$ is equivalent to the category of pointed $\pi_1^{orb}(M, p)$-sets.*

Proof. Given a covering space $(\bar{M}, p) \to (M, p)$, the preimages of p form a set with a $\pi_1^{orb}(M, p)$-action. This is one of the functors giving the category equivalence.
Given a $\pi_1^{orb}(M, p)$-set X, the other functor yields the associated bundle $(\bar{M}, p) \to (M, p)$. In other words, take a disjoint copy of the universal covering space for each element in X: $(\tilde{M} \times X, p)$. There is the $\pi_1^{orb}(M, p)$-action on $\tilde{M}$ by deck transformations and there is the given $\pi_1^{orb}(M, p)$-action on the set X. Hence, $\pi_1^{orb}(X, p)$ acts on $(\tilde{M} \times X, p)$. Divide out by this action to obtain the covering space $(\bar{M}, p) \to (M, p)$. □

We now define the contravariant functors Cov and $\pi_1^{orb}-$Sets from the category Orb of connected, orientable orbifolds with base point to the category Cat of categories.

Let Cov be the functor that assigns to an orbifold the category of covering spaces:

$$\begin{array}{lll} \text{Cov}: & \text{Orb} & \to \quad \text{Cat}^{op} \\ & (M,p) & \mapsto \quad \{(\bar{M},p) \to (M,p)\}. \end{array}$$

Similarly, let $\pi_1^{orb}-$Sets be the functor that assigns to an orbifold (M,p) the category of pointed $\pi_1^{orb}(M,p)$-sets:

$$\begin{array}{lll} \pi_1^{orb}-\text{Sets}: & \text{Orb} & \to \quad \text{Cat}^{op} \\ & (M,p) & \mapsto \quad \{\pi_1^{orb}(M,p)-\text{Sets}\}. \end{array}$$

The constructions in the proof are inverse natural transformations between the functors Cov and $\pi_1^{orb}-$Set.

Classification of Orbifold Covering Spaces

Corollary 2.3.14. *Connected covering spaces of an orientable, connected orbifold (M,p) correspond to subgroups of $\pi_1^{orb}(M,p)$ [Hat02, Theorem 1.38], regular covering spaces to normal subgroups [Hat02, Proposition 1.39]. Finite covering spaces can be specified by a representation of $\pi_1^{orb}(M,p)$ into S_n, namely by the action of $\pi_1^{orb}(M,p)$ on the fiber. If the covering space is regular, the fiber becomes a group G and the covering space is specified by a representation of $\pi_1^{orb}(M,p)$ into a group G.*

We call this representation $\pi_1^{orb}(M,p) \to G$ the *holonomy* of the covering space.

Corollary 2.3.15. *A regular covering space is a manifold if the holonomy sends an ssl to an element in G of the same order.*

2.4 Standard Orbifold Handle Decomposition

A surface can be glued together from 0-, 1-, and 2-handles yielding a handle decomposition (see, e.g., [GS99] for definition of handles and handle decomposition). Defining an *orbifold 0-handle* as a disk with a singular point, we can similarly obtain handle decompositions of 2-orbifolds. In other words, starting with a handle decomposition of a surface, we turn some 0-handles into orbifold 0-handles to add singular points to the surface yielding a 2-orbifold.

If the orbifold F has a base point p, we require p to be in its own 0-handle.

2.4.1 Standard Handle Decomposition

Usually, we consider the *standard handle decomposition* of a 2-orbifold (F, p) shown in Figure 2.7. This handle decomposition consists of the minimal number of handles such that we obtain the following finite presentation of the orbifold fundamental group:

$$\pi_1^{orb}(F,p) = \langle \sigma_1, \ldots, \sigma_k, \alpha_1, \beta_1, \alpha_2, \ldots, \beta_g | \prod \sigma_j \prod [\alpha_i; \beta_i] = \sigma_1^{\mathrm{ord}(s_1)} = \cdots = \sigma_k^{\mathrm{ord}(s_k)} = 1 \rangle.$$

In other words, this handle decomposition has the ordinary 1-handles of a genus g surface plus an extra orbifold 0-handle and 1-handle for each singular point $s_j \in \Sigma(F)$, the extra 1-handle connecting s_j to p.

If we remove the singular points from F, we obtain the following finite presentation of the fundamental group of the punctured surface:

$$\pi_1(X(F) \setminus \Sigma(F), p) = \langle \sigma_1, \ldots, \sigma_k, \alpha_1, \beta_1, \alpha_2, \ldots, \beta_g | \prod \sigma_j \prod [\alpha_i; \beta_i] = 1 \rangle.$$

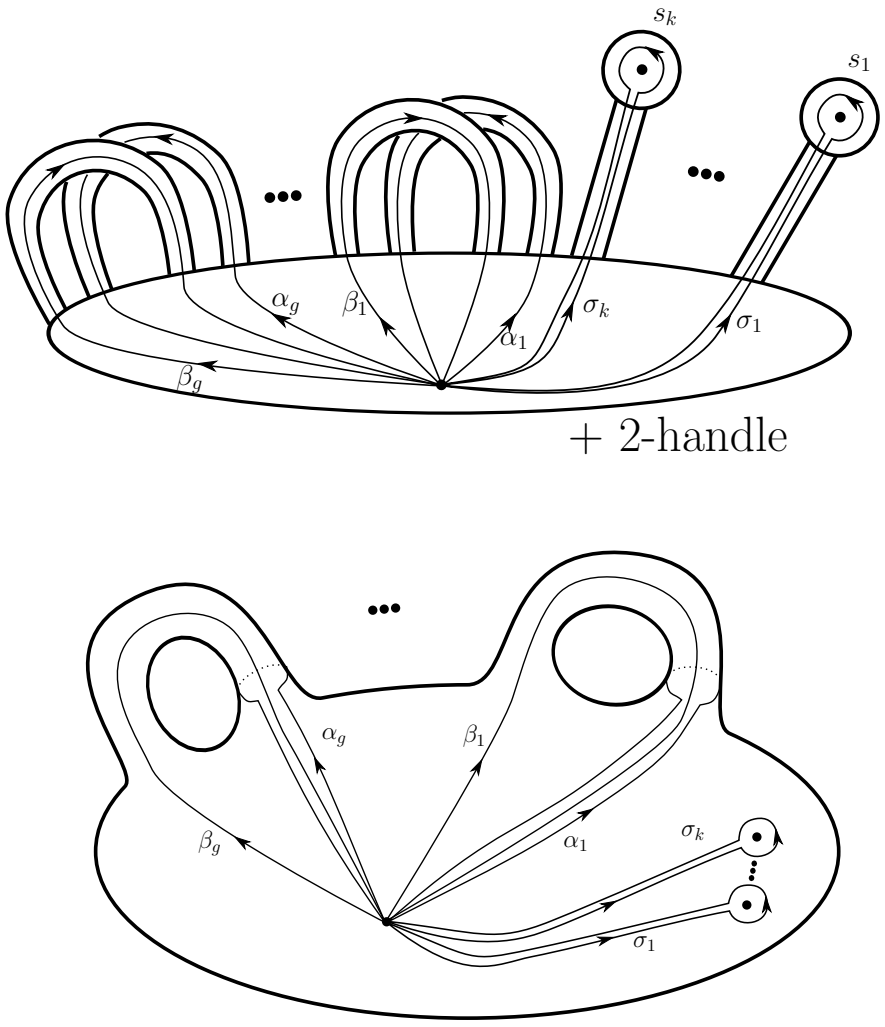

Figure 2.7: Standard handle decomposition of a 2-orbifold (F, p) with k singular points and genus g and standard generators of $\pi_1^{orb}(F, p)$.

2.5 Equivalence of Equivariant Morphisms

Let F be a regular map and M be a 3-manifold.

Definition 2.5.1. *Let $H \subseteq \mathrm{Aut}^+_{reg}(F), B \subseteq \mathrm{Aut}^+(M)$ be subgroups of automorphisms of the spaces F and M and $\eta : H \cong B$ be an isomorphism. An (H, B, η)-equivariant morphism is a morphism $F \to M$ such that for every $h \in H$, the following diagram commutes:*

$$\begin{array}{ccc} F & \longrightarrow & M \\ \downarrow{\scriptstyle h} & & \downarrow{\scriptstyle \eta(h)} \\ F & \longrightarrow & M \end{array}$$

Definition 2.5.2. *Let $m, m' : F \to M$ be an (H, B, η)- respectively (H', B', η')-equivariant morphism. The morphisms are equivalent if there exists $i \in \mathrm{Aut}_{reg}(F)$ and $c \in \mathrm{Aut}(M)$ such that the following conditions hold:*

1. *The following diagram commutes:*

$$\begin{array}{ccc} F & \xrightarrow{m} & M \\ \downarrow{\scriptstyle i} & & \downarrow{\scriptstyle c} \\ F & \xrightarrow{m'} & M \end{array}$$

2. *The respective groups are related through conjugation:*

$$H' = iHi^{-1}, B' = cBc^{-1}.$$

3. *The above diagram commutes in an H-equivariant fashion. More precisely, the following diagram commutes:*

$$\begin{array}{ccc} h & H & b \\ \downarrow & \downarrow \quad \xrightarrow[\eta]{\cong} \quad \downarrow & \downarrow \\ ihi^{-1} & H' \xrightarrow[\eta']{\cong} B' & cbc^{-1} \end{array}$$

2.6 Translation from Equivariant Morphisms to Orbifolds

Let F and M be a 2-, respectively, 3-dimensional smooth orientable manifolds. Given a subgroup $H \subset \mathrm{Aut}^+_{reg}(F)$, we obtain a covering space $F \to F/H$ where F/H is the quotient orbifold. The covering space has a holonomy $\pi_1^{orb}(F/H, p) \twoheadrightarrow H$. Namely, $p \in F/H$ has as preimage an H-fiber with $\pi_1^{orb}(F/H, p)$-action. The orbifold F/H together with the holonomy $\pi_1^{orb}(F/H, p) \twoheadrightarrow H$ encodes all information to recover F and the H-action. Similarly, for M/B.

Lemma 2.6.1. *(H, B, η)-equivariant morphisms $(F, p) \to (M, p)$ are in 1-1 correspondence with orbifold morphisms $(F/H, p) \to (M/B, p)$ such that the following diagram commutes:*

$$\begin{array}{ccc} \pi_1^{orb}(F/H, p) & \longrightarrow & \pi_1^{orb}(M/B, p) \\ \downarrow\!\!\downarrow & & \downarrow\!\!\downarrow \\ H & \xrightarrow{\quad\eta\quad} & B \end{array}$$

This holds for piecewise-linear/smooth functions, immersions, and embeddings.

Here, an orbifold immersion is an orbifold morphism that is an embedding when locally lifted to the orbifold charts. An **orbifold embedding** is an orbifold morphism that is an embedding on the topological spaces $X(F) \to X(M)$ and sends singular points to singular points of the same order.
To see that this is the right notion, notice that an (H, B, η)-equivariant embedding remains an embeddings when restricted to the interior of a fundamental domain of M under the B-action. Hence, an orbifold embedding $F \to M$ has to have the property that $X(F) \setminus \Sigma(F) \to X(M) \setminus \Sigma(M)$. This implies that near a singular point of F, the mapping $X(F) \to X(M)$ has degree one, and the singular point of F has to go to a singular point of the same degree.

2.7 Theory about Mappings and Immersions

Let (F, p) and (M, p) be good, connected, orientable orbifolds of dimension 2 and 3, respectively. Let $\tau : \pi_1^{orb}(F, p) \to \pi_1^{orb}(M, p)$ be a group homomorphism.

In this section, we list necessary and sufficient conditions for τ to be induced by an actual orbifold morphism or immersion $(F, p) \to (M, p)$. Theorem 2.7.7 does this in the mapping case. Lemma 2.7.6 and Theorem 2.7.30 do this in the immersion case.

These results are obtained by successively mapping the 0-, 1-, and 2-skeleton of F into M. Section 2.7.1 defines *simple singular loops*, *singular loops*, and *multiple singular loops* as extra

data on π_1^{orb}. They serve to detect when τ allows mapping and immersing the 0-skeleton in Section 2.7.2. The 1-skeleton is immersed into M in Section 2.7.3.

For the immersion case, we also need to understand when a 2-handle can be immersed into M so that it glues to the 1-skeleton in a compatible way. The boundary of the 1-skeleton consists of immersed ribbons (framed knots if perturbed). In Section 2.7.5, we define a $\mathbb{Z}/2$-framing invariant of an immersed ribbon that detects whether the immersed ribbon bounds an immersed 2-handle. In Section 2.7.6, we list all possible regular homotopy classes of immersions of the 1-skeleton. In Section 2.7.7, we apply the $\mathbb{Z}/2$-framing invariant to the immersions of the 1-skeleton yielding a cohomology class $[c(\tau)] \in H^2(X(F); \mathbb{Z}/2)$ that – if defined – is an obstruction to τ being realized by an immersion.

Section 2.7.8 classifies all regular homotopy classes of immersions $(F, p) \to (M, p)$ inducing τ.

2.7.1 Definitions of Singular Loops

In this section, we define three types of loops in π_1^{orb} to detect a necessary condition on a homomorphism $\tau : \pi_1^{orb}(F, p) \to \pi_1^{orb}(M, p)$: τ has to send a simple singular loop to

- a singular loop (sl) if τ is induced by an orbifold morphism,
- a multiple singular loop (msl) if τ is induced by an orbifold immersion,
- a simple singular loop (ssl) if τ is induced by an orbifold embedding.

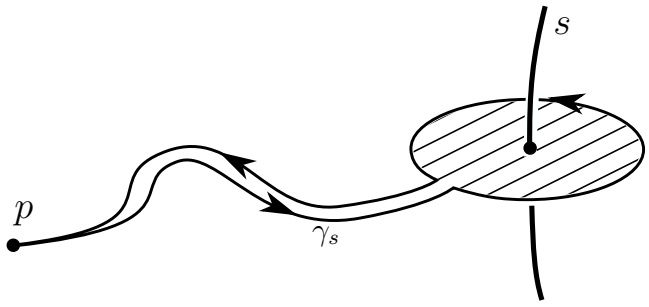

Figure 2.8: Simple Singular Loop.

Definition 2.7.1 (Simple singular loop)**.** *Let (M, p) be a good, connected, orientable 2- or 3-orbifold with base point. Take a loop bounding a small embedded disk in $X(M)$ that intersects $\Sigma(M)$ in one point s (not being a vertex of the trivalent singular graph if $\dim M = 3$).*

Connecting this loop through a path to p gives an element $\gamma_s \in \pi_1^{orb}(M,p)$*, see Figure 2.8. We call* γ_s *a* **simple singular loop (ssl)**.

Remark 2.7.2. Up to conjugacy and taking inverses, a ssl γ_s is determined by the point s.

Definition 2.7.3. *A* **singular loop (sl)** *is a (possibly trivial) multiple* γ_s^p *of a ssl* γ_s*. A* **multiple singular loop (msl)** *is a non-trivial element* $\gamma_s^n \in \pi_1^{orb}(M,p)$ *such that* $n \in \mathbb{Z}$ *divides* $\mathrm{ord}\,(\gamma_s)$ *and* γ_s *is a ssl.*

Remark 2.7.4. Consider an orbifold 0-handle of order two and four. Then there is an orbifold immersion from the first to the second orbifold 0-handle that is a 2-cyclic branched cover on the underlying topological space. Hence, the ssl is taken to twice a ssl in π_1^{orb}, i.e., a msl, motivating the above definition.

2.7.2 Mapping and Immersing Orbifold 0-Handles

Recall that an *orbifold 0-handle* was defined as a disk with a singular point. Consider a mapping of an orbifold 0-handle D with singular point d of order m into a good, connected, orientable 3-orbifold (M,p). The boundary of D in M represents a conjugacy class in $\pi_1^{orb}(M,p)$. Notice that we can homotope $\gamma_d = \partial D$ to a loop arbitrarily close to the singular point in D. Hence, the image of ∂D has to be a sl γ_s^n where s is the image of d. Lifting $D \to M$ to the orbifold charts, we obtain the following commutative diagram with D on the left and a neighborhood in M on the right:

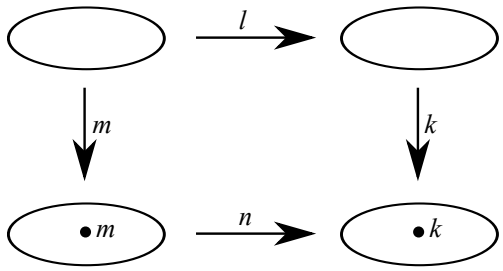

(2.5)

Lemma 2.7.5. *Let* D *be an orbifold 0-handle with singular point* d *of order* m *and* (M,p) *be a good, connected, orientable 3-orbifold. The elements* $\gamma \in \pi_1^{orb}(M,p)$ *represented (up to conjugacy) by mappings* $D \to M$ *are exactly the sl's* γ_s^n *with* $\mathrm{ord}(\gamma_s)|mn$*. The elements represented by immersions are exactly the sl's* γ_s^n *with* $\mathrm{ord}(\gamma_s) = \pm mn$*, i.e., the msl's* γ_s^n *with* $\mathrm{ord}(\gamma_s^n) = \pm m$*.*

Proof. Commutative Diagram 2.5 implies $mn = lk$ where $k = \mathrm{ord}(\gamma_s)$. If $D \to M$ is an immersion, then $l = \pm 1$. Hence, the conditions on γ are necessary.
Given a sl $\gamma_s^n \in \pi_1^{orb}(M,p)$, pick an n-fold cover of the underlying topological spaces $X(D) \to$

$X(M)$ branched over d mapping d to s. The conditions on γ_s^n are sufficient to complete Commutative Diagram 2.5. Hence, we obtain an orbifold morphism, respectively, immersion $D \to M$. □

2.7.3 Mapping and Immersing the 1-Skeleton

Lemma 2.7.6. *Let F_1 be the 1-skeleton of a good, connected, orientable 2-orbifold (F, p). Let (M, p) be a good, connected, orientable 3-orbifold. Let $\tau : \pi_1^{orb}(F_1, p) \to \pi_1^{orb}(M, p)$ be a group homomorphism. Then τ is induced by a mapping $t_1 : (F_1, p) \to (M, p)$ if and only if τ sends every ssl $\gamma_d \in \pi_1^{orb}(F_1, p)$ to a sl. τ is induced by an immersion if and only if τ sends every ssl $\gamma_d \in \pi_1^{orb}(F_1, p)$ to a msl and* $\mathrm{ord}(\tau(\gamma_d)) = \mathrm{ord}(\gamma_d)$.

Proof. Consider an orbifold 0-handle D with singular point d of order m in F_1. ∂D represents (up to conjugacy) a ssl $\gamma_d \in \pi_1^{orb}(F_1, p)$. $\mathrm{ord}(\tau(\gamma_d))|\mathrm{ord}(\gamma_d)$ because τ is a group homomorphism. Assume $\tau(\gamma_d)$ is a sl γ_s^n, then

$$\mathrm{ord}(\tau(\gamma_d)) = \mathrm{ord}(\gamma_s^n) = \frac{\mathrm{ord}(\gamma_s)}{\gcd(\mathrm{ord}(\gamma_s), n)} | \mathrm{ord}(\gamma_d) = m.$$

Hence, by Lemma 2.7.5, we can map D into M to represent $\tau(\gamma_d)$ up to conjugacy.
Similarly, if $\tau(\gamma_d)$ is a msl with $\mathrm{ord}(\tau(\gamma_d)) = \mathrm{ord}(\gamma_d)$, the same lemma implies that we can immerse the 0-handle.

The (non-orbifold) 0-handles can be immersed arbitrarily as long as their boundaries don't intersect and the base point $p \in F_1$ goes to the base point $p \in M$.

It is left to immerse the 1-handles. Pick an order for doing this such that each 1-handle is connected to p by previously immersed 1-handles. If a 1-handle is connecting an orbifold 0-handle D with singular point d, we get a ssl $\gamma_d \in \pi_1^{orb}(F_1, p)$. Immerse the 1-handle so that connecting the image of ∂D to p via the core of the 1-handle gives the conjugate equal to $\tau(\gamma_d)$ in the conjugacy class represented by ∂D. If a 1-handle closes a loop γ, pick the core to represent $\tau(\gamma)$. Otherwise, immerse the 1-handle arbitrarily. □

2.7.4 Main Theorem for Mappings

Theorem 2.7.7. *Let (F, p) respectively (M, p) be a good, connected, orientable 2- respectively 3-orbifold with base points. Let $\tau : \pi_1^{orb}(F, p) \to \pi_1^{orb}(M, p)$ be a group homomorphism. Then τ is induced by an orbifold morphism $t : (F, p) \to (M, p)$ if and only if τ sends sl's to sl's.*

Proof. Compose τ with the inclusion $F_1 \subset F$. Lemma 2.7.6 states that the above condition is sufficient and necessary for the 1-skeleton F_1 to map into M.
Each 2-handle in F is attached to F_1 along a circle γ that is zero in $\pi_1^{orb}(F,p)$. The image of γ in $\pi_1^{orb}(M,p)$ is also zero, hence, it spans some disk in M. Map the 2-handle onto this disk. □

2.7.5 Immersed Ribbons Spanning Immersed Disks

This section reviews framings of knots. Theorem 2.7.16 is the result needed later in the Main Theorem for Immersions.

Given a knot K in a connected, orientable 3-manifold M, a framing is specified by a nowhere-zero transverse vector field v to K. We denote a framed knot by (K,v). A framing v can also be thought of as a curve on the boundary $\partial\mathcal{N}(K)$ of a tubular neighborhood of K. A framed knot (K,v) is also equivalent to an embedded ribbon $S^1 \times I \to M$, one of the boundary components being K. We have the following well-known theorem:

Theorem 2.7.8. *Fixing the isotopy class of K, isotopy classes of framed knots (K,v) correspond to integers $\mathbb{Z}$.*

Definition 2.7.9. *If K is a null-homologous knot, the longitude on $\partial\mathcal{N}(K)$ is the generator of* $\mathrm{im}(H_1(M \setminus \mathcal{N}(K)) \to H_1(\partial\mathcal{N}(K)))$.

By the Mayer-Vietoris sequence, the longitude (up to multiplicity) is induced by any mapped surface $(S,\partial S) \to (M \setminus \mathcal{N}(K), \partial\mathcal{N}(K))$. The longitude is also realized by an embedded surface (not proven here). For a projection of a knot in S^3, the embedded surface can be seen directly using Seifert's algorithm.

Remark 2.7.10. We can also obtain the longitude from a surface $(S,\partial S) \to (M, \partial\mathcal{N}(K))$ in M if we count the intersections of S with K as meridians (after perturbing S to intersect K transversely). More precisely, S intersects $\mathcal{N}(K)$ in disks. Remove them from S producing new boundary components ∂S that are meridians in $\partial\mathcal{N}(K)$.

Remark 2.7.11. If K is not homologically trivial, a canonical longitude might not exist, e.g., take the core of a solid torus $S^1 \times D^2$.

Theorem 2.7.12. *If K is null-homologous in M, the correspondence in Theorem 2.7.8 is canonical, the 0-framing of K being given by a longitude on $\partial\mathcal{N}(K)$.*

Definition 2.7.13. *The framing number $f(K,v)$ is the number of right-handed full-twists needed to obtain the framing (K,v) from the 0-framing of K.*

Remark 2.7.14. Given (K, v), we can compute the framing number as the linking number of K and the curve in $\partial\mathcal{N}(K)$.
In a knot projection, the blackboard framing has framing number given by the writhe [GS99, Proposition 4.5.6] which can be computed counting the crossings of K with the appropriate signs.

Let us weaken the conditions on K and let K be an immersion $S^1 \to M$, thus allowing self-intersections. An immersed ribbon is an immersion of an annulus $S^1 \times I$ into M. We regard two immersed ribbons as equivalent if they are related through a regular homotopy. Generically, an immersed ribbon is a framed knot (K, v) and we can compute the framing number $f(K, v)$ if K is null-homologous. If K has a self-intersection, there is a choice how to perturb (K, v), hence, even for null-homologous (K, v), the framing number is defined only modulo two in this case. Thus, Theorem 2.7.12 becomes (notice that two homotopic immersed loops $S^1 \to M$ are also regular homotopic):

Theorem 2.7.15. *Fixing the (regular) homotopy class of K, regular homotopy classes of immersed ribbons (K, v) correspond to elements in $\mathbb{Z}/2$.*

This is proven later. If K is null-homologous, Theorem 2.7.12 applies again for immersed ribbons and $\mathbb{Z}/2$, and, if K is null-homotopic, the theorem becomes:

Theorem 2.7.16. *If K is null-homotopic, the immersed ribbon (K, v) has a canonical framing number in $\mathbb{Z}/2$ that is 0 if and only if (K, v) is spanned by an immersed disk in M. If a (mapped) disk $D \to M$ spans an immersed ribbon (K, v), perturb the disk such that it is locally an embedding except at n places where it has a branch point, see Figure 2.9. Then the framing of (K, v) is n modulo 2. This also applies for a null-homotopic immersed ribbon (K, v) in a good, orientable, connected 3-orbifold.*

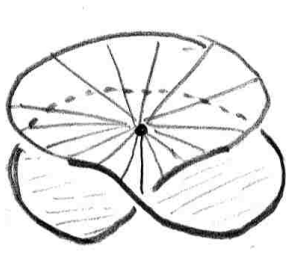

Figure 2.9: Branch point where a disk fails to be immersed.

Remark 2.7.17. The $\mathbb{Z}/2$-framing number of the blackboard framing of a projection of K is simply the number of crossings modulo two.

Example 2.7.18. Consider the blackboard framing of the projections of knots in S^3 in Figure 2.10. Notice that the cross-cap is a mapped disk inducing framing +1, but has a branch point.

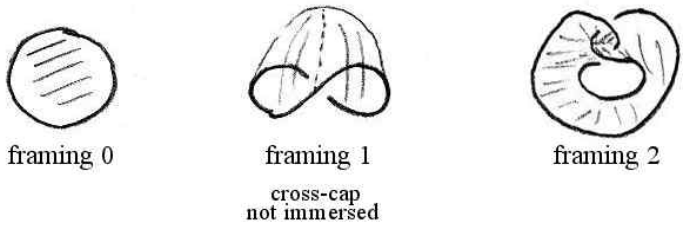

Figure 2.10: Blackboard framings of knots.

Remark 2.7.19. The condition that M is a good orbifold is necessary. The 2-orbifold F with $X(F) = S^2$ and $\Sigma(F)$ consisting of a single point s of order 2 is bad. Take a ribbon around the equator of F. The ribbon spans a disk, namely the hemisphere not containing s. Take the double cover of the ribbon. It also spans an immersed disk topologically branched over s. Compose the ribbons with the embedding $F \times p \subset F \times S^1$, now the two cases are related through a single full twist and a regular homotopy.

We now prove the theorems for immersed ribbons.

Proof of Theorem 2.7.16. Without loss of generality, perturb the immersed ribbon to a framed knot. Since M is a good orbifold, we can lift a disk $D \to M$ to the universal cover $\tilde{M}$ which is a manifold. Hence, we can assume that M is a 3-manifold. A regular homotopy between two knots extends to an ambient regular homotopy carrying potential immersed disks, thus the property of spanning an immersed disk stays invariant under regular homotopy.

The theorem follows from the following three facts:

Two curves γ and γ' in $\mathcal{N}(K)$ induced by immersed disks intersect an even number of times.

We can perturb the disks such that they intersect transversely. If γ and γ' intersect in a point, then the two disks intersect transversely in an arc that again ends on $\partial\mathcal{N}(K)$. Hence, γ and γ' intersect in an even number of points. This implies that the framing induced by the two disks differs by an even number of twists.

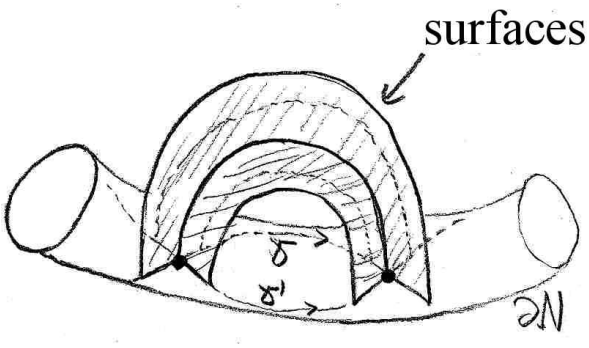

Two full twists of the framing can be achieved by a regular homotopy.

There is an immersed disk of the unknot in S^3 inducing the $+2$ framing:

Add this little immersed disk and unknot to K and then apply an ambient isotopy to straighten out the unknot:

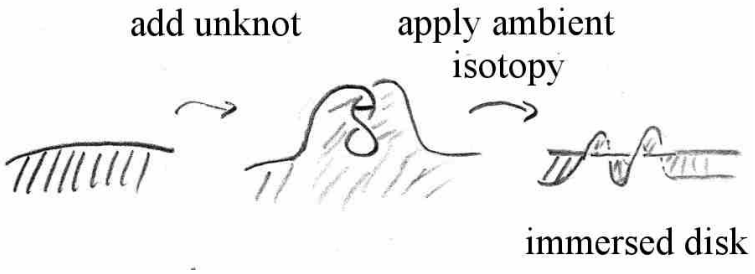

There is an immersed disk spanning K.

K spans a disk because it is null-homotopic. We can homotope the disk to be smooth or piecewise linear (e.g., by simplicial approximation). We can furthermore perturb the disk so that the points where it fails to be a local embedding are branch points of order 2, see Figure 2.9, i.e., the disk is locally the cone on a figure eight (see [Oer04, §1, Case2] or [Whi44]).

If there are two or more branch points, find a curve in D connecting two. "Zipping" along the curve, i.e., moving the branch points together, annihilates them as shown in the following picture (see [Oer04, §1, Case 2] or [Bin83]):

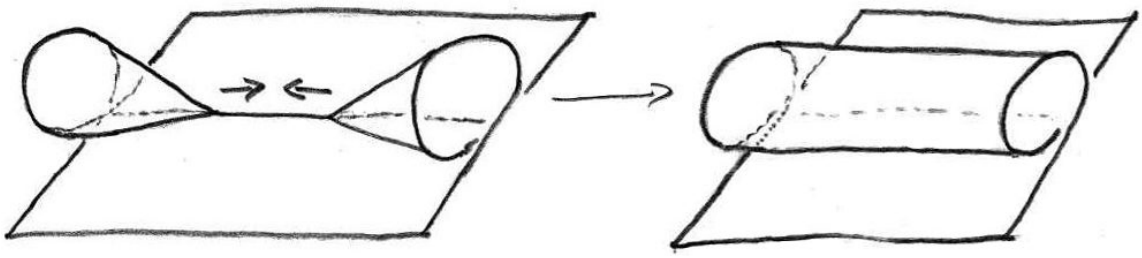

If there is only one branch point left, push it off over the boundary of D, this changes the framing the disk induces, see Figure 2.11.

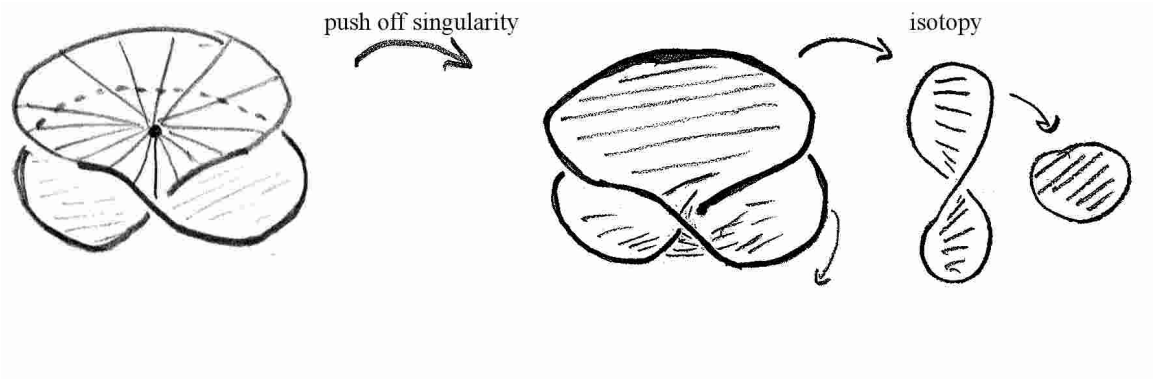

Figure 2.11: Pushing off a branch point over the boundary of a disk. The disk in the left picture has a branch point and the disk induces framing $+1$. After pushing off the branch point, the disk is immersed and consists of two disks glued by a vertical strip with a half-twist. The induced framing is 0 since the disk is even properly embedded.

□

Proof of Theorem 2.7.15. Two homotopic K are regular homotopic and we can change the framing by two through a regular homotopy. Hence, there are at most two regular homotopy classes of immersed ribbons. The two classes are related through a full-twist. It is left to show that the two classes are distinct, i.e., that a regular homotopy (K, v) cannot change the framing by a full-twist. Assume there is such a regular homotopy. Without loss of generality, the regular homotopy fixes a part U of (K, v). Let $(K, v)^{-1}$ be the ribbon with opposite orientation of S^1. We can perturb, cut, and glue (K, v) and $(K', v)^{-1}$ near U together to represent a null-homotopic 0-framed knot. The regular homotopy can act now on the glued ribbon by changing (K, v) but not $(K, v)^{-1}$. The glued ribbon being null-homotopic, Theorem 2.7.16 applies. □

2.7.6 Regular Homotopy Classes of the Immersed 1-Skeleton

Let $M = S^3/\Gamma$ with $\Gamma \subset \mathrm{SO}(4)$ be a spherical orbifold with base point p. Let F_1 be the 1-skeleton of a good, connected, orientable 2-orbifold. Let $\tau : \pi_1^{orb}(F_1, p) \to \pi_1^{orb}(M, p)$ be a group homomorphism mapping each ssl γ_s to a msl with $\mathrm{ord}(\tau(\gamma_s)) = \mathrm{ord}(\gamma_s)$.

Lemma 2.7.20. *Let $\gamma \in \pi_1^{orb}(M, p) \cong \Gamma$ be a non-trivial msl γ_s^n. Then, the conjugacy class of γ can be represented by an immersed orbifold 0-handle of order $\mathrm{ord}(\gamma) = \mathrm{ord}(\gamma_s)/n$ that is uniquely determined up to regular homotopy and up to a possible flip. By connecting the boundary of the orbifold 0-handle with an arc to p, we can represent γ exactly. This fixes an orientation of the orbifold 0-handle if and only if $\mathrm{ord}(\gamma) \neq 2$.*

Proof. Let $g \in \Gamma$ be the element corresponding to γ. Let s be the image of the singular point of the orbifold 0-handle. When the immersion is lifted to S^3, the point s has to go to a fixed point of g. The set of fixed points of g is a circle, all small immersed disk around the circle with the same orientation are in the same regular homotopy class. If $\mathrm{ord}(\gamma) \neq 2$, the orientation of the boundary of the immersed disk is determined. Sliding the immersed disk around the circle might result in immersed orbifold 0-handles around the same edge of $\Sigma(M)$ but with different orientations. Fixing an arc connecting the disk to p fixes the orientation on the orbifold 0-handle.
To see that the fixed point set of g is a circle, we can think of S^3 as $E^3 \cup \{\infty\}$ using the stereographic projection. Without loss of generality, the point s can be chosen to be the origin in E^3. Then, g induces an isometry of the tangent space at the origin. This is a rotation fixing an axis. The exponential map gives a circle in S^3. □

Remark 2.7.21. Let Γ be the symmetries of a regular tetrahedron in $E^3 \subset S^3$. Pick an order three symmetry axis of the tetrahedron. This axis intersects both a face and a vertex of a tetrahedron. Slide a embedded disk around the axis from one of these intersection to the other passing through the center of the tetrahedron.
The 3-orbifold S^3/Γ has $X(S^3/\Gamma) \cong S^3$ and $\Sigma(S^3/\Gamma)$ is the unique trivalent graph with two vertices and no reflexive edges. The order of the edges in $\Sigma(S^3/\Gamma)$ are two, three, and three. The embedded disk becomes an immersed orbifold 0-handle around an order three edge in $\Sigma(S^3/\Gamma)$. Sliding the above disk along the axis takes the orbifold 0-handle to the other order three edge.

Remark 2.7.22. Let Γ be the symmetries of a regular octahedron in $E^3 \subset S^3$. The 3-orbifold is similar to the one in the previous remark, but the orders of the edges of $\Sigma(S^3/\Gamma)$ are two, three, and four. Take a small embedded disk around an order three symmetry axis of the octahedron. Sliding the disk around results in immersed orbifold 0-handles around the same edge. The orientation however flips when the disk is going through the center of the octahedron. If we trace an arc connecting the orbifold 0-handle, the arc crosses $\Sigma(M)$ at this point as well.

Lemma 2.7.23. *All morphisms $(F_1 \setminus \Sigma(F_1), p) \to (M, p)$ inducing τ are in the same homotopy class.*

Proof. Notice that $F_1 \setminus \Sigma(F_1)$ has no singular points and deformation retracts to $G \subset F_1 \setminus \Sigma(F_1)$ being a wedge product of loops γ, some being ssl around singular points and some being generators of $\pi_1(X(F_1), p)$. The homotopy class of each loop γ is determined by its image under τ. □

To obtain all regular homotopy classes of immersions $t_1 : (F_1, p) \to (M, p)$, we need to consider all possible choices of thickening G in M and then filling the singular locus $\Sigma(F_1)$. This means that we need to pick a choice of framing on each loop of G. For a loop in G that is a generator of $\pi_1(X(F_1), p)$, we have a $\mathbb{Z}/2$ choice by Theorem 2.7.15. Consider a loop γ in $G \subset F_1 \setminus \Sigma(F_1)$ representing a ssl $\gamma_d \in \pi_1^{orb}(F_1, p)$. In order to fill the singular locus d, we need to homotope $(G, p) \to (M, p)$ so that γ becomes the boundary of a small disk D around an edge of $\Sigma(M)$ connected to p through an arc. By Lemma 2.7.20, this immersed disk is determined up to regular homotopy and a possible flip by γ. If $\mathrm{ord}(\gamma) \neq 2$, then the orientation in which γ is traversing ∂D is fixed. Hence, the framing on the arc connecting to p is fixed up to an even numbers of full-twists to match the orientation on the surface $F_1 \setminus \Sigma(F_1)$. If $\mathrm{ord}(\gamma) = 2$, then we can apply a flip to the disk, corresponding to a half-twist of a 1-handle containing the arc connecting to p or a full-twist around the loop γ, see Figure 2.12.

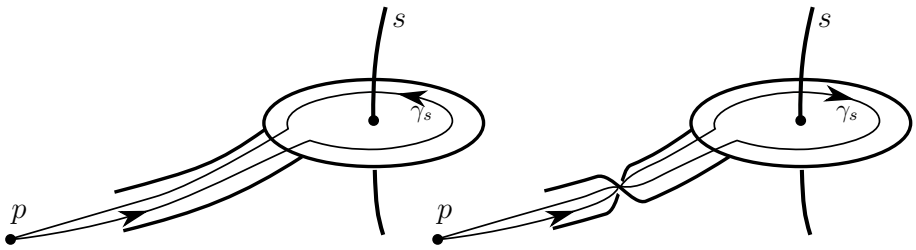

Figure 2.12: Flipping an orbifold 0-handle of order two.

Notice that we obtain all regular homotopy classes of immersions $t_1 : (F_1, p) \to (M, p)$ by full-twists on 1-handles and half-twists on 1-handles connecting to an orbifold 0-handle of order 2. The half-twist flips the orbifold 0-handle. If there is more than one 1-handle connecting the orbifold 0-handle, we first slide all other 1-handles off the orbifold 0-handle onto the 1-handle we half-twist and then slide them back on.

Lemma 2.7.24. *Let F_1 be the 1-skeleton of a good, connected, orientable 2-orbifold. Let (M, p) be a spherical orbifold as defined in the beginning of the section. Let $\tau : \pi_1^{orb}(F_1, p) \to$*

$\pi_1^{orb}(M,p)$ be a group homomorphism mapping each ssl γ_s to a msl with $\mathrm{ord}(\tau(\gamma_s)) = \mathrm{ord}(\gamma_s)$. *Then regular homotopy classes of immersions $t_1 : (F_1, p) \to (M, p)$ inducing τ are in (non-canonical) 1-1 correspondence to morphisms $f : \pi_1^{orb}(F_1, p) \to \mathbb{Z}/2$.*

Proof. An immersion $t_1 : (F_1, p) \to (M, p)$ exists by Lemma 2.7.6 and the resulting homotopy class of $(F_1 \setminus \Sigma(F_1), p) \to (M, p)$ is uniquely determined by Lemma 2.7.23. The above comments describe how to obtain all regular homotopy classes.
To establish the correspondence, fix one immersion $t_1 : (F_1, p) \to (M, p)$. Given another immersion t_1' and a loop $\gamma \in \pi_1^{orb}(F_1, p)$, we get two immersed ribbons in M representing the same $\pi_1^{orb}(F_1, p)$, hence by Theorem 2.7.16, we get an element in $\mathbb{Z}/2$ depending on the number of full twists needed to relate them. This is the image of γ under f for t_1'. □

2.7.7 Main Theorem for Immersions

Let $M = S^3/\Gamma$, $\Gamma \subset \mathrm{SO}(4)$, be a spherical orbifold with base point p. Let $\tau : \pi_1^{orb}(F,p) \to \pi_1^{orb}(M,p)$ be a group homomorphism mapping each ssl γ_s to a msl with $\mathrm{ord}(\tau(\gamma_s)) = \mathrm{ord}(\gamma_s)$.

Fix an immersion $t_1 : (F_1, p) \to (M, p)$ of the 1-skeleton of F inducing τ. This is possible by Lemma 2.7.6.

Pick a connected component $C \subset \partial F_1$ of the boundary of the 1-skeleton F_1. In $\pi_1^{orb}(F,p)$, C is trivial because it spans a 2-cell D in the handle decomposition. The immersion $t_1 : (F_1, p) \to (M, p)$ sends a collar neighborhood of C to an immersed ribbon K that is homotopically trivial because C is homotopically trivial in F and τ is a group homomorphism. The immersed ribbon K has a $\mathbb{Z}/2$-framing invariant by Theorem 2.7.16. Assign $f(K)$ to the corresponding 2-handle D in the cellular cohomology.

To be more precise, recall that the handle decomposition gives a cellular cochain complex of $X(F)$ with $\mathbb{Z}/2$ coefficients:

$$\begin{array}{ccccccccc} & & 0 & & (\mathbb{Z}/2)^r & & & & \\ & & \cong\uparrow & & \cong\uparrow & & & & \\ \cdots & \longleftarrow & C^3_{CW}(X(F);\mathbb{Z}/2) & \longleftarrow & C^2_{CW}(X(F);\mathbb{Z}/2) & \longleftarrow & C^1_{CW}(X(F);\mathbb{Z}/2) & \longleftarrow & \cdots \end{array}$$

where r is the number of 2-handles. Define $c(t_1) \in C^2_{CW}(X(F);\mathbb{Z}/2)$ by

$$\begin{array}{rcl} c(t_1) : C_2^{CW}(X(F);\mathbb{Z}/2) & \to & \mathbb{Z}/2 \\ \text{2-handle } D & \mapsto & \text{framing invariant } f(K) \end{array}$$

Definition 2.7.25. *Let (M,p), (F,p), and τ as above. The regular homotopy framing invariant of an immersion $t_1 : (F_1,p) \to (M,p)$ of the 1-skeleton inducing τ is $c(t_1) \in C_2^{CW}(X(F);\mathbb{Z}/2)$.*

Lemma 2.7.26. *The immersion $t_1 : (F_1,p) \to (M,p)$ extends to the 2-orbifold F if and only if $c(t_1) \in C^2_{CW}(X(F);\mathbb{Z}/2)$ is zero.*

Proof. A collar neighborhood of the boundary of a 2-cell D in F yields an immersed ribbon in M under t_1. By Theorem 2.7.16, this immersed ribbon bounds an immersed disk if and only if $c(t_1)(D)$ is zero for this 2-cell. We need these immersed disks to map the 2-cells of F into M extending t_1 such that it becomes an immersion on the boundary of the 2-cell. □

Definition 2.7.27. *Let (M,p), (F,p) and τ as above. The cohomology obstruction of an immersion $t_1 : (F_1,p) \to (M,p)$ inducing τ to extend to an immersion after full-twists is the class $[c(t_1)] \in H^2(X(F);\mathbb{Z}/2)$ represented by $c(t_1)$.*

Lemma 2.7.28. *The cohomology class* $[c(t_1)] \in H^2(X(F);\mathbb{Z}/2)$ *stays invariant if we apply full twists to the 1-handles of the immersion* $t_1 : (F_1, p) \to (M, p)$*. In particular, we can change* $c(t_1) \in C^2_{CW}(X(F);\mathbb{Z}/2)$ *to zero by applying full twists to the 1-handles if and only if* $[c(t_1)]$ *is zero in* $H^2(X(F);\mathbb{Z}/2)$*.*

Proof. If we perform a full-twist on a 1-handle, it changes the framing invariant f for the 2-handles that touch the 1-handle. This relationship also defines the coboundary operator $\delta : C^1_{CW}(X(F);\mathbb{Z}/2) \to C^2_{CW}(X(F);\mathbb{Z}/2)$. Hence, full-twists of 1-handles change $c(t_1)$ by an image of δ and hence leave $[c(t_1)]$ invariant. □

Lemma 2.7.29. *If there is no ssl* $\gamma_s \in \pi_1^{orb}(F, p)$ *with* $\mathrm{ord}(\tau(\gamma_s))) = 2$*, then the cohomology class* $[c(t_1)] \in H^2(X(F);\mathbb{Z}/2)$ *does not depend on the immersion* $t_1 : (F_1, p) \to (M, p)$*. We will write* $[c(\tau)]$ *in this case.*

Proof. Recall that in this case all regular homotopy classes of immersions $t_1 : (F_1, p) \to (M, p)$ inducing τ are obtained from full-twists, as shown in the comments to and proof of Lemma 2.7.24. □

Theorem 2.7.30 (Main Theorem for Immersions)**.** *Let* (F, p) *be a good, connected, orientable 2-orbifold and* (M, p) *a spherical 3-orbifold as defined above. Let* $\tau : \pi_1^{orb}(F, p) \to \pi_1^{orb}(M, p)$ *be a group homomorphism mapping each ssl* γ_s *to a msl with* $\mathrm{ord}(\tau(\gamma_s)) = \mathrm{ord}(\gamma_s)$*.*

1. *Assume there is no ssl* $\gamma_s \in \pi_1^{orb}(F, p)$ *such that* $\mathrm{ord}(\tau(\gamma_s)) = 2$*. Then an immersion* $t : (F, p) \to (M, p)$ *inducing* τ *exists if and only if* $[c(\tau)] \in H^2(X(F);\mathbb{Z}/2)$ *is zero.*
2. *Assume there is a ssl* $\gamma_s \in \pi_1^{orb}(F, p)$ *such that* $\mathrm{ord}(\tau(\gamma_s)) = 2$*. Then an immersion* $t : (F, p) \to (M, p)$ *inducing* τ *exists.*

Proof. By Lemma 2.7.6, an immersion $t_1 : (F_1, p) \to (M, p)$ of the 1-skeleton F_1 exists.
Case 1. By Lemma 2.7.29, the class $[c(t_1)]$ is independent of the choice of the immersion of the 1-skeleton. By Lemma 2.7.28, we can modify this immersion of the 1-skeleton by full-twists making $c(t_1) \in C^2_{CW}(X(F);\mathbb{Z}/2)$ vanish if and only if $[c(t_1)] = 0$. By Lemma 2.7.26, we can extend an immersion of 1-skeleton to F if and only if $c(t_1) = 0$.

Case 2. . If $[c(t_1)] = 0$, continue as in the previous case. Otherwise, alter the immersion of the 1-skeleton by picking the orbifold 0-handle corresponding to a γ_s with $\mathrm{ord}(\tau(\gamma_s)) = 2$ and flipping it, twisting the connecting 1-handle by a half-twist. The new immersion of the 1-skeleton F_1 induces the same τ. However, $[c(t_1)]$ has changed. To see this, lift γ_s to the manifold cover as shown in Figure 2.13. □

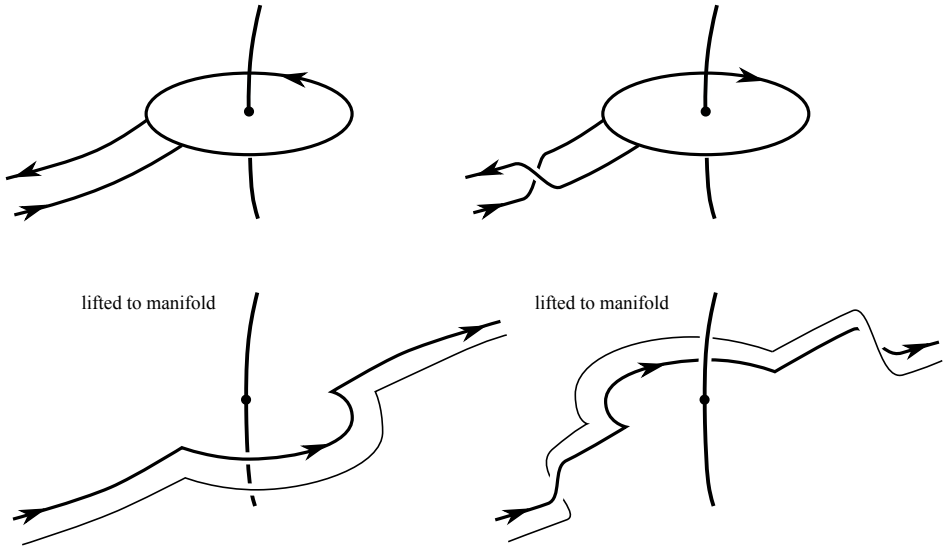

Figure 2.13: Framing change when flipping orbifold 0-handle.

2.7.8 Regular Homotopy Classes of Immersions

Consider a 2-orbifold (F, p) and a spherical 3-orbifold (M, p) as defined at the beginning of the previous section. Let $\tau : \pi_1^{orb}(F, p) \to \pi_1^{orb}(M, p)$ be a group homomorphism.

Let (F_1, p) be the 1-skeleton of (F, p). Let $t_1 : (F_1, p) \to (M, p)$ be an immersion. Recall Definition 2.7.25 of the regular homotopy framing invariant $c(t_1) \in C_2^{CW}(X(F); \mathbb{Z}/2)$. If $c(t_1) = 0$, then t_1 can be extended to an immersion of (F, p) and yields:

Lemma 2.7.31. *There is a 1-1 correspondence between*

- *regular homotopy classes of immersions* $t_1 : (F_1, p) \to (M, p)$ *inducing* τ *with* $c(t_1) = 0$
- *regular homotopy classes of immersions* $t : (F, p) \to (M, p)$ *inducing* τ.

Proof. If two immersions $t : (F, p) \to (M, p)$ are regular homotpic, so are their restrictions to the 1-skeleton.
Theorem 2.7.16 implies that there is only one regular homotopy class of immersed ribbons in S^3 bounding immersed disks. Furthermore, any two immersed disks are also regular homotopic. Hence, if possible, an immersion $t_1 : (F_1, p) \to (M, p)$ extends to F uniquely up to regular homotopy. □

Theorem 2.7.32. *Let* (F, p) *be a good, connected, orientable 2-orbifold. Let* (M, p) *be a spherical orbifold as defined in the beginning of the previous section. Let* $\tau : \pi_1^{orb}(F, p) \to$

$\pi_1^{orb}(M,p)$ be a group homomorphism mapping each ssl γ_s to a msl with $\mathrm{ord}(\tau(\gamma_s)) = \mathrm{ord}(\gamma_s)$. *Let g be the genus of $X(F)$ and k the number of order two singular points in F. Then, one of the following cases holds:*

- *$k = 0$ and there are zero regular homotopy classes immersion $t : (F,p) \to (M,p)$ inducing τ.*
- *$k = 0$ and there are 2^{2g} classes.*
- *$k > 0$ and there are 2^{2g+k-1} classes.*

These classes form an affine subspace of the $g + k$-dimensional $\mathbb{Z}/2$-vector space of group homomorphisms $f : \pi_1^{orb}(F,p) \to \mathbb{Z}/2$.

Remark 2.7.33. This theorem is the orbifold version of results about enumerating the regular homotopy classes of immersions of surfaces into $\mathbb{R}^3$ due to James and Thomas [JT66] using methods of Hirsch and Smale [Hir59]. Hass and Hughes give explicit constructions in [HH85].

Proof. Use a standard handle decomposition of (F,p). By Lemma 2.7.24, all regular homotopy classes of immersions $t_1 : (F_1,p) \to (M,p)$ are obtained by half-twists of a 1-handle connecting to an order two orbifold 0-handle and full-twists of 1-handles not connecting to orbifold 0-handles. The half-twists change $c(t_1)$, the full-twists do not. Hence, if there is no order two singular point in (F,p), all regular homotopy classes have the same $c(t_1)$. If there is an order two singular point, then exactly half of the regular homotopy classes have $c(t_1) = 0$. □

2.8 Theory about Embeddings

Let (F, p) and (M, p) be good, connected, orientable orbifolds with base points of dimension 2 and 3, respectively. Let $\tau : \pi_1^{orb}(F, p) \to \pi_1^{orb}(M, p)$ be a group homomorphism.

For 3-orbifolds (M, p) that are quotients of E^3 by a finite group of symmetries, the main theorem in Section 2.8.2 classifies all embeddings of a good, connected, orientable 2-orbifold (F, p) into (M, p) up to regular homotopy and choices of identifying the 2-orbifold with itself. A corollary of this theorem in Section 2.8.5 lists all $\tau : \pi_1^{orb}(F, p) \to \pi_1^{orb}(M, p)$ that can be realized by an embedding $(F, p) \to (M, p)$.

We prove the main theorem using a modified version of the Haken theory of normal surfaces. The method can be used to derive results similar to the main theorem for a much larger class of target 3-orbifolds.

We follow the notation and definitions used in [Mat07, Section 3]. A *normal surface* in a 3-manifold is defined with respect to a triangulation of the 3-manifold. A fundamental result of the Haken theory of normal surfaces is that the normal surfaces are in correspondence to non-negative integral solutions of a system of equations that can be derived from the triangulation. There exists a minimal set of these solutions that spans all solutions. This set is finit and can be computed effectively. The corresponding surfaces are referred to as *fundamental surfaces*.

Given a triangulation of a 3-manifold, "interesting" surfaces are isotopic to a normal surface and can be algorithmically found in this frame work. Here, the notion "interesting" depends on the application, for example, splitting surfaces to detect splittable links. The *normalization procedure* is a general technique to prove that an interesting surface is isotopic to a normal surface. For example, any incompressible surface in an irreducible 3-manifold is isotopic to a normal surface [Mat07, Proposition 3.3.24].

In Section 2.8.1, we extend the notion of normal surface by adding *beads* and *tunnels* and apply it to orbifolds. We show that every (not necessarily incompressible) embedded 2-orbifold in a 3-orbifold is isotopic to an "altered" normal surface. Using this fact, we can enlist all fundamental surfaces in the 3-orbifold, and then derive results about all embedded 3-orbifolds if the 3-orbifold is simple enough. We do this explicitly for S^3/B in Section 2.8.3, thus proving the main theorem.

2.8.1 "Altered" Normal Surfaces and the Normalization Procedure

Let M be a good, closed, connected, orientable 3-orbifold with a triangulation of the underlying topological space $X(M)$ such that the singular graph $\Sigma(M)$ is contained in the 1-skeleton. An embedded 2-orbifold $F \subset M$ is called a *normal 2-orbifold* if $X(F)$ is a normal surface.

Given an embedded 2-orbifold $F \subset M$, we can perform the normalization moves N_1 to N_4 as described in [Mat07, Section 3.3]. We ignore the orbifold structure during the process and perform the procedure on the underlying topological space $X(F)$. By [Mat07, Theorem 3.3.21], this process terminates after finitely many steps and results in a normal 2-orbifold. Notice that N_2 potentially changes the intersection of $X(F)$ with $\Sigma(M)$ thus changing the orbifold structure of F. Also, the normalization move N_1 can change the topology of $X(F)$ in a non-trivial way if F is not incompressible.

We alter the definition of normal surface and the normalization procedure to account for these cases.

Adding a tunnel amounts to surgery along a 3-dimensional 1-handle, see Figure 2.14:

Definition 2.8.1. *Let $F \subset M$ be an embedded 2-orbifold. Let $[0,1] \times D^2 \subset M \setminus \Sigma(M)$ be an embedded solid cylinder intersecting F in $\partial[0,1] \times D^2$. Remove $\partial[0,1] \times D^2$ from F and add $[0,1] \times \partial D^2$ to F. We call this surgery "adding a tunnel" to F.*

Definition 2.8.2. *Let $F \subset M$ be an embedded 2-orbifold. Let $B^3 \subset X(M) \setminus X(F)$ be an embedded ball intersecting $\Sigma(M)$ in an interval. Add a tunnel to $F \cup \partial B^3$ connecting F to ∂B^3. We call this surgery "adding a bead" to F.*

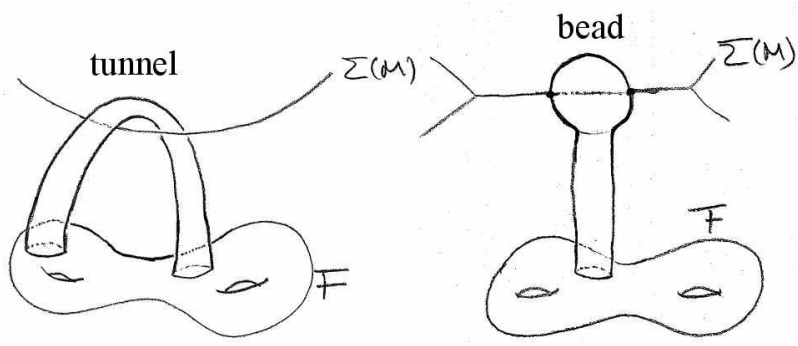

Figure 2.14: Tunnels and beads.

Adding a bead does not change the isotopy class of $X(F) \to X(M)$ but adds two singular points to F.

Definition 2.8.3. *An embedded 2-orbifold $F' \subset M$ is an altered normal surface if it can be obtained from a normal 2-orbifold $F \subset M$ by consecutively adding beads and tunnels with ends lying on the normal surface F.*

Theorem 2.8.4. *Every connected, orientable, embedded 2-orbifold $F \subset M$ is isotopic to an altered normal surface or an altered 2-sphere bounding a ball.*

Proof. We perform the normalization procedure to obtain a normal surface, modifying the moves in [Mat07, Section 3.3] to keep track of solid cylinders and balls as extra data. We use those solid cylinders and balls to add tunnels and beads yielding an altered normal surface isotopic to F:

N_1: Compress F along D and add a solid cylinder for a tunnel as shown in the following picture:

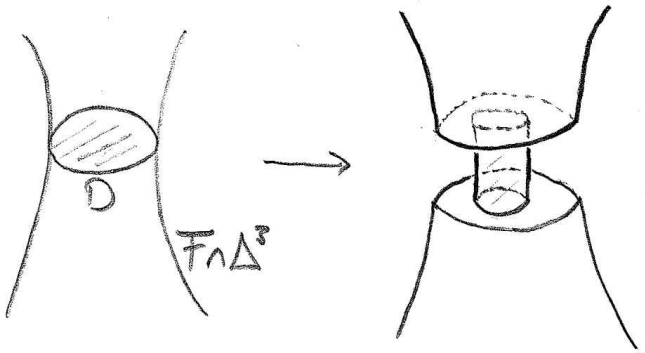

Notice that D might intersect other solid cylinders from previous normalization moves. If ∂D intersects such a solid cylinder, we can isotope the cylinder to avoid ∂D (see picture below). If the interior of D intersects a solid cylinder, then the cylinder does not touch ∂D because the corresponding altered normal surface is embedded. Hence, the cylinder intersects D in disks lying in the interior of D. If the cylinder intersects D in a circle compressible in the cylinder, we can isotope it to avoid D:

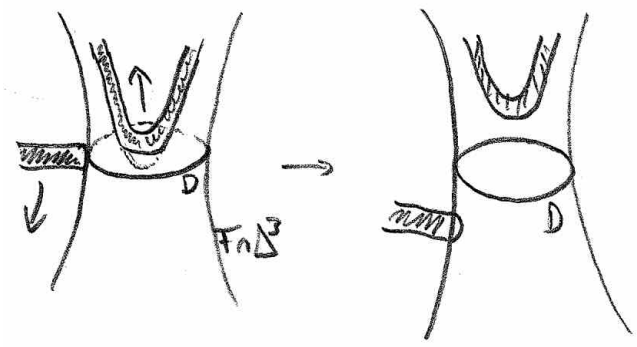

If the previous cylinder intersects D transversely, we obtain nested cylinders, i.e., solid cylinders modeled on "longer" solid cylinders sitting in "thicker" solid cylinders:

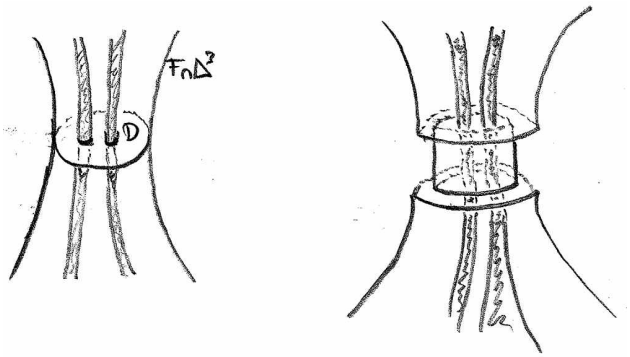

N_2: After isotoping F to avoid the edge e, we add a bead so that the altered normal surface still intersects $\Sigma(M)$ if $\Sigma(M)$ contains e:

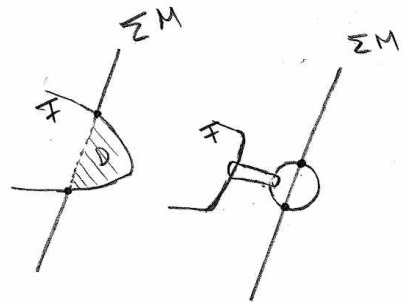

Notice that D might intersect some solid cylinders introduced at earlier steps. These cylinders have to be isotoped to lie within the bead:

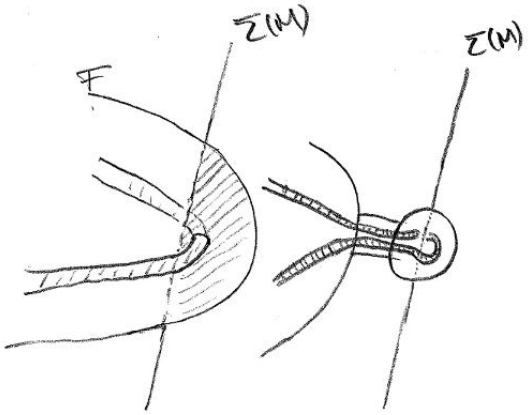

D might also intersect some beads, introducing nested beads.

N_3: Since we started with a connected 2-orbifold, the 2-sphere has to be connected to another component of F by some cylinder (otherwise the normalization procedure has already terminated in an altered 2-sphere). The solid cylinder and the ball bounded by the 2-sphere form a ball in $X(M) \setminus \Sigma(M)$. Use this ball for an ambient isotopy turning the 2-sphere into the other end of the cylinder:

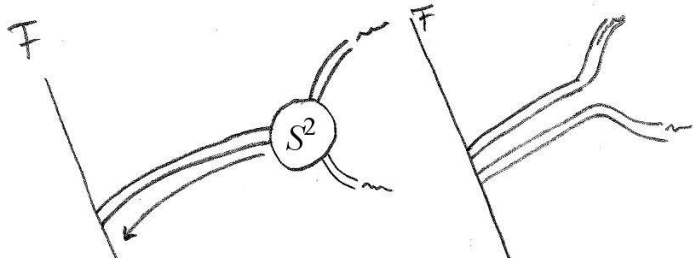

The 2-sphere disappears from the normal surface. Other cylinders connecting to the 2-sphere now connect to F.

N_4: Same as N_3.

□

Remark 2.8.5. The procedure might result in convoluted nested beads and tunnels, see Figure 2.15.

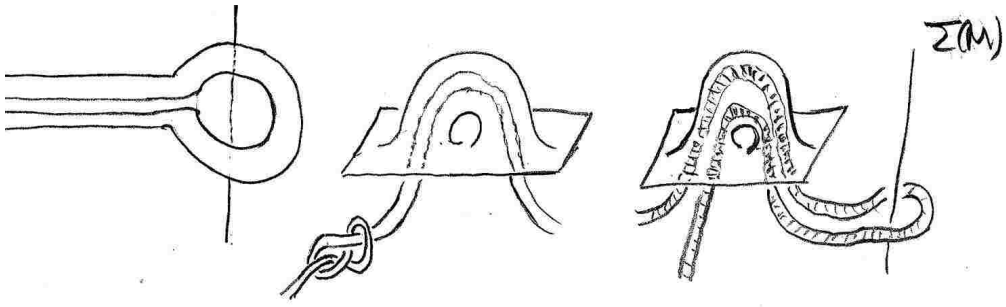

Figure 2.15: Nested beads and tunnels.

2.8.2 Main Theorem for Embeddings

Let $B \subset \mathrm{SO}(3)$ be a finite subgroup of $\mathrm{SO}(3) \subset \mathrm{SO}(4)$. Let $M = S^3/B$. The group B is a either a cyclic group or a triangle group $[p, q]^+$, see Section 2.2.1 and Table 2.1. In either case, $X(M) \cong S^3$.

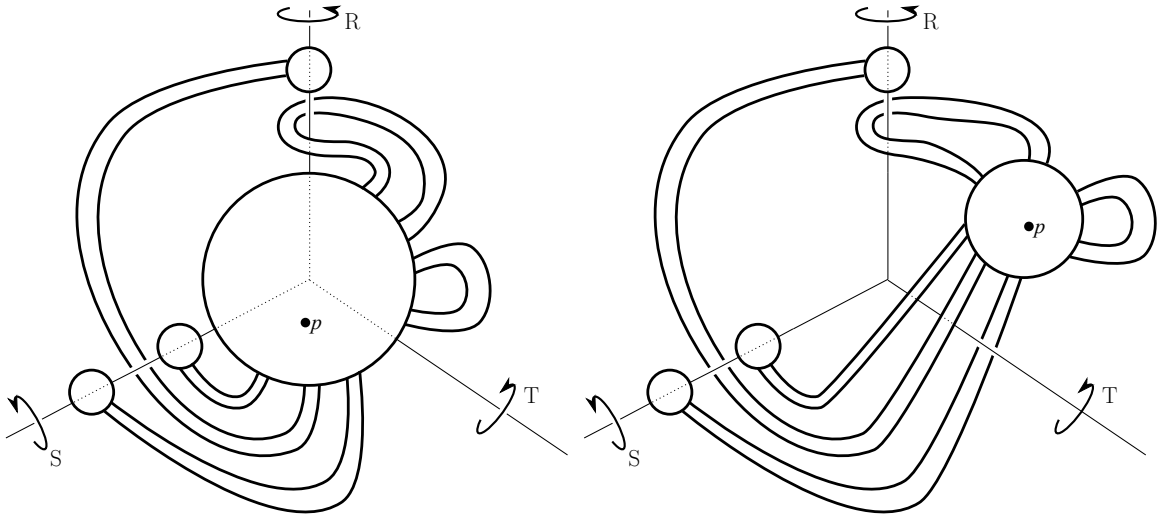

Figure 2.16: Prototypical embedded orbifold in S^3/B with B non-cyclic. In the left picture, the surface (F, p) is obtained by adding tunnels (Definition 2.8.1) and beads (Definition 2.8.2) to a sphere around a trivalent vertex of $\Sigma(M)$. In the right picture, we start with a small sphere around a generic point in M.

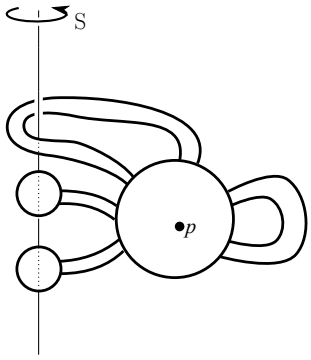

Figure 2.17: Prototypical embedded orbifold in S^3/B with B cyclic.

Theorem 2.8.6 (Main Theorem for Embeddings)**.** *Let $M = S^3/B$ be the quotient orbifold where B is a finite subgroup of $\mathrm{SO}(3) \subset \mathrm{SO}(4)$ with base point p. Every embedded orientable 2-orbifold $(F, p) \subset (M, p)$ is regular homotopic to one of the following forms:*

- *If B is not cyclic, adding tunnels and beads to a sphere around a trivalent vertex of $\Sigma(M)$ (left picture in Figure 2.16).*
- *Adding tunnels and beads to a small sphere around a generic point in M (right picture in Figure 2.16 if B is not cyclic; Figure 2.17 if B is cyclic).*

This is proven in the next section.

Remark 2.8.7. Notice that each bead intersects an edge of $\Sigma(M)$ twice. Assume that $B = [p, q]^+$ is not cyclic. Then the numbers of singular points of (F, p) lying on the axis for R, for S, and for T are either all odd or all even (left, respectively, right picture in Figure 2.16). We can detect the axis a singular point is lying on by determining the conjugacy class of the image of the corresponding ssl γ_s under $\tau : \pi_1^{orb}(F, p) \to \pi_1^{orb}(M, p) \cong B$ induced by $(F, p) \subset (M, p)$.

2.8.3 Proof of the Main Theorem for Embeddings

We want to find all orientable, connected, embedded 2-orbifolds in $M = S^3/B$ up to regular homotopy.

B non-cyclic

If B is not cyclic, we triangulate S^3 by four tetrahedra: construct a hexahedron by gluing two tetrahedra along one face, glue two hexahedron along their boundaries. The trivalent graph $\Sigma(M)$ embeds as follows:

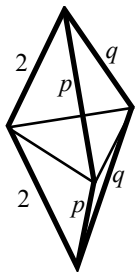

Using the 3-manifold software Regina [Bur09], we see that every fundamental surface is either a vertex linked or edge linked sphere, i.e., the boundary of a regular neighborhood of a vertex or edge in the 1-skeleton. Furthermore, two spheres linked to edges sharing a vertex do not have compatible quad types. This implies that every normal surface is just a disjoint union of fundamental spheres in $X(M)$. In order to enumerate all embedded surfaces, we can ignore most of these spheres by replacing them by a bead or by applying a regular homotopy so that they go away. For example, a sphere linked around a vertex other than the trivalent vertices of $\Sigma(M)$ can be replaced by a bead. Similarly, an edge linked sphere can be replaced by two beads if the edge is not part of $\Sigma(M)$.

Hence, we are left with an "altered" normal surface that consists of tunnels and beads added to either:

- a sphere not intersecting $\Sigma(M)$ (the case of an empty normal surface) or
- a bunch of spheres around one of the trivalent vertices of $\Sigma(M)$.

In the latter case, there must be tunnels connecting the spheres. If there are nested tunnels, then there is an outermost tunnel, and we can turn the two spheres it connects into three beads, as shown in Figure 2.18.

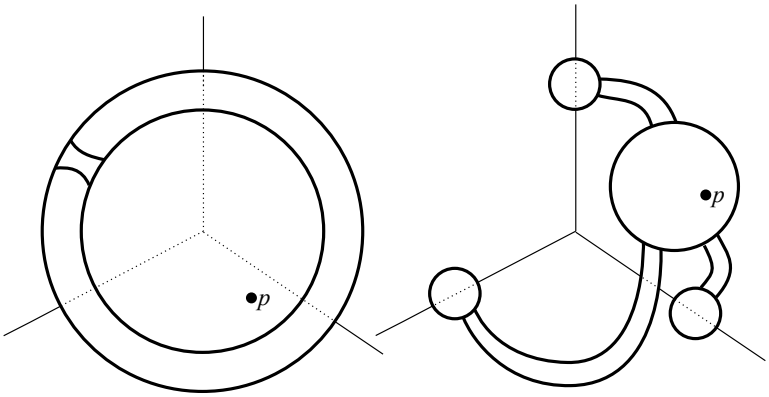

Figure 2.18: Two spheres around the trivalent vertex isotoped to three beads.

Thus we can successively reduce the number of spheres around the trivalent vertex by two until there is only one left. We can push all tunnels and beads outside and avoid them to be nested by a regular homotopy. Hence, up to regular homotopy, every embedded surface is of one of the forms shown in Figure 2.16.

B cyclic

Notice that $\Sigma(M)$ is a circle and can be embedded into the same triangulation of $S^3 \cong X(M)$. Using the same arguments, every embedded surface is, up to regular homotopy, of the form shown in Figure 2.17.

2.8.4 Identifying a Prototypical Embedded 2-Orbifold with the Standard Handle Decomposition

In this section, we explicitly fix one standard handle decomposition of an embedded orientable 2-orbifold $(F, p) \subset (M, p)$ as given in Theorem 2.8.6 and compute the induced group homomorphism $\tau : \pi_1^{orb}(F, p) \to \pi_1^{orb}(M, p)$. τ is given in the generators of the standard presentation of $\pi_1^{orb}(F, p)$ in Section 2.4.1. Here, $\pi_1^{orb}(M, p)$ is isomorphic to a cyclic group or a triangle group $B = [p, q]^+$ and is presented as in Equation 2.1.

Vice versa, we can embed (F, p) into (M, p) using Figure 2.16 or 2.17 if a 2-orbifold (F, p) has a standard handle decomposition such that τ is of one of the forms listed here with respect to the generators of $\pi_1^{orb}(M, p)$ coming from that standard handle decomposition. Section 2.8.5 discusses this in detail.

B non-cyclic, odd number of singular points

Assume (F, p) has an odd number $k = 2m+3$ of singular points. A picture of the embedded surface is given on the left of Figure 2.16. There are m beads. Label the singular points such that σ_{2j-1} and σ_{2j} are on the same bead and that $\sigma_{2m+1}, \sigma_{2m+2}$, and σ_{2m+3} lie on the sphere around the trivalent vertex of $\Sigma(M)$. Then, we can identify the embedded surface with the surface in Figure 2.7 such that

$$\begin{aligned} \tau(\sigma_{2j-1}) = \tau(\sigma_{2j})^{-1} = &\quad \text{conjugate of} \quad R^{\pm 1}, S^{\pm 1}, T^{\pm 1} \\ \tau(\sigma_{2m+1}) = &\quad R \\ \tau(\sigma_{2m+2}) = &\quad S \\ \tau(\sigma_{2m+3}) = &\quad T \\ \tau(\alpha_i) = &\quad \text{id} \end{aligned} \tag{2.6}$$

where $i = 1, \ldots, g$ and $j = 1, \ldots, m$. Notice that we can warp the beads and tunnels so that $\tau(\beta_i)$ can take arbitrary values and $\tau(\sigma_{2j-1})$ is an arbitrary conjugate of $R^{\pm 1}, S^{\pm 1}$, or $T^{\pm 1}$.

If we reverse the orientation of (F, p), we get:

$$\begin{aligned} \tau(\sigma_{2j-1}) = \tau(\sigma_{2j})^{-1} = &\quad \text{conjugate of} \quad R^{\pm 1}, S^{\pm 1}, T^{\pm 1} \\ \tau(\sigma_{2m+1}) = &\quad T^{-1} \\ \tau(\sigma_{2m+2}) = &\quad S^{-1} \\ \tau(\sigma_{2m+3}) = &\quad R^{-1} \\ \tau(\alpha_i) = &\quad \text{id} \end{aligned} \tag{2.7}$$

B non-cyclic, even number of singular points

Assume (F, p) has an even number $k = 2m$ of singular points. Then, we can identify the embedded surface in the right picture of Figure 2.16 with the surface in Figure 2.7 such that

$$\begin{aligned} \tau(\sigma_{2j-1}) = \tau(\sigma_{2j})^{-1} = &\quad \text{conjugate of} \quad R^{\pm 1}, S^{\pm 1}, T^{\pm 1} \\ \tau(\alpha_i) = &\quad \text{id} \end{aligned} \tag{2.8}$$

where i, j as above and the same comments apply.

B cyclic

The surface (F, p) has to have an even number $k = 2m$ of singular points. Then, we can identify the embedded surface in Figure 2.7 with the surface in Figure 2.7 such that

$$\begin{aligned} \tau(\sigma_{2j-1}) = \tau(\sigma_{2j})^{-1} = &\quad S^{\pm 1} \\ \tau(\alpha_i) = &\quad \mathrm{id} \end{aligned} \tag{2.9}$$

where i, j as above and the same comments apply.

2.8.5 Main Theorem for Embeddings Revisted

Given $\tau : \pi_1^{orb}(F, p) \to \pi_1^{orb}(M, p)$ in standard generators, the goal of this section is to decide whether it is induced by an embedding by letting the mapping class group act on τ and check the conditions in Section 2.8.4. This is stated Theorem 2.8.10 at the end.

Before we state the following corollary to the Main Theorem 2.8.6 for Embeddings, we want to discuss a technical subtlety even though it turns out that we can ignore it: two standard presentations of $\pi_1^{orb}(F, p)$ can be different if we permute singular points of different orders thus changing the relation $\sigma_j^{\mathrm{ord}(s_j)} = \mathrm{id}$. This means that, even if the genus and the number of singular points of a given order are the same for two 2-orbifolds, we might not be able to identify a standard handle decomposition of one 2-orbifold with one of the other 2-orbifold. A priori, we need to check that a singular point labeled s_j in one 2-orbifold has the same order as the singular point with the same label in the other 2-orbifold.

However, assuming τ sends ssl's to ssl's of the same order, this check becomes unnecessary, i.e., if we test the equations in Section 2.8.4 for τ, it follows that the singular points in (F, p) have the right orders automatically, also see Remark 2.11.1.

Corollary 2.8.8. *Let (F, p) be a good, connected, orientable 2-orbifold of genus g and with k singular points. Let $M = S^3/B$ be the quotient orbifold where B is a finite subgroup of $\mathrm{SO}(3) \subset \mathrm{SO}(4)$ with base point p. Let $\tau : \pi_1^{orb}(F, p) \to \pi_1^{orb}(M, p) \cong B$ be a group homomorphism mapping ssl's to ssl's of the same order. Then τ is induced by an embedding $(F, p) \to (M, p)$ if and only if there is a standard handle decomposition of (F, p) such that expressing τ in the resulting standard generators of $\pi_1^{orb}(F, p)$ is of one of the forms listed in Section 2.8.4.*

Looking forward, the algorithm in Section 2.11.1 computes the τ-tuple, i.e., the tuple of the images of the standard generators of $\pi_1^{orb}(F, p)$. To decide whether an embedding exists, run the algorithm with all possible choices of standard handle decomposition and check whether a τ-tuple is of one of the forms listed in Section 2.8.4.

Alternatively, fix one standard handle decomposition and let the mapping class group act on the τ-tuple. We choose the mapping class group of the punctured surface $(X(F) \setminus \Sigma(F), p)$ so that we can permute the singular points arbitrarily.

To state this in a theorem, define a forgetful functor from 2-orbifolds to punctured surfaces $(F, p) \mapsto (X(F) \setminus \Sigma(F), p)$ that forgets the order of each singular point. This functor carries $\tau : \pi_1^{orb}(F, p) \to B$ to $\tilde{\tau} : \pi_1(X(F) \setminus \Sigma(F), p) \to B$. Assume we have checked that τ sends ssl's to ssl's of the same order. Then, having applied the forgetful functor and thus knowing only $(X(F) \setminus \Sigma(F), p)$ and $\tilde{\tau}$, we can still reconstruct the order of each singular point (F, p) and thus we have effectively lost no information.

We can rewrite Corollary 2.8.8.

Corollary 2.8.9. *Let (F, p), (M, p), and τ as in Corollary 2.8.8. Then τ is induced by an embedding $(F, p) \to (M, p)$ if and only if there is a standard handle decomposition of $(X(F) \setminus \Sigma(F), p)$ such that expressing $\tilde{\tau}$ in the resulting standard generators of $\pi_1^{orb}(X(F) \setminus \Sigma(F), p)$ is of one of the forms listed in Section 2.8.4.*

An element ϕ in the mapping class group $\mathrm{Mod}(X(F) \setminus \Sigma(F), p)$ of the punctured surface induces a group automorphism

$$\phi_* : \pi_1(X(F) \setminus \Sigma(F), p) \to \pi_1(X(F) \setminus \Sigma(F), p)$$

and hence acts on $\tilde{\tau}$.

Theorem 2.8.10. *Let (F, p), (M, p), and τ as in Corollary 2.8.8. Pick a standard handle decomposition and write $\pi_1(X(F) \setminus \Sigma(F), p)$ in standard generators. Then τ is induced by an embedding $(F, p) \to (M, p)$ if and only if there is an element $\phi \in \mathrm{Mod}(X(F) \setminus \Sigma(F), p)$ such that $\tilde{\tau} \circ \phi_* : \pi_1(X(F) \setminus \Sigma(F), p) \to B$ is of one of the forms listed in Section 2.8.4.*

2.8.6 Mapping Class Group of a Punctured Surface

We follow the notation used in [FM]. Another classical reference for mapping class groups is [Bir75].

Let $\mathrm{Mod}(S_{g,n})$ denote the mapping class group of a genus g surface with n marked points, respectively, punctures. This group consists of equivalence classes of orientation-preserving homeomorphisms of the surface taking the marked points set-wise to itself. We regard two homeomorphisms equal if there is an isotopy between them fixing the marked points set-wise.

Given a non-separating curve in $S_{g,n}$, we can perform a Dehn twist about the curve and obtain an element in the mapping class group.

If a curve bounds a disk in $S_{g,n}$ containing two marked points, we can perform a half twist about the curve and rotate the disk to exchange the two marked points. We mark such a curve by $\frac{1}{2}$.

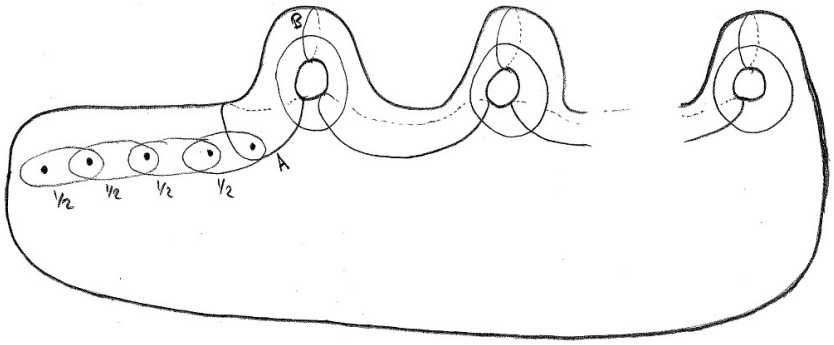

Figure 2.19: Generators of the mapping class group of a punctured surface.

Theorem 2.8.11. *The mapping class group* $\mathrm{Mod}(S_{g,n})$ *is generated by Dehn twists and half twists about the curves shown in Figure 2.19.*

Proof. Let $\mathrm{PMod}(S_{g,n})$ denote the pure mapping class group where the homeomorphisms and isotopies fix the marked points point-wise.

The push map

$$\mathcal{P}ush : \pi_1(S_{g,n}, x) \to \mathrm{PMod}(S_{g,n+1})$$

is defined in [FM, Section 4.2.1] and can be though of as "stick[ing] our finger on x and push[ing] x along α, dragging the rest of the surface along as we go" where $\alpha \in \pi_1(S_{g,n}, x)$.

There is a forgetful map $\mathrm{Mod}(S_{g,n}) \to \mathrm{Mod}(S_{g,0}) = \mathrm{PMod}(S_{g,0})$ ignoring the marked points. The Dehn twists in Figure 2.19 include the Lickorish generators in [FM, Theorem 4.13], thus they generate $\mathrm{PMod}(S_{g,0})$.

By applying a Dehn twist about A and the reverse Dehn twist about B, we can push the most right marked point x once around, thus realizing one standard generator of $\pi_1(S_{g,0}, x)$. Conjugation by appropriate Dehn twists allows realizing all standard generators of $\pi_1(S_{g,0}, x)$ as described in detail in the proof of [FM, Theorem 4.13]. Thus, we have shown that we generate the image of the push map $\mathcal{P}ush : \pi_1(S_{g,0}, x) \to \mathrm{PMod}(S_{g,1})$.

By the Birman exact sequence [FM, Theorem 4.6] for $n = 0$

$$1 \to \pi_1(S_{g,n}, x) \to \mathrm{PMod}(S_{g,n+1}) \to \mathrm{PMod}(S_{g,n}) \to 1,$$

this proves that we generate $\mathrm{PMod}(S_{g,1})$.

We want to use the Birman exact sequence inductively to show that the twists are enough to generate $\mathrm{PMod}(S_{g,n+1})$. This means we need to realize the image of $\mathcal{P}ush : \pi_1(S_{g,n}, x) \to \mathrm{PMod}(S_{g,n+1})$ by twists. The half twists can push a marked point x arbitrarily around the other marked points, thus realizing $\mathcal{P}ush$ for those loops around marked points that avoid the handles. Recall that we described earlier how Dehn twists realize the push map for the most right marked point. Conjugate those Dehn twists with half twists interchanging the point x with the most right point. This finishes the induction step.

The half twists generate all permutations of the marked points. Hence, the following short exact sequence in [FM, Chapter 4] implies that all twists together generate $\mathrm{Mod}(S_{g,n})$:

$$1 \to \mathrm{PMod}(S_{g,n}) \to \mathrm{Mod}(S_{g,n}) \to \Sigma_n \to 1.$$

□

This is also discussed in [FM, Section 4.4.4] and a similar picture [FM, Figure 4.10] is given.

2.8.7 Generalization to Other 3-Orbifolds

Results similar to Theorem 2.8.6 respectively 2.8.10 can be derived for a larger class of 3-orbifolds. Given a 2-orbifold F and a 3-orbifold M, compute all normal 2-orbifolds in M whose genus and number of singular points is less than those of F, then add tunnels and beads to match genus and singular point count. A problem might arise if tori appear as fundamental surfaces because then there are infinitely many normal surfaces of the same gender. In this case, adding a fundamental tori performs surgery on the surface, not changing the topology of the surface but the way the surface is embedded and thus the image of the surface in the fundamental group of M. For simple enough cases, this can still be computed explicitly. Another problem might arise if a fundamental surface splits the 3-orbifold into two connected components, each component having a different image in the fundamental group of M. In this case, the first tunnel can live in only one of the two connected components, the second tunnel can nest through the second tunnel, making the enumeration difficult.

In some cases though, the enumeration is still feasible. Consider, for example, the quotients of S^3 by the orientation-preserving subgroup of a Coxeter reflection group, i.e., the symmetry group of the 5-, 8-, 24-, or 120-cell in S^3. The resulting 3-orbifold quotient is topologically S^3 and the singular locus is the 1-skeleton of a tetrahedron. All fundamental surfaces are again vertex- and edge-linked spheres. And even though an edge-linked sphere separates some of the vertex-linked sphere from some of the other vertex-linked spheres, the enumeration of all possible tunnels is still feasible.

Dunbar classifies the non-hyperbolic geometric 3-orbifolds [Dun88].

2.9 Overview of the Algorithms

Let F be an orientable regular map presented as described in Section 2.9.1. We want to find all (H, B, η)-triples consisting of a subgroup $H \subset G = \mathrm{Aut}^+_{reg}(F)$, a subgroup $B \subset \mathrm{SO}(3)$ of symmetries of Euclidean 3-space, and an isomorphism $\eta : H \cong B$ such that an (H, B, η)-equivariant morphism, immersion, respectively, embedding exists. The algorithm has two steps, the first one is described in Section 2.10, the second one in Section 2.11.

Input	Regular map F.
Output	(H, B, η)-triples up to equivalence such that an (H, B, η)-equivariant morphism, immersion, or embedding exists.

Algorithm

1. Find all (H, B, η)-triples up to equivalence, see this Section 2.10.
2. For each (H, B, η)-triple:
   (a) Is there an (H, B, η)-equivariant morphism, immersion, respectively, embedding? See Section 2.11.
   (b) If yes, emit (H, B, η)-triple.

2.9.1 Presentation of a Regular Map

When we write "**Input:** Regular map F", we mean a finite presentation of $G = \mathrm{Aut}^+_{reg}(F)$ in the generators R and S as defined in Section 2.2.1.

If F is reflexible, then $\mathrm{Aut}_{reg}(F)$ is given as a finite presentation in R, S, and C and G is presented as the subgroup of $\mathrm{Aut}^+_{reg}(F)$ generated by R and S.

Conder and Dobcsianyi give such presentations of $\mathrm{Aut}_{reg}(F)$ for regular maps F up to genus 101 in [Con09] and also provide parsable text files [Con06b, Con06a]. Notice that Conder and Dobcsianyi use T for the reflection C. We replace T by C in the text files they provide, because we already use T to denote RS.

2.10 Algorithm to Find All (H, B, η)-triples

Recall the definition of (H, B, η)-equivariant morphism and the notion of equivalence in Section 2.5. In this section, ignore the underlying topological mapping of an equivariant morphism and just maintain the parts of the definitions involving the groups.

Given a regular map F, Table 2.2 shows an algorithm listing all valid (H, B, η)-triples up to equivalence.

In a naive implementation, produce all triples (H, B, η) and let elements $i \in G = \mathrm{Aut}_{reg}(F)$ and $c \in \mathrm{Isom}(E^3)$ act on the space of all triples (H, B, η) as described in Definition 2.5.2. Pick a representative of each orbit under this action.

To refine the implementation, notice that this action can take H to any conjugate of H in $\mathrm{Aut}_{reg}(F)$, similarly for B. Hence, to list all (H, B, η) up to equivalence, we only need to pick one representative for each conjugacy class of subgroups $H \subset \mathrm{Aut}^+_{reg}(F)$ and $B \subset \mathrm{Isom}^+(E^3)$.

Fix an H and an isomorphic B. An element $i \in G = \mathrm{Aut}_{reg}(F)$ can still act on a triple (H, B, η) by changing η if i is in the normalizer $\mathrm{N}_G(H)$ of H in G. Similarly, an element c can still act on a triple (H, B, η) if it is in the normalizer $\mathrm{N}_{\mathrm{Isom}(E^3)}(B)$ of B in $\mathrm{Isom}(E^3)$.

For the implementation, we present B as a normal subgroup of a triangle group $D = [p, q] \subset \mathrm{Isom}(E^3)$ presented by Equation 2.2. Hence, D acts on B by conjugation and therefore on η in an (H, B, η)-triple. We choose D such that the conjugation action by D is equal to the conjugation action by $\mathrm{N}_{\mathrm{Isom}(E^3)}(B)$. Table 2.1 shows the presentation of B and D. If B is not cyclic, D is equal to $\mathrm{N}_{\mathrm{Isom}(E^3)}(B)$. If B is cyclic, $\mathrm{N}_{\mathrm{Isom}(E^3)}(B)$ is infinite.

Remark 2.10.1. Notice that for the tetrahedral, octahedral, and icosahedral group, at least half of the automorphisms are inner automorphisms. This means that step A and step B cancel each other in a lot of cases, for example, if F is reflexible, and the algorithm could be simplified. However, we avoid special cases and implement the algorithm in its generality as in Table 2.2.

Table 2.1: Presentation of the target symmetry groups $B \subset \mathrm{Isom}^+(E^3)$ [Cox69, Table III, page 413] as subgroups of a triangle group D.

Spatial group B		Presentation[1] of B	D
tetrahedral	$[3,3]^+$	$\langle D.R, D.S \rangle$	$[3,3]$
octahedral	$[3,4]^+$	$\langle D.R, D.S \rangle$	$[3,4]$
icosahedral	$[3,5]^+$	$\langle D.R, D.S \rangle$	$[3,5]$
dihedral[2]	$[2,n]^+$	$\langle D.R, D.S^2 \rangle$	$[2,2n]$
cyclic[2]	$\mathbb{Z}/n$	$\langle D.S \rangle$	$[2,n]$

[1] $D.x$ denotes the generator x of the finitely presented group D.

[2] We choose n to be the order of an element in H.

Table 2.2: Algorithm to enumerate all (H, B, η)-triples up to the equivalence defined in Section 2.5.

Input Regular map F.

Output A representative for each equivalence class of (H, B, η).

Algorithm

1. To speed up computation, find permutation representations of
$$G = \mathrm{Aut}_{reg}(F)^+ \subset \mathrm{Aut}_{reg}(F) \quad \text{and} \quad \mathrm{Aut}_{reg}(F).$$
2. For a representative H of each conjugacy class of subgroups of $\mathrm{Aut}_{reg}(F)$:
If $H \subset \mathrm{Aut}^+_{reg}(F)$:
   (a) For each symmetry group $B \subset \mathrm{SO}(3) \cong \mathrm{Isom}^+(E^3, 0)$ from Table 2.1:
      i. Find an isomorphism $\eta' : H \cong B$.
      If η' exists:
         A. Find all isomorphisms $I = \{\eta : H \cong B\}$ by computing
         $$I = \{\eta' \circ h : h \in \mathrm{Aut}(H)\}.$$
         B. Compute (where D is from Table 2.1)
         $$I' = \text{Conjug. action by } D \setminus I / \text{Conjug. action by } \mathrm{N}_G(H).$$
         C. For a representative η of each double coset in I':
         Emit the triple (H, B, η).

2.11 Algorithm to Decide the Existence of (H, B, η)-Equivariant Morphism, Immersion, and Embedding

Input	Regular map F, (H, B, η)-triple.
Output	Three Booleans: (H, B, η)-equivariant morphism, immersion, respectively, embedding exists.
Algorithm	
	1. Compute τ-tuple, see Section 2.11.1.
	2. Apply decision tree in Figure 2.20.

Section 2.6 translates the question about the existence of equivariant morphisms into the orbifold language. Given a regular map F and an (H, B, η)-triple, recall that the regular covering space $(F, p) \to (F/H, p)$ is specified by a holonomy

$$h : \pi_1^{orb}(F/H, p) \to H.$$

The holonomy for $(S^3, p) \to (S^3/B, p)$ is an isomorphism:

$$\pi_1^{orb}(S^3/B, p) \cong B.$$

Lemma 2.6.1 translates the original question into the question whether

$$\tau = \eta \circ h$$

$$\tau : \pi_1^{orb}(F/H, p) \to B \cong \pi_1^{orb}(S^3/B, p)$$

is induced by an orbifold morphism, immersion, or embedding.

We compute τ in the generators of a standard presentation of $\pi_1^{orb}(F/H, p)$ as described in Section 2.4.1. We encode this in the *τ-tuple*:

$$(\tau(\sigma_1), \ldots, \tau(\sigma_k); \tau(\alpha_1), \tau(\beta_1), \ldots, \tau(\alpha_g), \tau(\beta_g)).$$

The algorithm to compute the τ-tuple is described in Section 2.11.1. Given the τ-tuple, we apply the decision tree in Figure 2.20, the steps are described in the following sections.

Notice that for Steps 1, 2, 3, 5, and 6 in the decision tree, we only need to compute the conjugacy classes of the images of the ssl's. This can be done without implementing all of Section 2.11.1 using Remark 2.11.2.

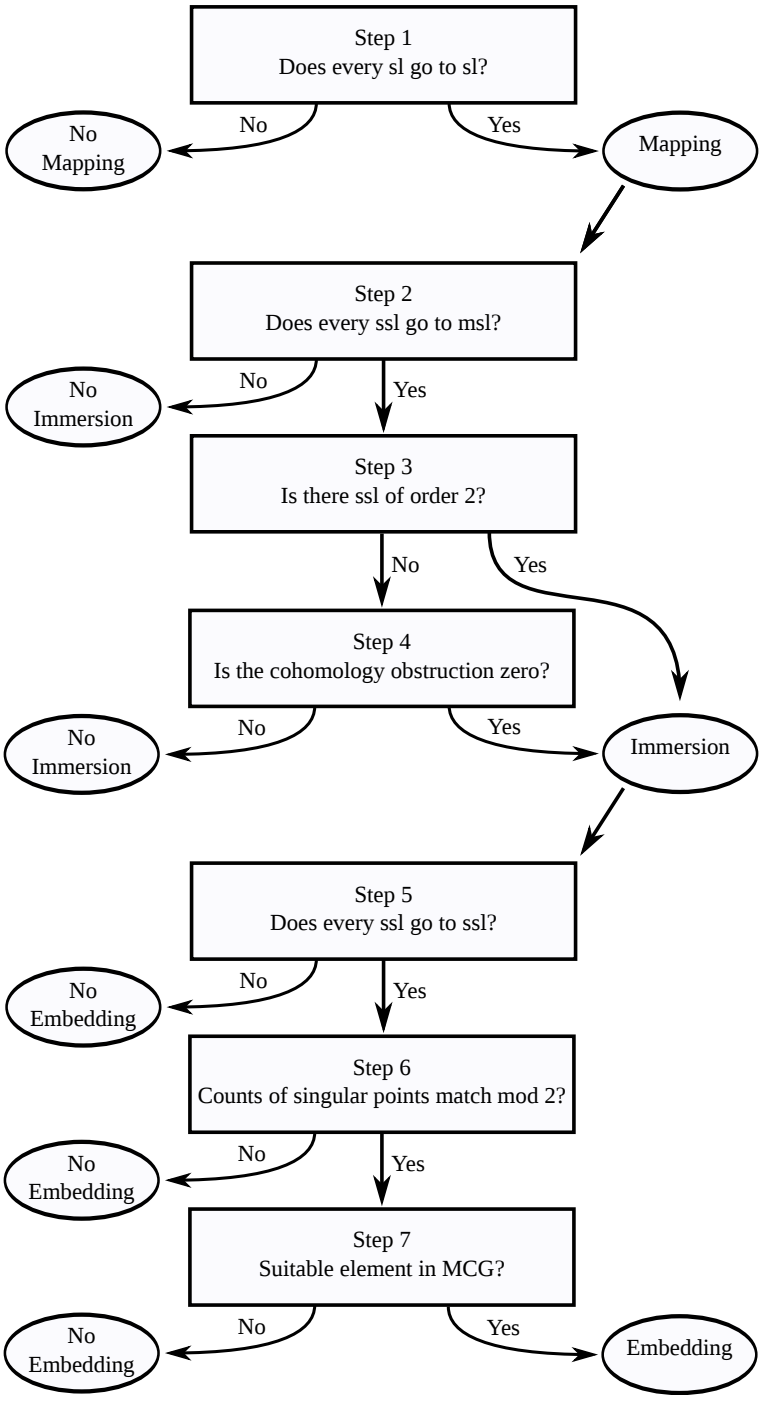

Figure 2.20: Decision tree for a given (H, B, η)-triple.

2.11.1 Computing the τ-Tuple

This algorithm identifies the orbifold $(F/H, p)$ with a standard handle decomposition as described in Section 2.4.1. This gives a presentation of $\pi_1^{orb}(F/H, p)$. For each generator in this presentation, we compute the image under the holonomy $h : \pi_1^{orb}(F/H, p) \to H$. We compose h with η to obtain τ and encode it in a data structure we call *τ-tuple.* Notice that the algorithm implicitly returns the number k of singular points of F/H and the genus g of $X(F/H)$, indicated by using ";" in the τ-tuple.

Input Regular map F, (H, B, η)-triple.

Output τ-tuple in B^{k+2g}

$$(\tau(\sigma_1), \ldots, \tau(\sigma_k); \tau(\alpha_1), \tau(\beta_1), \tau(\alpha_2), \ldots, \tau(\beta_g))$$

of the images under $\tau = \eta \circ h$.

Algorithm

1. Compute black-and-white triangulation of F/H.
2. Find embedded fat graph.
3. Perform handle slides.
4. Compute holonomy $h : \pi_1^{orb}(F/H, p) \twoheadrightarrow H$.
5. Apply η to h.

Remark 2.11.1. Notice that the order of σ_j, $h(\sigma_j)$, and $\tau(\sigma_j) = \eta(h(\sigma_j))$ agree, hence, an τ-tuple implicitly contains what order each singular point s_i in the associated handle decomposition has.
In other words, the algorithm makes a choice on how to label the singular points $s \in \Sigma(F/H)$. A priori, it should also return a tuple with the orders of the singular points s_i if we want to be able to reconstruct F from the τ-tuple. However, this information is already contained implicitly.

Computing the Black-and-White Triangulation of F/H

In this section, we describe the following algorithm:

Input	Regular map F, subgroup $H \subset G$.
Output	Black-and-white triangulation of F/H. (Conjugacy class of $h(\gamma_s) \in H$ for each singular point $s \in \Sigma(F/H)$.)
Algorithm	
	See text for the structure of triangulation.

Here γ_s denotes a ssl about the singular point $s \in \Sigma(F/H)$.

First, we describe the triangulation of F obtained by subdividing each p-gon into $2p$ triangles (Schwarz's triangles in [Cox73]) that we color black and white as in Figure 2.21. A triangle pair is a black and a white triangle sharing an edge as shown in the figure.

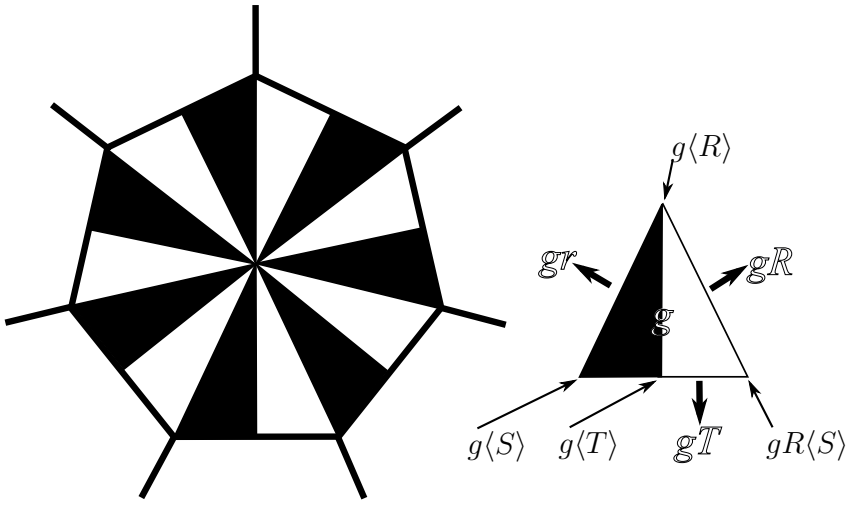

Figure 2.21: Triangulation of a regular map.

The triangle pairs correspond to the elements $g \in G = \mathrm{Aut}^+_{reg}(F)$ such that the automorphism $g \in G$ takes the triangle pair corresponding to id to g. More general, left-multiplication of a label of a triangle pair by an automorphism $g \in G$ gives the action of g on F. In particular, left-multiplication by one of the generators R, S, or T yields a rotation about one of the vertices of the black triangle labeled id. Right-multiplication by R, S, or T of a triangle pair g yields a rotation about one of the vertices of the black triangle labeled g.

This means that right-multiplication by R, $r = R^{-1}$, and T gives the adjacent triangle pairs. There are three classes of vertices in the triangulation of F corresponding to the p-gon

centers, edge centers, and vertices of the regular map F. Vertices in each class correspond to cosets $g\langle R\rangle$, $g\langle S\rangle$, and $g\langle T\rangle$. A triangle corresponding to g has vertices corresponding to those cosets, see Figure 2.21.

Let H be a subgroup of G. To obtain the orbifold F/H, let H act on the above structures from the left. The quotient F/H again posses a triangulation by triangle pairs of black and white triangles. The triangle pairs correspond to cosets Hg and the vertices to double cosets $Hg\langle R\rangle, Hg\langle S\rangle$, and $Hg\langle T\rangle$. The triangles in a triangle pair might share more than one edge, for example, if a conjugate of T is in H, we obtain the triangle pair shown in Figure 2.22.

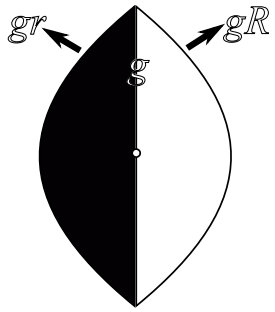

Figure 2.22: Triangle pair with shared edge.

Remark 2.11.2. Some of the vertices turn into singular points of F/H. Let $Hg\langle X\rangle$ represent a vertex s of F/H where $X = R, S$, or T. Take the least $k > 0$ such that $HgX^k = Hg$, i.e., take the least $k > 0$ such that $(gXg^{-1})^k \in H$. This means that rotating the orbifold by k notches about the vertex takes the orbifold to itself. Hence, the element $(gXg^{-1})^k$ is the image $h(\gamma_s)$ of a ssl $\gamma_s \in \pi_1^{orb}(F/H, p)$ about the vertex in H. Notice that the orientation of the ssl is compatible with the orientation of F/H. Apply η to obtain the conjugacy class of $\tau(\gamma_s)$.

Remark 2.11.3. Recall that γ_s is determined only up to conjugacy by the singular point s, as is $h(\gamma_s)$. Similarly, the above computation gives conjugate, but different $(gXg^{-1})^k$ for different representatives g of the same vertex s.

The Dual 2-Cell Complex

Section 2.11.1 constructs a triangulation of F/H. Take the dual 2-cell complex, see Figure 2.23. The vertices of the 2-cell complex are trivalent and colored black and white being the dual of black and white triangles. This makes the 1-skeleton of the 2-cell complex a bipartite graph. Call p the vertex corresponding to the black triangle labeled id. It serves as base point for F/H.

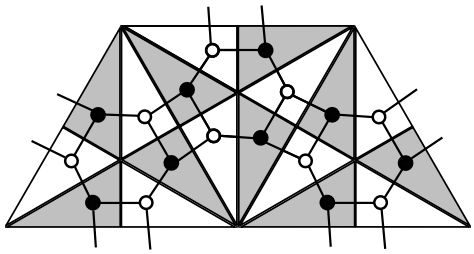

Figure 2.23: Dual 2-cell complex of the canonical triangulation of F/H.

Embedded (Fat) Graph

For each singular point s of F/H, remove the corresponding (open) 2-cell in the dual 2-cell complex. The homotopy type is now that of the punctured surface $X(F/H) \setminus \Sigma(F/H)$. Remove another random 2-cell. We obtain a surface with boundary and with free fundamental group.

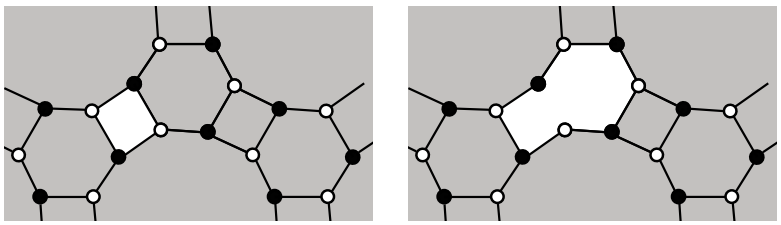

Figure 2.24: Simple homotopies on the 2-cell complex of punctured F/H.

Remove a 2-cell and an adjacent edge as in Figure 2.24. Repeat until there are no 2-cells left. If a vertex (except for p) is connected to only one edge, remove the vertex and the edge. Repeat until no such vertices are left. These steps are simple homotopies resulting in a graph embedded into the 1-skeleton of the 2-cell complex, see Figure 2.25.

Being embedded into a surface, it is naturally a *fat* graph G, i.e., the orientation of the surface induces a cyclic order of the edges incident to a vertex. The fat graph G is a deformation retract of the 1-skeleton of a handle decomposition of $X(F/H) \setminus \Sigma(F/H)$ with only one 2-handle.

Unzipping the Fat Graph

Given a fat graph G, we can perform the "unzip" move in Figure 2.26 to obtain a new fat graph G' that projects onto G.

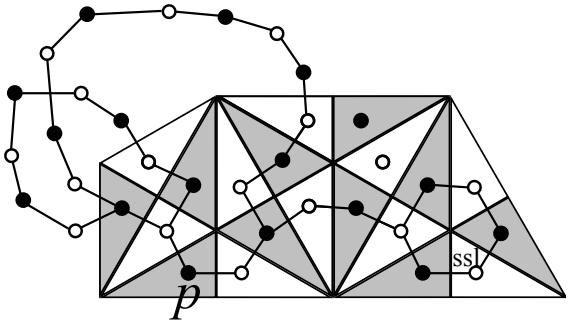

Figure 2.25: Embedded graph in 2-cell complex.

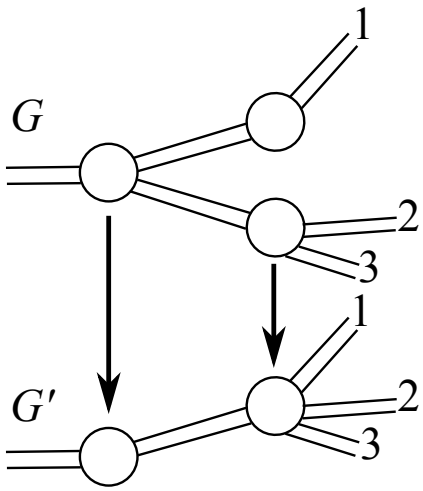

Figure 2.26: Unzip move on a fat graph.

Perform these moves on the fat graph G as long as possible avoiding the vertex p. We obtain an "unzipped" graph $\tilde{G}$ that projects onto G and such that only the vertex p has valence different from two. The unzipped fat graph $\tilde{G}$ explicitly illustrates a 1-skeleton of punctured F/H, as shown in Figure 2.27. Furthermore, $\tilde{G}$ has canonical loops γ_i generating $\pi_1(\tilde{G}, p)$. Each such loop projects to a loop in G and, hence, onto the 1-skeleton of the 2-cell complex.

Reading the Image of a Loop

Given a loop γ that is a canonical generator of $\pi_1(\tilde{G}, p)$, take its image in the 1-skeleton of the 2-cell complex. Split it at the black vertices into arcs. Each arc consists of two segments that "bend" around a vertex in the black and white triangulation, see Figure 2.28. Hence, we can assign $R^{\pm 1}, S^{\pm 1}$, or $T^{\pm 1} \in G$ to the arc. Write those in the order the loop traverses

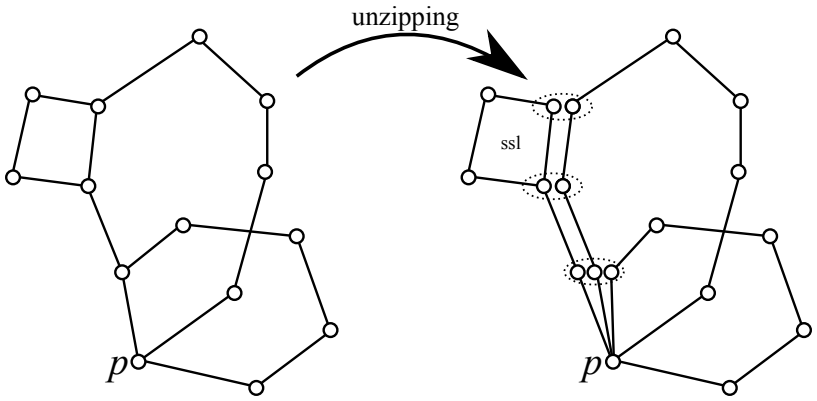

Figure 2.27: Unzipped fat graph making 1-skeleton structure apparent.

the arcs. The resulting word is the image $h(\gamma)$ of γ under the holonomy.

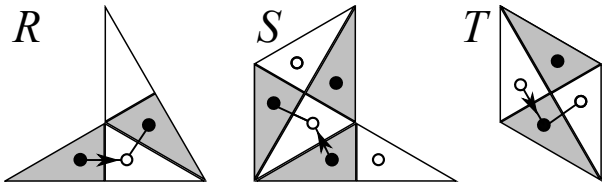

Figure 2.28: Arcs corresponding to the generators R, S, and T.

Handle Slides

The "unzipped" fat graph $\tilde{G}$ models a 1-skeleton of a handle decomposition of punctured F/H and we have computed a presentation the holonomy

$$h : \pi_1(\tilde{G}, p) \to \pi_1^{orb}(F/H, p) \to H$$

in the loops of $\tilde{G}$.

The kernel $\ker(\pi_1(\tilde{G}, p) \to \pi_1^{orb}(F/H, p))$ from the free group might not be generated by the relations in the standard presentation of $\pi_1^{orb}(F/H, p)$. This is equivalent to the fat graph $\tilde{G}$ not being in the standard form given in Figure 2.29, e.g., the left picture in Figure 2.30. To fix this, we use handle slides (see Figure 2.30) on the fat graph $\tilde{G}$ to bring it into the standard form. In the standard form, each boundary component of the fat graph $\tilde{G}$ is supposed to represent an ssl except for the "outer" boundary component representing the relation in π_1^{orb}. This can be checked by detecting whether the outer boundary component is sent to zero, and fixed by handle slides if not.

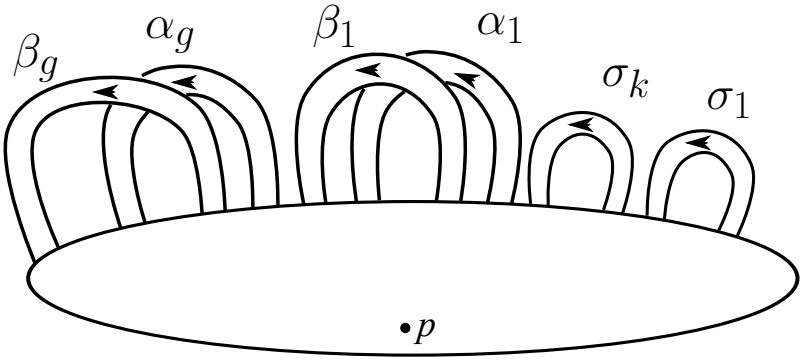

Figure 2.29: Standard fat graph serving as 1-skeleton of $X(F/H) \setminus \Sigma(F/H)$.

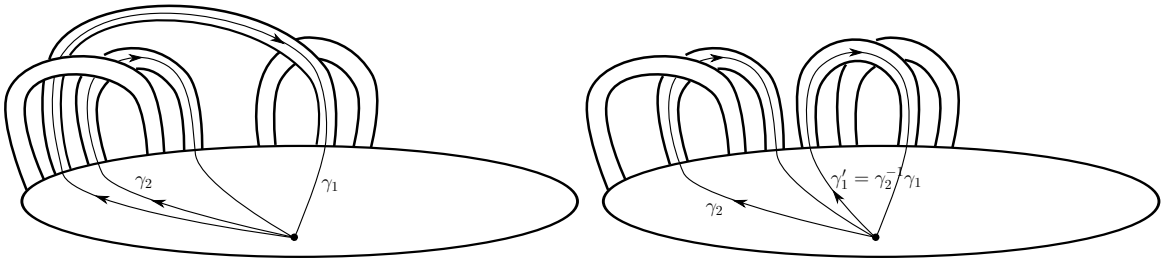

Figure 2.30: Handle slide on a fat graph.

Such a handle slides alters the fat graph $\tilde{G}$ and the way it maps into F/H. If $\tilde{G}'$ is, e.g., obtained from the handle slide in Figure 2.30, then we obtain a new presentation $h' : \pi_1^{orb}(\tilde{G}', p) \to H$ from $h : \pi_1^{orb}(\tilde{G}, p) \to H$ such that

$$h' : \gamma_1 \mapsto h(\gamma_2^{-1}\gamma_1).$$

Having performed the handle slides and kept track of the images of the generators of $\pi_1(\tilde{G}, p)$, we can now read the h-tuple, see Figure 2.29.

2.11.2 Step 1 in Decision Tree

This step is based on the Main Theorem 2.7.7 for mappings.

Input	Conjugacy class of $\tau(\gamma_s)$ for each singular point $s \in \Sigma(F/H)$.
Output	Boolean: τ is induced by orbifold map.
Algorithm	Check that each $\tau(\gamma_s)$ is a sl in B.

Remark 2.11.4. This step is unnecessary (i.e., always yes) for finite subgroups $B \subset \mathrm{SO}(3)$ regarded here. The reason is that every element in B fixes some axis. In other words, every element in $\pi_1^{orb}(S^3/B, p)$ is a sl and the condition is void.

This is not the case for other spherical 3-orbifolds. For example, take two axis in S^3 such that rotations about them commute. Let Γ be generated by a rotation about one axis by $2\pi/p$ and a rotation about the other axis by $2\pi/q$. The orbifold S^3/Γ is topologically S^3 with singular locus being the Hopf link, the components having order p and q. The multiples of the generators of Γ are sl, but the other elements in $\pi_1^{orb}(S^3/\Gamma, p) \cong \mathbb{Z}/p \oplus \mathbb{Z}/q$ are not.

2.11.3 Step 2 in Decision Tree

Input	Conjugacy class of $\tau(\gamma_s)$ for each singular point $s \in \Sigma(F/H)$.
Output	Boolean: τ is induced by immersion of 1-skeleton.
Algorithm	Check that each $\tau(\gamma_s)$ is a msl in B.

Remark 2.11.5. An element in B is a ssl if it is conjugate to $R^{\pm 1}$, $S^{\pm 1}$, or $T = T^{-1} = RS$ (only $S^{\pm 1}$ if B is cyclic). All msl in B are given by

$$\{X^n : X \text{ is a ssl}, \quad n|\mathrm{ord}(X), \quad n \neq \mathrm{ord}(X)\}.$$

This step is checking the conditions of Lemma 2.7.6 for immersing the 1-skeleton of $(F/H, p)$. In this case, the lemma simplifies to:

Lemma 2.11.6. *The homomorphism τ is induced by an immersion of the 1-skeleton of $(F/H, p)$ if and only if τ sends every ssl to an msl. In other words, this is a necessary condition for the existence of (H, B, η)-equivariant immersion.*

Proof. Since τ is induced from a (H, B, η)-triple, a sl in F/H or M/B gives an element in H and B, and, because η is an isomorphism, the image $\tau(\gamma_s) \in \pi_1^{orb}(S^3/B, p)$ of a ssl $\gamma_s \in \pi_1^{orb}(F/H, p)$ has the same order as the ssl γ_s. □

2.11.4 Step 3 in Decision Tree

Step 3 is an application of the Main Theorem 2.7.30 for Immersions.

Input	Conjugacy class of $\tau(\gamma_s)$ for each singular point $s \in \Sigma(F/H)$.
Output	Boolean: Order two loop exists.
Algorithm	Check that there is $\tau(\gamma_s)$ with $\text{ord}(\tau(\gamma_s)) = 2$.

This is equivalent to the existence of $h(\gamma_s)$ with $\text{ord}(h(\gamma_s)) = 2$ because η is an isomorphism.

2.11.5 Step 4 in Decision Tree

Input	τ-tuple
Output	Boolean: Cohomology obstruction for immersion
Algorithm	Construct loop to attach 2-handle, determine framing, compute framing invariant. See text for details.

The τ-tuple specifies how to immerse the 1-skeleton of the standard handle decomposition into S^3/B. The 1-skeleton is bounded by an immersed ribbon. By the Main Theorem 2.7.30, an immersion exists if and only if the $\mathbb{Z}/2$-framing invariant of the immersed ribbon is zero (the framing invariant is equal to the cohomology obstruction because there is only one 2-handle and the coboundary map is zero).

We construct an immersed loop in the black-and-white triangulation of S^2 corresponding to B. Then, we discuss how to modify the blackboard framing to obtain the immersed ribbon. For the implementation, we simplify the process.

While explaining the process we use the regular map R5.2 and icosahedral symmetry as a guiding example. In this case, an immersion does not exist. The calculations are computer assisted.

Example: R5.2 and Icosahedral Symmetry

The goal of this subsection is to introduce the example guiding through the rest of the section and to give the τ-tuple for it in Equation 2.11. We choose R5.2 because it is the first regular map in Conder's list that has a potential immersion realizing the icosahedral group which is the largest finite non-solvable subgroup of SO(3).

The regular map R5.2 is the unique regular map of type $\{3, 10\}$ and genus 5. Up to conjugacy, there are two subgroups of $\mathrm{Aut}^+_{reg}(\mathrm{R5.2})$ that are isomorphic to $B = [3, 5]$. This results in two (H, B, η)-triples up to equivalence. One of the triples fails Step 2 of the decision tree in Figure 2.20. The other one passes Step 2 and fails Step 3, so the computation of the cohomology obstruction in Step 4 decides the existence of an equivariant immersion.

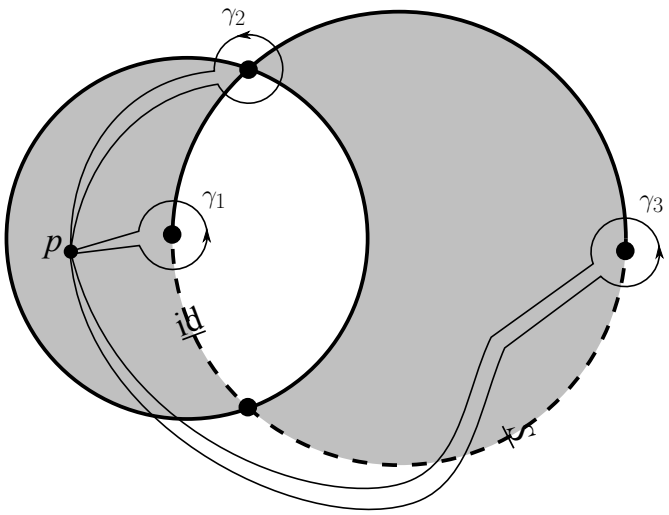

Figure 2.31: Black-and-white triangulation of $(F/H, p)$ for R5.2 and $H \cong B$ icosahedral symmetry.

Figure 2.31 shows the black-and-white triangulation of the quotient orbifold $(F/H, p)$ as described in Section 2.11.1. Topologically, F/H is a sphere. The dashed lines indicate which two triangles form a triangle pair. A group element $g \in \mathrm{Aut}^+_{reg}(F)$ representing the triangle pair Hg is written onto the dashed line, the label being oriented so that the vertex $Hg\langle R\rangle$ is up and the vertex $Hg\langle T\rangle$ is down. The figure implicitly also shows a standard handle decomposition of $(F/H, p)$.

We can read the holonomy $h : \pi_1^{orb}(F/H, p) \to H$ from the loops as described in Section 2.11.1:

$$\begin{aligned} h(\gamma_1) &= R \\ h(\gamma_2) &= S^2 \\ h(\gamma_3) &= TRT^{-1} \end{aligned} \tag{2.10}$$

We can apply η and write each group element as a conjugate of $X = R^{\pm 1}, S^{\pm 1}$ and then as

a word in the generators to obtain the τ-tuple $(\tau(\gamma_1), \tau(\gamma_2), \tau(\gamma_3))$:

$$\begin{aligned} \tau(\gamma_1) &= (S^2)R^{-1}(S^2)^{-1} \\ \tau(\gamma_2) &= (TR^{-1})S(TR^{-1})^{-1} \\ \tau(\gamma_3) &= SRS^{-1} \end{aligned} \tag{2.11}$$

Model of Target Space

Assume B is not cyclic. We construct the immersed ribbon in the black-and-white triangulation of S^2 corresponding to the symmetry group B as described in Section 2.11.1. For example, Figure 2.32 shows the black-and-white triangulation for B being the icosahedral group if we identify edges of the net shown. We have a copy of the base point p in each black triangle.

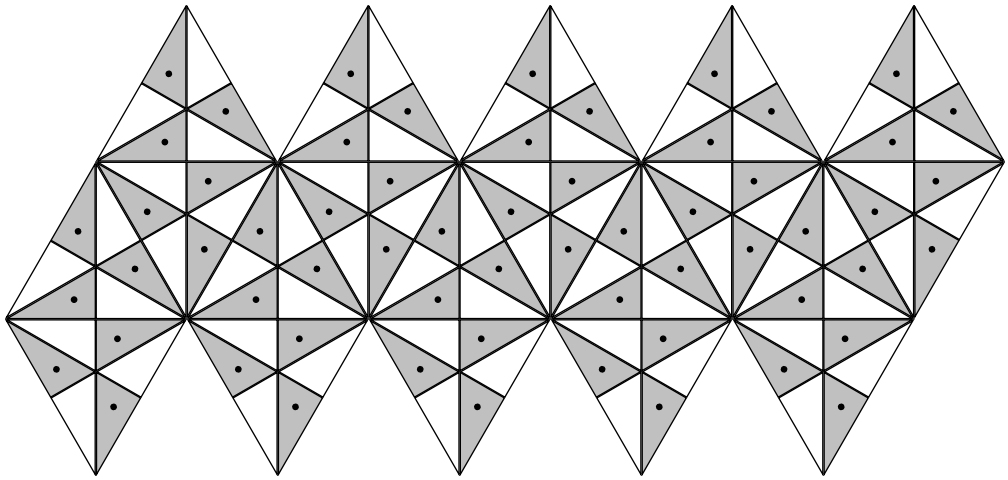

Figure 2.32: Black-and-white triangulation of S^2 for B being the icosahedral group. Glue the net to obtain a icosahedron.

Formally speaking, the orbifold S^3/B is the suspension of a triangle orbifold $\mathcal{O}$. Avoiding the trivalent vertices of $\Sigma(S^3/B)$, the ribbon is immersed into the product $I \times \mathcal{O}$. Lifted to S^3, the ribbon is immersed into a product of an interval I and a regular map, namely the surface of a tetrahedron, octahedron, icosahedron, or the dihedral group. We can triangulate this regular map as in Section 2.11.1 by black and white triangles.

Arcs for Generators and Paths for Words

Given a copy of the base point p in a black triangle and $X = R^{\pm 1}, S^{\pm 1}, T^{\pm 1}$, we can draw an arc for X in the 1-skeleton of the 2-cell complex dual to the black and white triangulation as in Figure 2.28. For better drawings, we perturb the arc for X so that it does not overlap with other arcs, see Figure 2.33.

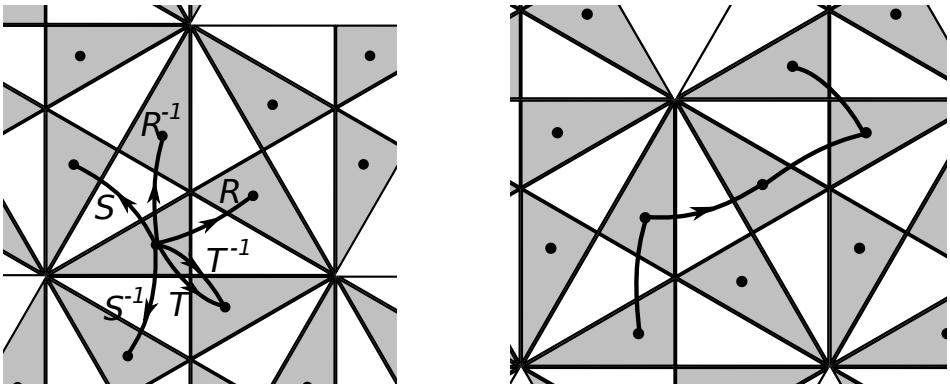

Figure 2.33: Arcs for the generators $R^{\pm 1}, S^{\pm 1}, T^{\pm 1}$ (notice that the arcs for T and T^{-1} are not the same.) Path for the word $R^{-1}SR^{-1}T$.

Given a word, we can connect the arcs to a path, see Figure 2.33 for an example. This is the reverse process of reading off a word from a loop that was described in Section 2.11.1.

Immersing the 0-Handle

We draw a little disk D around the base point p and fix $k + 4g$ points on ∂D counterclockwise. These points mark the ends of the 1-handles attaching to the 0-handle, see Figure 2.34. Split ∂D at the points into arcs. Figure 2.35 shows this in case of the guiding example of this section.

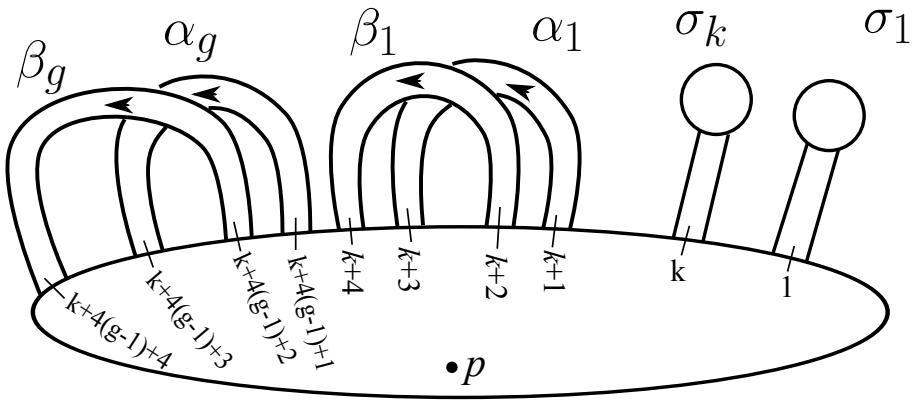

Figure 2.34: Arcs on the boundary ∂D of the 0-handle.

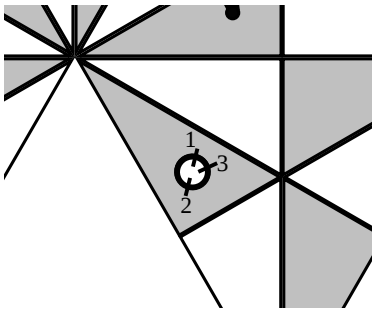

Figure 2.35: 0-handle for the guiding example of this section.

Constructing a Path for $\tau(\sigma_i)$

We write $\tau(\sigma_j)$ as word $w_j = \gamma_j X_j^n \gamma_j^{-1}$ with $X_j = R^{\pm 1}, S^{\pm 1}$ and γ_j a word in $R^{\pm 1}, S^{\pm 1}, T^{\pm 1}$. We construct a path for γ_j and perturb the first arc to connect to the point j on the 0-handle. We extend the path by X_j and then take a rotated and reversed copy of the path for γ_j to obtain the path for $\tau(\sigma_j)$. Figure 2.36 shows the path for $\tau(\gamma_1)$ in case of the guiding example of this section. The arc for X_j is marked bold.

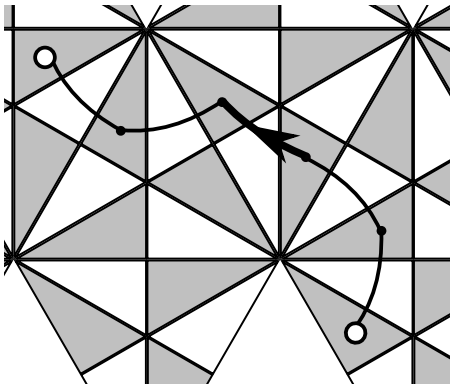

Figure 2.36: Path for $\tau(\gamma_1) = (S^2)R^{-1}(S^2)^{-1}$ in the guiding example of this Section.

Constructing a Path for $\tau(\alpha_i)$ and $\tau(\beta_i)$

We write $\tau(\alpha_i)$ and $\tau(\beta_i)$ as words in $R^{\pm 1}, S^{\pm 1}, T^{\pm 1}$. We denote these words by $w_{k+4(i-1)+1}$ and $w_{k+4(i-1)+2}$ and construct the path for these words as described earlier. For $\tau(\alpha_i)$, we perturb the first and last arc of the path to connect to the point $k + 4(i-1) + 1$ and $k + 4(i-1) + 3$ on the 0-handle. For $\tau(\beta_i)$, perturb the arcs to connect to the points $k + 4(i-1) + 4$ and $k + 4(i-1) + 2$.

Let $w_{k+4(i-1)+3} = w_{k+4(i-1)+1}^{-1}$ and $w_{k+4(i-1)+4} = w_{k+4(i-1)+2}^{-1}$.

Putting it Together to a Loop

To obtain the loop, we start with the first arc of ∂D from the point $k + 4g$ to the point 1 on the 0-handle. We add the path for $\tau(\sigma_1)$, the next arc of ∂D, $\tau(\sigma_2)$, and so on. Then, we take the path for $\tau(\alpha_1)$, the suitable arc of ∂D, $\tau(\beta_1)$, arc of ∂D, a reversed and rotated copy of the path for $\tau(\alpha_1)$, arc of ∂D, a reversed and rotated copy of the path for $\tau(\beta_1)$, and so on.

In other words, we build a loop for the word $w_1 \dots w_k w_{k+1} \dots w_{k+4g}$ with the arcs corresponding to the first and last letter of each w_i perturbed and connected by pieces of ∂D.

Figure 2.37 shows the resulting loop for the guiding example of this section.

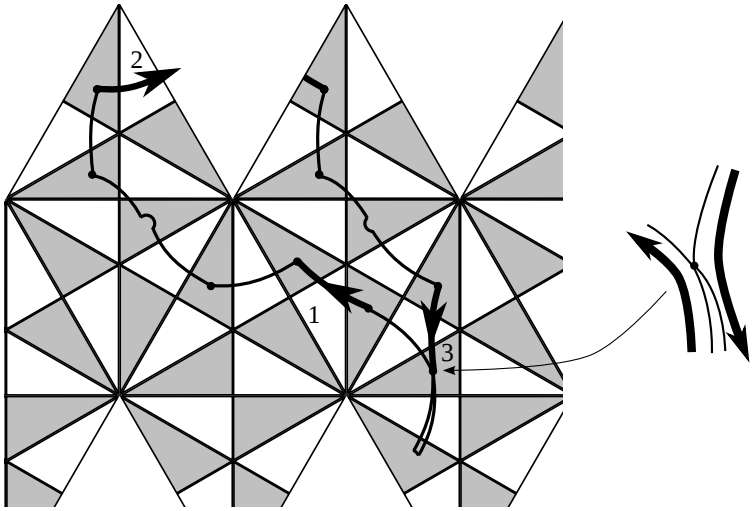

Figure 2.37: Loop serving as boundary of immersed 1-skeleton.

Loop is Immersed

If the words w_j do not contain XX^{-1}, then the loop is immersed. In particular, this is true if we choose the words w_j, respectively, γ_j to be of minimal length.

Framing

Pick the blackboard framing and imagine the 2-handle is attached from the right hand side when moving forward along the loop. This framing works except for the paths corresponding to $\tau(\sigma_j) = \gamma_j X_j^n \gamma_j^{-1}$ where we picked $X_j = R^{-1}$ or $X_j = S^{-1}$. In this case, the singular point s is to the right of the arc corresponding to X_j, and, hence, the 2-handle has to be attached from the left hand side. Figure 2.38 shows an example. We fix this by applying a half twist just before and after entering the arc. These twists have to be done "equivariantly", i.e., they are related by the rotation X_j^n about the singular point s. This changes the framing invariant by one, see Figure 2.38.

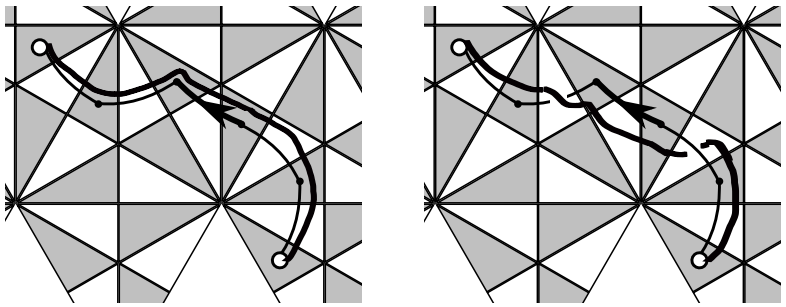

Figure 2.38: Changing framing if $X_j = R^{-1}$ or S^{-1}, here for $X_1 = R^{-1}$.

Corollary 2.11.7. *An immersion exists if and only if the number of self-intersections of the immersed loop constructed above plus the number of j with $\tau(\sigma_j) = \gamma_j X_j^n \gamma_j^{-1}$ where $X_j = R^{-1}$ or $X_j = S^{-1}$, $p > 0$ is even.*

The number of self-intersections of an immersed loop is defined modulo 2 because there might be choices of perturbing it to make the intersections transverse.

In the guiding example of this section, this happens once for $\tau(\sigma_1) = (S^2)R^{-1}(S^2)^{-1}$. Figure 2.39 shows the resulting framing. The framing invariant is odd, hence, an immersion does not exist.

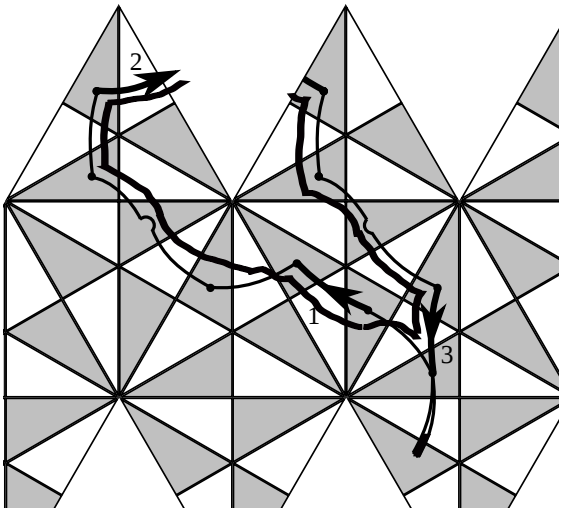

Figure 2.39: Immersed ribbon serving as boundary of immersed 1-skeleton.

Perturbing the Arcs Revisited

Recall that we perturbed the arcs corresponding to the first and last letter in a word w_i to connect them through parts of ∂D. The goal of this section is to avoid this perturbations, effectively collapsing the 0-handle. The resulting loop is easier to construct: it is simply the loop corresponding to the word $w_1 \dots w_{k+4g}$. The example in Figure 2.40 shows a well-behaved case where this results again in an immersed loop with blackboard framing in the same regular homotopy class.

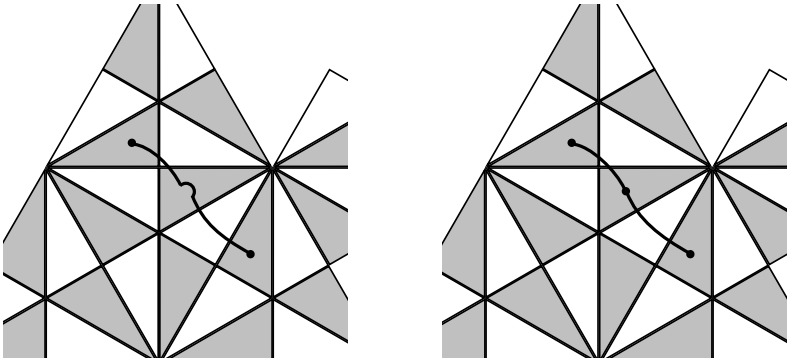

Figure 2.40: Collapsing a 0-handle.

In general, however, we might run into problems:

1. Potentially, the loop might traverse the 0-handle in the same black triangle more than once. This might cause several intersections between the different segments passing through the triangle. However, we are interested only in the parity of the intersection number, hence, we can apply a regular homotopy to each segment independently and can count the number of self-intersections after it, see Figure 2.41.

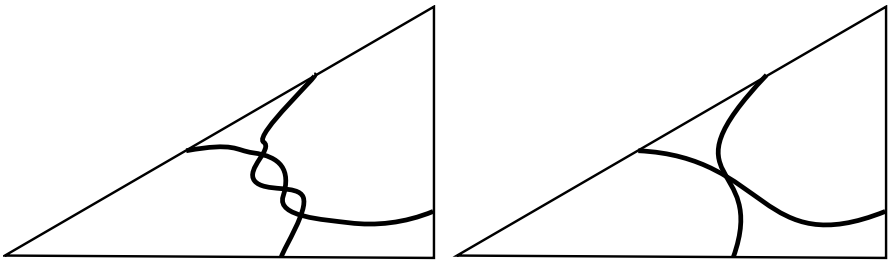

Figure 2.41: Loop traversing a black triangle twice with odd number of self-intersections.

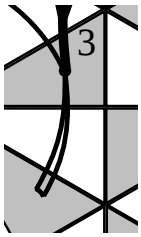

Figure 2.42: 0-handle collapse resulting in non-immersed loop.

2. **Loop no longer immersed.** If the last letter of the word w_j is the inverse of the first letter of w_{j+1} (cyclic indexing), then collapsing the 0-handle results in a loop that has a "hair pin" and is no longer immersed. Figure 2.42 shows an example that is part of the loop for the guiding example in Figure 2.37.

   We can always change a word $w_j = \gamma_j X_j^n \gamma_j^{-1}$ by prepending $R^{\pm p}$, $S^{\pm q}$, or $T^{\pm 2}$ to γ_j. For the words for $\tau(\alpha_i)$ and $\tau(\beta_i)$, we can prepend and append these as well. We can use this to avoid the pattern XX^{-1} anywhere in the (cyclic) word $w_1 \dots w_k w_{k+1} \dots w_{k+4g}$, thus fixing the problem.

3. **Change of framing.** When collapsing the 0-handle, the number of self-intersections of the immersed loop might change. Thus, the blackboard framing of the loop might yield a different $\mathbb{Z}/2$-framing invariant, this is shown in Figure 2.43. This happens if the incoming arc intersects the outgoing arc.

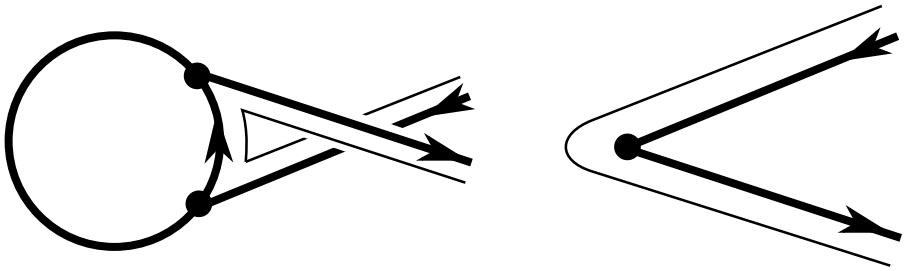

Figure 2.43: Wrong blackboard framing after 0-handle collapse.

Recall that the arcs connecting to the 0-handle D correspond to the first and last letter in the w_i. To see whether these arcs intersect, we fix a standard way to connect these arcs. This happens in an annulus D' around D. Notice that the arcs in Figure 2.33 hit D' at different angles. We obtain the picture shown in Figure 2.44.

Make a cut on ∂D between the vertices $k + 4g$ and 1, and a cut on $\partial D'$ between T^{-1} and R. Then, there is an induced ordering on the generators $R < R^{-1} < S < S^{-1} <$

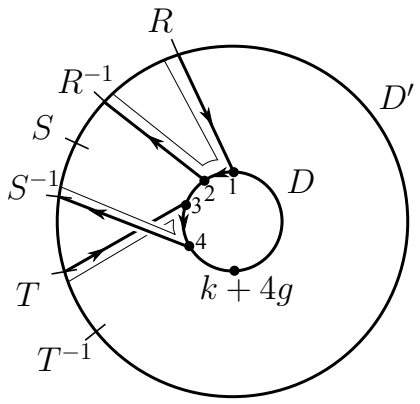

Figure 2.44: Standard way to connect arcs to the 0-handle.

$T < T^{-1}$. The incoming and outgoing arc intersect if the inverse of the last letter of w_i has higher order than the first letter of w_{i+1}.

To cover the case w_{k+4g} and w_1, we can apply cyclic indexing of the w_j. Notice that this case behave in the opposite way. We can fix this by adding one self-intersection to the total.

4. **Trivial words $\tau(\alpha_i)$, $\tau(\beta_i)$, and γ_j.** This might cause special cases. Avoid by applying the same trick of prepending or appending $R^{\pm p}, S^{\pm q}$, or $T^{\pm 2}$.

Algorithm

To summarize, we have the following algorithm:

Input τ-tuple.
Output Boolean: Cohomology obstruction for immersion.
Algorithm

1. Write each $\tau(\sigma_j)$ as word $w_j = \gamma_j X_j^n \gamma_j^{-1}$ with $X_j = R^{\pm 1}, S^{\pm 1}$ and γ_j a word in $R^{\pm 1}, S^{\pm 1}, T$ such that w_j contains no XX^{-1}.
2. Write each $\tau(\alpha_i)$ as word $w_{k+4(i-1)+1}$ in $R^{\pm 1}, S^{\pm 1}, T$ such that w_j contains no XX^{-1}.
3. Write each $\tau(\beta_i)$ as word $w_{k+4(i-1)+2}$ (same as $\tau(\alpha_i)$).
4. Prepend $R^{\pm p}, S^{\pm q}, T^{\pm 2}$ to γ_j, prepend or append to $w_{k+1}, \ldots, w_{k+4g}$ to avoid empty w_i, γ_j or XX^{-1} in the cyclic word $w_1 \ldots w_{k+4g}$ where $w_{k+4(i-1)+3} = w_{k+4(i-1)+1}^{-1}$ and $w_{k+4(i-1)+4} = w_{k+4(i-1)+2}^{-1}$.
5. Add the following numbers modulo 2. If sum is odd, no immersion exists.
   (a) Number of $i = 1, \ldots, k+4g$ such that the inverse of the the last letter of w_i has higher order than the first letter of w_{i+1} (cyclic indexing). The order is $R < R^{-1} < S < S^{-1} < T < T^{-1}$.
   (b) 1 (because the previous calculation is reversed for $i = k + 4g$)
   (c) Number of $j = 1, \ldots, k$ such that the word w_j is $\gamma_j X_j^n \gamma_j^{-1}$ with $X_j = R^{-1}, S^{-1}$.
   (d) Number of self-intersections of the immersed loop $w_1 \ldots w_{k+4g}$ in the black-and-white triangulation (see next section).

Number of Self-Intersections of An Immersed Loop

Consider an immersed loop described by a word $w = X_1 \ldots X_n$. Recall that an immersed loop can be perturbed to have transverse self-intersections, defining the number of self-intersections modulo two.

First, assume the loop intersects itself only at copies of p. Let ab and cd represent paths of two arcs each that intersect in the middle, see Figure 2.45.

There is a cyclic ordering of the letters $R < R^{-1} < S < S^{-1} < T < T^{-1} < R$ coming from

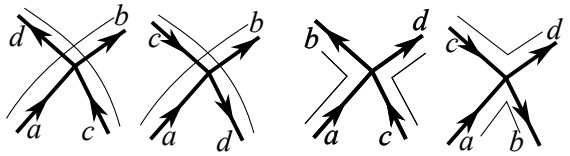

Figure 2.45: Two paths intersecting in a point and their intersection numbers.

the angles at which the arcs hit p in Figure 2.33. We can detect whether ab and cd intersect transversely yielding odd intersection number by checking whether the following holds:

$$a^{-1} < c^{-1} < b < d < a^{-1} \quad \text{or} \quad a^{-1} < d < b < c^{-1} < a^{-1}. \tag{2.12}$$

Now, drop the assumption. Let the loop traverse the same arc twice, either in the same or opposite orientations. We reduce to the previous case by perturbing the arcs so that the loop intersects itself only in points at copies of p again, see Figure 2.46.

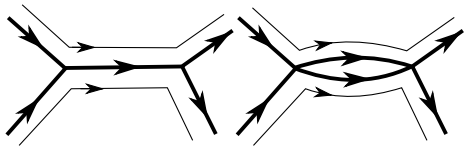

Figure 2.46: Perturbation such that loop intersects in points only.

To do this in a deterministic way, we parametrize a family of perturbed arcs by pairs (X, n) where $X = R^{\pm 1}, S^{\pm 1}$, or $T^{\pm 1}$ as in Figure 2.47. The angles at which the perturbed arcs hit p again induce a cyclic ordering:

$$\begin{aligned} &(R,1) < \cdots < (R,n) < (R^{-1},n) < \cdots < (R^{-1},1) \\ <&(S,1) < \cdots < (S,n) < (S^{-1},n) < \cdots < (S^{-1},1) \\ <&(T,1) < \cdots < (T,n) < (T^{-1},n) < \cdots < (T^{-1},1) < (R,1). \end{aligned} \tag{2.13}$$

We obtain the perturbed loop by using the arc (X_n, n) for the letter X_n at the n-th place in the word. Using the new cyclic ordering on these pairs, we can again apply Equation 2.12 to compute the parity of the intersection number of two paths $ab = (X_i, i)(X_{i+1}, i+1)$ and $cd = (X_j, j)(X_{j+1}, j+1)$.

We detect intersections by checking whether two subwords $X_1 \dots X_j$ and $X_1 \dots X_i$ are representing the same element in B. Thus, we have the following algorithm:

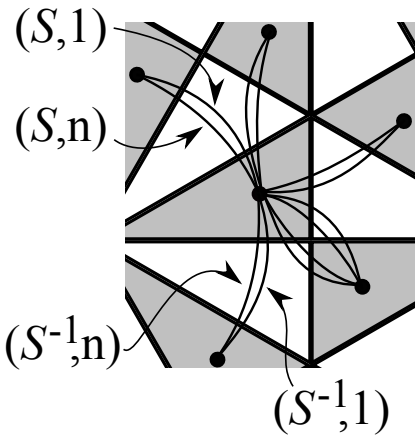

Figure 2.47: Family of perturbed arcs, also see Figure 2.33.

Input	Group B, a word $w = X_1 \dots X_n$ presenting an immersed loop in the black-and-white-triangulation.
Output	Number of self-intersections of immersed loop modulo 2.
Algorithm	

1. Compute $b_1, \dots, b_n$ where b_j is the element in B presented by the word $X_1 \dots X_j$.

2. Compute the number of pairs (i, j) with $1 \leq i < j \leq n$ such that

$$b_i = b_j \quad \text{and}$$

$$\Big((X_i^{-1}, i) < (X_j^{-1}, j) < (X_{i+1}, i+1) < (X_{j+1}, j+1) < (X_i^{-1}, i)$$

$$\text{or}$$

$$(X_i^{-1}, i) < (X_{j+1}, j+1) < (X_{i+1}, i+1) < (X_j^{-1}, j) < (X_i^{-1}, i) \Big)$$

where we use the cyclic ordering in Equation 2.13 and cyclic indexing for the X_i.

2.11.6 Step 5 in Decision Tree

Input	Conjugacy class of $\tau(\gamma_s)$ for each singular point $s \in \Sigma(F/H)$.
Output	Boolean: Necessary condition for embedding.
Algorithm	Check that each $\tau(\gamma_s)$ is a ssl in B.

Remark 2.11.5 explains how to detect ssl's.

Remark 2.11.8. Notice that msl is replaced by ssl when switching from immersions to embeddings. Let us construct an example illustrating that ssl is too restrictive for immersions. Embed a disk D into S^3 intersecting an axis in S^3 perpendicular. Compose the embedding with the trivial double covering map $F = D \times \mathbb{Z}/2 \to D$. F is immersed into $M = S^3$. Let the group $H = B = \mathbb{Z}/4$ act on F and M such that the generator b rotates D and M by a $\frac{1}{4}$th of a turn and also exchanges the two disks in F. Thus, b^2 rotates each disk in F by a half turn and does not exchange the disk. The quotient F/H thus is a disk with a singular point of order two, see Figure 2.48. A ssl in F/H goes to twice a generator of B, i.e, a msl but not a ssl. This happens for the immersed regular map R3.4, see Remark 2.12.1. However, this cannot happen for equivariant embeddings $F \to M$: Let $s \in M$ be a point fixed by a cyclic subgroup. Then, $f^{-1}(s)$ consists of at most one point in F and that point is fixed by the same cyclic subgroup.

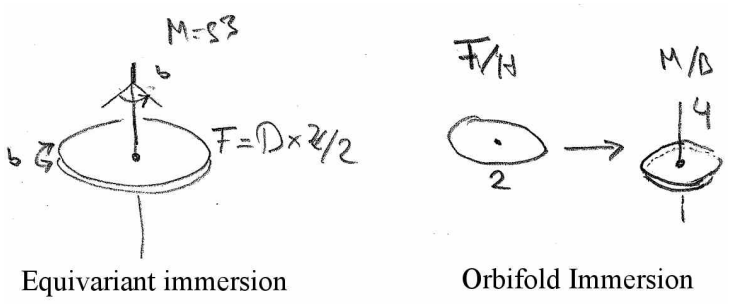

Figure 2.48: An equivariant immersion sending a ssl to a msl.

2.11.7 Step 6 in Decision Tree

Step 6 can be skipped in the decision tree but speeds up implementation, since it is a quick check not requiring a standard handle decomposition.

Input Conjugacy class of $\tau(\gamma_s)$ for each singular point $s \in \Sigma(F/H)$.
Output Boolean: τ passes counting argument similar to Remark 2.8.7.
Algorithm

Let α_X be the number of $\tau(\gamma_s)$ that are conjugate to X in B.

1. If B is the octahedral, icosahedral, or dihedral group D_{2n},
   check that α_{X_R}, α_{X_S}, and α_{X_T} are either all odd or all even.
2. If B is the tetrahedral group,
   check that $\alpha_{X_R} = \alpha_{X_{R^{-1}}}$ and ($\alpha_{X_R} > 0$ if α_{X_T} is odd).
3. If B is the dihedral group $D_{2n+1} = [2, 2n+1]^+$,
   check that α_{X_R} is even and ($\alpha_{X_R} > 0$ if α_{X_S} is odd).
4. If B is cyclic,
   check that $\alpha_{X_S} = \alpha_{X_{S^{-1}}}$.

These follow from counting arguments similar to the one presented in Remark 2.8.7: starting with a sphere around a generic point or the trivalent vertex of $\Sigma(S^3/B)$ in Figure 2.16, each bead increases α_X and then $\alpha_{X^{-1}}$ by one.

In case 1, the ssl R is conjugate to R^{-1} and S to S^{-1} in B, and furthermore $T = T^{-1}$.

In case 2, the ssl R is conjugate to S^{-1} and S to R^{-1} in B.

In case 3, the ssl S is conjugate to S^{-1} and $R = R^{-1}$ is conjugate to $T = T^{-1}$.

In the last case, B is Abelian and has only one generator S.

2.11.8 Step 7 in Decision Tree

Input	τ-tuple as defined and computed in Section 2.11.1
Output	Boolean: Embedding exists
Algorithm	

1. Compute the orbit of the τ-tuple under the action of the twists.

   The action of a twist is explicitly described in Section "Action on τ-Tuple".

2. For each τ-tuple in the orbit:

   (a) For each $b \in B$:

   i. Conjugate τ-tuple by b.

   ii. Check whether the τ-tuple of one of the forms in Section 2.8.4.

First, notice that the mapping class group is infinite, so, a priori, it is not clear that the algorithm is finite. However, the space of all τ-tuples B^{k+2g} is finite and, hence, computing the subspace closed under the moves described in Section "Action on τ-tuple" is still finite.

Issues with Base Point

The Dehn twists and half twists in Figure 2.19 act on $\tilde{\tau}$ and, hence, on τ-tuples. These twists give elements in $\mathrm{Mod}(S_{g,k}, p)$ and thus $\mathrm{Aut}(\pi_1(S_{g,k}, p))$, but do not necessarily generate $\mathrm{Mod}(S_{g,k}, p)$ as required in Theorem 2.8.10. However, by Theorem 2.8.11, the twists generate $\mathrm{Mod}(S_{g,k})$ under the natural map $\mathrm{Mod}(S_{g,k}, p) \to \mathrm{Mod}(S_{g,k})$.

Considering the Birman exact sequence [FM, Theorem 4.6]

$$1 \to \pi_1(S_{g,k}, p) \to \mathrm{Mod}(S_{g,k}, p) \to \mathrm{Mod}(S_{g,k}) \to 1,$$

we can thus fix the issue by conjugation:

Corollary 2.11.9. *An embedding exists if and only if conjugation by an element in B and the action by Dehn twists and half twists in Figure 2.19 can bring the τ-tuple (computed in Section 2.11.1) into one of the forms listed in Section 2.8.4.*

Action on τ-Tuple

Consider the τ-tuple

$$(\tau(\sigma_1), \ldots, \tau(\sigma_k); \tau(\alpha_1), \tau(\beta_1), \ldots, \tau(\alpha_{i-1}), \tau(\beta_{i-1}), \tau(\alpha_i) \qquad , \tau(\beta_i), \ldots, \tau(\beta_g)).$$

The Dehn twist about a_i turns this into the τ-tuple

$$(\tau(\sigma_1),\ldots,\tau(\sigma_k);\tau(\alpha_1),\tau(\beta_1),\ldots,\tau(\alpha_{i-1}),\tau(\beta_{i-1}),\tau(\alpha_i)\tau(\beta_i),\tau(\beta_i),\ldots,\tau(\beta_g)).$$

This is because the Dehn twist about a_i induces an automorphism of $\pi_1(S_{g,k},p)$ that fixes each generator except for sending α_i to $\alpha_i\beta_i$. We denote this by

$$a_i \mapsto (\alpha_i \mapsto \alpha_i\ \beta_i).$$

Using Figure 2.49, 2.50, 2.51, and 2.52, we have explicitly computed the automorphisms for each Dehn twist respectively half twist:

$$\begin{array}{lll}
a_i \mapsto & (\alpha_i \mapsto \alpha_i\ \beta_i) & \text{for} \quad i=1,\ldots,g \\
m_i \mapsto & (\beta_i \mapsto \beta_i\ \alpha_i) & \text{for} \quad i=1,\ldots,g \\
c_1 \mapsto & \left(\begin{array}{lll} \sigma_k & \mapsto & (\sigma_k\alpha_1)\ \sigma_k\ (\sigma_k\alpha_1)^{-1} \\ \alpha_1 & \mapsto & \sigma_k\ \alpha_1\ \sigma_k^{-1} \\ \beta_1 & \mapsto & \beta_1\ (\sigma_k\alpha_1)^{-1} \end{array}\right) & \\
c_i \mapsto & \left(\begin{array}{lll} \beta_{i-1} & \mapsto & (\beta_{i-1}\alpha_{i-1}^{-1}\beta_{i-1}^{-1}\alpha_i)\ \beta_{i-1} \\ \alpha_i & \mapsto & (\beta_{i-1}\alpha_{i-1}^{-1}\beta_{i-1}^{-1}\alpha_i)\ \alpha_i\ (\beta_{i-1}\alpha_{i-1}^{-1}\beta_{i-1}^{-1}\alpha_i)^{-1} \\ \beta_i & \mapsto & \beta_i\ (\beta_{i-1}\alpha_{i-1}^{-1}\beta_{i-1}^{-1}\alpha_i)^{-1} \end{array}\right) & \text{for} \quad i=2,\ldots,g \\
h_j \mapsto & \left(\begin{array}{lll} \sigma_j & \mapsto & \sigma_j\ \sigma_{j+1}\ \sigma_j^{-1} \\ \sigma_{j+1} & \mapsto & \sigma_j \end{array}\right) & \text{for} \quad j=1,\ldots,k-1
\end{array}$$

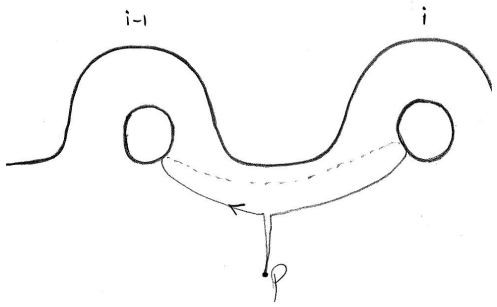

Figure 2.49: The curve $\beta_{i-1}\alpha_{i-1}^{-1}\beta_{i-1}^{-1}\alpha_i$ is helpful in the following computations.

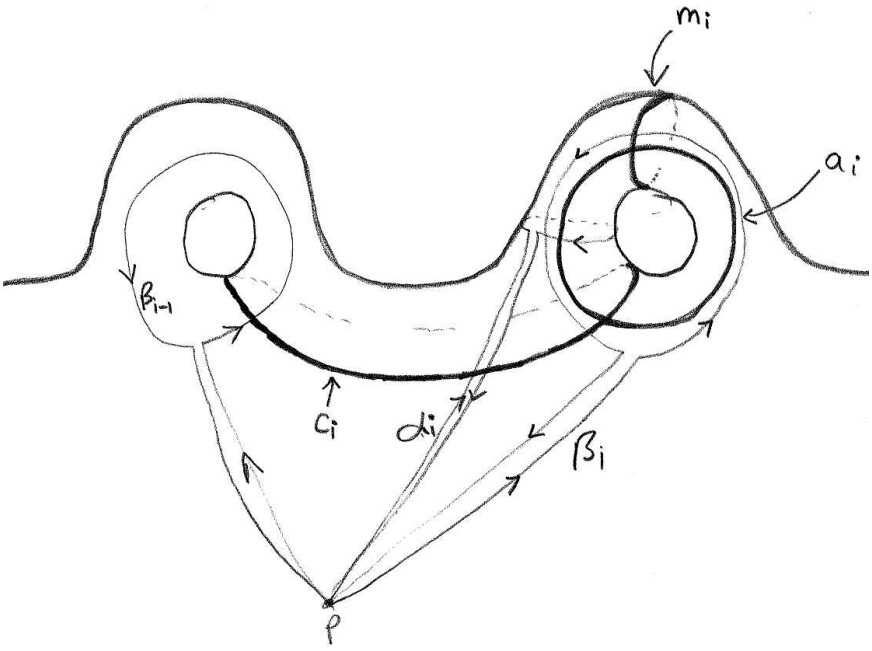

Figure 2.50: Dehn twists about the curves a_i, m_i, and c_i.

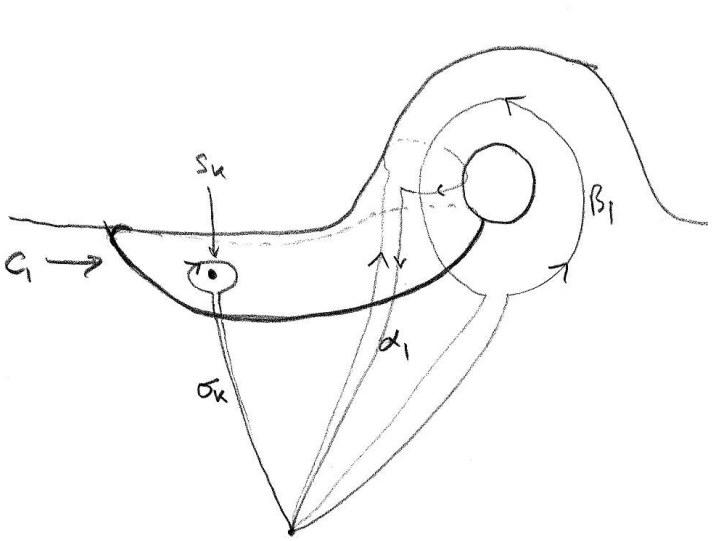

Figure 2.51: Dehn twist about the curve c_1.

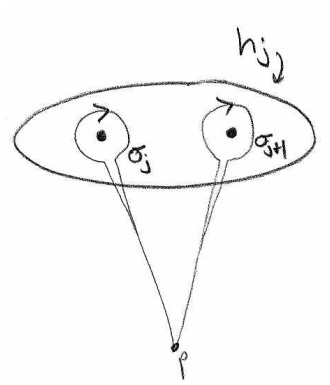

Figure 2.52: Half twist about the curve h_j.

2.12 Examples of Equivariant Morphisms, Immersions, and Embeddings

This section reviews new and well-known (e.g., regular star polyhedron $\left\{\frac{5}{2}, 5\right\}$) examples of equivariant morphisms, immersions, and embeddings of regular maps. Some of the examples are due to, or, grew out of discussions with Jeff Weeks and Carlo Séquin.

Let F be a regular map and B a finite group of isometries of E^3. The pair (F, B) appears in the subsection corresponding to the strongest case possible, e.g., R3.1 and C_7 appears in "Equivariant Morphisms" because there is no C_7-equivariant immersion of R3.1. Given a pair (F, B), we also write for each (H, B, η)-triple what step passing or failing in Figure 2.20 is decisive. We call a morphism $F \to M$ *faithfully equivariant* if every orientation-preserving automorphism of the regular map F is realized by a symmetry of M, usually E^3.

We focus on the ubiquitous Klein quartic R3.1 and the next Hurwitz surface, the Macbeath surface R7.1. The map R4.6 is included because it illustrates how a branched cover can be visualized as stellated polygon. The case of R3.4 provides an example of two subgroups being isomorphic but not conjugate, only one of them giving rise to an equivariant immersion that can be modified to a faithfully equivariant embedding into the 3-torus, but not to an equivariant embedding into E^3. This motivates the examples at the end of the section where we allow target spaces different from E^3.

We adopt the notation in [CD01] for Conder's census of regular maps. For example, the Klein quartic is denoted by "R3.1" because it is the "1"st reflexible ("R") regular map of genus "3" in the census. The letter "R" is replaced by "C" for chiral regular maps, and "N" for non-orientable regular maps. Since the indexing is rather non-descriptive, we also include the type $\{p, q\}$ of the regular map, and, if genus and type uniquely specify a chiral or reflexible regular map, we write "of type $\{p, q\}$ (unique)".

2.12.1 Morphisms into E^3

R4.6 and Icosahedral Symmetry: Small Stellated Dodecahedron

Passes: Step 1, **Fails:** Step 2

The regular star polyhedra are obtained by stellating the Platonic solids (see [Cox73]). A stellated polygon $\left\{\frac{p}{n}\right\}$ can be thought of as an n-cyclic branched cover of a p-gon, as shown in Figure 2.53. Hence, a regular star polyhedron is a mapping from a regular map F into E^3 that is cyclically branched at the vertices, respectively, face centers, and, therefore, not an immersion.

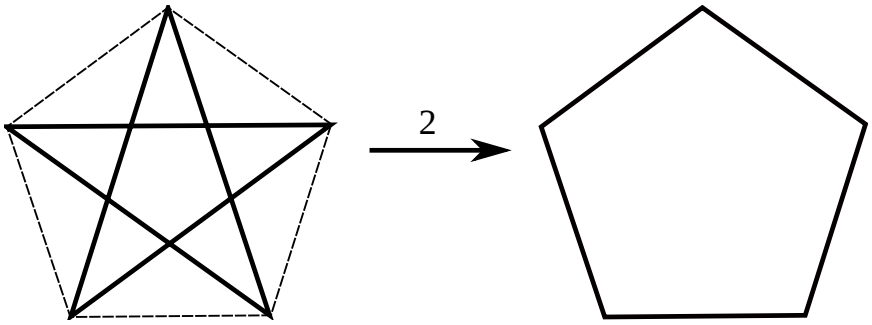

Figure 2.53: Stellated polygon as cyclic branched cover.

Up to duality, there are two regular star polyhedra known as the Kepler-Poinsot polyhedra:

- $\left\{\frac{5}{2}, 3\right\}$ and $\left\{3, \frac{5}{2}\right\}$ are mappings of the dodecahedron $\{5, 3\}$ and icosahedron $\{3, 5\}$.
- $\left\{\frac{5}{2}, 5\right\}$ and $\left\{5, \frac{5}{2}\right\}$ are mappings of the self-dual R4.6 of type $\{5, 5\}$ (unique).

Each mapping is branched at 12 places and is faithfully equivariant.

Klein Quartic R3.1 of Type $\{3, 7\}$ (Unique) and C_7-Symmetry

Passes: Step 1, **Fails:** Step 2

The Klein quartic R3.1 also appears in Section 1.2.1 and 2.2.2. Up to conjugacy, $\mathrm{Aut}^+_{reg}(\mathrm{R3.1})$ has one C_7 subgroup which is generated by rotating one heptagon by a $\frac{1}{7}$th of a turn. As described in [Ago], the generator of C_7 rotates one other heptagon by $\frac{2}{7}$th and a third by $\frac{4}{7}$th of a turn. Hence, Step 2 fails.

In other words, the C_7-equivariant mapping of R3.1 intersects the C_7-symmetry axis of E^3 in the face centers of three heptagons. At one of these points, the mapping is locally an embedding, but at the other two points, the mapping is a 2-, respectively, 4-cyclic branched cover resulting in stellated heptagons $\left\{\frac{7}{2}\right\}$ and $\left\{\frac{7}{4}\right\}$.

R5.2 of Type $\{3, 10\}$ (Unique) and Icosahedral Symmetry

First (H, B, η)**-triple Passes:** Step 1, **Fails:** Step 2
Second (H, B, η)**-triple Passes:** Step 1, **Fails:** Step 3 and Step 4

The cohomology obstruction (Step 4) for the second triple is computed in Section 2.11.5.

R3.4 of Type $\{4,6\}$ (Unique) and Octahedral Symmetry: Part I

First (H,B,η)-triple Passes: Step 1, **Fails:** Step 3 and Step 4

There are two non-conjugate subgroups of Aut^+_{reg}(R3.4) isomorphic to the octahedral group, resulting in two different equivariant mappings. Only one of those can be turned into an equivariant immersion. We describe that immersion later. Here, we study the other case as another example to compute the cohomology obstruction following Section 2.11.5.

The quotient orbifold $(F/H,p)$ has the same black-and-white triangulation as the guiding example in Section 2.11.5. We can again use Figure 2.31 (triangle pairs are labeled differently, but everything else is the same), and obtain the presentation of the holonomy $h : \pi_1^{orb}(F/H,p) \to H$ in Equation 2.10. Applying η to it, we obtain the following τ-tuple $(\tau(\sigma_1),\tau(\sigma_2),\tau(\sigma_3))$:

$$\begin{aligned} \tau(\gamma_1) &= RS^{-1}R^{-1} \\ \tau(\gamma_2) &= S^{-1}RS \\ \tau(\gamma_3) &= S^{-1} \end{aligned} \tag{2.14}$$

We continue as in Section 2.11.5 by constructing the immersed loop for gluing the 2-handle, see Figure 2.54. The loop has one transverse self-intersection, hence, the blackboard framing has non-trivial $\mathbb{Z}/2$-framing invariant. Two $\tau(\gamma_i)$ are expressed as conjugates of inverses of generators, thus we have to change the blackboard framing by two full twists in total. Hence, the framing invariant is still non-trivial, and so is the cohomology obstruction.

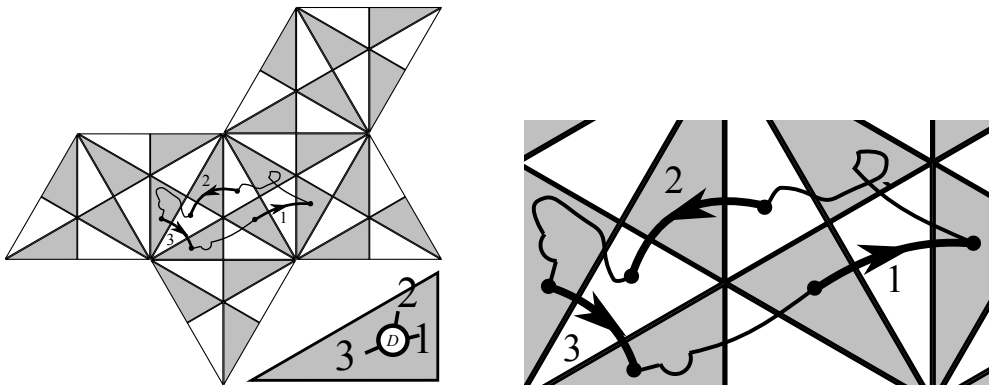

Figure 2.54: The arcs on the 0-handle D, the net of the tetrahedron, and the immersed loop for attaching the 2-handle in case of the equivariant immersion of R3.4.

2.12.2 Immersions into E^3

R3.4 of Type $\{4,6\}$ (Unique) and Octahedral Symmetry: Part II

Second (H, B, η)-triple Passes: Step 3, **Fails:** Step 5

Aut^+_{reg} contains (up to conjugacy) one subgroup H that is isomorphic to the octahedral group and and that passes Step 3.

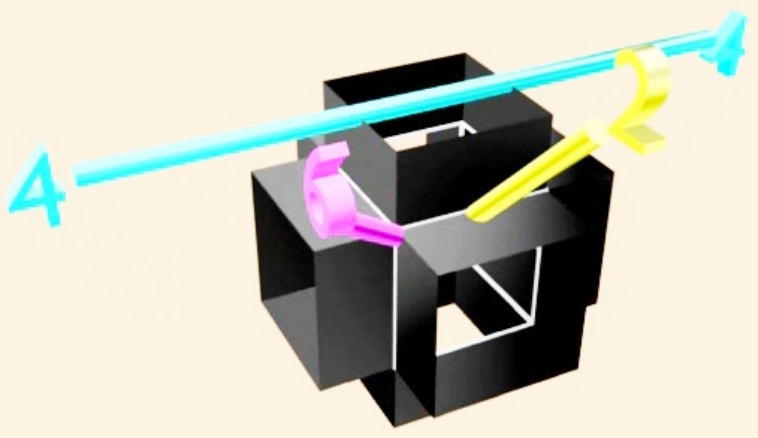

Figure 2.55: Faithfully equivariant embedding of R3.4 into the 3-torus.

We can explicitly construct the equivariant immersion as follows: as shown later in Section 2.12.4, there is a faithfully equivariant embedding of R3.4 into the 3-torus. Figure 2.55 shows the embedded surfaces in a cube serving as fundamental domain of the 3-torus. A face of a cube cuts a 4-gon of the regular map into two. Instead of identifying the faces of the cube, take the top square formed by the surface intersecting the face of the cube, shrink the square a bit and pull it half-way down into the cube. Similarly, take the bottom square shrink it, and pull it half-way up the cube and connect both. Proceed analogously for the other faces of the cube, creating transverse self-intersections of the surface.

Remark 2.12.1. The order four symmetry axis of the cube intersects the immersed surface in four 4-gons. A rotation by a quarter turn about that axis exchanges these 4-gons in pairs. However, a rotation by a half turn takes each of these 4-gons to itself by a half turn. Hence, the centers of the 4-gons turn into order two singular points in the quotient orbifold. This is an instance of the example in Remark 2.11.8.

Klein quartic R3.1 and Octahedral Symmetry

Passes: Step 3, **Fails:** Step 5

The octahedral group has the largest order among all subgroups of Aut^+_{reg}(R3.1) isomorphic to subgroups of SO(3), see the table in Section 2.13.

2.12.3 Embeddings into E^3

Platonic Solids and Spatial Symmetry Groups

The surfaces of Platonic solids are regular maps faithfully equivariantly embedded into E^3.

Klein quartic R3.1 and Tetrahedral Symmetry: "The Eightfold Way"

The tetrahedral group is the largest (in terms of inclusion and in terms of order) subgroup of Aut^+_{reg}(R3.1) that can be realized by an embedding of R3.1 into E^3, see table in Section 2.13.

This is illustrated by Helaman Ferguson's sculpture "The Eightfold Way" (see Figure 2.1) which was the starting point of this chapter.

Macbeath surface R7.1 of type $\{3,7\}$ (Unique) and D_7-Symmetry

First (H,B,η)-triple Passes: Step 1, **Fails:** Step 2
Second (H,B,η)-triple Passes: Step 1, **Fails:** Step 2
Third (H,B,η)-triple Passes: Step 7

The Macbeath surface is the only other Hurwitz surface (Section 2.2.2) for which equations are known to express it as an algebraic curve such that the automorphisms become birational transformations, see [Mac65].

Up to conjugacy (in Aut_{reg}(R7.1)), there is one subgroup $H \subset \mathrm{Aut}^+_{reg}$(R7.1) isomorphic to the dihedral group $B = D_7$. This yields three (H,B,η)-triples up to equivalence with different representations η, but only one passes Step 2. We will first show that this yields an equivariant embedding. We will then explain how to construct it through two cyclic covers from the quotient orbifold shown in Figure 2.56. Carlo Séquin has explicitly produced pictures of the D_7-equivariant embedding of R7.1 that will be published soon.

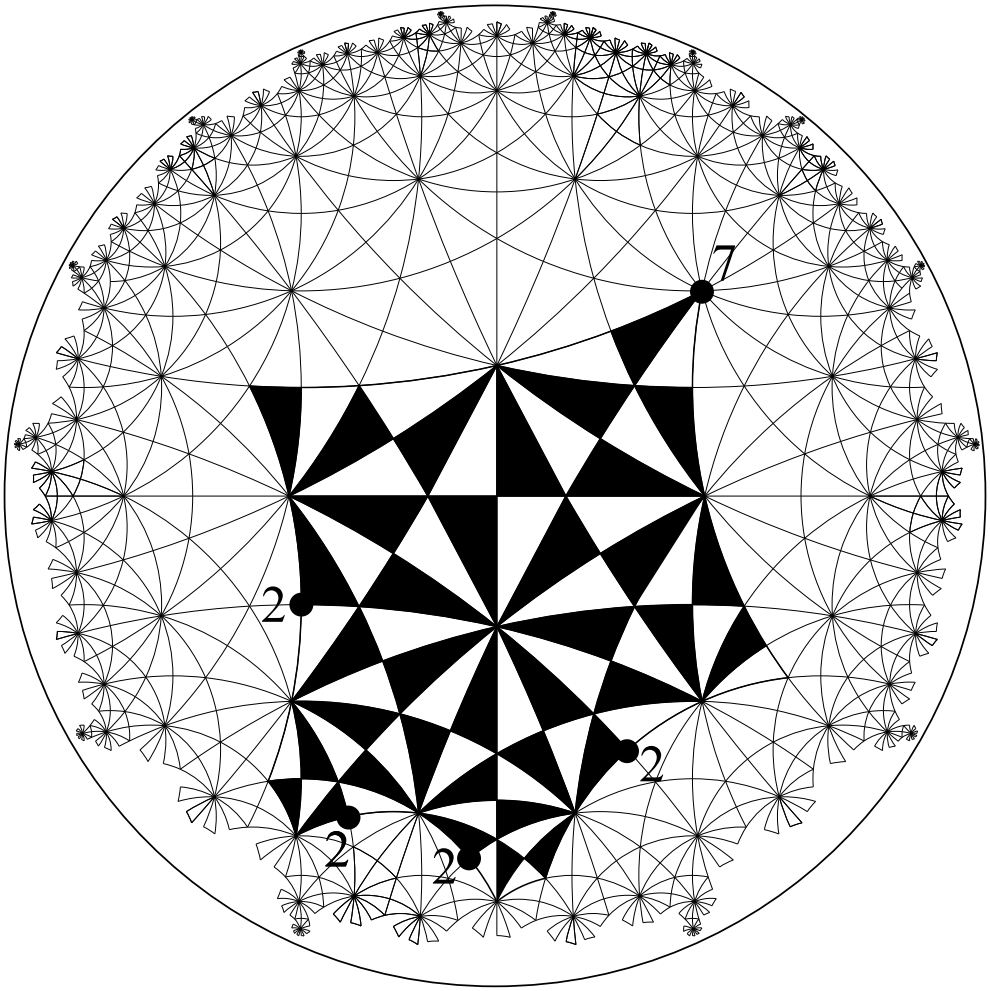

Figure 2.56: Fundamental domain of the quotient orbifold R7.1/D_7.

We compute the orbifold structure of F/H as described in Section 2.11.1. Figure 2.56 shows the quotient orbifold F/H which is S^2 topologically and has one order 7 and four order 2 singular points. There are only two conjugacy classes of ssl's in $\pi_1^{orb}(S^3/B, p) \cong B \cong D_7 = [2,7]^+$ (generators of $[2,7]^+$ as in Equation 2.1):

- The ssl S of order 7 is conjugate to S^{-1}.
- Every ssl corresponding to an order 2 singular point can be expressed as $S^n R S^{-n}$.

Thus, by pushing (in the sense defined in Section 2.8.6) the order 2 singular points around the order 7 singular point, we can obtain a presentation of τ that has one of the forms listed in Section 2.8.4, passing Step 7.

For the construction, we use that the group D_7 is solvable since $[D_7; D_7] \cong C_7$ is Abelian, the quotient group being $\mathbb{Z}/2$. Hence, F is the 7-cyclic branched cover of a 2-cyclic branched cover of F/H. Figure 2.57 sketches the construction of the embedding through cyclic covers. The 2-cyclic cover is uniquely specified by requiring that it unfolds the four singular points of order 2. The 2-cyclic cover is topologically a torus, the Deck transformation is the involution about the axis in Figure 2.57.

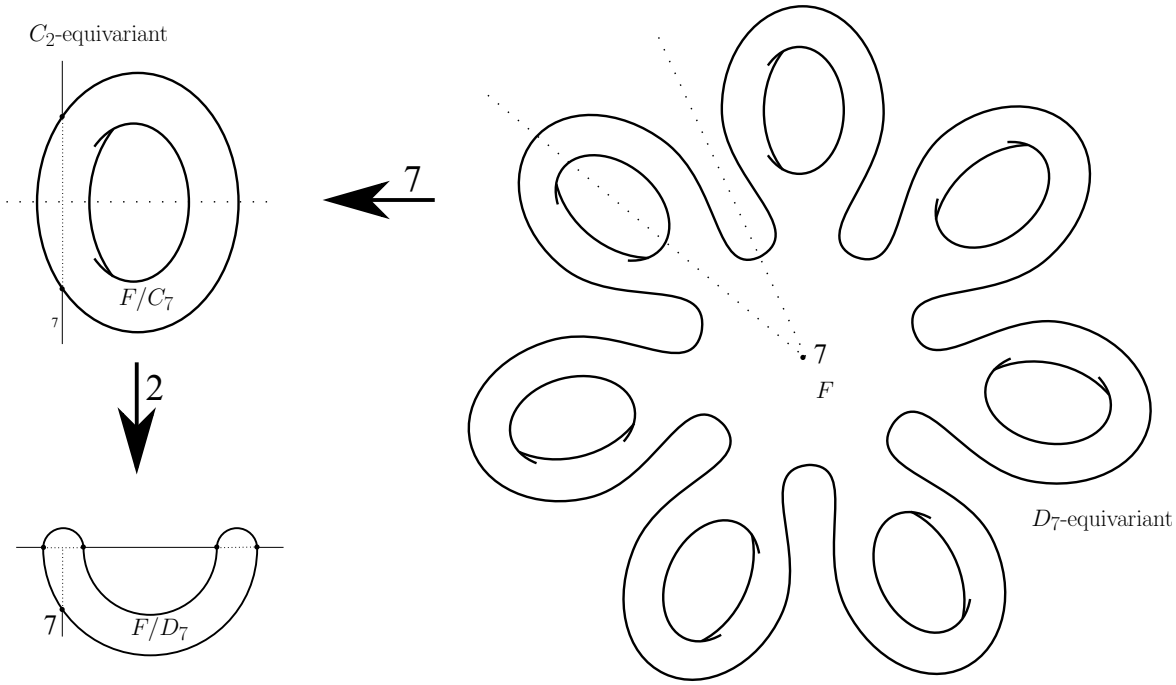

Figure 2.57: Unfolding the quotient orbifold R7.1/D_7 in S^3.

2.12.4 Faithfully Equivariant Immersions and Embeddings Into Other Spaces

Immersions into Cusped Hyperbolic 3-Manifolds

As explained in Section 1.2.1, there is an equivariant immersion of the punctured Klein quartic R3.1 into the complement of the Thurston congruence link [Ago]. Table 2.3 lists examples of other regular maps immersing into cusped hyperbolic 3-manifolds after puncturing the regular map at the vertices. See Section 1.1 and Section 1.15.1 for the definition of N_z^D and $\widehat{\mathrm{N}}_z^D$.

Table 2.3: Immersions of regular maps into cusped hyperbolic 3-manifolds.

Regular map	3-manifold	Link complement
R3.1 of type $\{3,7\}$ (unique)	$\mathrm{N}_{2+\zeta}^{-3}$	Thurston congruence link
R50.1 of type $\{3,13\}$ (unique)	$\mathrm{N}_{3+\zeta}^{-3}$	Yes (Section 1.14)
Type $\{3,19\}$ and genus 196	$\widehat{\mathrm{N}}_{3+2\zeta}^{-3}$	?
Type $\{3,21\}$ and genus 241	$\widehat{\mathrm{N}}_{4+\zeta}^{-3}$	?
R19.4 of type $\{4,7\}$ (unique)	$\widehat{\mathrm{N}}_{2+\zeta}^{-4}$	?

Immersion of Klein Quartic into the 7-Simplex

Carlo Séquin suggested to me that there is a connection between the Klein quartic and the 7-simplex. In fact, every face in the canonical triangulation of the complement $\mathrm{N}_{2+\zeta}^{-3}$ of the Thurston congruence link connects to three different cusps. There are eight cusps and $\binom{8}{3} = 56$ faces. Hence, when collapsing each cusp to a point, the faces of the triangulation become the 2-skeleton of a 7-simplex. The faces in the canonical triangulation of $\mathrm{N}_{2+\zeta}^{-3}$ form an immersed punctured Klein quartic, hence, the punctured Klein quartic is also immersed into the 2-skeleton of the 7-simplex. When filling the punctures, it is no longer an immersion near the vertices. Three vertices of the Klein quartic are sent to the same vertex in the 7-simplex.

Looking at only one vertex of the 7-simplex, the link of a vertex of the 2-skeleton is the complete graph K_7. We recover the connections of the Klein quartic to K_7 recognized by Thurston and described in [Ago]. For example, restricting the canonical triangulation of $\mathrm{N}_{2+\zeta}^{-3}$ to one cusp (see definition of cusp modulus in Section 1.5) gives a triangulation of the torus

with 1-skeleton K_7. The triangulation is a regular map F such that the automorphisms of F correspond to the symmetries of $\mathrm{N}_{2+\zeta}^{-3}$ fixing the cusp. The automorphisms also correspond to symmetries of the Klein quartic that fix a certain class of three heptagons. The three heptagons have the property that rotating one by a $\frac{1}{7}$th of a turn corresponds to rotating another one by a $\frac{2}{7}$th and the third by a $\frac{4}{7}$th of a turn.

Embedding R3.4 of Type $\{4,6\}$ (Unique) into The 3-Torus

This example is due to Jeff Weeks. The regular map R3.4 is of the same type as R2.2 shown in Figure 2.58 and thus the embedding can be thought of as adding one more handle to the embedding of R2.2.

Imagine a cube containing the surface in Figure 2.55 and identify opposite faces of the cube to obtain a 3-torus. The surface becomes R3.4. To show that every automorphism of R3.4 is realized by a symmetry of the torus we need to realize an orientation-reversing automorphism of R3.4, and a rotation by a half and a $\frac{1}{6}$th of a turn about the order 2 and order 6 axis in the Figure 2.55. The orientation-reversing automorphism of R3.4 and the rotation by a half turn are already realized as symmetries of the cube. To rotate R3.4 about a vertex by a $\frac{1}{6}$th of a turn, apply a $\pi/3$ rotation about the order 6 axis and then mirror about the plane perpendicular to the axis and through the vertex.

This yields a representation $\mathrm{Aut}_{reg}(F) \hookrightarrow \mathrm{GL}(4,\mathbb{Z}/4)$. To see this, recall that, using homogeneous coordinates, the isometries of E^3 can be expressed by 4×4 matrices $\begin{pmatrix} M & x \\ 0 & 1 \end{pmatrix}$ with real coefficients and $M \in O(3)$. The symmetries H fixing the cube correspond to matrices with $x = 0$ and coefficients in $\{-1,0,1\}$. H forms an index two subgroup of Aut_{reg}(R3.4). If we pick the side length of the cube to be four, then the additional generator needed is a translation by $x = (2,2,2)$. A translation by four fixes the torus, thus regard the coefficients modulo 4. Notice that if we use $\mathbb{Z}/2$ coefficients such that $-1 = 1$, the group H does not inject into $\mathrm{GL}(4,\mathbb{Z}/2)$.

Embedding $\{2n,2k\}$ into S^3

This family of embedded regular maps F of type $\{2n,2k\}$ and genus $(n-1)(k-1)$ is a generalization of an example due to Jeff Weeks. For $n = 2, k = 3$, we obtain the embedding of R2.2 shown in Figure 2.58.

Pick two axis A and B in S^3 such that the rotations commute. Pick n, respectively, k equidistant points on A and B, see Figure 2.59. Let G consist of all geodesics connecting a point on A with a point on B. Let G' be obtained from G by a rotation by π/k about A

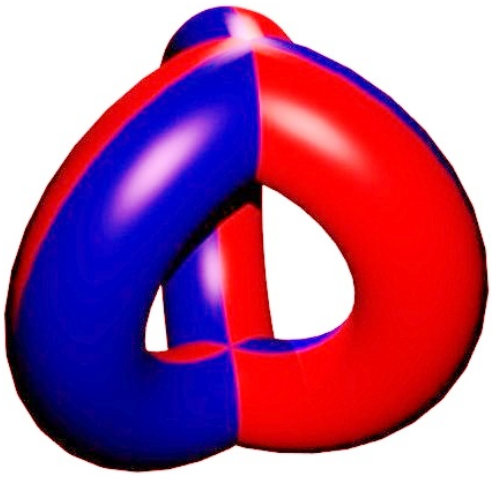

Figure 2.58: Faithfully equivariant embedding of R2.2 of type $\{4, 6\}$ (unique) into S^3.

followed by a rotation by π/n about B. In other words, G and G' intersect a torus around A or B in dual square lattices. All points with equal distance from G and G' form a smooth surface F. Figure 2.59 shows F in a fundamental domain of the quotient orbifold of S^3 (by rotations of $2\pi/k$, respectively, $2\pi/n$ about A and B). Intersect F with planes spanned by A and a geodesic in G or G' to obtain the edges (dashed lines) turning F into a regular map. The $2n$ vertices of F lie equidistantly on A, and the $2k$ face centers on B.

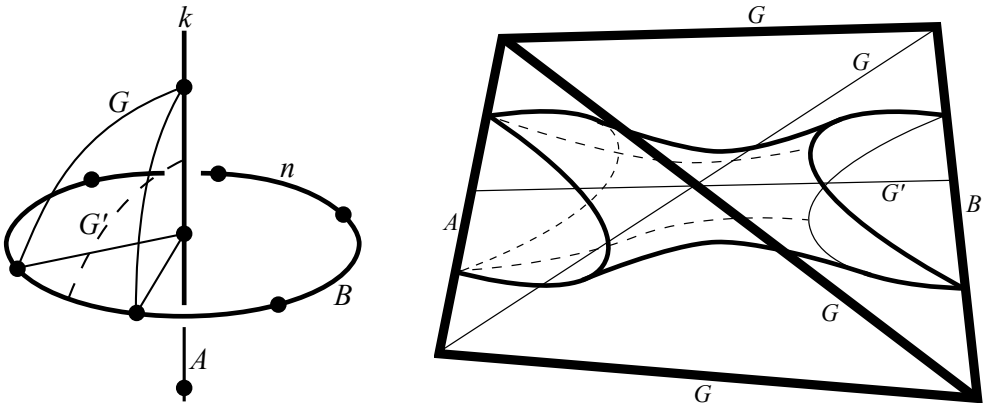

Figure 2.59: The graph G and G' in S^3 and the regular map $\{2n, 2k\}$ in a fundamental domain of the quotient orbifold.

Every automorphism of F is realized by a symmetry of S^3 in $O(4)$. To reserve the orientation of F, mirror about a plane through B and an edge in G. To obtain a half turn about an edge center of the regular map F, take the axis connecting a point of G' on A with a point of

G on B. To rotate by a $\frac{1}{2k}$th of a turn about a vertex of F, mirror about the plane through the vertex and B and rotate by a $\frac{1}{2k}$th of a turn about B. This reverses the orientation of S^3 and exchanges G and G', but does not change the orientation of F.

2.13 Results

In this section, we list for each orientable regular map F of genus 2, ..., 7 what subgroups fulfill necessary and sufficient conditions for the existence of an equivariant morphism, immersion, or embedding. A complete list for the entire census of orientable regular maps by Conder [CD01, Con09] up to genus 101 will be available on the ArXiV.

For example, C_7 is listed for R3.1 under "Mapping" but not under "necessary" conditions for "Immersions", hence there is a C_7-equivariant mapping, but not a C_7-equivariant immersion. C_3 appears under "necessary" for immersion, but not under "sufficient", this means that there might be a potential C_3-equivariant immersion, but the necessary step to decide it has not been implemented yet. However, the table implies that a D_4-equivariant immersion exists because the dihedral group D_4 is in "sufficient".

A group might be listed several times in a field, for example, "3 C_7" in mappings of R7.1. This means that there are three (H, B, η)-triples up to equivalence with $B = C_7$. This can be caused by different subgroups H of $\mathrm{Aut}^+_{reg}(F)$ that are isomorphic but not conjugate, and by different isomorphisms η from the same subgroup H to B, here C_7.

Tet, Oct, and Ico refer to the orientation-preserving isometry groups of the tetrahedron, octahedron, and icosahedron.

To derive these tables, we have implemented the algorithm to find all (H, B, η)-triples and the algorithms in Step 1, 2, 3, 5, and 6 described in Section 2.10 and 2.11. The implementation is done in gap [GAP08] and takes a couple of days to run through the entire census up to genus 101 on a current personal computer.

Remark 2.13.1. For genus $g = 7, 23, 32, 38$, the only equivariant morphisms into E^3 are cyclic or dihedral.

2.13.1 Reflexible Maps

	Mapping	Immersion		Embedding
	necessary and sufficient	necessary	sufficient	necessary
Genus 2				
R2.1	2 C_2, C_3, C_4, C_6, C_8, 2 D_2, D_3, D_4, D_6	2 C_2, C_3, C_4, C_6, 2 D_2, D_3, D_4, D_6	2 C_2, C_4, C_6, 2 D_2, D_3, D_4, D_6	2 C_2, C_3, 2 D_2, D_3
R2.2	3 C_2, C_3, C_4, 2 C_6, 4 D_2, D_3, D_4, D_6	3 C_2, C_3, C_4, 2 C_6, 4 D_2, D_3, D_4, D_6	3 C_2, C_4, C_6, 4 D_2, D_3, D_4, D_6	3 C_2, C_3, 4 D_2, D_3
R2.3	2 C_2, 2 C_4, C_8, 2 D_2, D_4	2 C_2, 2 C_4, 2 D_2, D_4	2 C_2, 2 C_4, 2 D_2, D_4	2 C_2, 2 D_2
R2.4	C_2, 2 C_5, 2 C_{10}	C_2	C_2	C_2
R2.5	3 C_2, C_3, 3 C_6, 3 D_2	3 C_2, C_3, 3 C_6, 3 D_2	3 C_2, C_6, 3 D_2	3 C_2, C_3, 3 D_2
R2.6	C_2, C_4, 2 C_8	C_2, C_4	C_2, C_4	C_2
Genus 3				
R3.1	**Tet**, **Oct**, C_2, C_3, C_4, C_7, D_2, D_3, D_4	**Tet**, **Oct**, C_2, C_3, C_4, D_2, D_3, D_4	**Tet**, **Oct**, C_2, C_4, D_2, D_3, D_4	**Tet**, C_2, C_3, D_2, D_3
R3.2	**Tet**, **Oct**, 2 C_2, C_3, 3 C_4, C_8, 3 D_2, D_3, 2 D_4	**Tet**, **Oct**, 2 C_2, C_3, 3 C_4, 3 D_2, D_3, 2 D_4	**Tet**, **Oct**, 2 C_2, 2 C_4, 3 D_2, D_3, 2 D_4	**Tet**, 2 C_2, C_3, 3 D_2, D_3
R3.3	2 C_2, C_3, 2 C_4, C_6, 2 C_{12}, 2 D_2, D_4	2 C_2, C_3, 2 C_4, C_6, C_{12}, 2 D_2, D_4	2 C_2, C_4, C_6, 2 D_2, D_4	2 C_2, 2 D_2
R3.4	**Tet**, 2 **Oct**, 5 C_2, C_3, 2 C_4, C_6, 16 D_2, 2 D_3, 4 D_4, D_6	**Tet**, 2 **Oct**, 5 C_2, C_3, 2 C_4, C_6, 16 D_2, 2 D_3, 4 D_4, D_6	**Tet**, **Oct**, 3 C_2, C_4, C_6, 16 D_2, D_3, 4 D_4, D_6	**Tet**, 5 C_2, C_3, C_4, 16 D_2, D_3, 2 D_4
R3.5	3 C_2, 5 C_4, C_8, 4 D_2, 2 D_4	3 C_2, 5 C_4, 4 D_2, 2 D_4	3 C_2, 3 C_4, 4 D_2, 2 D_4	3 C_2, 4 D_2
R3.6	5 C_2, 3 C_4, 2 C_8, 13 D_2, 3 D_4	5 C_2, 3 C_4, C_8, 13 D_2, 3 D_4	3 C_2, 2 C_4, 13 D_2, 3 D_4	5 C_2, C_4, 13 D_2, D_4
R3.7	3 C_2, C_3, 2 C_4, C_6, C_{12}, 3 D_2, 2 D_3, D_6	3 C_2, C_3, 2 C_4, C_6, 3 D_2, 2 D_3, D_6	2 C_2, 2 C_4, C_6, 3 D_2, D_3, D_6	3 C_2, C_3, 3 D_2, D_3

	Mapping	Immersion		Embedding
	necessary and sufficient	necessary	sufficient	necessary
R3.8	**Tet**, 3 C_2, C_3, C_6, 6 D_2	**Tet**, 3 C_2, C_3, C_6, 6 D_2	**Tet**, 2 C_2, C_6, 6 D_2	**Tet**, 3 C_2, C_3, 6 D_2
R3.9	C_2, 3 C_7, 3 C_{14}	C_2	C_2	C_2
R3.10	2 C_2, 2 C_4, 2 C_8, 2 D_2	2 C_2, 2 C_4, 2 D_2	2 C_2, C_4, 2 D_2	2 C_2, 2 D_2
R3.11	3 C_2, 2 C_4, 4 C_8, 3 D_2	3 C_2, 2 C_4, 2 C_8, 3 D_2	2 C_2, C_4, 3 D_2	3 C_2, C_4, 3 D_2
R3.12	C_2, C_3, C_4, C_6, 2 C_{12}	C_2, C_3, C_4, C_6	C_2, C_4, C_6	C_2, C_3
Genus 4				
R4.1	2 **Tet**, **Oct**, 2 C_2, 3 C_3, C_4, 2 C_6, C_{12}, 3 D_2, D_3, D_4	2 **Tet**, **Oct**, 2 C_2, 3 C_3, C_4, 2 C_6, 3 D_2, D_3, D_4	2 **Tet**, **Oct**, 2 C_2, C_6, 3 D_2, D_3, D_4	2 C_2, C_3, C_4, 3 D_2, D_3, D_4
R4.2	**Tet**, **Oct**, **Ico**, 2 C_2, C_3, C_4, C_5, C_6, 3 D_2, 2 D_3, D_4, D_5, D_6	**Tet**, **Oct**, 2 C_2, C_3, C_4, C_6, 3 D_2, 2 D_3, D_4, D_6	**Tet**, **Oct**, 2 C_2, C_6, 3 D_2, 2 D_3, D_4, D_6	2 C_2, C_3, C_4, 3 D_2, 2 D_3, D_4
R4.3	3 C_2, 2 C_3, C_4, 2 C_6, 4 D_2, 4 D_3, D_4, 2 D_6	3 C_2, 2 C_3, C_4, 2 C_6, 4 D_2, 4 D_3, D_4, 2 D_6	3 C_2, C_6, 4 D_2, 4 D_3, D_4, 2 D_6	3 C_2, 2 C_3, C_4, 4 D_2, 4 D_3, D_4
R4.4	3 C_2, C_4, 2 C_5, 4 C_{10}, 4 D_2, D_4, 2 D_5, 2 D_{10}	3 C_2, C_4, C_5, 2 C_{10}, 4 D_2, D_4, D_5, D_{10}	3 C_2, C_4, C_{10}, 4 D_2, D_4, D_5, D_{10}	3 C_2, C_5, 4 D_2, D_5
R4.5	2 C_2, 2 C_4, 2 C_8, 2 C_{16}, 2 D_2, D_4, 2 D_8	2 C_2, 2 C_4, C_8, 2 D_2, D_4, D_8	2 C_2, 2 C_4, C_8, 2 D_2, D_4, D_8	2 C_2, 2 D_2
R4.6	**Tet**, 2 **Ico**, C_2, C_3, 2 C_5, D_2, D_3, 2 D_5	**Tet**, C_2, C_3, D_2, D_3	**Tet**, C_2, D_2, D_3	C_2, C_3, D_2, D_3
R4.7	3 C_2, 3 C_3, 2 C_6, 3 D_2, 5 D_3, 2 D_6	3 C_2, 3 C_3, 2 C_6, 3 D_2, 5 D_3, 2 D_6	3 C_2, 3 D_2, 5 D_3, 2 D_6	3 C_2, 3 C_3, 3 D_2, 5 D_3
R4.8	3 C_2, 3 C_3, 5 C_6, 3 D_2, 2 D_3, D_6	3 C_2, 3 C_3, 5 C_6, 3 D_2, 2 D_3, D_6	3 C_2, 4 C_6, 3 D_2, 2 D_3, D_6	3 C_2, C_3, 3 D_2, 2 D_3
R4.9	3 C_2, C_3, C_4, 3 C_6, C_{12}, 4 D_2, D_4	3 C_2, C_3, C_4, 3 C_6, 4 D_2, D_4	3 C_2, C_6, 4 D_2, D_4	3 C_2, C_4, 4 D_2, D_4
R4.10	C_2, C_3, C_6, 3 C_9, 3 C_{18}	C_2, C_3, C_6	C_2, C_6	C_2
R4.11	3 C_2, 2 C_5, 6 C_{10}, 3 D_2	3 C_2, C_5, 3 C_{10}, 3 D_2	3 C_2, C_{10}, 3 D_2	3 C_2, C_5, 3 D_2
R4.12	C_2, C_4, 2 C_8, 4 C_{16}	C_2, C_4, C_8	C_2, C_4, C_8	C_2

	Mapping	Immersion		Embedding
	necessary and sufficient	necessary	sufficient	necessary
Genus 5				
R5.1	**Tet**, **Oct**, 4 C_2, C_3, 3 C_4, C_6, 2 C_8, 12 D_2, D_3, 3 D_4, D_6	**Tet**, **Oct**, 4 C_2, C_3, 3 C_4, C_6, C_8, 12 D_2, D_3, 3 D_4, D_6	**Oct**, 2 C_2, 2 C_4, C_8, 11 D_2, D_3, 3 D_4, D_6	**Tet**, **Oct**, 4 C_2, C_3, C_4, 12 D_2, D_3, 2 D_4
R5.2	**Tet**, 2 **Ico**, 3 C_2, C_3, 2 C_5, C_6, 2 C_{10}, 7 D_2, 2 D_3, 4 D_5, D_6, 2 D_{10}	**Tet**, **Ico**, 3 C_2, C_3, C_5, C_6, C_{10}, 7 D_2, 2 D_3, 2 D_5, D_6, D_{10}	2 C_2, C_6, C_{10}, 6 D_2, D_3, D_5, D_6, D_{10}	**Tet**, 3 C_2, C_3, C_5, 7 D_2, 2 D_3, D_5
R5.3	4 C_2, 3 C_4, 2 C_5, 21 D_2, 6 D_4, 2 D_5	4 C_2, 3 C_4, C_5, 21 D_2, 6 D_4, D_5	2 C_2, C_4, 17 D_2, 6 D_4, D_5	4 C_2, 2 C_4, C_5, 21 D_2, 4 D_4, D_5
R5.4	**Tet**, **Oct**, 6 C_2, C_3, 3 C_4, 2 C_6, 26 D_2, D_3, 5 D_4, D_6	**Tet**, **Oct**, 6 C_2, C_3, 3 C_4, 2 C_6, 26 D_2, D_3, 5 D_4, D_6	**Oct**, 3 C_2, C_4, C_6, 21 D_2, D_3, 5 D_4, D_6	**Tet**, **Oct**, 6 C_2, C_3, 2 C_4, 26 D_2, D_3, 4 D_4
R5.5	6 C_2, 3 C_4, C_8, 27 D_2, 3 D_4	6 C_2, 3 C_4, 27 D_2, 3 D_4	3 C_2, 2 C_4, 21 D_2, 3 D_4	6 C_2, C_4, 27 D_2, 2 D_4
R5.6	6 C_2, 5 C_4, 2 C_8, 19 D_2, 3 D_4	6 C_2, 5 C_4, C_8, 19 D_2, 3 D_4	3 C_2, 4 C_4, C_8, 17 D_2, 3 D_4	6 C_2, C_4, 19 D_2, 2 D_4
R5.7	5 C_2, C_3, 2 C_4, 3 C_6, 2 C_{12}, 13 D_2, 2 D_3, 4 D_6	5 C_2, C_3, 2 C_4, 3 C_6, C_{12}, 13 D_2, 2 D_3, 4 D_6	3 C_2, 2 C_4, C_6, 11 D_2, D_3, 3 D_6	5 C_2, C_3, C_6, 13 D_2, 2 D_3, D_6
R5.8	3 C_2, 2 C_4, 2 C_5, 2 C_{10}, 2 C_{20}, 3 D_2, 4 D_5, 2 D_{10}	3 C_2, 2 C_4, C_5, C_{10}, 3 D_2, 2 D_5, D_{10}	2 C_2, 2 C_4, C_{10}, 3 D_2, D_5, D_{10}	3 C_2, C_5, 3 D_2, D_5
R5.9	3 C_2, 2 C_5, 15 D_2	3 C_2, C_5, 15 D_2	C_2, 11 D_2	3 C_2, C_5, 15 D_2
R5.10	**Tet**, 7 C_2, C_3, 3 C_6, 31 D_2	**Tet**, 7 C_2, C_3, 3 C_6, 31 D_2	3 C_2, 2 C_6, 23 D_2	**Tet**, 7 C_2, C_3, 31 D_2
R5.11	C_2, C_3, 2 C_5, C_6, 2 C_{15}, 2 D_5	C_2, C_3, C_5, C_6, D_5	C_2, C_6, D_5	C_2, C_5, D_5
R5.12	4 C_2, 2 C_4, 2 C_8, 10 D_2, 2 D_4	4 C_2, 2 C_4, 10 D_2, 2 D_4	2 C_2, 2 C_4, 8 D_2, 2 D_4	4 C_2, 10 D_2
R5.13	5 C_2, 3 C_4, 4 C_8, 13 D_2	5 C_2, 3 C_4, 2 C_8, 13 D_2	2 C_2, 3 C_4, 2 C_8, 11 D_2	5 C_2, 13 D_2
R5.14	C_2, 5 C_{11}, 5 C_{22}	C_2	C_2	C_2
R5.15	3 C_2, C_3, 2 C_4, 3 C_6, 4 C_{12}, 3 D_2	3 C_2, C_3, 2 C_4, 3 C_6, 2 C_{12}, 3 D_2	2 C_2, 2 C_4, C_6, 3 D_2	3 C_2, C_3, C_6, 3 D_2

	Mapping	Immersion		Embedding
	necessary and sufficient	necessary	sufficient	necessary
R5.16	C_2, C_4, 2 C_5, 2 C_{10}, 4 C_{20}	C_2, C_4, C_5, C_{10}	C_2, C_4, C_{10}	C_2, C_5
Genus 6				
R6.1	C_2, C_3, 4 C_5, 2 C_{10}, D_3, 2 D_5	C_2, C_3, 3 C_5, C_{10}, D_3, 2 D_5	C_2, C_{10}, D_3, 2 D_5	C_2, C_3, 2 C_5, D_3, 2 D_5
R6.2	**Tet**, **Oct**, **Ico**, 2 C_2, C_3, C_4, C_5, C_6, 3 D_2, 2 D_3, D_4, D_5, D_6	**Tet**, **Oct**, **Ico**, 2 C_2, C_3, C_4, C_5, C_6, 3 D_2, 2 D_3, D_4, D_5, D_6	**Tet**, **Oct**, **Ico**, 2 C_2, C_4, 3 D_2, 2 D_3, D_4, D_5, D_6	**Tet**, 2 C_2, C_3, C_5, C_6, 3 D_2, 2 D_3, D_5, D_6
R6.3	2 C_2, C_3, C_4, C_6, 3 C_9, 3 D_2, D_3, D_4, D_6, 3 D_9	2 C_2, C_3, C_4, C_6, C_9, 3 D_2, D_3, D_4, D_6, D_9	2 C_2, C_4, C_6, 3 D_2, D_3, D_4, D_6, D_9	2 C_2, C_3, 3 D_2, D_3
R6.4	3 C_2, C_4, 3 C_7, 6 C_{14}, 4 D_2, D_4, 3 D_7, 3 D_{14}	3 C_2, C_4, C_7, 2 C_{14}, 4 D_2, D_4, D_7, D_{14}	3 C_2, C_4, C_{14}, 4 D_2, D_4, D_7, D_{14}	3 C_2, C_7, 4 D_2, D_7
R6.5	2 C_2, C_3, 2 C_4, C_6, C_8, 2 C_{12}, 2 C_{24}, 2 D_2, D_3, D_4, D_6, 2 D_{12}	2 C_2, C_3, 2 C_4, C_6, C_{12}, 2 D_2, D_3, D_4, D_6, D_{12}	2 C_2, 2 C_4, C_6, C_{12}, 2 D_2, D_3, D_4, D_6, D_{12}	2 C_2, C_3, 2 D_2, D_3
R6.6	C_2, 8 C_5, 2 C_{10}, 2 D_5	C_2, 6 C_5, C_{10}, 2 D_5	C_2, C_{10}, 2 D_5	C_2, 4 C_5, 2 D_5
R6.7	3 C_2, C_3, C_4, 2 C_6, 2 C_8, C_{12}, 4 D_2, D_3, 2 D_4, D_6, 2 D_8, D_{12}	3 C_2, C_3, C_4, 2 C_6, C_8, C_{12}, 4 D_2, D_3, 2 D_4, D_6, D_8, D_{12}	3 C_2, C_6, 4 D_2, D_3, 2 D_4, D_6, D_8, D_{12}	3 C_2, C_3, C_4, 4 D_2, D_3, 2 D_4
R6.8	2 C_2, C_3, C_4, C_6, C_8, 2 D_2, D_3, D_4, D_6	2 C_2, C_3, C_4, C_6, 2 D_2, D_3, D_4, D_6	2 C_2, C_4, C_6, 2 D_2, D_3, D_4, D_6	2 C_2, C_3, 2 D_2, D_3
R6.9	C_2, C_3, C_6, 3 C_9, D_2	C_2, C_3, C_6, C_9, D_2	C_2, C_6, D_2	C_2, C_3, D_2
R6.10	C_2, C_3, 2 C_5, 2 C_{10}, 2 C_{15}, D_3	C_2, C_3, C_5, C_{10}, D_3	C_2, C_{10}, D_3	C_2, C_3, D_3
R6.11	C_2, 6 C_{13}, 6 C_{26}	C_2	C_2	C_2
R6.12	3 C_2, 3 C_7, 9 C_{14}, 3 D_2	3 C_2, C_7, 3 C_{14}, 3 D_2	3 C_2, C_{14}, 3 D_2	3 C_2, C_7, 3 D_2
R6.13	C_2, C_3, C_4, C_6, 2 C_8, 2 C_{12}, 4 C_{24}	C_2, C_3, C_4, C_6, C_{12}	C_2, C_4, C_6, C_{12}	C_2, C_3

	Mapping	Immersion		Embedding
	necessary and sufficient	necessary	sufficient	necessary
Genus 7				
R7.1	C_2, C_3, 3 C_7, 3 C_9, 3 D_2, D_3, 3 D_7, 3 D_9	C_2, C_3, C_7, 3 C_9, 3 D_2, D_3, D_7, 3 D_9	C_2, 3 D_2, D_3, D_7, 3 D_9	C_2, C_3, C_7, 3 D_2, D_3, D_7
R7.2	2 C_2, 3 C_3, 2 C_4, 3 C_6, 3 C_{12}, 2 D_2, D_3, D_4, D_6, D_{12}	2 C_2, 3 C_3, 2 C_4, 3 C_6, 2 C_{12}, 2 D_2, D_3, D_4, D_6, D_{12}	2 C_2, 2 C_4, 3 C_6, 2 C_{12}, 2 D_2, D_3, D_4, D_6, D_{12}	2 C_2, C_3, 2 D_2, D_3
R7.3	3 C_2, 4 C_4, 2 C_8, 2 C_{16}, 4 D_2, 2 D_4, D_8	3 C_2, 4 C_4, C_8, 4 D_2, 2 D_4, D_8	3 C_2, 3 C_4, 4 D_2, 2 D_4, D_8	3 C_2, C_4, 4 D_2, D_4
R7.4	5 C_2, 3 C_4, 4 C_8, 4 C_{16}, 13 D_2, 3 D_4, 6 D_8	5 C_2, 3 C_4, 3 C_8, C_{16}, 13 D_2, 3 D_4, 5 D_8	3 C_2, 2 C_4, 13 D_2, 2 D_4, 3 D_8	5 C_2, C_4, C_8, 13 D_2, 2 D_4, D_8
R7.5	3 C_2, 2 C_4, 3 C_7, 3 C_{14}, 3 C_{28}, 3 D_2, 6 D_7, 3 D_{14}	3 C_2, 2 C_4, C_7, C_{14}, 3 D_2, 2 D_7, D_{14}	2 C_2, 2 C_4, C_{14}, 3 D_2, D_7, D_{14}	3 C_2, C_7, 3 D_2, D_7
R7.6	C_2, 3 C_3, C_6, 6 C_9, D_3, 3 D_9	C_2, 3 C_3, C_6, 4 C_9, D_3, 3 D_9	C_2, C_6, D_3, 3 D_9	C_2, 2 C_3, D_3
R7.7	2 C_2, C_3, 2 C_4, C_6, 2 C_{12}, 2 D_2, D_4	2 C_2, C_3, 2 C_4, C_6, C_{12}, 2 D_2, D_4	2 C_2, 2 C_4, C_6, C_{12}, 2 D_2, D_4	2 C_2, 2 D_2
R7.8	C_2, C_3, C_6, 3 C_7, 3 C_{21}, 3 D_7	C_2, C_3, C_6, C_7, D_7	C_2, C_6, D_7	C_2, C_7, D_7
R7.9	C_2, C_3, 2 C_5, C_6, 2 C_{10}, 4 C_{15}, 4 C_{30}	C_2, C_3, C_6	C_2, C_6	C_2
R7.10	3 C_2, 2 C_4, 4 C_8, 8 C_{16}, 3 D_2	3 C_2, 2 C_4, 3 C_8, 2 C_{16}, 3 D_2	2 C_2, C_4, 3 D_2	3 C_2, C_4, C_8, 3 D_2
R7.11	2 C_2, 2 C_4, 3 C_8, 4 C_{16}, 2 D_2	2 C_2, 2 C_4, C_8, 2 D_2	2 C_2, C_4, 2 D_2	2 C_2, C_4, 2 D_2
R7.12	C_2, C_4, 3 C_7, 3 C_{14}, 6 C_{28}	C_2, C_4, C_7, C_{14}	C_2, C_4, C_{14}	C_2, C_7

2.13.2 Chiral Maps

	Mapping	Immersion		Embedding
	necessary and sufficient	necessary	sufficient	necessary
Genus 2, 3, 4, 5, 6				
None				
Genus 7				
C7.1	C_2, 2 C_3, C_6, 2 C_9, D_3, D_9	C_2, 2 C_3, C_6, C_9, D_3, D_9	C_2, C_6, D_3, D_9	C_2, C_3, D_3
C7.2	C_2, 3 C_7, 3 D_2	C_2, C_7, 3 D_2	C_2, 3 D_2	C_2, C_7, 3 D_2

2.14 Discussion

This chapter provided a complete theoretical answer to the question what orientation-preserving symmetries of a regular map can be made directly visible in space by an equivariant morphism, immersion or embedding. We have implemented and ran some of the algorithms for the census of orientable regular maps up to genus 101 by Conder. Section 2.13 shows the results up to genus 7 listing which regular maps and symmetry groups fulfill sufficient or necessary conditions for an equivariant morphism, immersion, and embedding. The answer is exact in case of equivariant morphisms. To complete the work for equivariant immersions and give an exact answer, an implementation of the missing steps in Section 2.10 and 2.11 is straight-forward.

However, for equivariant embeddings, the decision algorithm shown in Step 7 does not have feasible run-time because it has to search a space growing exponentially in the genus and number of singular points of the quotient orbifold F/H. Several observations suggest that there is a decision algorithm to replace Step 7 that has run-time growing linear in the genus and number of singular points, thus allowing to give an exact answer for equivariant embeddings of all regular maps in Conder's census. We discuss this at the end.

The cohomology obstruction as defined in 2.7.7 is only well-defined if there is no ssl of order two. We can change the formalism to make the theory more elegant, though the resulting pictures are less intuitive. Instead of putting singular points into the 0-handles, define a orbifold 2-handle to be a disk D with singular point of order k. In a handle decomposition of a 2-orbifold F, let a 1-handle go around a singular point s so that it represents a ssl $\gamma_s \in \pi_1^{orb}(F,p)$. Gluing the orbifold 2-handle such that it covers s then enforces the relation $\gamma_s^k = 0$ in $\pi_1^{orb}(F,p)$. Under the coboundary map $C^1_{CW}(F;\mathbb{Z}/2) \to C^2_{CW}(F;\mathbb{Z}/2)$, a 1-handle touching D is sent to k times the generator of $C^2_{CW}(F;\mathbb{Z}/2)$ corresponding to D. Now, the cohomology obstruction of τ is well-defined even if there is an ssl of order two, in which case it will be automatically zero.

Related work includes Rafalski's investigation of triangle orbifolds immersed into hyperbolic 3-orbifolds [Raf10].

Future work might also extend the theory to include subgroups $H \subset \mathrm{Aut}_{reg}(F)$ that contain orientation-reversing automorphisms.

2.14.1 Deciding the Existence of an Equivariant Embedding in Linear Time

In Step 7, the existence of an equivariant embedding is decided by checking whether a given τ-tuple can be brought into one of the forms listed in Section 2.8.4 by the action of the mapping class group. Computing the complete orbit of a τ-tuple in the exponentially growing space B^{k+2g} under the action of the mapping class group is infeasible.

However, the following arguments suggest though that a decision algorithm with run time linear in the genus and number of singular points exists.

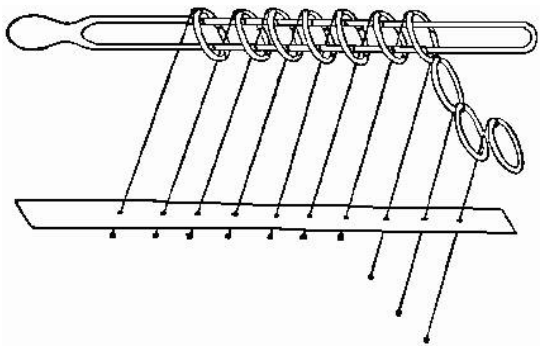

Figure 2.60: The Chinese rings puzzle. Picture from [Wal]. See [Bri] for solution.

Notice that an individual Dehn or half twist in Figure 2.19 operates on at most four consecutive entries in the τ-tuple, i.e., all other entries in the τ-tuple are neither affected by the twist nor influence the outcome of the twist. Furthermore, checking that a τ-tuple is of one of the forms in Section 2.8.4 can be done independently on groups of at most three consecutive entries in the τ-tuple. There might be an algorithm that splits the τ-tuple into such groups and solves the problem group for group in a way similar to solving the Chinese rings puzzle shown in Figure 2.60. Performing the solution to the Chinese rings puzzle follows a binary counting scheme and, hence, the time is exponential in the number of rings. Yet, we can prove that a solution to the Chinese Rings puzzle exists in time linear in the number of rings. We do this inductively by showing for each ring that we can solve the part of the puzzle to the right of the ring while bringing the ring from some configuration to some other configuration. Similarly, even though, the number of necessary Dehn twists might grow exponentially, we might be able to prove that a sequence of Dehn twists exists. Unfortunately, I have not had time to work out such an algorithm.

Bibliography

[Ago] Ian Agol, *Thurston's congruence link*, `http://www.math.uic.edu/~agol/conglink.pdf`.

[Ago00] Ian Agol, *Bounds on exceptional Dehn filling*, Geom. Topol. **4** (2000), 431–449. MR 1799796 (2001j:57019)

[AK80] Selman Akbulut and Robion Kirby, *Branched covers of surfaces in 4-manifolds*, Math. Ann. **252** (1979/80), no. 2, 111–131. MR 593626 (82j:57001)

[AR92] I. R. Aitchison and J. H. Rubinstein, *Combinatorial cubings, cusps, and the dodecahedral knots*, Topology '90 (Columbus, OH, 1990), Ohio State Univ. Math. Res. Inst. Publ., vol. 1, de Gruyter, Berlin, 1992, pp. 17–26. MR 1184399 (93i:57016)

[Bak01] Mark D. Baker, *Link complements and the Bianchi modular groups*, Trans. Amer. Math. Soc. **353** (2001), no. 8, 3229–3246. MR 1695016 (2001j:57007)

[BH96] Steven A. Bleiler and Craig D. Hodgson, *Spherical space forms and Dehn filling*, Topology **35** (1996), no. 3, 809–833. MR 1396779 (97f:57007)

[Bia92] Luigi Bianchi, *Sui gruppi di sostituzioni lineari con coefficienti appartenenti a corpi quadratici immaginarî*, Math. Ann. **40** (1892), no. 3, 332–412. MR 1510727

[Bia93] ———, *Sui gruppi di sostituzioni lineari*, Math. Ann. **42** (1893), no. 1, 30–57. MR 1510766

[Bin83] R. H. Bing, *The geometric topology of 3-manifolds*, American Mathematical Society Colloquium Publications, vol. 40, American Mathematical Society, Providence, RI, 1983. MR 728227 (85j:57001)

[Bir75] Joan S. Birman, *Erratum: "braids, links, and mapping class groups" (Ann. of Math. Studies, No. 82, Princeton Univ. Press, Princeton, N. J., 1974)*, Princeton University Press, Princeton, N. J., 1975, Based on lecture notes by James Cannon. MR 0425944 (54 #13894)

[BLVŽ94] A. Björner, L. Lovász, S. T. Vrećica, and R. T. Živaljević, *Chessboard complexes and matching complexes*, J. London Math. Soc. (2) **49** (1994), no. 1, 25–39. MR 1253009 (95c:52021)

[Bri] Jill Britton, *Solving the chinese ring puzzle*, `http://britton.disted.camosun.bc.ca/chinesering/ninering_sol.html`.

[Bur09] Benjamin A. Burton, *Regina: Normal surface and 3-manifold topology software*, `http://regina.sourceforge.net/`, 1999–2009.

[CD01] Marston Conder and Peter Dobcsányi, *Determination of all regular maps of small genus*, Journal of Combinatorial Theory, Series B **81** (2001), 224–242.

[CDGT91] John Horton Conway, Peter Doyle, Jane Gilman, and William Thurston, *Geometry and the imagination*, `http://www.math.ntnu.no/~dundas/SIF5034/GeometryandtheImagination.pdf`, 1991.

[CDW] Marc Culler, Nathan M. Dunfield, and Jeffrey R. Weeks, *Snappy – a computer program for studying the geometry and topology of 3-manifolds*.

[CM80] H. S. M. Coxeter and W. O. J. Moser, *Generators and relations for discrete groups*, fourth ed., Ergebnisse der Mathematik und ihrer Grenzgebiete [Results in Mathematics and Related Areas], vol. 14, Springer-Verlag, Berlin, 1980. MR 562913 (81a:20001)

[Con06a] Marston Conder, *All chiral (irreflexible) orientably-regular maps on surfaces of genus 2 to 101, up to isomorphism, duality and reflection, with defining relations for their automorphism groups*, `http://www.math.auckland.ac.nz/~conder/ChiralMaps101.txt`, 2006.

[Con06b] ———, *All orientable regular maps on surfaces of genus 2 to 101, up to isomorphism and duality, with defining relations for their automorphism groups*, `http://www.math.auckland.ac.nz/~conder/OrientableRegularMaps101.txt`, 2006.

[Con09] ———, *Regular maps and hypermaps of Euler characteristic* -1 *to* -200, J. Combin. Theory Ser. B **99** (2009), no. 2, 455–459. MR 2482963 (2010b:05084)

[Cox69] H. S. M. Coxeter, *Introduction to geometry*, second ed., John Wiley & Sons Inc., New York, 1969. MR 0346644 (49 #11369)

[Cox73] ———, *Regular polytopes*, third ed., Dover Publications Inc., New York, 1973. MR 0370327 (51 #6554)

[DT03] Nathan M. Dunfield and William P. Thurston, *The virtual Haken conjecture: experiments and examples*, Geom. Topol. **7** (2003), 399–441. MR 1988291 (2004i:57024)

[Dun88] William D. Dunbar, *Geometric orbifolds*, Rev. Mat. Univ. Complut. Madrid **1** (1988), no. 1-3, 67–99. MR MR977042 (90k:22011)

[Eis95] David Eisenbud, *Commutative algebra*, Graduate Texts in Mathematics, vol. 150, Springer-Verlag, New York, 1995, With a view toward algebraic geometry. MR 1322960 (97a:13001)

[EP88] D. B. A. Epstein and R. C. Penner, *Euclidean decompositions of noncompact hyperbolic manifolds*, J. Differential Geom. **27** (1988), no. 1, 67–80. MR 918457 (89a:57020)

[Epp] David Eppstein, *Is the 4x5 chessboard complex a link complement?*, `http://mathoverflow.net/questions/36791`.

[FM] Benson Farb and Dan Margalit, *A primer on mapping class groups, version 5.0*, `http://www.math.uchicago.edu/~margalit/mcg/mcgv50.pdf`.

[GAP08] The GAP Group, *GAP – Groups, Algorithms, and Programming, Version 4.4.12*, 2008.

[Gar79] Peter Freedman Garst, *COHEN-MACAULAY COMPLEXES AND GROUP ACTIONS*, ProQuest LLC, Ann Arbor, MI, 1979, Thesis (Ph.D.)–The University of Wisconsin - Madison. MR 2628756

[Gor02] C. McA. Gordon, *Links and their complements*, Topology and geometry: commemorating SISTAG, Contemp. Math., vol. 314, Amer. Math. Soc., Providence, RI, 2002, pp. 71–82. MR 1941623 (2004c:57012)

[Gra99] Jeremy Gray, *From the history of a simple group*, The eightfold way, Math. Sci. Res. Inst. Publ., vol. 35, Cambridge Univ. Press, Cambridge, 1999, pp. 115–131. MR 1722415 (2001a:14001)

[GS81] Fritz J. Grunewald and Joachim Schwermer, *Arithmetic quotients of hyperbolic 3-space, cusp forms and link complements*, Duke Math. J. **48** (1981), no. 2, 351–358. MR 620254 (82j:10046)

[GS99] Robert E. Gompf and András I. Stipsicz, *4-manifolds and Kirby calculus*, Graduate Studies in Mathematics, vol. 20, American Mathematical Society, Providence, RI, 1999. MR 1707327 (2000h:57038)

[Hat83a] Allen Hatcher, *Bianchi orbifolds of small discriminant*, `http://www.math.cornell.edu/~hatcher/bianchi.html`, 1983.

[Hat83b] ———, *Hyperbolic structures of arithmetic type on some link complements*, J. London Math. Soc. (2) **27** (1983), no. 2, 345–355. MR 692540 (84m:57005)

[Hat02] ———, *Algebraic topology*, Cambridge University Press, 2002.

[HH85] Joel Hass and John Hughes, *Immersions of surfaces in* 3*-manifolds*, Topology **24** (1985), no. 1, 97–112. MR 790679 (87a:57037)

[Hir59] Morris W. Hirsch, *Immersions of manifolds*, Trans. Amer. Math. Soc. **93** (1959), 242–276. MR 0119214 (22 #9980)

[Hun80] Thomas W. Hungerford, *Algebra*, Graduate Texts in Mathematics, vol. 73, Springer-Verlag, New York, 1980, Reprint of the 1974 original. MR 600654 (82a:00006)

[Hur92] A. Hurwitz, *Ueber algebraische Gebilde mit eindeutigen Transformationen in sich*, Math. Ann. **41** (1892), no. 3, 403–442. MR 1510753

[JT66] Ioan James and Emery Thomas, *Note on the classification of cross-sections*, Topology **4** (1966), 351–359. MR 0212820 (35 #3685)

[Kle78] Felix Klein, *Ueber die Transformation siebenter Ordnung der elliptischen Functionen*, Math. Ann. **14** (1878), no. 3, 428–471. MR 1509988

[Kle99] ———, *On the order-seven transformation of elliptic functions*, The eightfold way, Math. Sci. Res. Inst. Publ., vol. 35, Cambridge Univ. Press, Cambridge, 1999, Translated from the German and with an introduction by Silvio Levy, pp. 287–331. MR 1722419 (2001i:14042)

[Lac00] Marc Lackenby, *Word hyperbolic Dehn surgery*, Invent. Math. **140** (2000), no. 2, 243–282. MR 1756996 (2001m:57003)

[Lan02] Serge Lang, *Algebra*, third ed., Graduate Texts in Mathematics, vol. 211, Springer-Verlag, New York, 2002. MR 1878556 (2003e:00003)

[Lar01] Michael Larsen, *How often is* $84(g-1)$ *achieved?*, Israel J. Math. **126** (2001), 1–16. MR 1882031 (2002m:30056)

[Lev99] Silvio Levy (ed.), *The eightfold way*, Mathematical Sciences Research Institute Publications, vol. 35, Cambridge University Press, Cambridge, 1999, The beauty of Klein's quartic curve. MR 1722410 (2000f:14001)

[Mac61] A. M. Macbeath, *On a theorem of Hurwitz*, Proc. Glasgow Math. Assoc. **5** (1961), 90–96 (1961). MR 0146724 (26 #4244)

[Mac65] ———, *On a curve of genus* 7, Proc. London Math. Soc. (3) **15** (1965), 527–542. MR 0177342 (31 #1605)

[Mac99] ———, *Hurwitz groups and surfaces*, The eightfold way, Math. Sci. Res. Inst. Publ., vol. 35, Cambridge Univ. Press, Cambridge, 1999, pp. 103–113. MR 1722414 (2001c:14002)

[Mat07] Sergei Matveev, *Algorithmic topology and classification of 3-manifolds*, second ed., Algorithms and Computation in Mathematics, vol. 9, Springer, Berlin, 2007. MR 2341532 (2008e:57021)

[Men79] Eduardo R. Mendoza, *Cohomology of* PGL_2 *over imaginary quadratic integers*, Bonner Mathematische Schriften [Bonn Mathematical Publications], 128, Universität Bonn Mathematisches Institut, Bonn, 1979, Dissertation, Rheinische Friedrich-Wilhelms-Universität, Bonn, 1979. MR 611515 (82g:22012)

[Mey86] Robert Meyerhoff, *Sphere-packing and volume in hyperbolic* 3*-space*, Comment. Math. Helv. **61** (1986), no. 2, 271–278. MR 856090 (88e:52023)

[MR03] Colin Maclachlan and Alan W. Reid, *The arithmetic of hyperbolic 3-manifolds*, Graduate Texts in Mathematics, vol. 219, Springer-Verlag, New York, 2003. MR 1937957 (2004i:57021)

[MS74] John W. Milnor and James D. Stasheff, *Characteristic classes*, Princeton University Press, Princeton, N. J., 1974, Annals of Mathematics Studies, No. 76. MR 0440554 (55 #13428)

[NR92] Walter D. Neumann and Alan W. Reid, *Arithmetic of hyperbolic manifolds*, Topology '90 (Columbus, OH, 1990), Ohio State Univ. Math. Res. Inst. Publ., vol. 1, de Gruyter, Berlin, 1992, pp. 273–310. MR 1184416 (94c:57024)

[Oer04] Ulrich Oertel, *Incompressible maps of surfaces and Dehn filling*, Topology Appl. **136** (2004), no. 1-3, 189–204. MR 2023417 (2004j:57032)

[Raf10] Shawn Rafalski, *Immersed turnovers in hyperbolic 3-orbifolds*, Groups Geom. Dyn. **4** (2010), no. 2, 333–376. MR 2595095 (2011a:57036)

[Rat94] John G. Ratcliffe, *Foundations of hyperbolic manifolds*, Graduate Texts in Mathematics, vol. 149, Springer-Verlag, New York, 1994. MR 1299730 (95j:57011)

[Ril83] Robert Riley, *Applications of a computer implementation of Poincaré's theorem on fundamental polyhedra*, Math. Comp. **40** (1983), no. 162, 607–632. MR 689477 (85b:20064)

[Roh85] J. Rohlfs, *On the cuspidal cohomology of the Bianchi modular groups*, Math. Z. **188** (1985), no. 2, 253–269. MR 772354 (86e:11042)

[Rol90] Dale Rolfsen, *Knots and links*, Mathematics Lecture Series, vol. 7, Publish or Perish Inc., Houston, TX, 1990, Corrected reprint of the 1976 original. MR 1277811 (95c:57018)

[Sco83] Peter Scott, *The geometries of* 3*-manifolds*, Bull. London Math. Soc. **15** (1983), no. 5, 401–487. MR 705527 (84m:57009)

[Thu86] William P. Thurston, *Hyperbolic structures on* 3*-manifolds. I. Deformation of acylindrical manifolds*, Ann. of Math. (2) **124** (1986), no. 2, 203–246. MR 855294 (88g:57014)

[Thu98] ———, *How to see* 3*-manifolds*, Classical Quantum Gravity **15** (1998), no. 9, 2545–2571, Topology of the Universe Conference (Cleveland, OH, 1997). MR 1649658 (99i:57030)

[Vog85] Karen Vogtmann, *Rational homology of Bianchi groups*, Math. Ann. **272** (1985), no. 3, 399–419. MR 799670 (87a:22025)

[vW09] Jake J. van Wijk, *Symmetric tiling of closed surfaces: visualization of regular maps*, ACM Trans. Graph. **28** (2009), no. 3, 1–12.

[Wal] Jeffrey Walker, *Chinese ring puzzle applet*, `http://www.cs.oberlin.edu/~jwalker/puzzle/`.

[Wed] N. S. Wedd, *Regular map database*, `http://www.weddslist.com/rmdb/`.

[Whi44] Hassler Whitney, *The singularities of a smooth* n*-manifold in* $(2n-1)$*-space*, Ann. of Math. (2) **45** (1944), 247–293. MR 0010275 (5,274a)

[Zie94] Günter M. Ziegler, *Shellability of chessboard complexes*, Israel J. Math. **87** (1994), no. 1-3, 97–110. MR 1286818 (95e:06010)

[Zim73] R. Zimmert, *Zur* SL_2 *der ganzen Zahlen eines imaginär-quadratischen Zahlkörpers*, Invent. Math. **19** (1973), 73–81. MR 0318336 (47 #6883)